Yves Konigshofer's

Thesis

March 18, 2005

STUDIES OF
GAMMA DELTA T CELL ACTIVATION:
FROM THE INTESTINE TO THE SPLEEN
AND ALSO IN SILICON

A DISSERTATION

SUBMITTED TO THE PROGRAM IN IMMUNOLOGY

AND THE COMMITTEE ON GRADUATE STUDIES

OF STANFORD UNIVERSITY

IN PARTIAL FULFILLMENT OF THE REQUIREMENTS

FOR THE DEGREE OF

DOCTOR OF PHILOSOPHY

Yves Konigshofer

March 2005

© Copyright by Yves Konigshofer 2005

All Rights Reserved

I certify that I have read this dissertation and that, in my opinion, it is fully adequate in scope and quality as a dissertation for the degree of Doctor of Philosophy.

_____

Yueh-hsiu Chien Principal Adviser

I certify that I have read this dissertation and that, in my opinion, it is fully adequate in scope and quality as a dissertation for the degree of Doctor of Philosophy.

_____

Eugene C. Butcher

I certify that I have read this dissertation and that, in my opinion, it is fully adequate in scope and quality as a dissertation for the degree of Doctor of Philosophy.

_____

Mark M. Davis

I certify that I have read this dissertation and that, in my opinion, it is fully adequate in scope and quality as a dissertation for the degree of Doctor of Philosophy.

_____

Patricia P. Jones

Approved for the University Committee on Graduate Studies

_____

Abstract

The roles of gamma delta T cells in the immune system have remained unclear. In the spleens and lymph nodes of adult animals, only about 5% of lymphocytes are gamma delta T cells. On the other hand, about half of the approximately 10 million lymphocytes in the murine intraepithelial lymphocyte (IEL) compartment of the small intestine are gamma delta T cells. A microarray analysis of gamma delta IELs from normal mice and from mice infected with the enteric pathogen *Yersinia pseudotuberculosis* was performed to analyze how these cells respond to infection and revealed that their mRNA transcripts do not show major changes following infection and that gamma delta IELs appear to be constitutively activated. To further study gamma delta T cells, RAG2-deficient BALB/c mice that were transgenic for the G8 gamma delta T cell receptor (TCR) were used. G8 gamma delta T cells can be activated through the recognition of the MHC class Ib molecules T10 and T22 of the b but not of the d haplotype. Microarray studies of G8 gamma delta IELs reveal that they are also constitutively activated – even in the apparent absence of a stimulatory TCR ligand. In addition, while the exposure of G8 gamma delta IELs to ligand-expressing splenocytes leads to their expression of CD69 and blasting, this only leads to minor changes to their transcripts. On the other hand, the coculture of splenic gamma delta T cells from these mice with stimulatory TCR ligand-expressing splenocytes leads to their activation and their expression of cell-surface molecules like CD5, CD6, CD44, CD69, Lag-3, and PD-1. Furthermore, activated splenic gamma delta T cells are found to produce interferon gamma and interleukin 4 that act synergistically to activate B cells. In fact, the presence of both of these cytokines leads to the expression of CD69 by about 80 – 90% of B cells and their upregulation of B7.2, MHC class II, and T10/T22. Finally, in order to study gamma delta T cell activation and immunological synapse formation, a simulation of cell-to-cell contact was designed using the JAVA programming language.

Acknowledgements

First and foremost, I would like to thank my parents, Ilse and Friedrich, and my sister, Marilyn, for being so supportive during my many years at Stanford.

I would like to thank my adviser, Chien. She was about as hands-on as advisers can get. This was very helpful during my first few years at Stanford because I learned a lot about how to design and critically evaluate experiments. There are advisers who appear as if they could not care less about their graduate students. Chien is definitely not one of those advisers.

I would like to thank all of the members, past and present, of the Chien and Davis labs. All of them were nice and helpful, both inside and outside of the labs. Mark and Chien did a great job of putting together labs where someone almost always knew how to answer some difficult problem or how to perform certain types of experiments. Of past Chien and Davis lab members, I would especially like to thank Rudy Chaparro, Ashley Chi, Aude Fahrer, Corwyn Hopke, Kirk Jensen, Sunny Shin, and Tony Yao for being good friends.

I would like to thank the ASSU Nominations Commission for allowing me to serve on the Administrative Panels on Biosafety, on Human Subjects in Medical Research, and on Laboratory Animal Care over a five year span. This allowed me to learn the rules and regulations that apply to medical research and taught me a lot about different areas of medical research.

I would like to thank my past coworkers in intramural sports for their support on the field. I think that every graduate student should spend at least one quarter refereeing a sport before TA-ing his or her first class. Students sometimes complain, and what they say to referees (which might not always be in accordance with the Fundamental Standard) is often a lot worse than what they would dare say to TAs. However, as a referee, as a TA, and as a scientist, you have to be able to back up your positions and defend your decisions in order to be effective.

I would like to thank all of my teammates in intramural sports (there were a lot) and, especially, those I had the privilege to captain. It was almost always fun and I learned a lot from it. We even won a championship in co-ed softball.

Finally, during my sophomore year at McGill University, I was forced to take a course in physical chemistry for bioscience students. In the first class, the professor teaching that course, Adi Eisenberg, mentioned that it was not possible to teach this course using examples that were relevant to us and, for the next few months, we had to memorize one complicated equation after another. However, some of these equations did become relevant during my graduate school years. In fact, I am pretty sure that the course could have been taught using interesting examples from the biosciences. Chapter 5 of this thesis is dedicated to all the bioscience students who had to endure this physical chemistry class.

Table of Contents

List of Tables

List of Illustrations

General Introduction

The immune system is subject to natural selection. The innate immune system, which operates in plants and animals, consists of physical barriers, cells, mechanisms and effector functions that can deal with infections in a fixed way. The adaptive immune system, which is only found in vertebrate animals, is characterized by cells that express diverse receptors as a consequence of somatic gene rearrangement. In mammals, the adaptive immune system is comprised of B and T lymphocytes, which, unlike cells of the innate immune system that express receptors that are germline-encoded, are capable of antigen-specific responses to infection. These antigen-specific responses are essential for the maintenance of host immune competence.

T lymphocytes can be subdivided into αβ T cells and γδ T cells based on the rearranged receptors they express. Early studies revealed that γδ T cells are the first to appear in thymic ontogeny and that, as the appearance and the development of αβ T cells progresses, the number of γδ T cells remains similar but ends up only representing about 5% of the lymphocytes in the spleen and lymph nodes. On the other hand, γδ T cells appear to contribute more to the lymphocyte pools in various mucosal tissues including the small intestine, the uterus, and the skin.

In general, γδ T cells and αβ T cells were found to be able to mount similar immune responses. Along those lines, $CD16^+$ γδ T cell clones were capable of antibody-dependent cellular cytotoxicity (Borst, van de Griend et al. 1987), γδ T cell clones were often capable of killing tumor target cells while freshly-isolated γδ T cells were not (Lanier, Kipps et al. 1985), freshly-isolated $Thy\text{-}1^+$ γδ T cells in the intraepithelial lymphocyte compartment of the small intestine (γδ IELs) were capable of killing cells in redirected lysis experiments (Klein and Kagnoff 1984; Klein 1986; Goodman and Lefrancois 1988; Lefrancois and Goodman 1989), and, collectively, γδ T cells and cell lines and hybridomas thereof were reported to be capable of producing cytokines such as IL-2 (Yokoyama, Koning et al. 1987), GM-CSF, IL-4 (Roberts, Yokoyama et al. 1991), IFNγ, and TNFα (Christmas and Meager 1990).

An apparent similarity between γδ T cells and αβ T cells may have been due to the assays that were performed because it was possible that γδ T cells performed yet unknown functions. Early experiments suggested that T cells were important in controlling intravenous primary *Listeria* infection and that γδ T cells could partially substitute for αβ T cells, although αβ T cells were needed for the development of memory responses while γδ T cells had an effect on controlling lesion formation in infected livers (Mombaerts, Arnoldi et al. 1993). Similar results were observed in an HSV-1 infection model, where both γδ T cells and αβ T cells were sufficient to resolve infections (Sciammas, Kodukula et al. 1997). In the case of coxsackievirus B3 infection, it has been suggested that differences in IFNγ and IL-4 production by Vγ4Vδ4- and Vγ1Vδ4-expressing γδ T cells influence the cytokine production of $CD4^+$ αβ T cells and determine whether mice develop myocarditis (Huber, Graveline et al. 2001). Additional studies have implicated γδ T cells in immune responses against pathogens such as Influenza virus (Carding, Allan et al. 1990), *Mycobacterium tuberculosis* (Janis, Kaufmann et al. 1989), *Nippostrongylus brasiliensis* (Ferrick, Schrenzel et al. 1995), *Nocardia brasiliensis* (King, Hyde et al. 1999), Sendai virus (Ogasawara, Emoto et al. 1994), and *Toxoplasma gondii* (Kasper, Matsuura et al. 1996), although the reason and significance of their involvement has remained mostly unclear.

The observations that γδ TCRs, unlike αβ TCRs, do not have a propensity for recognizing peptides associated with MHC molecules, that γδ TCRs can recognize antigens directly without requiring their processing and presentation, and that the CDR3 length distribution of the TCR δ chain is more similar to that of the immunoglobulin heavy chain than to that of the TCR α and β chains (Rock, Sibbald et al. 1994), suggested that γδ T cells and αβ T cells recognized different types of antigens (reviewed in (Chien, Jores et al. 1996)). While this may partially explain why these two cell types have different functions, it also presents a major problem because the antigens recognized by γδ T cells have been and still remain difficult to identify. In fact, to date, the only natural ligands that have been identified for murine γδ T cells are the MHC class Ib molecules T10 and T22 (Crowley, Fahrer et al. 2000).

The lack of known γδ TCR ligands has stymied efforts to determine the function of γδ T cells because, without this information, it is difficult to know when and where γδ T cells activate and how γδ T cells act upon recognition of γδ TCR ligands. One such example is the oral *Yersinia pseudotuberculosis* infection model developed by Elizabeth M. Kerr in Mark M. Davis' lab. She found that, compared to wild-type mice, TCR δ chain-deficient mice that were orally infected with *Yersinia pseudotuberculosis* had bacteria spread to the spleen one day faster and, unlike wild-type mice, frequently still had bacteria in their mesenteric lymph nodes (MLNs) 5 days after infection (Kerr 1998). Because the murine small intestine contains a large number of IELs of which a sizeable amount are γδ T cells (Goodman and Lefrancois 1988), because oral *Yersinia* infection occurs through the small intestine, and because it had been reported that the presence of γδ IELs may play a role in the turnover of epithelial cells and their expression of MHC class II (Komano, Fujiura et al. 1995), this suggested that γδ IELs may play a role in the defense against oral *Yersinia* infection and that this infection model could be used to study how γδ T cells respond to infection.

Chapter 1 deals with the *Yersinia* infection model, where I helped analyze the responses of γδ IELs using microarray analysis. Interestingly, γδ IELs showed only minor changes to their transcripts in response to infection. In addition, γδ IELs were found to constitutively express genes associated with effector functions. This differed from MLN $CD8^+$ αβ T cells, which only expressed such genes in response to infection. While these results indicated that γδ IELs function differently than MLN $CD8^+$ αβ T cells, the question of why γδ T cells are important in *Yersinia* infection remained unanswered.

It has been reported that γδ IELs can express keratinocyte growth factor following γδ TCR crosslinking (Boismenu and Havran 1994) but we did not find this gene to be expressed in our analysis. This raised the possibility that, when γδ IELs recognize antigens through their γδ TCRs, they may mount different responses than during *Yersinia* infection. In addition, it is unclear why γδ IELs express diverse γδ TCRs when they appear to constitutively express genes associated with effector functions.

In **Chapter 2**, I take advantage of the availability of the mice that are transgenic for the G8 γδ TCR (Dent, Matis et al. 1990), which is specific for T10 and T22, in order to address the transcriptional responses of γδ IELs to the recognition of stimulatory γδ TCR ligands. In **Chapter 3**, these experiments are extended to study the responses of splenic γδ T cells. Surprisingly, the splenic G8 γδ T cells were not the only cells that became activated when they were cocultured with splenocytes that expressed their ligands. B cells were also found to activate based on their expression of CD69 and their enhanced expression of B7.2, MHC class II, and T10/T22. In **Chapter 4**, I show that this activation of B cells is primarily due to the synergistic effects of two cytokines, IFNγ and IL-4, which are produced in response to G8 γδ T cell activation. Lastly, when a T cell encounters a TCR ligand-expressing cell, the interaction can lead to the formation of an immunological synapse where there is an accumulation and often-ordered distribution of molecules at the contact area between the cells. This process may influence the outcome of the T cell activation and the T cell's subsequent effector functions. **Chapter 5** deals with a simulation of cell-to-cell contact that I designed and its use to study T cell activation and synapse formation.

Overall, the transcriptional responses to the recognition of stimulatory γδ TCR ligands differ greatly between γδ IELs and splenic γδ T cells. However, the genes expressed by γδ and αβ T cells in the spleens of G8 γδ TCR-transgenic mice do not appear to differ much, and the same has been reported for CD8αα$^+$ γδ and αβ IELs in conventional mice (Shires, Theodoridis et al. 2001). Thus, it will be important to determine the ligands that are recognized by γδ T cells in order to determine when these cells encounter their ligands *in vivo*.

In addition, one of the exiting observations of all of these experiments is that not all γδ T cells activate, not all B cells express the same amount of T10/T22, not all γδ T cells downregulate their γδ TCRs by the same amount, not all γδ T cells express the same amount of PD-1 or Lag-3 after activation, not all γδ T cells express IFNγ, etc. There is an amazing diversity in a system that is based around a single γδ TCR and two high affinity ligands. In the future, it will be necessary to characterize γδ T cells, and all cells, at a single cell level.

Chapter 1: Attributes of γδ Intraepithelial Lymphocytes as Suggested by Their Transcriptional Profile

Aude M. Fahrer[*†], Yves Konigshofer[‡], Elizabeth M. Kerr[‡], Ghassan Ghandour[‖], David H. Mack[‖], Mark M. Davis[*‡**], and Yueh-hsiu Chien[*‡]

[*] Department of Microbiology and Immunology, [‡] Program in Immunology, and [**] Howard Hughes Medical Institute, Stanford University, Stanford, CA 94305; and [‖] Eos Biotechnology, South San Francisco, CA 94080

Foreword

This chapter has been reproduced from Proceedings of the National Academy of Sciences of the United States of America, 2001, vol. 98, no. 18, pp 10216 – 10266 and is Copyright 2001 National Academy of Sciences, U.S.A. Some of the genes listed in the tables have been updated with respect to their names. Y.C., together with M.M.D., A.M.F., and E.M.K. are responsible for the experimental designs. A.M.F. and E.M.K. set up and performed the γδ IEL-related as well as the MLN $CD8^+$ αβ T cell experiments together. A.M.F. and Y.C. performed the initial analyses of the microarray data and Y.K. performed subsequent analyses. Y.C., M.M.D., A.M.F., and Y.K. are responsible for the interpretation of the results. G.G. provided expertise in statistical analysis of the microarray data and D.H.M. provided experimental expertise and microarrays from Affymetrix.

Copyright 2001 National Academy of Sciences, U.S.A. Reproduced from Proceedings of the National Academy of Sciences of the United States of America; 2001, vol. 98, no. 18, pp 10216 – 10266

Abstract

γδ T lymphocytes in the intestinal intraepithelial layer (γδ IELs) are thought to contribute to immune competence, but their actual function remains poorly understood. Here we used DNA microarrays to study the gene expression profile of γδ IELs in a *Yersinia* infection system to better define their roles. To validate this approach, mesenteric lymph node $CD8^+$ αβ T cells were similarly analyzed. The transcription profiles show that, whereas lymph node $CD8^+$ αβ T cells must be activated to become cytotoxic effectors, γδ IELs are constitutively activated and appear to use different signaling cascades. Our data suggest that γδ IELs may respond efficiently to a broad range of pathological situations irrespective of their diverse T cell antigen receptor repertoire. γδ IELs may modulate local immune responses and participate in intestinal lipid metabolism, cholesterol homeostasis, and physiology. This study provides a strong basis for further investigations of the roles of these cells as well as mucosal immune defense in general.

Copyright 2001 National Academy of Sciences, U.S.A. Reproduced from Proceedings of the National Academy of Sciences of the United States of America; 2001, vol. 98, no. 18, pp 10216 – 10266

Introduction

Despite intense efforts, the functional roles of γδ T cells in maintaining host immune defense remain enigmatic. One unique feature of γδ T cells that distinguishes them from αβ T cells is their tissue distribution. Although γδ T cells represent a small percentage (<5%) of the lymphocytes in the central immune system of humans and mice, they are a sizable population (10 – 50%) in the mucosal epithelia (Sim 1995; Kaufmann 1996). The murine γδ T lymphocytes in the intestinal intraepithelial layer (γδ IELs) exhibit a diverse T cell antigen receptor (TCR) repertoire (Asarnow, Goodman et al. 1989; Takagaki, DeCloux et al. 1989) and thus have the potential to recognize a variety of antigens. These cells have been implicated in regulating the development of epithelial cells (Komano, Fujiura et al. 1995) and in controlling intestinal αβ T cell responses in an *Eimeria vermiformis* infection model (Roberts, Smith et al. 1996). Recently, we found that mice lacking γδ T cells ($TCR\delta^{-/-}$) are much less resistant than either normal mice or mice without αβ T cells ($TCR\beta^{-/-}$) to the dissemination of the enteric pathogen *Yersinia pseudotuberculosis* to the liver and spleen 1 – 4 days following oral infection (Kerr 1998). To gain insight into the scope of γδ IEL responses in this system, we compared the gene expression of γδ IELs isolated from mice orally infected with *Yersinia* to that of γδ IELs isolated from uninfected animals by using the Affymetrix (Santa Clara, CA) GeneChip technology (Lipshutz, Fodor et al. 1999). This approach allowed us to examine a large number of transcripts including many not associated with lymphocyte functions and to gain insight into the cellular mechanisms operating in γδ IELs. To validate the experimental approach, and to serve as a basis of comparison for the γδ IEL data, we also analyzed the expression profiles of mesenteric lymph node (MLN) $CD8^+$ αβ T cells at the peak of the peripheral responses to oral *Yersinia* infection (Kerr 1998).

We find that, whereas transcripts associated with cytotoxic functions and activation are significantly induced in $CD8^+$ αβ T cells by the infection, γδ IELs from infected and uninfected animals appear to be constitutively activated and to express very high levels of cytotoxic genes. Interestingly, γδ IELs express several inhibitory receptors, which could keep their effector functions in check but allow them to be readily

Copyright 2001 National Academy of Sciences, U.S.A. Reproduced from Proceedings of the National Academy of Sciences of the United States of America; 2001, vol. 98, no. 18, pp 10216 – 10266

turned on with little or no *de novo* transcription. These properties could allow these cells to participate in both innate and acquired immune defense by responding quickly to a broad range of pathological situations irrespective of their diverse TCR repertoire. Our data also show that γδ IELs may recruit other leukocytes and down-regulate immune responses by targeting cells such as macrophages. Surprisingly, γδ IELs express genes associated with lipid and cholesterol metabolism that are complementary to those expressed by the intestinal epithelial cells, suggesting a new role for γδ IELs in intestinal homeostasis and physiology. Overall, this approach has allowed us to evaluate many more potential attributes of γδ IELs than previously possible and provides important insights into γδ IEL regulation and function.

Copyright 2001 National Academy of Sciences, U.S.A. Reproduced from Proceedings of the National Academy of Sciences of the United States of America; 2001, vol. 98, no. 18, pp 10216 – 10266

Methods

Sample Preparation

Seven- to twelve-week-old female C57Bl/6 mice (The Jackson Laboratory and Stanford University) deprived of food overnight were infected by oral gavage with *Y. pseudotuberculosis* YPIII or with a YopE mutant bacterium (kindly provided by Stanley Falkow, Stanford University). γδ IELs were isolated 5 days after mice were infected with $5x10^8$ colony-forming units (cfu) of *Y. pseudotuberculosis* YPIII. αβ T cells were isolated 10 days after mice were infected with $1x10^8$ cfu of *Y. pseudotuberculosis* YPIII or with a YopE mutant. αβ T cells isolated from YPIII- or YopE-mutant-infected animals showed virtually no difference in gene expression. Therefore, no distinction was made in the data analysis here.

Cells from the small intestine were isolated as described (Wang, Whetsell et al. 1997) but without the gradient step. γδ IELs were isolated by positively selecting with biotin-conjugated GL3 (anti-δ chain) antibody and avidin-conjugated magnetic beads (Dynal, Oslo). $CD8^+$ αβ T cells from mesenteric lymph nodes were isolated by negative depletion with FITC-conjugated antibodies against CD4, B220, CD11b, γδ TCR, and anti-FITC-conjugated magnetic beads (PerSeptive Biosystems, Framingham, MA) followed by FACS sorting with phycoerythrin-conjugated anti-CDα antibody. $CD8^+$ $FITC^-$ cells were collected. Epithelial cells were obtained by sorting intestinal cell suspensions on the basis of forward and side scatter profiles and propidium iodide exclusion. The purity of the cells was estimated to be greater than 95% for γδ IELs and epithelial cells and greater than 99% for $CD8^+$ αβ T cells. Analysis of RNA expression by using Affymetrix GeneChip microarrays was carried out according to published procedures (Glynne, Akkaraju et al. 2000) with at least $1x10^7$ cells for each sample, isolated from a minimum of three mice.

GeneChip Data Analysis

Each gene is represented by ≈20 probe pairs on the array. Each probe pair consists of a 25-mer oligo complementary to the gene of interest [the perfect match (PM)

Copyright 2001 National Academy of Sciences, U.S.A. Reproduced from Proceedings of the National Academy of Sciences of the United States of America; 2001, vol. 98, no. 18, pp 10216 – 10266

oligo] and a second mismatched (MM) oligo, which contains a single base change at the middle nucleotide. Expression values represent the median of PM-MM values for each gene after normalization. Chips were normalized on the basis of the 75^{th} percentile of PM-MM values for all probe pairs (PM-MM values for each chip were multiplied by the $42/75^{th}$ percentile for that chip). GeneChip 3.0 software (Affymetrix) was used to determine the presence or absence of mRNA for specific genes in each sample. Analysis specific for individual sets of data is described in the table legends.

Copyright 2001 National Academy of Sciences, U.S.A. Reproduced from Proceedings of the National Academy of Sciences of the United States of America; 2001, vol. 98, no. 18, pp 10216 – 10266

Results

Gene Expression Correlates Well with Known Protein Expression and Cell Function

To determine the gene expression patterns of γδ IELs and MLN $CD8^+$ αβ T cells from uninfected and *Yersinia*-infected mice, duplicate samples of mRNA were prepared from isolated cell populations. In addition, one sample of mRNA isolated from intestinal epithelial cells was also analyzed. Of the 6,352 probe sets found on the microarrays, about 2,100 genes were expressed by the lymphocytes (both αβ and γδ T cells), and about 800 genes were expressed by the epithelial cells. This difference in the number of genes expressed presumably reflects a bias in the database towards mRNAs identified from hematopoietic cells.

Genes expected to be expressed in αβ, γδ T cells, and epithelial cells were identified in the array analysis. These include the T cell receptors, lymphocyte cell surface markers and structural genes characteristic of each cell type. A partial list of cell surface molecules expressed in $CD8^+$ αβ T cells is shown in *Table 1.1* and *Supplemental Table 1.1*. As expected, there is no linear correlation between the expression levels of genes identified from epithelial cells and either T cell population. Interestingly, the differences in individual gene expression levels between mesenteric $CD8^+$ αβ T cells and γδ IELs are much greater than those observed between the same cell types isolated from infected and uninfected animals, as discussed in the next section (*Supplemental Figure 1.1*).

Effector Function Genes Are Constitutively Expressed in γδ IELs but Induced in MLN $CD8^+$ αβ T Cells

Many of the abundantly expressed genes in γδ IELs are associated with specialized functions. Genes coding for Granzymes A, B and RANTES are among the ten most abundantly expressed mRNAs (*Supplemental Table 1.2*). Surprisingly, these genes are expressed at similarly high levels in cells isolated from both infected and uninfected mice. In fact, only 37 genes and ESTs are identified as having statistically significant, albeit small (less than 3-fold), differences between infected and uninfected γδ

Copyright 2001 National Academy of Sciences, U.S.A. Reproduced from Proceedings of the National Academy of Sciences of the United States of America; 2001, vol. 98, no. 18, pp 10216 – 10266

IEL samples (*Supplemental Table 1.3*). None of these is thought to be associated with cell activation or effector function.

That almost all of the genes associated with effector function and activation are expressed at comparable levels in γδ IELs from infected and uninfected mice is clearly not a failure of the detection system. A large increase in the expression of genes encoding cytotoxic functions (e.g., Granzymes A and B), the chemokine RANTES, and activation markers (e.g., Ly-6E) was readily observed in mesenteric $CD8^+$ αβ T cells from infected mice compared with those from uninfected mice (*Table 1.1* and *Supplemental Table 1.4*). This difference was seen despite the fact that only 8% of the lymph node $CD8^+$ αβ T cell population from infected animals showed an activated phenotype ($CD44^{hi}$, L-$selectin^{low}$).

It is also unlikely that the γδ IEL transcription program is activated by the isolation procedure, which includes a 30-min 37°C incubation to detach the IELs (all subsequent steps in the isolation procedure are carried out at 0 – 4°C, precluding significant mRNA synthesis). RNA samples were obtained from a whole intestine manipulated only to remove Peyer's patches and from a whole intestine processed to detach, but not remove, epithelial cells and IELs. Similar levels of Granzyme A and RANTES were found in both samples by Northern analysis (*data not shown*). Consistent with this finding, all γδ IELs, but not most splenic γδ T cells that underwent the same isolation procedures, showed surface CD69 expression – a marker associated with activated natural killer (NK) cells, αβ T cells, and B cells (the gene is not represented on the chips) (*Figure 1.1A* and *data not shown*).

In addition, all γδ IEL samples express genes implicated in sustaining specialized cell functions. These include genes associated with growth arrest (e.g., *c-fes*, *gadd45*, *gadd153*, and *gas3*) and differentiation (e.g., *atf-4*, *blimp-1*, *cdc25*, *mad*, *tis21*, and *agp/ebp*). Several proteases and enzymes (e.g., Furin, Mep-1, CD73), which have been implicated in the maturation of molecules associated with growth and differentiation, are also expressed (*Table 1.2* and *Supplemental Table 1.5*). Taken together, these results indicate that γδ IELs in uninfected animals are constitutively activated to transcribe genes associated with effector functions.

Copyright 2001 National Academy of Sciences, U.S.A. Reproduced from Proceedings of the National Academy of Sciences of the United States of America; 2001, vol. 98, no. 18, pp 10216 – 10266

γδ IELs May Be Activated Through Signaling Pathways Distinct from Those in αβ T Cells

Despite γδ IELs having an activated phenotype, they do not appear to express transcripts for certain key signaling proteins used by αβ T cells. These include protein kinase C θ (PKCθ), an important component of TCR-mediated NF-κB activation in mature αβ T cells (Sun, Arendt et al. 2000), and diacylglycerol kinase α (Sakane and Kanoh 1997), a protein responsible for the removal of diacylglycerol, which normally activates PKCθ. Conversely, PI3-kinase (Rameh and Cantley 1999) levels are increased when compared with αβ T cells. Whereas the signal transduction genes preferentially expressed by MLN $CD8^+$ αβ T cells (*Table 1.1* and *Supplemental Table 1.6*) largely fit into known lymphocyte signaling pathways, those preferentially expressed by γδ IELs do not (*Table 1.2* and *Supplemental Table 1.5*).

In this context, it is interesting to note that although γδ IELs express high levels of RANTES, RFLAT-1, which is important in the later stages of RANTES expression after $CD8^+$ αβ T cell activation (Song, Chen et al. 1999), is not expressed. Because the RANTES promoter contains NF-κB- and interferon regulatory factor-binding sites, the expression of RANTES could result from signals from tumor necrosis factor (TNF)α and IFNγ, respectively (Lee, Hong et al. 2000). In fact, both the TNFα and IFNγ receptor genes are expressed in γδ IELs. Thus, some of the effector genes expressed by both γδ and peripheral αβ T cells appear to be triggered by different signaling cascades in the two cell types.

γδ IEL Function

Because the gene expression pattern of γδ IELs is characteristic of that of effector cells, whereas the gene expression pattern of αβ T cells is typical of that of naïve cells, we analyzed the genes preferentially expressed in γδ IELs to identify potential γδ IEL functions. This analysis was complemented by a search through all the data sets for the

Copyright 2001 National Academy of Sciences, U.S.A. Reproduced from Proceedings of the National Academy of Sciences of the United States of America; 2001, vol. 98, no. 18, pp 10216 – 10266

expression of particular genes. Some of these genes, subdivided by function, are shown in *Table 1.2* and *Supplemental Table 1.5*.

γδ IELs Have the Potential to Kill a Variety of Targets by Using Different Mechanisms

In addition to Granzymes A and B, γδ IELs were found to express other cytotoxic mediators. These include the antimicrobial peptide cryptdin, an α-IFN homolog, lymphotoxin β, Fas ligand, and genes implicated in generating or enhancing the lytic response of NK cells such as NKR-P1A, NKR-P1C, LAG-3, and 2B4. LAG-3 has been reported to bind class II MHC (Baixeras, Huard et al. 1992), suggesting that macrophages, B cells, and epithelial cells may interact with γδ IELs. 2B4 is related to CD2 and binds to the same ligand, CD48 (Brown, Boles et al. 1998). The expression of 2B4, but not CD2, on virtually all γδ IELs can be demonstrated by FACS (*Figure 1.1B* and *data not shown*).

Intriguingly, mRNAs coding for a variety of inhibitory receptors (CTLA-4, gp49, PD-1, and the NK inhibitory receptors Ly49-E, F, and G) are found in the γδ IEL samples. Because our data suggest that γδ IELs are actively transcribing genes related to effector functions, it seems likely that these cells, although ready to act, are being held back by inhibitory receptors *in situ*. Most functions could thus be kept in check and yet be readily turned on, with little or no *de novo* transcription. This interpretation would also be consistent with the very few differences in gene expression seen between γδ IELs from infected versus uninfected mice (*Supplemental Table 1.3*).

γδ IELs Can Recruit Other Leukocytes, Down-Regulate Immune Responses, and Present Antigens on Class II MHC

γδ IELs express genes that are known to down-regulate immune responses. These include TGFβ and TJ6/J6B7. Perhaps the most intriguing one is Eta-1 (osteopontin), which has been postulated to be part of a surprisingly rapid T cell-dependent response to infection preceding classical forms of T cell-dependent immunity. Recent experiments

Copyright 2001 National Academy of Sciences, U.S.A. Reproduced from Proceedings of the National Academy of Sciences of the United States of America; 2001, vol. 98, no. 18, pp 10216 – 10266

indicate that Eta-1 can differentially regulate macrophage IL-10 and -12 expression and thereby play a key role in the establishment of cell-mediated immune responses to viral and bacterial infections (Ashkar, Weber et al. 2000). After *Listeria* infection, mice deficient in Eta-1 fail to form granulomas – a phenotype that is also observed in mice deficient in γδ T cells (Mombaerts, Arnoldi et al. 1993; Fu, Roark et al. 1994).

Transcripts corresponding to chemokines such as RANTES, lymphotactin, macrophage inflammatory protein (MIP)-1α, and MIP-1β are present in γδ IEL populations. It is worth noting that other than very low levels of IL-2, none of the other cytokines on the arrays, including IL-1 – 5, -7, -10 – 12, -15, and -17 and IFNγ, were expressed. This expression pattern suggests that, whereas γδ IELs may play a role in recruiting other leukocytes, their ability to modify immune responses may be more focused.

With respect to cytokine receptor genes, γδ IELs express the β and γ chains of the IL-2R, the IL-4R, the β chain of the IL-12R, receptors for IFNs α, β, and γ, tumor necrosis factor receptors 1 and 2, and also 114/A10, a responsive element of IL-3. Cytokine receptor gene transcripts not found in γδ IELs include the receptors for IL-3, -5 – 11, -15, and -17. Additionally, γδ IELs transcribe the gene encoding the (bacterial) lipopolysaccharide-induced chemokine receptor (L-CCR), but lack transcripts for CXCR4 and CCR7 that are associated with peripheral homing. In fact, the transcripts for L-selectin, α-actinin-1, and lymphocyte function-associated antigen-1 are also absent in γδ IELs. Thus, γδ IELs lack both the extracellular and intracellular components required for peripheral homing.

γδ IELs expressed both the invariant chain and MHC class II molecules. FACS analysis showed that 15% of the γδ IELs express I-A on the surface (*Figure 1.1C*). This finding indicates that γδ IELs may serve as antigen-presenting cells for $CD4^+$ αβ T cells, possibly presenting peptides from intestinal lumen- or epithelial cell-derived antigens.

Copyright 2001 National Academy of Sciences, U.S.A. Reproduced from Proceedings of the National Academy of Sciences of the United States of America; 2001, vol. 98, no. 18, pp 10216 – 10266

γδ IELs May Contribute to Intestinal Lipid Metabolism, Cholesterol Homeostasis, and Physiology

The most surprising result is the expression of many genes relating to lipid and cholesterol metabolism in the γδ IELs samples (*Table 1.2* and *Supplemental Table 1.5*). Cholesterol is a major structural component of the plasma membrane lipid rafts where many signaling proteins are found in activated T and B cells (reviewed in (Langlet, Bernard et al. 2000)). Thus, the enhanced expression of genes involved in the cholesterol biosynthetic pathway is compatible with our proposal that γδ IELs are constitutively activated. In addition, the expression of these genes may also be important in intestinal physiology.

Although it is well known that the small intestine plays a major role in the metabolism of dietary lipids, it is commonly assumed that these functions are carried out by enterocytes, a major population of epithelial cells. Indeed, high levels of transcripts for fatty acid-binding protein and apolipoproteins A-I, A-IV, and C-III were detected in epithelial cell mRNA. Unexpectedly, mRNAs for apolipoprotein E, phospholipid-binding protein, low-density lipoprotein receptor, and some enzymes involved in fatty acid, lipid, and cholesterol biosynthesis were expressed only in the γδ IEL samples. The expression of these transcripts raises the possibility that lipid metabolism is carried out through the collaboration of epithelial cells and γδ IELs. These results also suggest that γδ IELs may play a role in the generation of lipoprotein particles including chylomicrons, very low density lipoprotein, and high-density lipoprotein. The lipoprotein particles may promote the efflux of cholesterol from the membranes of dying cells and provide cholesterol to the rapidly dividing epithelial cells, thereby maintaining homeostasis. Consistent with the supposition that γδ IELs are involved in lipid/cholesterol metabolism, two of the six genes that show an increase in cells isolated from infected versus uninfected animals are involved in glycolipid metabolism (*Supplemental Table 1.3*).

The protein encoded by *adh-1*, ADH-A2, is the only known murine class I alcohol dehydrogenase that is capable of oxidizing retinol (vitamin A) to retinaldehyde. This process is the first enzymatic step in the conversion of retinol into its biologically active metabolite, retinoic acid, a potent inducer of cellular differentiation and morphogenesis.

Copyright 2001 National Academy of Sciences, U.S.A. Reproduced from Proceedings of the National Academy of Sciences of the United States of America; 2001, vol. 98, no. 18, pp 10216 – 10266

The expression of ADH-A2 is absent in the αβ T cell samples and is expressed at a lower level in epithelial cells. Carbonic anhydrase II may regulate the acid-base balance within IELs. The abundance of transcripts encoding this protein suggests that IELs may exist in an environment where the pH may reach drastically different levels compared with the normal blood circulation.

The production of keratinocyte growth factor (KGF) by *in vitro* culturing of γδ IELs with TCR crosslinking (Boismenu and Havran 1994) has led to a proposed role for these cells to maintain intestinal homeostasis. We failed to detect KGF expression in any γδ IEL samples.

Copyright 2001 National Academy of Sciences, U.S.A. Reproduced from Proceedings of the National Academy of Sciences of the United States of America; 2001, vol. 98, no. 18, pp 10216 – 10266

Discussion

In this report, we have characterized the gene expression pattern of γδ IELs in an effort to understand why these cells are important in the initial protection against oral *Yersinia* infection. Surprisingly, we found hardly any transcriptional changes in γδ IELs as the result of infection. Instead, γδ IELs from uninfected as well as infected animals appeared to be activated and transcribed high levels of cytotoxic and other genes associated with specialized functions. Although these results preclude us from estimating the magnitude of the γδ IEL response to *Yersinia* infection, they provide an important and unexpected clue for understanding how γδ IELs may function as a "first line of defense" against pathogens entering the digestive system.

It is commonly assumed that γδ IELs require antigen recognition to induce effector functions. This is because almost all the well-defined functions attributed to freshly isolated γδ IELs were observed in *in vitro* assays with anti-CD3 antibody to crosslink the TCR. These include the spontaneous lytic response of γδ IELs as assayed in anti-CD3 redirected lysis (Lefrancois and Goodman 1989) and the transcription of KGF (Boismenu and Havran 1994) and lymphotactin (Boismenu, Feng et al. 1996) mRNAs in γδ IELs after *in vitro* activation with plate bound anti-CD3 antibody. Our data show that freshly isolated γδ IELs constitutively express very high levels of Granzymes A and B and RANTES transcripts, that these cells express NK-activating and inhibitory receptors, and that the activation of γδ IELs and peripheral αβ T cells appears to be triggered by different signaling cascades. These features raise the interesting possibility that the lytic activity of γδ IELs may not be induced exclusively through the antigen receptors. Instead, it could be induced through activating receptors such as those expressed by NK cells. This method of activation would allow γδ IELs to deal with a broad range of pathological situations very quickly, despite the diversity of γδ TCR expressed by these cells, and with little or no requirement for new gene expression – an effective way to participate in innate immune responses.

If γδ IELs are able to function in this fashion, what is the role of the γδ T cell receptor? One possibility is that it gives these cells an alternative route to induce

Copyright 2001 National Academy of Sciences, U.S.A. Reproduced from Proceedings of the National Academy of Sciences of the United States of America; 2001, vol. 98, no. 18, pp 10216 – 10266

cytotoxicity, free from the constraints imposed by the use of activating receptors. As γδ TCRs recognize intact antigens directly (reviewed in (Chien, Jores et al. 1996)), this ability could allow γδ IELs to detect infected or diseased cells through the recognition of activation- (Crowley, Fahrer et al. 2000) or stress-induced (Hayday 2000) self antigens. γδ IELs could also recognize and kill pathogens directly [a herpesvirus-specific γδ T cell has been described (Sciammas, Kodukula et al. 1997)]. It is also possible that a different set of effector programs is triggered by TCR engagement. The induction of KGF mRNA (Boismenu and Havran 1994) may be such an example.

Although we do not have any evidence for such new gene expression here in the γδ IELs of *Yersinia*-infected mice, it may be that such genes are below the limits of detection here or are not represented on the arrays. In the case of the MLN $CD8^+$ αβ T cells, where 8% of them are activated in response to the infection, the most clearly up-regulated effector genes are the very abundant ones, which encode components of the cytotoxic granules. Cytokines, which are known to be expressed in activated $CD8^+$ αβ T cells and can detected by sensitive reverse transcription-PCR in this infection system (Kerr 1998), are not detectable above background. In addition, as mentioned above, we do not know what fraction of the γδ IELs for are responding to *Yersinia* antigens or to antigens induced by the infection.

Our earlier studies showed that mice lacking γδ T cells ($TCR\delta^{-/-}$) are much less resistant than either normal mice or mice without αβ T cells ($TCR\beta^{-/-}$) to the early dissemination of *Yersinia*. These findings suggest that γδ IELs are important and functionally distinct from αβ IELs in this infection model. We have tested some of the effector genes that are preferentially expressed in γδ IELs and found that they are similarly expressed in αβ IELs. Similar observations were made from a more extensive serial analysis of gene expression (SAGE) analysis carried out by A. Hayday and colleagues on αβ and γδ IELs isolated from uninfected animals (*A. Hayday, personal communication*). This similarity between αβ and γδ IEL gene expression suggests that the differences between γδ and αβ IELs in contributing to immune competence are most likely because of their differences in antigen recognition (reviewed in (Chien, Jores et al. 1996)) and the functional consequences of such recognition.

Copyright 2001 National Academy of Sciences, U.S.A. Reproduced from Proceedings of the National Academy of Sciences of the United States of America; 2001, vol. 98, no. 18, pp 10216 – 10266

In any event, this approach has allowed us to evaluate many more potential attributes of γδ IELs than previously possible and has provided important insights into their regulation and function.

Copyright 2001 National Academy of Sciences, U.S.A. Reproduced from Proceedings of the National Academy of Sciences of the United States of America; 2001, vol. 98, no. 18, pp 10216 – 10266

Figure Legends

Figure 1.1: γδ IELs express (A) CD69, (B) 2B4, and (C) I-A

IELs were isolated and stained with FITC conjugates of anti-CD69, -2B4, and -I-A (Pharmingen) and phycoerythrin (PE)-conjugated GL3 (anti-δ-TCR) (purified and conjugated to PE according to standard protocols). Cy-chrome-conjugated G235-2356 (anti-2,4,6-trinitrophenol, hamster isotype control) and propidium iodide-positive cells were excluded from analysis.

Supplemental Figure 1.1: Transcripts of γδ T lymphocytes in the intestinal intraepithelial layer (γδ IELs) do not change significantly after *Yersinia* infection but differ from those of mesenteric lymph node (MLN) $CD8^+$ T cells and epithelial cells

Normalized gene expression values of genes expressed in γδ IELs isolated from uninfected animals were compared with those from γδ IELs isolated from infected animals (a), MLN $CD8^+$ αβ T cells isolated from uninfected animals (b), and epithelial cells (c). In each graph, only genes called present in at least one of the two samples are included. All expression values less than 1 were made equal to 1 before representation on the logarithmic plots.

Copyright 2001 National Academy of Sciences, U.S.A. Reproduced from Proceedings of the National Academy of Sciences of the United States of America; 2001, vol. 98, no. 18, pp 10216 – 10266

Table Legends

Table 1.1: Expression levels of genes expressed preferentially by MLN CD8$^+$ αβ T cells (A and B) and of genes upregulated by these cells after *Yersinia* infection (C)

(A) Gene expression values are shown for a partial list of cell surface molecules that are preferentially expressed by MLN CD8$^+$ αβ T cells (αβ T; averaged from all six samples) together with their averaged expression values in γδ IELs (γδ T; averaged from all four samples). Genes called absent are indicated by 'A.'

(B) Gene expression values are shown for signal transduction molecules and transcription factors that are preferentially expressed by MLN CD8$^+$ αβ T cells.

(C) Gene expression values are shown for genes expressed at least two fold higher in cells isolated from *Yersinia*-infected (Inf) as compared to uninfected (Uninf) animals. These genes had to be called present with minimum expression values greater than 30 in at least one of the duplicate samples of αβ T cells isolated from either *Yersinia*-infected mice or from uninfected mice. A comprehensive list, including accession numbers, can be found in *Supplemental Tables 1, 4* and *6*.

Table 1.2: Expression levels of genes expressed preferentially by γδ IELs

A partial list of genes identified as being more abundantly-expressed in γδ IELs than mesenteric lymph node CD8$^+$ αβ T cells by ANOVA. The complete list can be found in *Supplemental Table 5*. Average gene expression values are shown for γδ IELs (γδ T), mesenteric CD8$^+$ αβ T cells (αβ T), and epithelial cells (Epi.). Because the differences in gene-expression between the infected and uninfected samples of either the αβ or the γδ T cells were very small, all four γδ IEL samples were compared against all six CD8$^+$ αβ T cell samples. In all, 235 genes fit the following criteria. These genes (*i*) have a P value $<7.87\text{x}10^{-6}$ (1,206 / 6,352 genes), (*ii*) are more highly expressed in γδ than in the αβ T cells (449 / 1,206 genes), (*iii*) are called "present" or "moderate" in at least two γδ IEL samples (344 / 449 genes), (*iv*) have a difference in median expression of at least 15 between the γδ and αβ T cell samples (246 / 344 genes), and (*v*) show at least a 1.5 fold difference in median expression between the γδ and αβ T cell samples (235 / 246

Copyright 2001 National Academy of Sciences, U.S.A. Reproduced from Proceedings of the National Academy of Sciences of the United States of America; 2001, vol. 98, no. 18, pp 10216 – 10266

genes). To avoid large differences in expression because of negative or very small values in αβ T cell gene expression, all αβ T cell expression values <1 were made equal to 1 before calculating the absolute and fold differences in steps (*iv*) and (*v*).

Supplemental Table 1.1: Cell-surface molecules expressed by MLN CD8$^+$ αβ T cells

Gene expression values of a partial list of cell surface molecules expressed by MLN CD8$^+$ αβ T cells (αβ T; averaged from all six samples), together with their expression values in γδ IELs (γδ T; averaged from all four samples) are shown. Genes called absent are indicated by 'A.'

Supplemental Table 1.2: Fifteen most abundantly-expressed genes of γδ IELs (A), MLN CD8$^+$ αβ T cells (B), and epithelial cells (C)

Gene expression values for the 15 most highly-expressed genes in γδ IELs (γδ T; averaged from all four samples), MLN CD8$^+$ αβ T cells (αβ T; averaged from all six samples), and epithelial cells (Epi) are shown.

Supplemental Table 1.3. Genes up- or down-regulated by γδ IELs after *Yersinia* infection

Gene expression values are shown for genes with 1.4-fold or greater differences in the expression levels identified from γδ IEL samples isolated from uninfected (Un) and *Yersinia*-infected (Inf) animals. To identify genes differentially expressed between γδ IELs from infected and uninfected mice, ANOVA tests were carried out by comparing individual probe pairs from the GeneChip arrays. To be considered differentially expressed, genes had to (*i*) have a P value $<7.87 \times 10^{-6}$ (60 / 6,352 genes met this criterion), (*ii*) be called "present" or "moderate" in at least one γδ IEL sample, according to GeneChip 3.0 software (58 / 60 remaining genes), (*iii*) have an absolute difference in median expression of at least 10 between the two populations from infected and uninfected mice (54 / 58 genes), and (*iv*) exhibit at least a 1.4-fold change between infected and uninfected samples. Of the 6,352 genes tested, 37 met these criteria, 6 being increased after infection and 31 being decreased after infection.

Copyright 2001 National Academy of Sciences, U.S.A. Reproduced from Proceedings of the National Academy of Sciences of the United States of America; 2001, vol. 98, no. 18, pp 10216 – 10266

Supplemental Table 1.4: Genes upregulated by MLN CD8$^+$ αβ T cells following *Yersinia* infection

Gene expression values are shown for genes expressed at least 2-fold higher in cells isolated from *Yersinia*-infected (Inf) as compared to uninfected (Uninf) animals. The criteria were determined as follows: genes had to be called present with minimum expression values greater than 30 in at least one of the duplicate samples of αβ T cells isolated from either *Yersinia*-infected mice or from uninfected mice. The gene expression values of the resulting genes were averaged.

Supplemental Table 1.5: Genes expressed preferentially by γδ IELs

A list of genes identified as being more abundantly expressed in γδ IELs than MLN CD8$^+$ αβ T cells by ANOVA. Average gene expression values are shown for γδ IELs (γδ T), MLN CD8$^+$ αβ T cells (αβ T), and epithelial cells (Epi). Because differences in gene-expression between the infected and uninfected samples of the αβ and γδ T cells were small, all four γδ IEL samples were compared against all six CD8$^+$ αβ T cell samples by ANOVA tests. In all, 235 genes fit the following criteria. These genes (*i*) have a P value <7.87x10^{-6} (1,206 / 6,352 genes), (*ii*) are more highly expressed in γδ than in αβ T cells (449 / 1,206 genes), (*iii*) are called "present" or "moderate" in at least two γδ IEL samples (344 / 449 genes), (*iv*) have a difference in median expression of at least 15 between the γδ and αβ T cell samples (246 / 344 genes), and (*v*) show at least a 1.5-fold difference in median expression between the γδ and αβ T cell samples (235 / 246 genes). To avoid large differences in expression because of negative or very small values in αβ T cell gene expression, all αβ T cell expression values <1 were made equal to 1 before calculating the absolute and fold differences in steps (*iv*) and (*v*).

Supplemental Table 1.6: Signal transduction and transcription factors expressed preferentially by MLN CD8$^+$ αβ T cells

Gene expression values are shown for γδ IELs (γδ T; averaged from all four samples) and MLN CD8$^+$ αβ T cells (αβ T; averaged from all six samples).

Copyright 2001 National Academy of Sciences, U.S.A. Reproduced from Proceedings of the National Academy of Sciences of the United States of America; 2001, vol. 98, no. 18, pp 10216 – 10266

Acknowledgements

This work was supported by grants from the National Institutes of Health (Y.-h.C.) and Howard Hughes Medical Institute (M.M.D.). A.M.F. was supported by a Stanford Dean's fellowship and a Katherine McCormick fellowship. We thank Mamatha Mahatir and Suzanne Ybarra for expert technical advice and Drs. Richard Glynne and Jen-Tsan (Ashley) Chi for helpful discussions.

Copyright 2001 National Academy of Sciences, U.S.A. Reproduced from Proceedings of the National Academy of Sciences of the United States of America; 2001, vol. 98, no. 18, pp 10216 – 10266

Figure 1.1: γδ IELs express (A) CD69, (B) 2B4, and (C) I-A

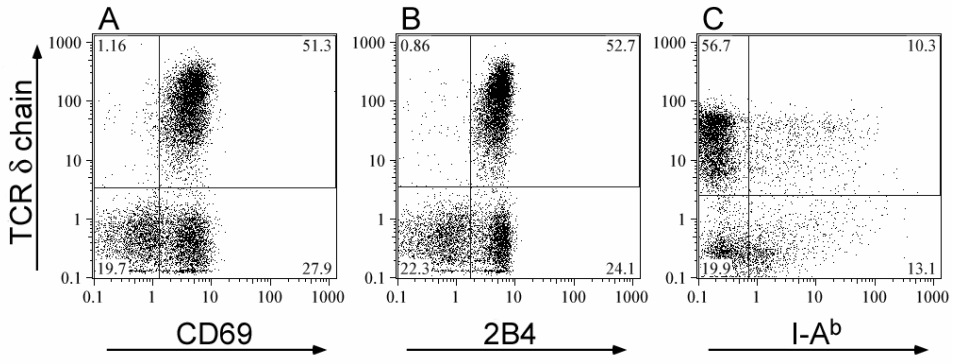

Supplemental Figure 1.1: Transcripts of γδ T lymphocytes in the intestinal intraepithelial layer (γδ IELs) do not change significantly after *Yersinia* infection but differ from those of mesenteric lymph node (MLN) $CD8^+$ T cells and epithelial cells

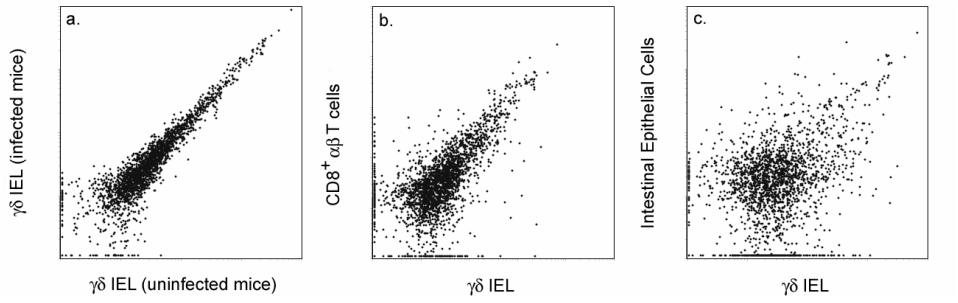

Copyright 2001 National Academy of Sciences, U.S.A. Reproduced from Proceedings of the National Academy of Sciences of the United States of America; 2001, vol. 98, no. 18, pp 10216 – 10266

Table 1.1: Expression levels of genes expressed preferentially by MLN $CD8^+$ αβ T cells (A and B) and of genes upregulated by these cells after *Yersinia* infection (C)

A. Cell-surface molecules

αβ T	γδ T	Description
Cytokine/Chemokine/Similar		
367	A	CCR7
179	A	IL-7 Receptor
115	11	CXCR4
72	A	Thromboxane A2 Receptor
64	A	IL-6 Receptor
54	A	IL-17 Receptor
Other Surface Molecules		
1653	303	pB7
822	64	Thy-1
454	A	Ly-6C
298	A	CD2
264	A	L-Selectin
226	16	CD97
224	26	Lectin L-14
220	A	Ly-6E
164	A	Semaphorin B
148	A	CD5
113	A	CD6
84	A	CD97
63	A	LFA-1
60	12	CD47
50	A	ICAM-2

B. Upregulated following *Yersinia* infection

Uninf.	Inf.	Description
Effector Functions		
139	779	RANTES
A	173	Granzyme A
A	87	Granzyme B
27	71	Flt3 ligand
Activation, Proliferation, Cell Cycle		
153	325	Nucleolin
56	303	Ly-6E
64	114	Proliferation-associated Protein 1 (p38-2G4)
56	108	CDC47
51	99	Pim-2
14	80	CDKN2A/INK4a/MTS1
22	73	Stathmin
21	55	Gamma-Glutamyl transpeptidase (Ggtp)
21	52	Mdm2
Chromosomal Structure		
144	431	HMG2
166	306	HMG14
55	141	HMG17
Protein Synthesis/Degradation/Targeting		
126	214	Proteasome sub., alpha type 2
115	190	Cathepsin S
86	169	Cytosolic Chaperone Containing TCP-1, theta
59	158	Cathepsin D
54	99	Splicing Factor Srp20/X16
54	91	Valosin Containing Protein (VCP)
31	74	Ubiquitin-conjugating Enzyme E2H (E20-20K)
22	60	FXR1
17	52	U2-snRNP b'' (pRNP31), homolog
A	51	Ac39/Physophilin
Surface Molecules		
68	301	Lectin L-14
128	255	CD48
36	85	Galectin-3 (Mac-2)
43	76	Integrin beta-1 subunit
Signal Transduction and Transcription Factors		
50	98	NF-YB
34	81	Maid
41	75	Protein Phosphatase 2A, cat.sub.alpha, hmlg.
36	73	Protein Phosphatase 2A, B'alpha3 reg.sub.
28	55	Protein Phosphatase 2A, cat.sub.beta, hmlg.
39	75	FK506-binding Protein (FKBP-12)
33	74	MyD88
39	68	NFATx/NFAT4/NFATc3

C. Preferentially expressed Signal and Transcription factors

αβ T	γδ T	Description
Signal transduction		
9792	1944	Receptor for Activated C Kinase
199	38	GTPase-activating protein GapIII
134	A	Diacylglycerol Kinase, alpha
117	15	Jak1, homolog
111	A	Diacylglycerol Kinase, alpha
83	A	Dual-specificity phosphatase PAC-1
51	A	Protein Kinase C, theta
Transcription factors		
554	A	Kruppel-like factor LKLF
407	18	SATB1
148	27	RFLAT-1, homolog
144	12	TCF-1
140	A	LEF-1
73	A	Kruppel-like factor 3
60	A	HMG-I(Y)

Copyright 2001 National Academy of Sciences, U.S.A. Reproduced from Proceedings of the National Academy of Sciences of the United States of America; 2001, vol. 98, no. 18, pp 10216 – 10266

Table 1.2: Expression levels of genes expressed preferentially by γδ IELs

γδ T	αβ T	Epi.	Description
Immune defense mediators			
	Cytokines/Chemokines		
3065	566	A	RANTES
215	49	A	Lymphotactin
58	25	A	TIS7/PC4, homolog
39	A	A	MIP-1-alpha
38	A	A	MIP-1-beta
36	A	A	Eta-1
30	A	A	Transforming Growth Factor, beta 3
22	8	A	TIS7/PC4/IFN-related developmental regulator 1
	Cytotoxic Proteins/Related		
2630	116	19	Granzyme A
2117	59	8	Granzyme B
583	258	22	Serglycin
275	A	A	Fas Ligand
222	8	153	Cryptdin
	Enzymes, Inflammation		
174	97	19	Leukotriene A-4 Hydrolase
73	35	40	p47phox
Cholesterol/Lipid biosynthesis and metabolism			
110	A	A	Apolipoprotein E
66	27	A	Farnesyl diphosphate synthase, homolog
65	16	A	Squalene Synthase
61	11	A	Plasma Phospholipid Binding Protein
54	29	A	Acetyl CoA Dehydrogenase, long-chain
51	A	A	LDL Receptor
50	A	A	Squalene Epoxidase
44	23	A	Stearoyl-Coenzyme A desaturase 2
38	A	A	Adipose Differentiation Related Protein
Intestinal function and homeostasis			
289	A	A	Carbonic Anhydrase isozyme II
226	A	A	Fibrinogen-like Protein
152	8	A	Spi2/EB1 Proteinase Inhibitor
116	A	A	Furin
116	59	A	Cystatin 7 (Cst7/leukocystatin)
91	A	A	p6-5 (preproelastase, homolog)
21	A	A	Platelet-activating factor acetylhydrolase, 1b, a1
45	A	91	Monocyte/neutrophil elastase inhibitor, homolog
108	A	111	Serine protease inhibitor, Kazal type 3 (Spink3)
165	14	150	Alcohol dehydrogenase class I (ADH-A-2)
104	A	297	Meprin 1 beta
Cell-surface molecules			
	TCR associated		
726	394	A	CD3-gamma
597	16	17	Fc-epsilon-RI gamma subunit
	NK Activating/Inhibitory Receptors		
182	A	A	NK Cell Receptor 2B4
138	A	A	LAG-3
87	A	A	Ly-49E-GE (Klra5)
58	A	A	NK Cell Receptor gp49B
55	A	13	PD-1/Programmed Cell Death 1
49	A	A	CTLA-4
38	A	A	NK Cell Receptor NKR-P1A
	Cytokine/Chemokine/Similar		
262	46	A	Tumor Necrosis Factor Receptor 2
125	49	100	Tumor Necrosis Factor Receptor 1
225	91	30	Interferon gamma Receptor
209	70	A	Interleukin 2 Receptor, beta chain
31	A	A	Interleukin 12 Receptor, beta 1
40	A	A	L-CCR chemokine receptor
62	A	A	Prostaglandin E Receptor, EP4 subtype

γδ T	αβ T	Epi.	Description
Signal transduction			
1020	A	A	Regulator of G-protein signalling 1 (RGS1)
620	101	77	MAPK phosphatase 1 (3CH134)
337	195	A	Stat3/APRF
271	94	113	Pim-1
185	41	17	A1
155	62	A	SH2 containing inositol-5-phosphatase (Ship)
123	77	A	ASM-like phosphodiesterase 3a
122	14	A	PI-3-kinase, regulatory subunit p85alpha
22	A	A	PI-3-kinase, catalytic subunit, beta, homolog
109	55	A	Rb2/p130
36	A	A	Rb1/p105Rb
105	36	A	TNF receptor-associated factor 5 (Traf5)
98	59	A	Serine/threonine kinase (MAP4K1, homolog)
95	28	A	cAMP-dependent protein kinase, beta-cat. sub.
39	27	A	cAMP-dependent protein kinase, alpha subunit
88	A	A	cAMP-responsive element modulator (CREM)
86	50	A	MAP kinase kinase kinase 1 (Mekk1)
86	41	A	Guanine Nucleotide Binding Protein, alpha 13
66	26	91	Mitogen Activated Protein kinase (erk-1)
61	27	51	Early Growth Response 1 (Egr1/zif/268)
61	17	A	Cytokine-inducible SH2-containing protein (CIS)
57	A	A	Protein Tyrosine phosphatase STEP61
56	14	A	MyD118
23	A	A	Ddit1/Gadd45
56	A	A	c-Fes (tyrosine kinase)
54	26	A	Lithium-sensitive myo-inositol monop'tase A1
52	A	A	Caspase-3/CPP32
52	25	A	Fyn proto-oncogene (Fyn/p59fyn)
48	25	A	Protein Tyrosine kinase, tec type I
38	17	A	G protein gamma-2 subunit, homolog
35	A	45	Phospholipase C beta3
34	A	27	Lyn-B protein tyrosine kinase
Transcription factors			
1251	353	271	ATF-4/CREB2
478	167	A	Id-2
59	11	188	Id
454	233	58	Jun-B
299	171	26	H3 histone, family 3B (H3f3b)
298	125	100	c-Fos
281	80	50	Max/Myn (Myc-associated factor X)
157	49	A	Nur77/N10/NGFI-B
152	99	A	Butyrate Response Factor 1/TIS11
92	26	A	A20/TNF Induced Protein 3
86	14	A	TG Interacting Factor (TGIF)
76	24	A	Gfi-1
70	24	61	Ddit3/Chop-10/Gadd153
68	33	A	General transcription factor IIB (GTF2B), hmlg.
64	31	A	MafK
59	A	104	Kruppel-like factor 4 (gut) (Klf4/Ezf/Zie)
58	A	A	PEBP2a1/PEBP2alphaA/CBFA1
57	30	A	TSC-22-like protein, homolog
51	15	A	X box binding protein-1 (Xbp1)
51	21	36	p45 NF-E2 related factor 2
49	A	A	Son of Sevenless 2
48	A	A	C/EBP beta
48	A	A	Interferon Concensus Sequence Binding Protein
47	A	A	Arylhydrocarbon Receptor
44	A	73	LRG-21
36	A	41	TSC-22
35	18	A	c-Jun
33	A	A	Blimp1

Copyright 2001 National Academy of Sciences, U.S.A. Reproduced from Proceedings of the National Academy of Sciences of the United States of America; 2001, vol. 98, no. 18, pp 10216 – 10266

Supplemental Table 1.1: Cell-surface molecules expressed by MLN $CD8^+$ αβ T cells

αβ T	γδ T	Accession	Description
TCR/associated			
137	15	M26417	T-cell receptor beta, variable 8.3
55	A	X06305	T-cell receptor alpha, variable 8
Cytokine/Chemokine/Similar			
367	A	L31580	chemokine (C-C motif) receptor 7
179	A	M29697	interleukin 7 receptor
115	11	X99581	chemokine (C-X-C motif) receptor 4
72	A	D10849	thromboxane A2 receptor
64	A	X53802	interleukin 6 receptor, alpha
54	A	U31993	interleukin 17 receptor
Other Surface Molecules			
1653	303	M55561	CD52 antigen
822	64	M12379	thymus cell antigen 1, theta
454	A	D86232	lymphocyte antigen 6 complex, locus C
298	A	Y00023	CD2 antigen
264	A	M25324	selectin, lymphocyte
226	16	W20922	CD97 antigen
224	26	W13002	lectin, galactose binding, soluble 1
220	A	X04653	lymphocyte antigen 6 complex, locus A
164	A	X85991	semaphorin 4A
148	A	M15177	CD5 antigen
113	A	U37543	CD6 antigen
84	A	AA118715	CD97 antigen
63	A	M60778	integrin alpha L
60	12	AA072961	CD47 antigen
50	A	AA028405	intercellular adhesion molecule 2

Copyright 2001 National Academy of Sciences, U.S.A. Reproduced from Proceedings of the National Academy of Sciences of the United States of America; 2001, vol. 98, no. 18, pp 10216 – 10266

Supplemental Table 1.2: Fifteen most abundantly-expressed genes of γδ IELs (A), MLN $CD8^+$ αβ T cells (B), and epithelial cells (C)

γδ IELs

γδ T	αβ T	Epi.	Description
6853	15236	3843	Trt (21 kDa)
3795	5230	1547	Ubiquitin
3065	566	A	RANTES
2643	4612	1258	Beta actin
2630	116	19	Granzyme A
2331	3213	369	Prothymosin beta 4
2117	59	8	Granzyme B
1944	9792	192	Gnb2-rs1
1823	2093	726	Ubiquitin C
1321	21	A	TCR gamma chain
1310	2349	100	Ribosomal Protein S16
1290	170	A	CD7
1251	353	271	ATF4
1234	1117	272	Gamma actin
1207	21	12	RGS1

MLN $CD8^+$ αβ T cells

γδ T	αβ T	Epi.	Description
6853	15236	3843	Trt (21 kDa)
1944	9792	192	Gnb2-rs1
1177	6645	133	Ribosomal protein PO
3795	5230	1547	Ubiquitin
2358	5022	1259	Beta actin
1044	4183	108	Ribosomal protein L5
2331	3213	369	Prothymosin beta 4
980	2954	70	Repeat family 3 gene
715	2932	81	Ribosomal protein S5
1115	2777	66	Ribosomal protein L27a
535	2771	32	Ribosomal protein L36
666	2428	115	Ribosomal protein fau
736	2401	48	Ribosomal protein L6
1310	2349	100	Ribosomal protein S16
941	2317	45	Ribosomal protein L3

Epithelial Cells

γδ T	αβ T	Epi.	Description
6853	15236	3843	Trt (21 kDa)
816	A	2670	FABP2, intestinal
79	A	1567	Trefoil factor 3, intestinal
3795	5230	1547	Ubiquitin
2358	5022	1259	Beta actin
109	A	842	CD13/aminopeptidase N
336	372	835	Prothymosin beta 4
153	A	810	FABP1, liver
199	A	749	Apolipoprotein A-I
1823	2093	726	Ubiquitin C
71	A	599	Cytokeratin EndoA
396	427	592	Thioredoxin
493	930	590	ATP synthase, F1, beta
383	128	564	Selenoprotein P
89	2	526	Apolipoprotein A-IV

Copyright 2001 National Academy of Sciences, U.S.A. Reproduced from Proceedings of the National Academy of Sciences of the United States of America; 2001, vol. 98, no. 18, pp 10216 – 10266

Supplemental Table 1.3: Genes up- or down-regulated by γδ IELs after *Yersinia* infection

Genes Upregulated After *Yersinia* Infection

Uninf.	Inf.	Accession	Description
5441	8264	X06407	tumor protein, translationally-controlled 1
445	625	D00472	cofilin 1, non-muscle
111	156	U27340	prosaposin
62	113	AA145371	interferon stimulated gene 12
65	108	L25885	beta-1,4-N-acetylgalactosaminyltransferase
34	48	W40735	EH-domain containing 1

Genes Downregulated After *Yersinia* Infection

Uninf.	Inf.	Accession	Description
972	590	U12236	integrin, alpha E, epithelial-associated
614	337	U58494	Intracisternal A-particle mRNA (5' to IL-3 gene)
451	281	U58888	osteoclast stimulating factor 1
239	137	AA114811	ATP synthase gamma 1 (Atp5c1)
238	160	AA008136	actinin alpha 4
212	139	AA123463	SET translocation
211	130	U09351	signal transducer and activator of transcription 4
203	86	W13875	RIKEN cDNA 2900073G15 gene
181	136	D37837	lymphocyte cytosolic protein 1
172	72	U50413	PI3-kinase, reg. sub., polypeptide 1 (p85 alpha)
164	103	W29730	protein phosphatase 1, cat. sub., alpha isoform
161	86	U10484	lymphoid-restricted membrane protein
135	50	W35962	suppressor of Ty 4 homolog
134	75	W83337	glutathione peroxidase 4
124	53	M60285	CAMP responsive element modulator
121	79	AA152884	DnaJ (Hsp40) homolog, subfamily A, member 1
119	76	AA168184	core promoter element binding protein
111	61	X89749	TG interacting factor
110	57	AA003990	splicing factor, arginine/serine-rich 7
92	57	U41736	ancient ubiquitous protein
75	36	D87990	UDP-galactose translocator 2
75	42	W29669	interferon-related developmental regulator 1
72	32	U54803	caspase 3
63	34	X05719	cytotoxic T-lymphocyte-associated protein 4
57	28	W46019	14-3-3 theta
48	16	AA162093	DEAH (Asp-Glu-Ala-His) box polypeptide 15
46	33	X59421	friend leukemia integration 1
45	19	AA105582	CD53 antigen
39	20	AA008095	general transcription factor II I
34	16	D83585	proteasome (prosome, macropain) sub., beta 7
32	9	D87691	Eukaryotic translation termination factor 1

Copyright 2001 National Academy of Sciences, U.S.A. Reproduced from Proceedings of the National Academy of Sciences of the United States of America; 2001, vol. 98, no. 18, pp 10216 – 10266

Supplemental Table 1.4: Genes upregulated by MLN CD8$^+$ αβ T cells following *Yersinia* infection

Uninf.	Inf.	Accession	Description
Effector Functions			
139	779	U02298	chemokine (C-C motif) ligand 5
A	173	M13226	granzyme A
A	87	X04072	granzyme B
27	71	U29875	FMS-like tyrosine kinase 3 ligand
Activation, Proliferation, Cell Cycle			
153	325	X07699	nucleolin
56	303	X04653	lymphocyte antigen 6 complex, locus A
64	114	U43918	proliferation-associated 2G4
56	108	D26091	minichromosome maintenance deficient 7
51	99	L41495	proviral integration site 2
14	80	D00208	S100 calcium binding protein A4
22	73	AA117100	stathmin
21	55	U30509	gamma-glutamyltransferase 1
21	52	X58876	transformed mouse 3T3 cell double minute 2
26	48	L16462	B-cell leukemia/lymphoma 2 related protein A1a
18	40	AA120142	replication factor C (activator 1) 2
A	38	X82786	antigen identified by monoclonal antibody Ki 67
Chromosomal Structure			
144	431	Z46757	high mobility group protein 2
55	141	X12944	high mobility group protein 17
A	46	X56683	chromobox homolog 3
166	306	X53476	high mobility group protein 14
Protein Synthesis/Degradation/Targeting			
126	214	X70303	proteasome (prosome, macropain) sub., alpha 2
115	190	AA146437	cathepsin S
86	169	Z37164	chaperonin subunit 8 (theta)
59	158	X52886	cathepsin D
54	99	X53824	splicing factor, arginine/serine-rich 3
54	91	Z14044	valosin containing protein
31	74	U19854	ubiquitin-conjugating enzyme E2H
22	60	X90875	fragile X mental retardation gene 1
17	52	AA146248	U2 small nuclear ribonucleoprotein B
A	51	U21549	ATPase, H+transporting, V0 subunit D iso. 1
26	47	AA002605	KDEL ER protein retention receptor 1
22	45	X60831	upstream binding transcr. fact., RNA pol. I
A	42	AA003841	splicing factor 3a, subunit 3
12	42	X56602	interferon, alpha-inducible protein
A	29	U05837	hexosaminidase A

Uninf.	Inf.	Accession	Description
Surface Molecules			
68	301	W13002	lectin, galactose binding, soluble 1
128	255	X17501	CD48 antigen
36	85	X16834	lectin, galactose binding, soluble 3
43	76	Y00769	integrin beta 1
17	40	X69902	integrin alpha 6
Signal Transduction and Transcription Factors			
50	98	X55316	nuclear transcription factor-Y beta
34	81	U50734	cyclin D-type binding-protein 1
41	75	AA116706	protein phosphatase 2a, cat. sub., alpha
39	75	X60203	FK506 binding protein 1a
33	74	X51397	myeloid differentiation primary response gene 88
36	73	U37353	protein phosphatase 2, reg. sub. B, gamma
39	68	U28807	nuclear factor of activated T-cells, cyt. 3
28	55	W82881	protein phosphatase 2a, cat. sub., beta
18	39	X80937	RalA binding protein 1
17	37	AA008566	peptidylprolyl isomerase E
21	36	X71327	metal response element binding TF 1
15	32	L28117	nuclear factor-kappaB p50
Other			
226	448	AA002621	nucleoside diphosphate kinase B
173	388	W34296	split hand/foot deleted gene 1
146	303	D38379	pyruvate kinase, muscle
131	267	AA027404	ATPase, Na+/K+transporting, beta 3
74	159	AA002979	ATPase, Na+/K+transporting, beta 3
53	103	U05809	transketolase
35	98	D10024	annexin A2
42	98	X57024	glutamate dehydrogenase 1
40	93	W99875	M2-type Pyruvate Kinase, homolog
36	73	U14172	eukaryotic translation initiation factor 3, sub. 10
25	63	Z48043	coagulation factor II (thrombin) receptor-like 1
29	60	L32974	IFN-induced prot. w. tetratricopeptide repeats 3
29	58	D88793	cysteine and glycine-rich protein 1
25	51	Z11911	glucose-6-phosphate dehydrogenase X-linked
22	42	U19119	interferon inducible protein 1
A	39	X78874	chloride channel 3
14	34	X97650	myosin IF

Copyright 2001 National Academy of Sciences, U.S.A. Reproduced from Proceedings of the National Academy of Sciences of the United States of America; 2001, vol. 98, no. 18, pp 10216 – 10266

Supplemental Table 1.5: Genes expressed preferentially by γδ IELs (page 1 of 2)

γδ T	αβ T	Epi.	Accession	Description
Immune defense mediators				
Cytokines/Chemokines				
3065	566	A	U02298	chemokine (C-C motif) ligand 5
215	49	A	D43769	chemokine (C motif) ligand 1
58	25	A	W29669	interferon-related developmental regulator 1
39	A	A	M73061	chemokine (C-C motif) ligand 3
38	A	A	M23503	chemokine (C-C motif) ligand 4
36	A	A	X16151	secreted phosphoprotein 1
30	A	A	M32745	transforming growth factor, beta 3
22	8	A	J00424	interferon-related developmental regulator 1
Cytotoxic Proteins/Related				
2630	116	19	M13226	granzyme A
2117	59	8	X04072	granzyme B
583	258	22	X16133	proteoglycan 1, secretory granule
275	A	A	U06948	tumor necrosis factor (ligand) superfamily, 6
222	8	153	M33225	defensin related cryptdin peptide 1
25	A	107	M33226	defensin related sequence cryptdin peptide
22	A	A	X58861	complement component 1, q, alpha
Enzymes, Inflammation				
174	97	19	M63848	leukotriene A4 hydrolase
73	35	40	L11455	neutrophil cytosolic factor 1
Cholesterol/Lipid biosynthesis and metabolism				
110	A	A	D00466	apolipoprotein E
66	27	A	AA036251	farnesyl diphosphate synthetase
65	16	A	D29016	farnesyl diphosphate farnesyl transferase 1
61	11	A	U37226	phospholipid transfer protein
54	29	A	U21489	acetyl-Coenzyme A dehydrogenase
51	A	A	X64414	low density lipoprotein receptor
50	A	A	D42048	squalene epoxidase
44	23	A	M26270	stearoyl-Coenzyme A desaturase 2
38	A	A	M93275	adipose differentiation related protein
22	A	48	AA014996	apolipoprotein B
26	A	40	M13366	glycerol-3-phosphate dehydrogenase 1
35	A	41	AA016485	sulfotransferase family, cytosolic, 2B, 1
38	A	187	W17412	apolipoprotein C-III
44	A	406	U00938	fatty acid binding protein 6, ileal (gastrotropin)
51	A	356	Z22216	apolipoprotein C-II
89	A	526	M64250	apolipoprotein A-IV
101	39	125	D29639	L-3-hydroxyacyl-CoA dehydrogenase
153	A	810	AA087320	fatty acid binding protein 1, liver
199	A	749	X64263	apolipoprotein A-I
816	A	2670	M65034	fatty acid binding protein 2, intestinal
Enzymes, Metabolic				
107	48	282	X53333	triosephosphate isomerase 1
89	34	37	X13752	aminolevulinate, delta-, dehydratase
80	24	29	X64837	ornithine aminotransferase
66	A	101	X63023	cytochrome P450, fam. 3, subfam. a, 13
26	6	A	D50834	cytochrome P450, fam, 4, subfam. b, 1
64	A	85	U16818	UDP glycosyltransferase 1 family, A6
59	25	A	Z14986	S-adenosylmethionine decarboxylase 1
45	A	205	Z13968	creatine kinase, mitochondrial 1, ubiquitous
45	A	129	M74570	aldehyde dehydrogenase fam.1, subfam.A1
36	A	A	U60987	glycerol phosphate dehydrogenase 2, mito.
27	A	30	U27014	sorbitol dehydrogenase 1
138	75	A	W99875	pyruvate kinase 3, homolog
45	A	106	AA023491	amiloride binding protein 1
35	A	A	AA109909	amiloride binding protein 1
27	A	49	J05663	aldo-keto reductase family 1, member B7
Enzymes, Nucleotide metabolism				
93	32	218	M10319	adenosine deaminase
46	22	A	X56548	purine-nucleoside phosphorylase
65	24	99	X75129	xanthine dehydrogenase
44	13	A	L12059	CD73 5' nucleotidase, ecto

γδ T	αβ T	Epi.	Accession	Description
Intestinal function and homeostasis				
289	A	A	K00811	carbonic anhydrase 2
226	A	A	M16238	fibrinogen-like protein 2
152	8	A	M64085	serine proteinase inhibitor, clade A, 3G
116	A	A	L26489	furin
116	59	A	AA089339	cystatin F (leukocystatin)
91	A	A	M27347	elastase 1, pancreatic
21	A	A	U57746	PAF acetylhydrolase, 1b, a1
23	A	42	L19932	transforming growth factor, beta induced
45	A	91	AA145127	serine proteinase inhibitor, clade B, 1a
108	A	111	AA106468	serine protease inhibitor, Kazal type 3
165	14	150	M22679	alcohol dehydrogenase 1 (class I)
104	A	297	L15193	meprin 1 beta
79	A	1567	D38410	trefoil factor 3, intestinal
Cell-surface molecules				
TCR/associated				
1321	21	A	M12836	T cell receptor gamma chain, constant 2
740	11	A	L36135	T cell receptor delta chain, constant
71	18	A	AA118701	T cell receptor delta chain, variable
62	A	A	AA119287	T cell receptor delta chain, variable
726	394	A	Y00635	CD3 antigen, gamma polypeptide
597	16	17	W41745	Fc receptor, IgE, high affinity I, gamma
NK Activating/Inhibitory Receptors				
182	A	A	L19057	CD244 natural killer cell receptor 2B4
138	A	A	X98113	lymphocyte-activation gene 3
87	A	A	U10091	killer cell lectin-like receptor, subfamily A, 5
58	A	A	U05265	leukocyte Ig-like receptor, subfamily B, 4
55	A	13	X67914	programmed cell death 1
49	A	A	X05719	cytotoxic T-lymphocyte-associated protein 4
38	A	A	M77753	killer cell lectin-like receptor subfamily B, 1A
Cytokine/Chemokine/Similar				
262	46	A	M59378	TNF receptor beta chain
125	49	100	X57796	TNF receptor alpha chain
225	91	30	J05265	interferon gamma receptor 1
209	70	A	M28052	interleukin 2 receptor, beta chain
31	A	A	U23922	interleukin 12 receptor, beta 1
40	A	A	AA034646	chemokine (C-C motif) receptor-like 2
62	A	A	D13458	prostaglandin E receptor 4 (subtype EP4)
Other Surface Molecules				
1290	170	A	D31956	CD7 antigen
781	152	14	U12236	integrin, alpha E, epithelial-associated
335	111	62	U25708	CD98 antigen
268	69	304	X16834	lectin, galactose binding, soluble 3
177	A	280	M76124	tumor-associated calcium signal transducer 1
166	A	A	Y00864	kit oncogene
109	A	842	U77083	CD13
96	50	A	L22143	insulin-like growth factor 2 receptor
85	27	A	X55184	ATPase, H+ transp., lysosomal V0 sub. a 2
81	16	A	M33581	ATP-binding cassette, sub-family B, 1A
79	35	A	U39827	G-protein coupled receptor 65
74	35	61	W08454	transmembrane 4 superfamily member 8
65	A	268	V01527	histocompatibility 2, class II antigen A, beta 1
64	A	144	J04634	lymphocyte antigen 64
62	A	35	X60961	cadherin 1
61	33	A	U07890	flotillin 2
47	A	38	M29961	glutamyl aminopeptidase
38	A	6	AA008624	integrin alpha-1, homolog
27	4	11	AA170355	integrin alpha X
23	A	A	L11332	CD38 antigen
Protein Processing/Related				
278	175	30	D78645	heat shock 70kD protein 5
151	85	266	J05185	prolyl 4-hydroxylase, beta polypeptide
107	21	A	AA144887	cathepsin C
72	24	79	U51014	peptidase 4
66	35	A	AA124985	insulin degrading enzyme
42	A	A	X92523	calpain 3
33	13	37	X59379	amyloid beta (A4) precursor protein
63	34	A	U10119	vacuolar protein sorting 4b
56	35	29	D87990	UDP-galactose translocator 2
54	A	A	M85153	glycoprotein galactosyltransferase alpha 1, 3
22	A	A	X93999	sialyltransferase 7B

Copyright 2001 National Academy of Sciences, U.S.A. Reproduced from Proceedings of the National Academy of Sciences of the United States of America; 2001, vol. 98, no. 18, pp 10216 – 10266

Supplemental Table 1.5: Genes expressed preferentially by γδ IELs (page 2 of 2)

γδ T	αβ T	Epi.	Accession	Description
Transcription factors				
1251	353	271	M94087	activating transcription factor 4
478	167	A	M69293	inhibitor of DNA binding 2
59	11	188	M31885	inhibitor of DNA binding 1
454	233	58	J03236	Jun-B oncogene
299	171	26	X13605	H3 histone, family 3B
298	125	100	V00727	FBJ osteosarcoma oncogene
281	80	50	M63903	Max protein
27	A	36	X83106	Max dimerization protein
157	49	A	X16995	nuclear receptor subfamily 4, group A, 1
152	99	A	M58566	zinc finger protein 36, C3H type-like 1
92	26	A	U19463	TNF alpha-induced protein 3
86	14	A	X89749	TG interacting factor
76	24	A	U78312	growth factor independent 1
70	24	61	X67083	DNA-damage inducible transcript 3
68	33	A	AA023287	general transcription factor IIB
64	31	A	D42124	nuclear factor, erythroid derived 2, ubiquitous
59	A	104	U70662	Kruppel-like factor 4 (gut)
58	A	A	D14636	runt related transcription factor 2
57	30	A	AA015076	TSC22-related inducible leucine zipper 2
51	15	A	AA016424	X-box binding protein 1
51	21	36	U20532	nuclear factor, erythroid derived 2, like 2
49	A	A	Z11664	son of sevenless homolog 2
48	A	A	X62600	CCAAT/enhancer binding protein, beta
48	A	A	M32489	IFN consensus sequence binding protein 1
47	A	A	D38417	aryl-hydrocarbon receptor
44	A	73	U19118	activating transcription factor 3
36	A	41	X62940	TGF beta 1 induced transcript 4
35	18	A	J04115	Jun oncogene
33	A	A	U08185	B lymphocyte induced maturation protein
20	A	A	U16322	transcription factor 4
19	A	A	X76654	nuclear receptor subfamily 2, grp. F, 6
Signal transduction				
1207	21	A	AA154742	regulator of G-protein signaling 1
1020	A	A	AA138863	regulator of G-protein signaling 1
620	101	77	X61940	dual specificity phosphatase 1
479	308	27	M90388	protein tyrosine phosphatase, non-receptor 8
337	195	A	U08378	stat3
271	94	113	M13945	proviral integration site 1
185	41	17	L16462	B-cell leukemia/lymphoma 2 related prot. A1a
155	62	A	U52044	inositol polyphosphate-5-phosphatase D
123	77	A	Y08135	sphingomyelin P'diesterase, acid-like 3A
122	14	A	U50413	PI3-kinase, regulatory subunit, 1
22	A	A	AA111021	PI3-kinase, catalytic subunit, beta
109	55	A	U36799	retinoblastoma-like 2
36	A	A	M26391	retinoblastoma 1
105	36	A	D78141	TNF receptor-associated factor 5
98	59	A	Y09010	hematopoietic progenitor kinase 1
95	28	A	X61434	protein kinase, cAMP dep., catalytic, beta
39	27	A	M19960	protein kinase, cAMP dep., catalytic, alpha
88	A	A	M60285	cAMP responsive element modulator
86	50	A	L13103	MEK kinase
86	41	A	M63660	guanine nucleotide binding protein, alpha 13
66	26	91	Z14249	mitogen activated kinase 3
61	27	51	M22326	early growth response 1
61	17	A	D31943	cytokine inducible SH2-containing protein
57	A	A	U28217	protein tyrosine P'tase, non-receptor 5
56	14	A	X54149	gadd45 beta
23	A	A	L28177	gadd45 alpha
56	A	A	X12616	feline sarcoma oncogene
54	26	A	AA124192	inositol (myo)-1(or 4)-monophosphatase 1
52	A	A	U54803	caspase 3
52	25	A	U70324	Fyn proto-oncogene
48	25	A	X55663	cytoplasmic tyrosine kinase, Dscr28C related
38	17	A	W83658	G protein gamma 2
35	A	45	U43144	phospholipase C, beta 3
34	A	27	M57696	Lyn protein tyrosine kinase
24	A	A	W82116	death-associated kinase 2
20	A	A	L20899	Ras guanine release factor beta

γδ T	αβ T	Epi.	Accession	Description
Cytoskeletal				
158	77	245	D10024	annexin A2
71	A	599	X12789	keratin complex 2, basic, gene 8
59	27	A	X97650	myosin IF
56	8	63	X59990	catenin alpha 1
55	38	A	AA032596	kinesin 2
50	A	196	M98454	villin 1
41	A	A	U04354	scinderin
39	A	A	X61452	septin 4
29	A	33	U49739	myosin VI
RNA-related				
213	111	32	M38381	CDC-like kinase 1
186	141	247	–	18SRNAMur-3
153	93	18	AA008245	poly(A)-binding protein, cytopl. pseudo.
103	53	A	D78135	cold inducible RNA binding protein
82	46	A	M12130	RNA polymerase II 1
82	21	25	W90866	elongation factor 2 (ef-2), homolog
71	30	A	U75680	stem-loop binding protein
47	32	A	D83033	zinc finger, matrin-like
40	15	A	AA125097	ribonucleoprotein H3, homolog
40	27	A	W82026	RNA binding motif, single strand. interact. 2
Other				
647	79	A	M64292	B-cell translocation gene 2, anti-proliferative
74	40	A	Z72000	B-cell translocation gene 3
383	128	564	X99807	selenoprotein P, plasma, 1
275	A	375	D13509	pancreatitis-associated protein
215	92	39	U37351	cyclin L2
204	59	211	X61433	ATPase, Na+/K+ transporting, beta 1
124	41	A	U10484	lymphoid-restricted membrane protein
120	A	189	D14010	regenerating islet-derived 1
97	A	421	AA123026	regenerating islet-derived 3 gamma
101	A	196	AA064246	solute carrier family 5, member 1
36	A	75	W18827	solute carrier family 5, member 1
128	47	A	L04961	inactive X specific transcripts
119	51	43	M96823	nucleobindin 1
95	41	A	U42386	fibroblast growth factor inducible 14
78	40	100	U53591	Fau-ps3 retropseudogene
72	11	35	M55154	transglutaminase 2, C polypeptide
68	26	A	D00812	replication protein A2
53	29	A	AA114648	T-cell, immune regulator 1
44	21	16	D13003	reticulocalbin 1
41	14	A	W40735	EH-domain containing 1
37	A	23	U68064	ceroid lipofuscinosis, neuronal 3, juvenile
35	19	A	X17459	RBP-J kappa
27	A	15	M32032	selenium binding protein 1
25	A	86	M32240	peripheral myelin protein
24	A	68	U00478	deoxyribonuclease I
32	A	A	M34897	ecotropic viral integration site 2a
29	A	A	M11024	Endogenous mammary tumor virus (MMTV)
82	41	A	AA154451	replication protein A1

Copyright 2001 National Academy of Sciences, U.S.A. Reproduced from Proceedings of the National Academy of Sciences of the United States of America; 2001, vol. 98, no. 18, pp 10216 – 10266

Supplemental Table 1.6: Signal transduction and transcription factors expressed preferentially by MLN $CD8^+$ αβ T cells

γδ T	αβ T	Accession	Description
Signal transduction			
1944	9792	X75313	G protein, beta polypeptide 2-like 1
38	199	U20238	RAS p21 protein activator 3
A	134	AA066032	diacylglycerol kinase, alpha
15	117	AA066354	janus kinase 1
A	111	AA110453	diacylglycerol kinase, alpha
A	83	L11330	dual specificity phosphatase 2
A	51	D11091	protein kinase C, theta
Transcription factors			
A	554	U25096	Kruppel-like factor 2 (lung)
18	407	U05252	special AT-rich sequence binding protein 1
27	148	AA015486	Kruppel-like factor 13
12	144	X61385	transcription factor 7, T-cell specific
A	140	D16503	lymphoid enhancer binding factor 1
A	73	U36340	Kruppel-like factor 3 (basic)
A	60	J04179	high mobility group AT-hook 1

Copyright 2001 National Academy of Sciences, U.S.A. Reproduced from Proceedings of the National Academy of Sciences of the United States of America; 2001, vol. 98, no. 18, pp 10216 – 10266

Chapter 2: Antigen-Specific γδ Intraepithelial Lymphocyte Responses

Introduction

The results from Chapter 1 implied, first, that γδ IELs constitutively express genes that are normally expressed by activated T cells, such as those coding for Granzymes A and B, second, that γδ IELs do not drastically change the genes they express in the presence of *Yersinia* and, third, that γδ IELs differ from activated MLN CD8αβ$^+$ αβ T cells in the expression or lack of expression of some genes. Around the same time, Adrian C. Hayday's group found that CD8αα$^+$ αβ IELs and CD8αα$^+$ γδ IELs exhibited very few differences in gene expression (Shires, Theodoridis et al. 2001). This suggested that a difference between γδ and αβ IELs is important in delaying the dissemination of *Yersinia* and that this difference may be the γδ TCR.

In order to study the responses of γδ IELs to the recognition of γδ TCR ligands it is possible to use mice that are transgenic for γδ TCRs that recognize known ligands. Although the scope of such ligands is still unknown, the MHC class Ib molecules T10 and T22 have been found to be recognized by two separate γδ TCRs, G8 and KN6 (Bluestone, Cron et al. 1988; Bonneville, Ito et al. 1989; Crowley, Reich et al. 1997), and γδ T cells in normal mice appear to recognize these molecules based on tetramer staining experiments (Crowley, Fahrer et al. 2000). The G8 γδ TCR was originally derived from the G8 γδ T cell clone (Houlden, Matis et al. 1989) that was obtained by first immunizing BALB/c *nu/nu* mice with irradiated B10.BR splenocytes (Matis, Cron et al. 1987). G8 mice are transgenic for the G8 γδ TCR (Dent, Matis et al. 1990) that has been shown to recognize T10^b with the relatively high affinity of 0.13 μM (Crowley, Fahrer et al. 2000) and G8 γδ T cells can be stimulated by T10/T22^{b,k} but not by T10^d.

I compared the genes G8 γδ IELs express immediately following isolation to the genes they express after 2 days of *in vitro* coculture with T10/T22^b-expressing splenocytes. Amazingly, the genes expressed by freshly-isolated G8 γδ IELs did not change much after two days of coculture. In addition, freshly-isolated G8 γδ IELs expressed similar genes to the ones previously identified using the *Yersinia* infection model and also appeared to be constitutively transcribing genes associated with effector functions. Thus, γδ IELs always appear to constitutively transcribe genes associated with

effector functions and may regulate their function at the level of translation and/or secretion as opposed to transcription. That way, they may be able to respond quickly to activating signals, but in a controlled manner.

Materials and Methods

Mice

G8 BALB/c mice were maintained by crossing G8 BALB/c mice with BALB/c mice. G8 BALB/c mice were crossed with $RAG2^{KO}$ BALB/c mice from Taconic (C.129S6(B6)-$Rag2^{tm1Fwa}$ N12) to generate G8 $RAG2^{KO}$ BALB/c mice that were maintained by crossing with $RAG2^{KO}$ BALB/c mice. $H2^{b/d}$ BALB/c mice were produced by crossing *b* haplotype-expressing BALB.B mice from Harlan with BALB/c mice.

Screening for G8 Transgenic Mice

Approximately four copies of the rearranged γ and δ chains are co-integrated into the genome of G8 mice (Dent, Matis et al. 1990). For this reason, mice were screened by genomic PCR with primers for the rearranged V-D and J segments of the δ chain. The expected PCR product had a size of only 71 bp and the primer sequences were as follows (5'->3'):

G8-VD-71:	TAC	TTC	TGT	GCT	GCT	GAC	ACG
G8-J-71:	CCA	AAG	ACG	AGT	TTG	TCG	GTA

The initial denaturing was carried out for 10 minutes at 94°C. 34 cycles were performed using 1 minute 94°C denaturing, 1 minute 55°C annealing, and 2 minute 72°C elongating steps. The final elongation was performed at 72°C for an additional 10 minutes.

Isolation of γδ IELs and Splenocytes

IELs were isolated from the small intestine of a G8 $RAG2^{KO}$ BALB/c mouse based on a published protocol (Mosley and Klein 1992) except that the nylon wool and Percoll fractionation steps were omitted. This resulted in a mixture of IELs and epithelial cells. IELs were then enriched as follows. Cells were resuspended in media

supplemented with 5 mM EDTA (M+E) in order to prevent clumping, because E-Cadherin/E-Cadherin interactions are dependent on divalent cations. Cells from one intestine were blocked on ice for 20 minutes with 1 ml M+E containing 20 μg of FcBlock (clone 2.4G2, BD Biosciences Pharmingen). Thereafter, 1 ml of M+E containing 20 μg of biotinylated anti-CD69 antibody (clone H1.2F3, BD Biosciences Pharmingen) was added to the mixture for an additional 30 minutes on ice. After the stain, the cells were washed twice with M+E, resuspended with 200 μl of anti-biotin MACS microbeads (Miltenyi Biotec) and 800 μl of M+E, and incubated at 4°C for 15 minutes. The cells were washed once with M+E, resuspended in 2 ml of M+E, and passed through an LS column (Miltenyi Biotec) in the absence of a magnet to remove adherent cells. IELs were obtained by enriching for cells that remained bound in the column in the presence of a magnetic field using two sequential LS columns and the manufacturer's recommended protocol. IELs were then washed three times in media without EDTA and resuspended at a concentration of 10^7 cells/ml.

Splenocytes were obtained from G8 RAG2^{KO} BALB/c mice and H2$^{b/d}$ BALB/c mice using standard isolation procedures and resuspended at concentrations of 10^7 cells/ml.

In Vitro γδ T cell Activation and RNA Isolation

Either G8 RAG2^{KO} BALB/c γδ IELs or splenocytes were combined in a 1:5 ratio with H2$^{b/d}$ BALB/c splenocytes and were cocultured at 37°C for 2 days in RPMI supplemented with 10% FCS, β-ME, glutamine, antibiotics and sodium pyruvate. Immediately after the γδ IEL isolation, 10^7 cells were dissolved in 1 ml of Trizol (Invitrogen) and frozen at -80°C for later analysis. After 2 days, the cells in the two cultures were stained with APC-labeled antibodies to the δ chain of the γδ TCR (clone GL3) and to Vγ2 (clone UC3-10A6), FITC-labeled antibodies to T10/T22 (clone 7H9), PE-labeled antibodies to CD69 (clone H1.2F3), and Cy7PE-labeled antibodies to B220 (clone RA3-6B2). Splenic γδ T cells and γδ IELs were enriched by using anti-APC MACS microbeads (Miltenyi) where the cells that bound to two sequential LS columns in magnetic fields were dissolved in 1 ml of Trizol after removing aliquots for analysis by

flow cytometry. RNA was isolated from all three samples, converted into RNA probes using the standard Affymetrix protocol, and hybridized to Affymetrix Mouse Expression Set 430 GeneChips.

Results and Discussion

The Activation of γδ IELs

Because γδ TCR ligands for the majority of γδ IELs are not known, it was necessary to use a system where the γδ IELs expressed a γδ TCR that was specific for a known γδ TCR ligand. For this reason, G8 RAG2^{KO} BALB/c mice, which lack αβ T cells and B cells, were used. These mice contain γδ T cells that can be activated through their recognition of the MHC class Ib molecules T10 and T22 of the *b*, but not of the *d*, haplotype.

IELs in normal mice and G8 RAG2^{KO} BALB/c mice were found to express low levels of CD69. This was also the case for the IELs of OT-I RAG2^{KO} C57Bl/6 mice in the absence of an activating peptide like SIINFEKL, suggesting that the expression of CD69 by IELs can be due to factors other than the recognition of agonist TCR ligands.

Thus, IELs were isolated based on their expression of CD69 because the isolation of γδ IELs based on their expression of γδ TCRs may lead to the unintended activation of these cells – especially, when coupled with the addition of magnetic beads that can bind to more than one anti-γδ TCR antibody. This resulted in a high purity of γδ IELs. 80% of cells enriched during the IEL isolation were alive and 95% of these cells expressed the γδ TCR, although, 1.5% of theses cells did not express the α_E integrin that is an adhesion molecule characteristic of IELs. Approximately 96% of living cells expressed the α_E integrin and not all of these expressed the γδ TCR, suggesting that there were some α_E-expressing CD69$^+$ cells that were not γδ T cells. Strangely, the majority of isolated IELs did not appear to express CD8α, which was not the case for the IELs of an OT-I RAG2^{KO} C57Bl/6 mouse that expressed very high levels. RNA was prepared from some of the G8 γδ IELs immediately after isolation in order to determine the transcripts that are normally expressed by these cells.

In order to activate γδ IELs, these cells were cocultured with a 5-fold excess of T10/T22^b-expressing splenocytes for 2 days. 2 days of activation were used because this provides for sufficient time for activation and because surface TCR levels after one day of activation are very low and sometimes undetectable for splenic γδ T cells. In order to

compare γδ IELs to γδ T cells of the central immune system, splenocytes from G8 RAG2^{KO} BALB/c mice were also cocultured with T10/T22^{b}-expressing splenocytes for 2 days.

Following the 2 day cocultures, the production of additional RNA was observed. 0.24 pg/cell of RNA from 10^7 freshly-isolated γδ IELs (2.4 μg), 0.62 pg/cell of RNA from 5.4x10^6 2 day-activated IELs (3.3 μg), and 1.9 pg/cell of RNA from 1.4x10^6 2 day-activated splenic γδ T cells (2.6 μg) was obtained. Thus, the total RNA of activated IELs was about twice that of freshly-isolated IELs and activated splenic γδ T cells expressed even more. In addition, the 5.4x10^6 activated IELs resulted from about 4x10^6 input IELs so some cell division appeared to have taken place.

The coculture also led to pronounced blasting, an increase in granularity, the expression of activation markers, and the expression of IFNγ. B220 may be an activation marker of γδ IELs (Guehler, Bluestone et al. 1996) and B220 was expressed on the γδ IELs following two days of activation. As expected, B220 was not expressed on activated splenic γδ T cells. In addition, both γδ IELs and splenic γδ T cells expressed elevated levels of T10/T22 and high levels of CD69 after activation. However, in the absence of ligand-expressing splenocytes, γδ IELs lost their expression of CD69 and RNA levels were not above background levels. In order to determine if there were any changes to the transcripts expressed by γδ IELs after activation and to see if these differed from those of activated splenic γδ T cells, microarray analyses of the isolated RNAs were performed.

The Activation of IELs through Their TCRs has Little Effect on Their Transcripts

The previous *Yersinia* microarray experiments showed that, based on the genes expressed by γδ IELs in conventional mice, γδ IELs are constitutively activated. Adrian C. Hayday's group reached similar conclusions through SAGE analysis and found that transcripts for Granzymes A and B and the chemokine RANTES comprise about 3% of IEL mRNA (Shires, Theodoridis et al. 2001). The analysis of the freshly-isolated G8 RAG2^{KO} BALB/c γδ IEL mRNA showed that these IELs did not differ much from what was observed in IELs during the *Yersinia* microarray experiments (*Tables 2.1* and *2.2*).

In terms of immune defense mediators, transcripts for MIP-1α/CCL3, MIP-1β/CCL4, RANTES/CCL5, Lymphotactin/XCL1, TGFβ, Granzyme A, Granzyme B, Serglycin/Prg1, Fas ligand/Tnfsf6, Leukotriene A4 hydrolase and various Defensins were observed. In terms of proteins associated with intestinal function and homeostasis, transcripts for Carbonic anhydrase 2, Fibrinogen-like protein 2, Furin, Cystatin F and Alcohol dehydrogenase 1 were observed. In terms of cell-surface molecules, transcripts for CD3γ, FcεRI γ subunit, 2B4/CD244, Lag3/CD223, Glycoprotein 49B/Lilrb4, CTLA-4/CD152, Tnfrsf1a, Tnfrsf1b, IFNγR1, IL-12Rβ1 and β2 and Prostaglandin E receptor, EP4 subtype were observed. Overall, the genes expressed by the IELs of G8 $RAG2^{KO}$ BALB/c mice indicated that, even in the apparent absence of stimulatory TCR ligands, IELs express genes that are consistent with their being in a state of constitutive activation.

Following 2 days of activation, γδ IELs and splenic γδ T cells were found to express a large number of genes differentially (*Figure 2.1A*). Surprisingly, freshly-isolated IELs and 2 day-activated IELs exhibited almost no major differences in gene expression as indicated by the tighter diagonal (*Figure 2.1B*) and suggested that there was little to no serum response (Iyer, Eisen et al. 1999), little to no response to the recognition of TCR ligands, and little to no response to two days of culture. The changes that were observed suggested that the function of IELs may be to protect against epithelial cell damage and bacteria.

Along those lines, the expression of Claudin 3 was induced after activation. This protein is important in the remodeling of tight junctions and suggests that IELs may help mend holes in the epithelial barrier. Transcripts encoding the secreted proteins RegIIIβ/Pap and RegIIIγ, which appear to have growth stimulating effects, and transcripts encoding Trefoil factor 3, which is a peptide that is important in repairing the epithelial barrier, were also increased.

Transcripts for antibacterial proteins were also upregulated. These included those coding for Lysozyme and the Defensin-related cryptdins 5 and 6. The expression of these genes appeared to be specific to γδ T cells in the IEL compartment and additional related genes were also preferentially-expressed by γδ IELs but were not upregulated after activation.

The expression of Trefoil factor 3 and antibacterial proteins has commonly been attributed to goblet cells and Paneth cells, respectively. However, antibodies to Trefoil factor 3 were observed to stain IEL-like cells in the days following the administration of methotrexate to rats (Verburg, Renes et al. 2002). It has been reported that cells other than Paneth cells are stained by an antibody to Lysozyme where this staining was attributed to background staining (Ariza, Lopez et al. 1996). In addition, cryptdin mRNA could be detected inside the villi of 24 day-old mice (Ouellette, Greco et al. 1989), an age where many IELs are $B220^{+}$. It will be necessary to analyze the expression of these genes in sorted IELs in order to be sure that IELs are responsible for the observed expression of antibacterial and protective proteins.

Regardless, IELs show very few changes to their transcripts following activation that includes two days of *in vitro* culture, which exposes them to an environment that is quite unlike that of the small intestine. This reinforces the idea that IELs are, at all times, ready to act. Whether this still requires translation or whether the majority of the proteins are already synthesized remains to be seen. If IEL function is translation-dependent, then it will be important to understand the kinetics thereof following TCR-dependent and TCR-independent types of activation.

Autoreactive IELs May Be Disarmed

The *Yersinia* experiments indicated that the γδ IELs expressed reduced levels of certain signaling molecules and transcription factors. However, the G8 $RAG2^{KO}$ BALB/c γδ IEL activation data showed that transcripts for Janus kinase 1, Diacylglycerol kinase alpha, Dual specificity phosphatase 2, and Receptor for activated C kinase were present in freshly-isolated γδ IELs while transcripts for Protein Kinase C theta were still absent (*Table 2.1*). In addition, it has been reported that autoreactive IELs are not deleted but that their ability to respond at all to TCR signals may be lost or reduced (Barrett, Tatsumi et al. 1993; Guehler, Finch et al. 1998). This suggests that these differences in expression between γδ IELs of normal mice and γδ IELs of G8 $RAG2^{KO}$ BALB/c mice may be behind the unresponsiveness towards TCR ligands that has been reported in Thy-1^{-} $CD8\alpha\alpha^{+}$ αβ IELs (Viney and MacDonald 1992; Siebrecht, Hsia et al. 1993). Because

G8 BALB/c mice that have been crossed onto *b* haplotype-expressing backgrounds, such as BALB.B, still contain IELs, it will be interesting to see if their γδ IELs lack the expression of some signaling molecules that are found in the γδ IELs of G8 BALB/c mice.

Conclusion

Cumulatively, the γδ IEL microarray experiments show that γδ IELs do not appear to respond to *Yersinia* infection or to γδ TCR ligation by profoundly changing the transcripts they express and raise the original question of why there is a difference between the dissemination of *Yersinia* in wild-type C57Bl/6 mice and TCR δ chain-deficient mice. First, this may be due to the activation of only a small fraction of γδ IELs where their transcriptional changes would go unnoticed amidst the transcripts of the other γδ IELs. However, even γδ TCR ligation does not lead to large transcriptional changes. Second, this may be due to differences in translation following the recognition of γδ TCR ligands, which would be helpful if a cell had to respond quickly to a stimulus. Third, this may be due to the mere presence of γδ T cells in mice before and/or during *Yersinia* infection. It has been found that mice deficient in αβ T cells show both an enhanced expression of autoreactive antibodies and larger percentages of antibodies that are of the T cell-dependent IgG and IgE isotypes compared to normal mice (Wen, Roberts et al. 1994). In addition, some γδ T cells in normal mice express proteins that are consistent with these cells having been activated at some point. Thus, γδ T cells may influence the function and development of epithelial cells (Komano, Fujiura et al. 1995), B cells and other cells of the immune system that could then slow the dissemination of *Yersinia* in the first few days after infection.

Figure Legends

Figure 2.1: Activated IELs and splenic γδ T cells show differences in gene expression while TCR-mediated IEL activation only leads to minor changes in gene expression

Gene expression levels were analyzed for freshly-isolated γδ IELs from a G8 RAG2^{KO} BALB/c mouse and splenic γδ T cells and γδ IELs from a G8 RAG2^{KO} BALB/c mouse that had been cocultured for 2 days with γδ TCR ligand-expressing H2$^{b/d}$ BALB/c splenocytes. Transcripts that were called "present" in at least one of the three samples are represented in the graphs. (A) A comparison between gene expression levels in the 2 day-activated splenic γδ T cell and γδ IEL samples is shown. (B) A comparison between the gene expression levels in the freshly-isolated and the 2 day-activated γδ IEL samples is shown.

Table Legends

Table 2.1: Expression levels of genes expressed preferentially by MLN CD8$^+$ αβ T cells

Gene expression values are shown for signal transduction molecules and transcription factors that had been identified as being preferentially expressed by MLN CD8$^+$ αβ T cells (αβ T; averaged from all six samples) compared to γδ IELs (γδ T; averaged from all four samples) in Chapter 1 using the Affymetrix Murine Genome 6500 set. Values from 2 day-activated IELs (act IEL), freshly-isolated IELs (iso IEL), and 2 day-activated splenic γδ T cells (S. γδ T) have been added as well as their probe set numbers in the newer Affymetrix Mouse Expression Set 430. Transcripts in the *Yersinia* experiments that were called absent are indicated by 'A'. Transcripts called absent also have their expression values shaded gray.

Table 2.2: Expression levels of genes expressed preferentially by γδ IELs

Average gene expression values are shown for genes that had been identified as being preferentially expressed by γδ IELs (γδ T) compared to MLN CD8$^+$ αβ T cells (αβ T) in Chapter 1 using the Affymetrix Murine Genome 6500 set. Expression levels in epithelial cells (Epi.) are also shown. In addition, values from 2 day-activated IELs (act IEL), freshly-isolated IELs (iso IEL), and 2 day-activated splenic γδ T cells (S. γδ T) have been added as well as their probe set numbers in the newer Affymetrix Mouse Expression Set 430. Transcripts in the *Yersinia* experiments that were called absent are indicated by 'A'. Transcripts called absent also have their expression values shaded gray.

Figure 2.1: Activated IELs and splenic γδ T cells show differences in gene expression while TCR-mediated IEL activation only leads to minor changes in gene expression

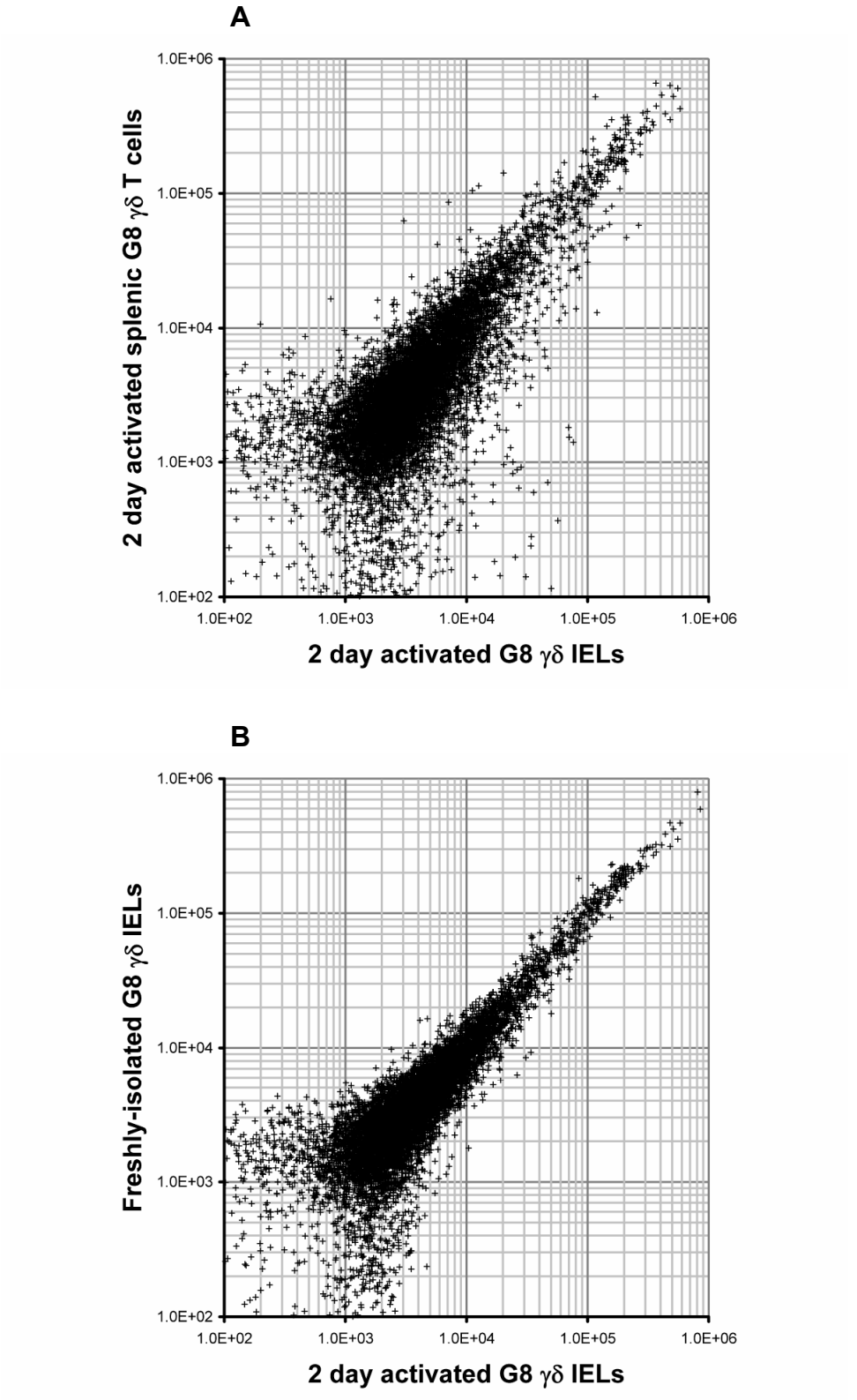

Table 2.1: Expression levels of genes expressed preferentially by MLN $CD8^+$ αβ T cells

Signal transduction

αβ T	γδ T	act IEL	iso IEL	S. γδ T	Description	Probe set
9792	1944	272616	292035	299127	Gnb2-rs1 (receptor of activated prot. kinase C)	1455168_a_at
199	38	699	846	1833	Rasa3 (RAS p21 protein activator 3/GapIII)	1415850_at
134	A	19417	15144	9021	Dgka (diacylglycerol Kinase, alpha)	1418578_at
111	A	---	---	---	Dgka (diacylglycerol Kinase, alpha)	---
117	15	14766	13910	5713	Jak1 (janus kinase 1)	1433803_at
---	---	2935	2186	712	Jak1 (janus kinase 1)	1433804_at
---	---	25065	22746	11872	Jak1 (janus kinase 1)	1433805_at
83	A	5099	6632	10890	Dusp2 (dual specificity phosphatase 2)	1450698_at
51	A	4020	1437	7182	Prkcq (protein kinase C, theta)	1426044_a_at

Transcription factors

αβ T	γδ T	act IEL	iso IEL	S. γδ T	Description	Probe set
554	A	2937	1275	100	Klf2 (Kruppel-like factor 2 (lung))	1448890_at
407	18	16013	10662	26944	Satb1 (special AT-rich sequence binding prot. 1)	1416007_at
---	---	6828	3838	12995	Satb1 (special AT-rich sequence binding prot. 1)	1416008_at
---	---	1218	286	3949	Satb1 (special AT-rich sequence binding prot. 1)	1436182_at
148	27	3746	2147	3410	Klf13 (Kruppel-like factor 13)	1432543_a_at
144	12	23299	15508	7513	Tcf7 (transcription factor 7, T-cell specific)	1433471_at
---	---	6560	6963	1284	Tcf7 (transcription factor 7, T-cell specific)	1450461_at
140	A	1758	170	1192	Lef1 (lymphoid enhancer binding factor 1)	1421299_a_at
73	A	1423	567	107	Klf3 (Kruppel-like factor 3 (basic))	1421604_a_at
---	---	3155	3999	1540	Klf3 (Kruppel-like factor 3 (basic))	1429360_at
---	---	5666	3675	3148	Klf3 (Kruppel-like factor 3 (basic))	1431630_a_at
60	A	7335	11813	14308	Hmga1 (high mobility group AT-hook 1)	1416184_s_at

Table 2.2: Expression levels of genes expressed preferentially by γδ IELs (page 1 of 4)

Immune defense mediators

γδ T	αβ T	Epi.	act IEL	iso IEL	S. γδ T	Description	Probe set
Cytokines/Chemokines							
3065	566	A	69594	39894	1800	Ccl5 (RANTES)	1418126_at
215	49	A	17600	19554	4519	Xcl1 (Lymphotactin)	1419412_at
58	25	A	12651	7996	3611	Ifrd1 (TIS7/PC4, homolog)	1416067_at
22	8	A	---	---	---	Ifrd1 (TIS7/PC4, homolog)	---
39	A	A	1323	3110	4509	Ccl3 (MIP-1-alpha)	1419561_at
38	A	A	5682	6365	5814	Ccl4 (MIP-1-beta)	1421578_at
36	A	A	1055	1397	97	Spp1 (Eta-1)	1449254_at
30	A	A	672	898	205	Tgfb3 (Transforming Growth Factor, beta 3)	1417455_at
---	---	---	10538	11978	13030	Tgfb1 (Transforming Growth Factor, beta 1)	1420653_at
Cytotoxic Proteins/Related							
2630	116	19	119521	89613	13032	Gzma (Granzyme A)	1417898_a_at
2117	59	8	116228	127846	521763	Gzmb (Granzyme B)	1419060_at
583	258	22	84510	70292	60400	Prg1 (Serglycin)	1417426_at
275	A	A	4165	4424	2028	Tnfsf6 (Fas Ligand)	1418803_a_at
---	---	---	12626	8377	5858	Tnfsf6 (Fas Ligand)	1449235_at
222	8	153	30927	8478	141	Defcr1,3,6 (Cryptdin)	1450631_x_at
Enzymes, Inflammation							
174	97	19	6129	6881	6021	Leukotriene A-4 Hydrolase	1434790_a_at
---	---	---	994	467	1151	Leukotriene A-4 Hydrolase	1426807_at
---	---	---	352	419	1178	Leukotriene A-4 Hydrolase	1453528_at
73	35	40	3610	5595	1514	Ncf1 (p47phox)	1425609_at
---	---	---	4106	3744	2359	Ncf1 (p47phox)	1451767_at

Cholesterol/Lipid biosynthesis and metabolism

γδ T	αβ T	Epi.	act IEL	iso IEL	S. γδ T	Description	Probe set
110	A	A	269	191	194	Apoe (Apolipoprotein E)	1432466_a_at
66	27	A	7430	6896	13281	Fdps (Farnesyl diphosphate synthase)	1423418_at
65	16	A	1430	851	2181	Fdft1 (Squalene Synthase)	1438322_x_at
---	---	---	1139	1528	1082	Fdft1 (Squalene Synthase)	1448130_at
61	11	A	1135	597	328	Pltp (Plasma Phospholipid Binding Protein)	1417963_at
54	29	A	11957	13513	9789	Acadl (Acetyl CoA Dehydrogenase, long-chain)	1448987_at
51	A	A	6074	5192	4881	Ldlr (LDL Receptor)	1421821_at
---	---	---	405	558	485	Ldlr (LDL Receptor)	1431947_at
50	A	A	3655	3719	5263	Sqle (Squalene Epoxidase)	1415993_at
44	23	A	5754	11688	41825	Scd2 (Stearoyl-Coenzyme A desaturase 2)	1415822_at
---	---	---	2528	2794	16238	Scd2 (Stearoyl-Coenzyme A desaturase 2)	1415823_at
---	---	---	899	2356	3520	Scd2 (Stearoyl-Coenzyme A desaturase 2)	1415824_at
38	A	A	4697	5128	5515	Adfp (Adipose Differentiation Related Protein)	1448318_at

Table 2.2: Expression levels of genes expressed preferentially by γδ IELs (page 2 of 4)

Intestinal function and homeostasis

γδ T	αβ T	Epi.	act IEL	iso IEL	S. γδ T	Description	Probe set
289	A	A	11632	6526	555	Car2 (Carbonic Anhydrase isozyme II)	1448752_at
226	A	A	6002	4478	285	Fgl2 (Fibrinogen-like Protein)	1421854_at
---	---	---	5795	4782	866	Fgl2 (Fibrinogen-like Protein)	1421855_at
152	8	A	7980	9752	6437	Serpina3g (Spi2/EB1 Proteinase Inhibitor)	1424923_at
116	A	A	13404	4463	3529	Furin	1418518_at
116	59	A	11870	11520	16576	Cst7 (Cystatin F/leukocystatin)	1419202_at
91	A	A	1523	2336	108	Ela1 (p6-5/preproelastase, homolog)	1423693_at
21	A	A	2894	4080	3145	Pafah1b3 (PAF acetylhydrolase, 1b, a1)	1416410_at
45	A	91	455	175	106	Serpinb1a (Monocyte/neutrophil elastase inhib.)	1448301_s_at
108	A	111	2410	907	153	Spink3 (Serine protease inhibitor, Kazal type 3)	1415938_at
165	14	150	6665	5779	467	Adh1 (Alcohol dehydrogenase class I)	1416225_at
104	A	297	206	275	82	Mep1b (Meprin 1 beta)	1418215_at
79	A	1567	16585	5266	678	Tff3 (trefoil factor 3, intestinal)	1417370_at

Cell-surface molecules

γδ T	αβ T	Epi.	act IEL	iso IEL	S. γδ T	Description	Probe set
TCR associated							
726	394	A	62564	47811	14483	Cd3g (CD3-gamma)	1419178_at
597	16	17	9357	5906	738	Fcer1g (Fc-epsilon-RI gamma subunit)	1418340_at
NK Activating/Inhibitory Receptors							
182	A	A	2855	2552	447	CD244 (2B4)	1449991_at
138	A	A	6441	8624	11950	Lag3	1449911_at
87	A	A	2722	2052	1550	Klra5 (Ly-49E-GE)	1420789_at
58	A	A	4292	3860	8645	Lilrb4 (NK Cell Receptor gp49B)	1420394_s_at
55	A	13	2437	1776	5627	Pdcd1 (PD-1/Programmed Cell Death 1)	1449835_at
49	A	A	3676	4951	4171	Ctla4	1419334_at
38	A	A	59	608	377	Klrb1a (NK Cell Receptor NKR-P1A)	1450296_at
Cytokine/Chemokine/Similar							
262	46	A	25339	13861	3813	Tnfrsf1b (Tumor Necrosis Factor Receptor 2)	1418099_at
---	---	---	6331	6258	2247	Tnfrsf1b (Tumor Necrosis Factor Receptor 2)	1448951_at
125	49	100	4463	5360	2453	Tnfrsf1a (Tumor Necrosis Factor Receptor 1)	1417291_at
225	91	30	33877	25550	3561	Ifngr1 (Interferon gamma Receptor)	1448167_at
209	70	A	18790	13909	31026	Il2rb (Interleukin 2 Receptor, beta chain)	1417546_at
---	---	---	15743	11673	22759	Il2rb (Interleukin 2 Receptor, beta chain)	1448759_at
31	A	A	2528	2980	6880	Il12rb1 (Interleukin 12 Receptor, beta 1)	1418166_at
40	A	A	1801	1328	1804	Ccrl2 (L-CCR chemokine receptor)	1427736_a_at
62	A	A	1247	678	664	Ptger4 (Prostaglandin E Receptor, EP4 sub.)	1421073_a_at

Table 2.2: Expression levels of genes expressed preferentially by γδ IELs (page 3 of 4)

Transcription factors

γδ T	αβ T	Epi.	act IEL	iso IEL	S. γδ T	Description	Probe set
1251	353	271	33747	24454	24832	Atf4 (CREB2)	1448135_at
478	167	A	3567	2988	2640	Idb2 (Id-2)	1422537_a_at
---	---	---	3227	4695	2944	Idb2 (Id-2)	1435176_a_at
59	11	188	1582	1376	1227	Idb1 (Id)	1425895_a_at
454	233	58	22398	16347	5549	Junb (Jun-B oncogene)	1415899_at
299	171	26	22526	17233	11290	H3f3b (H3 histone, family 3B)	1420376_a_at
---	---	---	92356	63569	57342	H3f3b (H3 histone, family 3B)	1455725_a_at
298	125	100	28226	13752	918	Fos (FBJ osteosarcoma related oncogene)	1423100_at
281	80	50	8413	6743	5741	Max (Myc-associated factor X)	1423501_at
157	49	A	12120	10190	11648	Nr4a1 (Nur77/N10/NGFI-B)	1416505_at
152	99	A	6316	3870	2451	Zfp36l1 (Butyrate Response Factor 1/TIS11)	1422528_a_at
---	---	---	10804	4920	1704	Zfp36l1 (Butyrate Response Factor 1/TIS11)	1450644_at
92	26	A	11174	10897	2079	Tnfaip3 (A20/TNF Induced Protein 3)	1450829_at
86	14	A	6325	2860	1798	Tgif (TG Interacting Factor)	1422286_a_at
76	24	A	2738	1810	3540	Gfi1	1417679_at
70	24	61	13341	7627	2030	Ddit3 (Chop-10/Gadd153)	1417516_at
68	33	A	12288	6929	4345	Gtf2b (General transcription factor IIB)	1451135_at
64	31	A	6537	5656	3847	Mafk	1418616_at
59	A	104	1109	494	68	Klf4 (Kruppel-like factor 4 (gut))	1417394_at
---	---	---	1664	1002	734	Klf4 (Kruppel-like factor 4 (gut))	1417395_at
58	A	A	993	1592	2496	Runx2 (PEBP2a1/PEBP2alphaA/CBFA1)	1424704_at
---	---	---	1059	1903	1066	Runx2 (PEBP2a1/PEBP2alphaA/CBFA1)	1425389_a_at
---	---	---	2265	340	1553	Runx2 (PEBP2a1/PEBP2alphaA/CBFA1)	1426034_a_at
57	30	A	7232	8513	5012	TSC-22-like protein, homolog	1448412_a_at
---	---	---	902	696	887	TSC-22-like protein, homolog	1425206_a_at
51	15	A	5186	4568	6522	Xbp1 (X box binding protein-1)	1420011_s_at
---	---	---	15477	13377	18359	Xbp1 (X box binding protein-1)	1420886_a_at
---	---	---	13009	9911	19016	Xbp1 (X box binding protein-1)	1437223_s_at
51	21	36	2451	2606	2093	Nfe2l2 (p45 NF-E2 related factor 2)	1416543_at
49	A	A	960	1852	1181	Sos2 (Son of Sevenless homolog 2)	1452281_at
48	A	A	3824	3693	2465	Cebpb (C/EBP beta)	1427844_a_at
---	---	---	6489	3337	2304	Cebpb (C/EBP beta)	1418901_at
---	---	---	3338	3187	3376	Cebpb (C/EBP beta)	1427843_at
48	A	A	5409	6397	13421	Icsbp1 (Interferon Concensus Sequence BP 1)	1416714_at
---	---	---	2516	2077	13322	Icsbp1 (Interferon Concensus Sequence BP 1)	1448452_at
47	A	A	16487	9218	508	Ahr (Arylhydrocarbon Receptor)	1422631_at
---	---	---	3036	3897	1489	Ahr (Arylhydrocarbon Receptor)	1450695_at
44	A	73	4853	4043	2611	Atf3 (LRG-21)	1449363_at
36	A	41	2601	2879	404	Tgfb1i4 (TSC-22)	1425742_a_at
---	---	---	164	697	794	Tgfb1i4 (TSC-22)	1433899_x_at
---	---	---	1036	1096	399	Tgfb1i4 (TSC-22)	1439111_at
---	---	---	1692	96	335	Tgfb1i4 (TSC-22)	1454758_a_at
---	---	---	1457	1897	130	Tgfb1i4 (TSC-22)	1454971_x_at
---	---	---	36	89	24	Tgfb1i4 (TSC-22)	1456132_x_at
35	18	A	6817	4823	937	Jun	1417409_at
---	---	---	3972	1961	1093	Jun	1448694_at
33	A	A	1452	2684	2123	Prdm1 (Blimp1)	1420425_at

Table 2.2: Expression levels of genes expressed preferentially by γδ IELs (page 4 of 4)

Signal transduction

γδ T	αβ T	Epi.	act IEL	iso IEL	S. γδ T	Description	Probe set
1020	A	A	58114	37676	11352	Rgs1 (Regulator of G-protein signalling 1)	1417601_at
1207	21	A	---	---	---	Rgs1 (Regulator of G-protein signalling 1)	
---	---	---	24132	11740	823	Rgs2	1419247_at
---	---	---	8739	3550	697	Rgs2	1419248_at
620	101	77	27055	14569	642	Dusp1 (MAPK phosphatase 1)	1448830_at
479	308	27	22620	11285	7801	Ptpn8	1417995_at
337	195	A	4248	3262	2534	Stat3	1424272_at
---	---	---	28938	24389	28366	Stat3	1426587_a_at
271	94	113	8679	7513	5488	Pim1 (proviral integration site 1)	1423006_at
---	---	---	21388	11717	12024	Pim1 (proviral integration site 1)	1435458_at
185	41	17	11272	15401	9394	Bcl2a1a (A1)	1419004_s_at
---	---	---	931	595	343	Bcl2a1a (A1)	1437913_at
---	---	---	463	356	109	Bcl2a1a (A1)	1450812_at
155	62	A	6714	9307	3112	Inpp5d (Ship)	1418110_a_at
---	---	---	3336	4107	4506	Inpp5d (Ship)	1424195_a_at
123	77	A	7296	6700	668	Smpdl3a (ASM-like phosphodiesterase 3a)	1416635_at
122	14	A	6888	2748	190	Pik3r1 (PI-3-kinase, reg. subunit p85alpha)	1425515_at
---	---	---	18755	8636	1737	Pik3r1 (PI-3-kinase, reg. subunit p85alpha)	1451737_at
22	A	A	---	---	---	Pik3cb (PI-3-kinase, cat. subunit, beta)	
109	55	A	6135	5088	2901	Rbl2 (Rb2/p130)	1418146_a_at
---	---	---	6313	3569	4030	Rbl2 (Rb2/p130)	1425981_a_at
36	A	A	3631	2246	1974	Rb1 (p105Rb)	1417850_at
105	36	A	1409	281	1471	Traf5 (TNF receptor-associated factor 5)	1448861_at
98	59	A	3837	4639	3704	Map4k1 (Serine/threonine kinase)	1439323_a_at
95	28	A	3808	2458	1046	Prkacb (cAMP-dep. prot. kin., beta-cat. sub.)	1420610_at
---	---	---	11669	8534	998	Prkacb (cAMP-dep. prot. kin., beta-cat. sub.)	1420611_at
39	27	A	3217	4440	4870	Prkaca (cAMP-dep. prot. kin., alpha subunit)	1450519_a_at
88	A	A	4508	5663	3852	Crem (cAMP-responsive element modulator)	1418322_at
---	---	---	8789	8476	6472	Crem (cAMP-responsive element modulator)	1449037_at
86	50	A	2851	1888	1992	Map3k1 (MAP kinase kinase kinase 1)	1424850_at
86	41	A	22126	13321	7702	Gna13 (Guanine Nucleotide BP, a13)	1422555_s_at
---	---	---	13169	7661	5334	Gna13 (Guanine Nucleotide BP, a13)	1422556_at
---	---	---	10085	6615	868	Gna13 (Guanine Nucleotide BP, a13)	1430295_at
---	---	---	9926	5409	2535	Gna13 (Guanine Nucleotide BP, a13)	1450656_at
---	---	---	19168	9105	4070	Gna13 (Guanine Nucleotide BP, a13)	1453470_a_at
---	---	---	8646	5792	3580	Gna13 (Guanine Nucleotide BP, a13)	1460317_s_at
66	26	91	5322	7172	6280	Mapk3 (Mitogen Activated Protein kinase (erk-1))	1427060_at
61	27	51	6385	5275	3359	Egr1 (Early Growth Response 1)	1417065_at
61	17	A	9331	5798	12174	Cish (Cytokine-inducible SH2-containing protein)	1448724_at
57	A	A	1069	2154	2060	Ptpn5 (Protein Tyrosine phosphatase STEP61)	1423544_at
56	14	A	5178	5208	2502	Gadd45b (MyD118)	1449773_s_at
---	---	---	5679	7080	3455	Gadd45b (MyD118)	1450971_at
23	A	A	1825	721	98	Gadd45a	1449519_at
56	A	A	4258	3211	436	c-Fes (tyrosine kinase)	1427368_x_at
---	---	---	5069	2638	1404	c-Fes (tyrosine kinase)	1452410_a_at
54	26	A	4725	4762	5595	Impa1 (myo-inositol monop'tase 1)	1423127_at
---	---	---	537	706	1618	Impa1 (myo-inositol monop'tase 1)	1436848_x_at
52	A	A	2056	2185	4029	Casp3 (Caspase-3/CPP32)	1426165_a_at
---	---	---	5908	8427	12426	Casp3 (Caspase-3/CPP32)	1449839_at
52	25	A	13415	8289	5033	Fyn (p59fyn)	1417558_at
---	---	---	4573	5247	1908	Fyn (p59fyn)	1448765_at
48	25	A	3085	3048	658	Tec (Protein Tyrosine kinase, tec type I)	1460204_at
38	17	A	1091	740	3339	Gng2 (G protein gamma-2 subunit)	1418451_at
---	---	---	148	109	55	Gng2 (G protein gamma-2 subunit)	1418452_at
35	A	45	2573	1594	299	Plcb3 (Phospholipase C beta3)	1448661_at
34	A	27	683	1038	1017	Lyn	1451318_a_at
---	---	---	1945	2775	1854	Lyn	1425598_a_at

Chapter 3: Microarray-Based Studies of Antigen-Specific Splenic γδ T cell Responses Using Mice that are Transgenic for the G8 γδ TCR and are Deficient in RAG2

Introduction

The roles of γδ T cells in the immune system have been difficult to ascertain and the majority of past studies were limited to the analysis of functions known to be carried out by lymphocytes. In addition, the scarceness of known γδ TCR ligands made it difficult to study certain aspects of γδ T cells during immune responses. For instance, an accumulation of γδ T cells at a site of infection could indicate that the accumulating γδ T cells were encountering and responding to a ligand at that site but could also indicate that the accumulating γδ T cells merely happened to express a particular combination of homing receptors.

In order to understand how γδ T cells contribute to the immune system, it was necessary to obtain a fuller picture of how these cells respond to the recognition of γδ TCR ligands. The recognition of T10/T22 on splenocytes by splenic γδ T cells was studied, in part, because 0.6 – 2% of γδ T cells in normal mice recognize these molecules (Crowley, Fahrer et al. 2000) and because G8 γδ TCR transgenic mice (Dent, Matis et al. 1990) were available, whose γδ T cells recognized these molecules in an allele-dependent manner. Thus, in order to determine how naïve γδ T cells respond to the recognition of γδ TCR ligands, G8 BALB/c and G8 $RAG2^{KO}$ BALB/c mice were further characterized, the expression of T10/T22 on different splenocytes was analyzed, and microarray experiments were performed that compared the mRNA transcripts of activated G8 $RAG2^{KO}$ BALB/c γδ T cells to those of naïve G8 $RAG2^{KO}$ BALB/c γδ T cells. Because G8 $RAG2^{KO}$ BALB/c γδ T cells were rare and because microarray experiments require large amounts of RNA, protocols were developed for analyzing the transcripts that are present in limited numbers of cells.

Materials and Methods

Details about the mice and the G8 γδ T cell activation protocol can be found in the Materials and Methods section of Chapter 2.

T10/T22 Expression Analysis

The 7H9 monoclonal antibody was used (Crowley, Fahrer et al. 2000), which is capable of recognizing the T10 and T22 molecules but cannot distinguish between them. A streptavidin-APC conjugate was used to detect the biotinylated 7H9 antibody because APC is excited using a different laser than FITC, PE, and PI and, thus, the detected T10/T22 levels were not greatly affected by the detected FITC, PE, and PI levels.

Histology

Organs were removed from mice and embedded in OCT. 10 – 15 μm tissue sections were cut on a cryostat and placed onto Fisher SuperFrost Plus slides. The sections were air-dried and placed, two at a time, into 50 ml conical tubes containing a ball of Drierite and stored at -20°C until use.

For fixation, slides were immersed in -20°C acetone for 10 minutes, air dried for an additional 10 minutes, and placed into PBS. In order to block nonspecific binding of antibodies, sections were covered for an hour with at least 200 μl of a mixture of 2% BSA, 5% normal hamster serum, 5% normal mouse serum, and 10 μg/ml of anti-CD16/CD32 (FcBlock; BD Pharmingen). Thereafter, this mixture was poured off the slide and replaced by at least 200 μl of a similar mixture that was supplemented with labeled antibodies. These antibodies were usually used at a 1:100 dilution, which corresponded to a concentration of 2 μg/ml – 10 μg/ml. Finally, the sections were washed in DAPI-containing PBS and were covered with Fluoromount-G (Southern Biotechnology Associates, Inc.) and a cover glass.

Microarray Analysis Using Two Rounds Of *In Vitro* Transcription (IVT)

A published protocol that had been designed for cDNA microarrays (Wang, Miller et al. 2000) was adapted for probe-based Affymetrix microarrays. In short, first-strand synthesis was carried out on the RNA of about $1x10^6$ cells using two primers. One primer was composed of oligo-dT and a T7 RNA polymerase promoter (T7-$(dT)_{15}$ primer) and the other primer was a template-switch primer (TSP) whose complementary sequence could be incorporated at the 3' end of completed first strands. This was followed by second-strand synthesis where the complementary sequence of the template-switch primer served as a binding site for that primer that was then elongated by a thermostable DNA polymerase. IVT was performed on the double-stranded cDNA and the resulting complementary RNA (cRNA) was reverse transcribed using random hexamers. The T7-$(dT)_{15}$ primer was then used for second-strand synthesis along with a thermostable polymerase in order to generate amplified cDNA. Subsequently, IVT was performed on the amplified cDNA in the presence of biotinylated ribonucleotides in order to generate amplified cRNA that was then analyzed using Affymetrix microarrays.

Microarray Analysis Using PCR-Based Amplification

Due to the low level of mRNA 5' end representation in the cRNAs produced by the previous protocol, a new protocol based on the SMART PCR cDNA synthesis kit (BD Clontech), the standard Affymetrix GeneChip™ cRNA synthesis protocol, and a published protocol (Wang, Miller et al. 2000) was used to make biotinylated RNA probes for microarray analysis. This protocol was composed of three major steps: (1) an initial double-stranded cDNA synthesis, (2) a PCR-based amplification, and (3) IVT.

For the synthesis of single-stranded cDNA, RNA was isolated from cells using Trizol (Invitrogen) where 1 μl of 5 μg/μl linear acrylamide (Ambion) was added to the aqueous phase prior to the addition of isopropanol in order to visualize the RNA pellet. The RNA pellet was air dried and resuspended in ddH_2O so that 1 μl of RNA was derived from 10,000 cells. 9 μl of RNA, equivalent to that obtained from 90,000 cells, was reverse transcribed by first adding 1 μl of 0.5 μg/μl T7-$(dT)_{15}$ primer, denaturing at 70°C for 5 minutes, snap cooling on ice, adding 12 μl of a mix containing 4 μl of 5x first-stand

buffer, 2 µl of 0.1 M DTT, 2 µl of 10 mM dNTPs, 1 µl of 1 µg/µl TSP, 1 µl RNaseIN, and 2 µl SuperScriptII, and incubating at 42°C for 90 minutes.

For the synthesis of double-stranded cDNA, 10 µl of single-stranded cDNA was added to 90 µl of a mix containing 10 µl of Advantage PCR buffer (BD Clontech), 3 µl of 10 mM dNTPs, 2 µl of Advantage cDNA polymerase (BD Clontech), 1 µl of RNaseH, 1 µl of 1 µg/µl T7 primer (same sequence as the T7-$(dT)_{15}$ primer without the $(dT)_{15}$), 1 µl of 1 µg/µl of TSP, and 72 µl of ddH_2O. The sample was incubated at 37°C for 5 minutes, at 94°C for 2 minutes, at 65°C for 1 minute, and at 75°C for 30 minutes and, thereafter, the sample was subjected to 12 to 18 cycles of PCR with 1 minute denaturing at 94°C, 1 minute annealing at 65°C, and 10 minute elongating at 68°C.

To purify the double-stranded cDNA, 5 µl of 1 M NaOH and 2 mM EDTA was first added and the sample was incubated at 65°C for 10 minutes to degrade residual RNA. 45 µl of ddH_2O, 1 µl of 5 µg/µl linear acrylamide, and 150 µl of phenol:chloroform:isoamyl alcohol (Ambion) were then added and mixed. The 300 µl samples were transferred to pre-spun phase-lock light gel tubes (Eppendorf) and spun at 14,000 rpm for 5 minutes. The 150 µl upper aqueous phase was collected and added to 150 µl of 5 M ammonium acetate. 1 ml of 100% ethanol was added, mixed, and spun at 14,000 rpm for 20 minutes. The supernatant was removed and the pellet was washed twice by adding 500 µl of 95% ethanol, spinning at 14,000 rpm for 6 minutes, and removing the supernatant. The pellet was air-dried and resuspended in 60 µl of ddH_2O. To remove additional small molecules, a Bio-6 chromatography column (Bio-Rad) was pre-equilibrated with ddH_2O and the 60 µl sample was applied to it, spun at 3,000 rpm for 4 minutes, and the 60 µl eluted sample was collected. The sample was dried in a Speed-Vac and resuspended in 12 µl of ddH_2O.

IVT was performed by mixing 2 µl of 10x HY reaction buffer, 2 µl of 10x biotin-labeled NTPs, 2 µl of 10x DTT, 2 µl of 10x RNase inhibitor mix, and 1 µl of 20x T7 RNA polymerase (all from Enzo) and adding 11 µl of the sample to it. The 20 µl mix was incubated at 37°C for 5 hours with occasional mixing. The RNA was isolated in a total volume of 30 µl from the sample using the RNeasy kit (Ambion) and the OD260/280 was determined using 5 µl thereof. To concentrate the RNA by ethanol

precipitation, 35 μl of ddH_2O, 60 μl of 5 M ammonium acetate, and 200 μl of 100% ethanol was added and mixed. The sample was placed at -20°C for overnight precipitation. The precipitated sample was spun at 14,000 rpm for 30 minutes at 4°C. The supernatant was removed and the pellet was washed twice with 500 μl of 80% ethanol and 14,000 rpm 5 minute spins. The supernatant was removed and the pellet was air-dried and resuspended in ddH_2O at a concentration of 0.6 μg/μl under the assumption that RNA recovery from precipitation was 100%. A fourth volume of fragmentation buffer (Affymetrix) was added and the sample was incubated at 94°C for 35 minutes. The fragmented RNA sample was submitted to the Stanford PAN facility for hybridization to Murine U74 and U74v2 GeneChip^{TM} microarrays (Affymetrix).

G8 RAG2^{KO} BALB/c γδ T cell Activation for Microarray Analysis

Stimulator splenocytes were washed in Hank's Balanced Salt Solution (HBSS) to remove primary amine-containing compounds and then labeled in 10 ml of HBSS with 5 μM 5-(and-6)-carboxyfluorescein diacetate, succinimidyl ester (Molecular Probes), which is also known as CFDASE and CFSE, for 20 minutes at room temperature. The labeled cells, which fluoresced brightly in the FITC channel of a cell sorter, were washed three times with media, cultured for three hours, and washed again because they were otherwise found to transfer some of the dye to the responder cells. Thereafter, the stimulator and responder cells were combined and cocultured. Following the cocultures, the cells were placed on ice and stained with a PE-conjugated antibody to the γδ TCR (GL3) and with propidium iodide. Alive $PE^+FITC^-PI^-$ G8 RAG2^{KO} BALB/c γδ T cells were subsequently sorted.

Results and Discussion

T10/T22 Expression is Cell Type and Strain Dependent

To identify which cells could potentially activate γδ T cells, the expression of T10 and T22 was analyzed in different strains of mice. T10/T22 levels were found to be mouse strain and cell-type dependent. B10.BR mice were found to express the highest T10/T22 levels of any strain (*Figure 3.1A*). Unlike other strains tested, their NK cells and T cells expressed clearly-detectable levels above background. In addition, their $CD11c^+$ $Mac1^+$ dendritic cells expressed 10-fold higher levels than those of BALB/c or C57Bl/6 mice. This is interesting given that B10.BR splenocytes are less capable than C57Bl/6 splenocytes at activating G8 γδ T cells.

The expression of T10/T22 was detected on granulocytes. In addition, a two-fold upregulation thereof could be observed after culturing them in the presence of bacteria for 2 hours (*Figure 3.1B*). γδ T cells are known to play a role early during some infections. Perhaps the detection of T10/T22 on activated granulocytes plays a role in this process.

B cells were found to express some of the highest levels of T10/T22 and those in the blood expressed higher levels than those in the spleen (*Figure 3.1C*). In addition, higher levels were observed on rare $CD19^+$ $B220^{low}$ B cells that expressed CD5 and low levels of IgD (*Figure 3.1D*). Given that B cells are abundant in the spleen and given that B cells express some of the highest levels of T10/T22, B cells may be the targets of T10/T22-reactive γδ T cells that comprise 0.6 – 2% of γδ T cells in the spleen.

Histological Analysis of G8 BALB/c Mice

G8 BALB/c mice contain about as many γδ T cells as αβ T cells that appear to be naïve based on their cell-surface marker expression. For the most part, these γδ T cells express the same G8 γδ TCR. In order to get an understanding of where naïve γδ T cells are found, the lymph nodes, thymuses, and spleens of G8 BALB/c mice were sectioned for histological analysis.

In the spleen and lymph nodes, G8 γδ T cells were found in the characteristic T cell areas of these organs along with αβ T cells (*Figure 3.2A* and *B*). However, some αβ T cells could also be observed inside the B cell areas while this was not the case for G8 γδ T cells. The movement into the B cell areas is generally a characteristic of activated $CD4^+$ αβ T cells so that these cells can provide help to B cells that have the ability to recognize the same foreign protein as the T cells. Given that G8 γδ T cells are not found in the B cell areas, this suggests that these γδ T cells are still naïve and/or that their function is not to move into the B cell areas.

In the thymus, G8 γδ T cells and αβ T cells were distributed differently (*Figure 3.2C*). It is generally accepted that early thymocytes are found in the outer portion of the cortex while those in the later stages of development that are undergoing positive selection are found closer to the medulla. Negative selection appears to occur in the medulla that is heavily populated by MHC class II^+ stromal cells. Staining for both the γδ TCR and the αβ TCR reveals that the γδ TCR is expressed closer to the outer portion of the cortex than the αβ TCR. This may be because the expression of the transgenic G8 γδ TCR does not require rearrangement and thus the γδ TCR could be expressed earlier than the αβ TCR. In addition, while some γδ T cells can be found in the medulla, this area is mostly occupied by αβ T cells.

Gene Expression Comparisons between G8 BALB/c γδ T cells and αβ T Cells

The fact that G8 BALB/c mice had large numbers of γδ T cells, that the transgenic γδ T cells were probably naïve, that some αβ T cells were probably not naïve, and that there was a subtle difference in the lymphoid organ distribution between γδ T cells and αβ T cells suggested that a comparison between γδ T cells and αβ T cells in these mice could give an indication of whether and how naïve γδ T cells differ from αβ T cells. For this reason, the transcripts expressed by G8 γδ T cells and αβ T cells were analyzed by microarray.

There were not many major differences between the transcripts expressed by γδ T cells and αβ T cells (*Figure 3.3*). However, the expression of some genes was found to

differ between naïve γδ T cells and αβ T cells and some of the differences were expected. For instance, G8 γδ T cells do not, for the most part, express CD8α and CD8α expression was only found in the αβ T cells. In addition, some of the differences supported the assertion that G8 γδ T cells are naïve while some αβ T cells are activated or memory cells. Transcripts for cell-surface markers expressed primarily by αβ T cells included those for CD5, CD6, the activation marker CD44, the memory marker Klrg1 (Robbins, Terrizzi et al. 2003), and the chemokine receptor CXCR3. In addition, αβ T cells preferentially expressed transcripts for Granzyme B, CCL5/RANTES, Ki-67, Syntaxin 11, Integrin β1, Bcl2, Schlafen2, and BTLA. On the other hand, G8 γδ T cells preferentially expressed transcripts for Endoglin, Myb, and the stem-cell marker Sca-1.

Analysis of the G8 RAG2^{KO} BALB/c Mouse

The use of G8 BALB/c mice as a source of γδ T cells for studying γδ T cell activation has a few difficulties. First, allelic exclusion is far from perfect for T cells and it is possible to find T cells in G8 BALB/c mice that express both γδ and αβ TCRs. Second, in order to study the activation of G8 γδ T cells by primary cells, it is necessary to use cells derived from *b* or *k* haplotype-expressing mice because no T10/T22^{b}-expressing transgenic BALB/c mice are available. Unfortunately, G8 BALB/c mice express αβ T cells and B cells, of which some may be alloreactive against these haplotypes. Third, while it is technically possible to deplete splenocytes of αβ T cells and B cells through the use of magnetic beads and antibodies directed against the αβ TCR and CD19, the fact that this involves αβ TCRs being bound to magnetic beads leads to the possibility that αβ T cells will become activated. Negative selection would need to be 100% efficient in order not to contaminate γδ T cells with activated αβ T cells. Fourth, the commonly-used anti-γδ TCR antibodies lead to the activation of positively-selected γδ T cells in culture based on CD69 expression; especially, when used in conjunction with magnetic beads.

G8 BALB/c mice that are deficient in RAG present a solution for generating a source of γδ T cells with a known specificity in the absence of αβ T cells and B cells. Although, it should be noted that it has recently been reported that mice that are deficient

in αβ T cells show some abnormalities with respect to the function of their γδ T cells (Pennington, Silva-Santos et al. 2003; Silva-Santos, Pennington et al. 2005). RAG2-deficient mice cannot rearrange their TCR and immunoglobulin loci and this leads to a complete lack of αβ T cells and B cells. Consequently, the thymuses of G8 RAG2^{KO} BALB/c mice are very small (*Figure 3.4A*), the mesenteric lymph nodes are barely visible (*Figure 3.4B*), and the lack of B cells also leads to the absence of Peyer's patches on the small intestine.

A histological analysis of the spleens of G8 RAG2^{KO} BALB/c mice revealed that most of the γδ T cells were found in small areas of white pulp around the central arterioles. However, there were some abnormalities because a stain for CD11c revealed that dendritic cells were primarily found surrounding the T cell areas (*Figure 3.4C*) instead of mostly overlapping with them, as would be the case in normal mice. This was similar to what had been reported for B cell knockout mice (Crowley, Reilly et al. 1999), where marginal zone dendritic cells were found surrounding the T cell areas.

Interestingly, it was possible to detect structures resembling lymphocyte-filled villi (*Figure 3.4D*) that have been reported to be the rat equivalent of murine cryptopatches that are involved in the development of intestinal intraepithelial lymphocytes. γδ IELs were detected and, similar to IELs in conventional mice, these cells expressed low levels of the activation marker CD69.

Splenic γδ T cells Activate in Response to T10/T22^{b}-Expressing Cells

The spleen was chosen as the source of γδ T cells from G8 RAG2^{KO} BALB/c mice because it contained the second largest amount of γδ T cells next to the IEL compartment and because IELs appeared to be constitutively activated as was shown in Chapter 2. However, it was only possible to isolate on the order of one million γδ T cells from the spleen. In order to activate G8 γδ T cells, the stimulator cells have to express T10/T22 of an appropriate haplotype and should not be alloreactive against the *d* haplotype. Thus, H2$^{b/d}$ BALB/c spleen-derived stimulator cells were chosen to serve as stimulator cells and were added in a 5-fold excess to ensure that G8 RAG2^{KO} BALB/c γδ T cells had access to ample γδ TCR ligand-expressing cells.

As expected, G8 γδ T cells incubated in the presence of $H2^b$-expressing splenocytes expressed the very early activation marker CD69 and exhibited a striking decrease in γδ TCR levels, where the most severe reduction was observed after 1 day of activation and where levels returned to near starting levels after 2 days of activation (*Figure 3.5A – C*). Activated γδ T cells also upregulated their levels of CD44 (*Figure 3.5D*), increased in cell size (*Figure 3.5E*), and divided twice during four days of activation (*Figure 3.5F*).

G8 γδ T cell Activation Using Splenocytes of Other Strains

B10.BR and $H2^{k/d}$ BALB/c were also analyzed for their ability to activate G8 γδ T cells. B10.BR mice have the *k* haplotype for their MHC class I and II molecules but are reported to have $T18^a$. Cells from B10.BR mice were originally used to create the G8 cell line and are thus known to activate G8. However, their alleles of T10 and T22 are, as yet, unknown. $H2^{k/d}$ BALB/c mice are a cross of BALB.K ($T18^b$) and BALB/c ($T18^c$) mice. BALB.K mice are congenic for the *k* haplotype MHC locus of C3H/He mice that, while expressing $T18^b$, should not contain a functional T22 gene and, thus, should only express the inducible T10. BALB/c mice also do not express a functional T22 gene. $H2^{k/d}$ BALB/c mice can thus be used to analyze the effects of T10 expression in the absence of T22.

Unlike splenocytes from C57Bl/6 mice or $H2^{b/d}$ BALB/c mice, neither B10.BR (*Figure 3.6A*) nor $H2^{k/d}$ BALB/c splenocytes (*Figure 3.6B*) led to substantial γδ TCR downregulation. In addition, not all γδ T cells were $CD69^+$ after 24 hours suggesting that the cells capable of activating G8 γδ T cells were less abundant in these mice than in other strains of mice and/or that the T10 and T22 alleles expressed by these mice did not stimulate as well. Given that the original studies of G8 showed that B10.BR "APCs" are very effective at activating G8 and given that G8 activation by B10.BR and $H2^{k/d}$ BALB/c lead to similar outcomes, the most-likely explanation is that T22 is not recognized in B10.BR and that, in both strains, the inducible T10 molecule is being recognized.

Identifying Novel Responses to Activation Using Microarrays

The expression of CD69 accompanied by blasting and cell division clearly indicated that the G8 γδ T cells became activated in cocultures with T10/T22^{b}-expressing splenocytes. Thus, this system represented an excellent way determine additional changes that take place following γδ T cell activation.

12 hour and 4 day timepoints were chosen for microarray analysis where G8 γδ T cells that had been incubated in the presence of T10^{b}, T22^{b}, and T10^{d} (H2$^{b/d}$ BALB/c stimulator cells) were compared to G8 γδ T cells that had been incubated in the presence of only T10^{d} (BALB/c stimulator cells). The 12 hour timepoint was chosen since this timepoint occurs before G8 γδ T cell division, allows for sufficient time for activation-dependent mRNA synthesis, and minimizes the effects of activation-induced proteins acting back on γδ T cells, directly or indirectly. The 4 day timepoint was chosen to look at longer term changes to γδ T cells in culture.

Following the 12 hour and 4 day cocultures, G8 γδ T cells were sorted. Yields were rather low and only on the order of 10^{5} cells could be obtained. This made it impossible to use the conventional Affymetrix GeneChip protocol to generate the biotinylated cRNA probes for analysis. Therefore, a PCR-based protocol was designed that was based on the SMART PCR cDNA synthesis kit (BD Clontech), the standard Affymetrix GeneChip^{TM} cRNA synthesis protocol, and a published protocol (Wang, Miller et al. 2000).

The use of this protocol had a few caveats because it was not clear whether all mRNAs would be reverse transcribed and amplified equally well in all samples being compared. First, it relied on the reverse transcriptase SuperScriptII's tendency to incorporate extra cytosines upon reaching the end of an mRNA and this may be dependent upon the presence of a 7-methylguanosine cap. Thus, even though the mRNA sequences detected by the Affymetrix microarrays were biased to the 3' ends in order to be more tolerant of mRNA degradation and secondary structures, it may have been difficult to detect cap-less mRNAs and mRNAs whose secondary structures would have prevented the reverse transcriptase from reaching the 5' end. Second, this protocol relied on PCR-based amplification of cDNA using the same set of primers for each gene. This

assumed that the amplification of one type of cDNA would not affect the amplification of another and that amplification would be equally efficient for all transcripts, for all cycles. Thus, validation of gene expression will be essential.

For the 12 hour timepoint, 500,000 G8 γδ T cells were sorted from the BALB/c cocultures and 287,000 G8 γδ T cells were sorted from the $H2^{b/d}$ BALB/c cocultures. For the 4 day timepoint, 230,000 γδ T cells were sorted from the BALB/c cocultures and 528,000 γδ T cells were sorted from the $H2^{b/d}$ BALB/c cocultures. The cDNA of these samples was amplified using 12 cycles of PCR. A gel analysis of these amplified samples revealed that the 4 day sample containing ligand-activated γδ T cells had, by far, the most amount of product. This was also observed when quantifying the cRNA after in vitro transcription that yielded between 5 and 11 μg for the other samples and 16 μg for the 4 day $H2^{b/d}$ BALB/c sample using only half as much cDNA. Thus, this sample contained about 3- to 6-fold more mRNA than the other samples. The 12 hour activated sample yielded twice as much product from half as many cells as the 12 hour naïve sample suggesting that 12 hours of activation led to 4-fold higher levels of mRNA than 12 hours of culture.

An additional 12 hour timepoint experiment was performed to determine if BALB/c cells affect G8 γδ T cell activation by $H2^{b/d}$ BALB/c cells. G8 γδ T cells were incubated with BALB/c splenocytes, $H2^{b/d}$ BALB/c splenocytes, or a 1:1 mixture thereof. 500,000 G8 γδ T cells were sorted from the BALB/c coculture, 176,000 G8 γδ T cells were sorted from the $H2^{b/d}$ BALB/c coculture, and 255,000 G8 γδ T cells were sorted from the mixed coculture. In order to increase the future *in vitro* transcription yields above 5 μg, 18 cycles, as opposed to 12 cycles, of PCR were performed on the cDNA of 40,000 cells. The *in vitro* transcription yielded about 10.8, 16.4 and 13.8 μg of cRNA for the BALB/c, $H2^{b/d}$ BALB/c, and mixed samples, respectively.

As shown in *Figure 3.7A*, the expression levels 12 hours and 4 days in the absence of activation correlated reasonably well with one another. On the other hand, activated γδ T cells showed more differences 12 hours and 4 days after activation (*Figure 3.7B*). For instance, IFNγ was primarily expressed in the 12 hour sample while CTLA-4 and Ki-67, on the other hand, were more abundant in the 4 day sample. There were large

differences between 4 day naïve and 4 day activated γδ T cell samples (*Figure 3.7C*) as well as between 12 hour naïve and 12 hour activated samples (*Figures 3.7D* and *3.7E*).

The activation of G8 γδ T cells led to the expression of large numbers of genes and also led to the downregulation of others. For instance, the expression of CD69 was induced and the expression of α_V integrin (CD51) increased while the expression of β_7 integrin and L-selectin was reduced (*Table 3.1*).

γδ T cell Activation Leads to Changes in TCR-Associated Transcripts

The downregulation of γδ TCRs from the cell surface was accompanied by a downregulation of transcripts encoding the components of the γδ TCR (*Table 3.2*). After 12 hours of activation, there were reductions in transcripts encoding the γδ TCR and CD3. The SNARE protein Syntaxin 11 (Valdez, Cabaniols et al. 1999) was expressed after activation and may have played a role in the degradation of activated TCRs that had been endocytosed.

On the other hand, transcript levels of Lck remained mostly unchanged following activation and those of Fyn and Zap70 increased. Lck and Fyn are Src-family kinases that are important in TCR signaling because they phosphorylate CD3, which leads to the recruitment of Zap70 and the activation thereof by the Src-family kinases. The activation of Zap70 has been found to lead to the phosphorylation of Lat, Lcp2/Slp76, and Vav1 whose transcripts did not change greatly following activation.

The loss of TCR expression and enhancement of Zap70 expression suggests that the reduced likelihood of generating a signal may be coupled with an increased ability to signal or prolong signaling. In support of the latter, there is a reduction in diacylglycerol kinase alpha transcripts. This enzyme converts diacylglycerol (DAG) that is produced by phospholipase C gamma (PLCγ) into phosphatidic acid. A reduction in this enzyme should prolong the effects of DAG-dependent signaling, such as the activation of protein kinase C theta (PKCθ). On the other hand, there is also a reduction in transcripts for an ER calcium channel, inositol 1,4,5-triphosphate receptor 5. This would suggest that future signals generated by the TCR may be less likely to trigger strong calcium signals and, in turn, less likely to activate calcineurin.

Complexes of the adapter proteins Lat and Slp76 allow for the accumulation of Tec family kinases, including Itk. While transcripts for Itk are not greatly changed after activation, those for Tec and, most notably, Txk/Rlk are. Txk phosphorylation induces the expression of IFNγ (Kashiwakura, Suzuki et al. 2002) to whose promoter it can bind directly (Takeba, Nagafuchi et al. 2002). The reduction of Txk levels may serve to reduce the intensity of its signal. IFNγ production increases between 12 and 24 hours of activation so the reduction of Txk expression does not immediately cause IFNγ production to stop. However, γδ T cells that have undergone 4 days of activation no longer express IFNγ. The reduction of Txk may play a role in that event.

TCR activation leads to synapse formation where proteins expressing Pleckstrin-homology (PH) domains, which bind phosphatidylinositol 4,5-biphosphate (PIP2) and some variants thereof with a high affinity (Paterson, Savopoulos et al. 1995), have been found to accumulate (Huppa, Gleimer et al. 2003). However, after activation, synapse formation needs to end. Along those lines, the expression of Pitpnc1/rdgB-beta, a member of the phosphatidylinositol transfer protein family, is reduced, and transcripts for Dock2 (Sanui, Inayoshi et al. 2003), Evl, and Fyb (Krause, Sechi et al. 2000) are also found to decrease following activation. Additionally, transcripts of the PH domain-containing, Rho-GTPase activating protein family members ArhGAP9 (Furukawa, Kawasoe et al. 2001) and ArhGAP15 (Seoh, Ng et al. 2003) are reduced after activation, and transcripts for ArhGEF18 (Niu, Profirovic et al. 2003) disappear.

γδ T cell Activation Leads to Changes in the NF-κB-Associated Transcripts

TCR signaling is coupled to NF-κB activation through Malt1 and its associations with Bcl10 and Card11 (Carma1) (Che, You et al. 2004). NF-κB (Nfkb1; p50) is a member of the Rel family of transcription factors that is normally bound to IκBs that keep it in an inactive state outside of the nucleus. An additional inhibitor, Tnip2, appears to work by binding to A20 (Van Huffel, Delaei et al. 2001) and/or by blocking the interaction of RIP with IκKγ (Liu, Yen et al. 2004). Iκ kinases (IκKs) that have been activated by PKCθ phosphorylate IκBs, which then causes these IκBs to become

ubiquitinated and subsequently destroyed. This, in turn, allows the now uninhibited NF-κBs to translocate to the nucleus and promote the expression of genes, such as IL-2.

Genes associated with the NF-κB pathway exhibited changes in expression following activation (*Table 3.3*) and suggest that the NF-κB pathway may be reinforced after activation. Following activation, Malt1 and NF-κB transcripts were increased, suggesting that there may be an increased ability to express NF-κB-dependent genes following activation because extra unbound NF-κB would be expected to act immediately as a transcription factor. However, transcripts for its inhibitors Tnip2 (ABIN-2), IκBα (Nfkbia), IκBβ (Nfkbib), and IκBNS were also increased, suggesting that increased NF-κB levels are balanced by increased inhibitor levels. In addition, the expression of IκK-i (Ikbke), which phosphorylates inhibitors of NFκB in order to activate NF-κB, was decreased, suggesting that it may become more difficult to initiate the NF-κB pathway. The induction of IκBNS has also been observed on thymocytes following TCR ligation that leads to negative selection (Fiorini, Schmitz et al. 2002).

γδ T cell Activation Leads to the Expression of Transcripts that are Associated with Effector Functions

The activation of γδ T cells led to the expression of transcripts for proteins that have direct effects on other cells (*Table 3.4*). For instance, transcripts for Granzyme B appear following activation and are very abundant. Granzyme B is a serine protease that is capable of initiating apoptosis in target cells. In order to protect themselves from the effects of Granzyme B, cytotoxic lymphocytes are known to express Serpinb9 (PI-9), a serine proteinase inhibitor (Sun, Bird et al. 1996). Serpinb9 transcripts were detected in γδ T cells following activation. While γδ IELs were found to express abundant transcripts for Granzymes A and B, Granzyme A expression was not detected 12 hours after activation and low amounts were detected after 4 days of activation. Granzyme B expression has been reported to be a marker of antigen-specific T cell activation (Jacob and Baltimore 1999). However, 4 day cultures of γδ T cells in the absence of T10/T22[b] were found to express Granzymes A and B and Serpinb9. The expression of these genes

in what should have been naïve cells suggests that either $T10^d$ can be recognized by G8 γδ T cells or that there are antigen-unspecific ways to activate γδ T cells.

It addition to Granzyme B, lymphocytes can also induce apoptosis on target cells through the expression of Fas ligand (FasL). FasL-expression is upregulated by the expression of Pdcd11 (Alg-4) (Lacana and D'Adamio 1999), whose transcripts were detected following activation. Strangely, both γδ and αβ T cells isolated from a normal G8 mouse appeared to express Pdcd11 similarly so the expression thereof is not necessarily an indicator of FasL expression.

Activated γδ T cells may also express antibacterial genes. Transcripts for Pla2g12a, group XIIa Phospholipase A2, were increased after activation. Phospholipases catalyze the release of lipids from phospholipids and some of the secreted forms have been shown to exhibit bactericidal activity against gram-positive bacteria. The human homolog of Pla2g12a has been found to be bactericidal against the gram-negative bacterium *E. coli* (Koduri, Gronroos et al. 2002). Thus, activated γδ T cells may produce bactericidal proteins. $CD4^+$ Th2 cells, as opposed to $CD4^+$ Th1 cells, have also been observed to upregulate their levels of Pla2g12a in response to anti-CD3 (Ho, Arm et al. 2001). Given that activated γδ T cells express large amounts of IFNγ, a Th1 cytokine, it is interesting that they also express a molecule associated with Th2 responses.

Finally, activated γδ T cells upregulated their expression of endothelial cell growth factor 1 (Ecgf1) and expressed the endothelin converting enzyme Ece1. This enzyme activates endothelin, which acts as a potent vasoconstrictor. Before activation, γδ T cells also expressed transcripts for Endoglin, a marker of endothelial cells that serves as an auxiliary receptor for the TGFβ-related family of cytokines. Endoglin expression has also been found on hematopoietic stem cells (Chen, Li et al. 2002). However, I have never managed to stain γδ T cells for Endoglin with the available antibody.

γδ T cell Activation Leads to Changes in Cytokine-Related Transcripts

The activation of γδ T cells led to the production of cytokines and associated genes (*Table 3.5*). One of the most upregulated genes following activation was IFNγ

whose production is characteristic of Th1 responses. IFNγ plays an important role in antiviral immunity and signals through Jak1. The effects of IFNγ may have led to the expression of some genes including those encoding Isg20, which degrades RNA (Nguyen, Espert et al. 2001), and Icsbp1/IRF-8 (Tsujimura, Nagamura-Inoue et al. 2002), which is a transcriptional regulator that has been found to downregulate the expression of the anti-apoptotic molecule Bcl-2 (Burchert, Cai et al. 2003). The expression of IFNγ may have also led to the downregulation of responses to IFNγ by G8 γδ T cells since transcripts of Jak1 decreased after activation.

In addition to IFNγ, transcripts for TNFα appeared following activation. TNFα is capable of causing cell death. The expression of TNFα and FasL has been found to be dependent on the early growth response (Egr) family of proteins (Droin, Pinkoski et al. 2003) and increases in transcripts for Egr-1, Egr-2 and Egr-3 were detected following activation. Transcripts for Lymphotoxin α (TNFβ) also appeared following activation.

Activated γδ T cells may also be subject to altered responses to cytokines. Transcripts for Cish (Cis) increased after activation and this protein has been found to associate with phosphorylated cytokine receptors though its SH2 domain whereby it prevents the binding of signaling molecules. While Cish transcripts increased, transcripts for Socs3, which negatively regulates Jaks, decreased.

In addition to being subject to altered responses to cytokines, γδ T cells may also be subject to altered responses to chemokines. Transcripts for the GTPase-activating protein Rgs16 (De Vries, Zheng et al. 2000; Hollinger and Hepler 2002; Lippert, Yowe et al. 2003) were barely detected prior to activation but became some of the most abundant transcripts after activation. Rgs16 may play a role in desensitizing the activated γδ T cells to the chemokines they produce and in preventing the activated γδ T cells from straying too far away from where they became activated. The expression of Rgs16 may be an indirect effect of γδ T cell activation because its expression can be induced through IL-2 (Beadling, Druey et al. 1999) and IL-2 was found in the supernatants of cultures after γδ T cell activation. Rgs14 transcripts behaved the opposite way by exhibiting lower expression after activation.

γδ T cells can be cultured with the addition of IL-2 and in some cases IL-7. IL-7 has been reported to be a cytokine necessary for the growth of naïve and memory T cells while IL-2 works well for the growth of activated cells. Activation of G8 γδ T cells led to a reduction in transcripts for the IL-7 receptor and corresponding reductions in the cell-surface levels thereof have been observed. Transcripts for the IL-6 receptor α chain, IL-10 receptor β chain, IL-17 receptor, and IL-18 receptor 1 were also reduced while transcripts for the IL-2 receptor β chain were increased following activation. It was not possible to detect the IL-2 receptor α chain, which leads to high affinity IL-2 binding, using the PCR-based amplification of cDNA. However, it was possible to detect it using the standard Affymetrix cRNA synthesis protocol using bead-selected γδ T cells two days after activation. This suggests that activated γδ T cells lose their responsiveness to IL-7 and perhaps other cytokines while increasing their ability to detect IL-2.

Additional changes to cytokine-related genes included those to IL-16, Gpr65, Gadd45b, Irf4, and Gfi1. Activated γδ T cells lost their expression of IL-16, a chemokine for $CD4^+$ T cells (Lynch, Heijens et al. 2003), but increased their expression of Gpr65 (Gpcr25; TDAG8), a receptor for the glycosphingolipid psychosine. Transcripts for Gadd45b increased after activation and its expression has been found to be required for a variety of T cell responses including cytokine production (Lu, Ferrandino et al. 2004). Irf4, a transcriptional regulator, was expressed following activation. Irf4 expression in Jurkat cells has been reported to lead to the expression of IL-2 as well as the Th2 cytokines IL-4, IL-10, and IL-13 and may bind cooperatively to the IL-2 and IL-4 promoters with NFATc1 (Hu, Jang et al. 2002). In addition, Irf4 may enhance Fas-mediated apoptosis (Fanzo, Hu et al. 2003) but has also been observed to be anti-apoptotic (Lohoff, Mittrucker et al. 2004). The expression of Gfi1, a Stat6-dependent transcriptional repressor, was upregulated after activation and this protein has been found to inhibit apoptosis and promote the growth of Th2 cells (Zhu, Guo et al. 2002) and has now been shown to prevent the proliferation of hematopoietic stem cells (Hock, Hamblen et al. 2004).

γδ T cell Activation Leads to Increased Amounts of Transcripts Associated with Protein Synthesis

In order to increase translation, γδ T cell activation resulted in the expression of genes associated with ribosome production and protein synthesis (*Table 3.6*). Ribosome synthesis takes place in nucleoli, and transcripts for nucleolar proteins were also more abundant following activation. Transcripts for proteins involved in nuclear mRNA splicing were increased, as were those for translation initiation factors, translation elongation factors, and translation termination factors. Transcripts for enhancing transcription and translation appeared following activation. Increased protein production also requires increased amounts of tRNA and some transcripts for enzymes used in tRNA formation were upregulated.

In addition to upregulating the expression of genes necessary for increased protein synthesis, γδ T cells also upregulated the expression of genes necessary for the proper folding of these proteins (*Table 3.7*) such as chaperones and heat shock proteins (HSPs). Transcripts for some proteins that interact with HSPs were also upregulated as were those for proteins that thread other proteins into mitochondria.

γδ T cell activation led to an increase in proteins that are important in nuclear import (*Table 3.8*). Importins bind to and serve as carriers for proteins with nuclear import signals in the cytoplasm that are destined for the nucleus. Once inside the nucleus, Ran-GTP binds to protein/carrier complexes and leads to their dissociation. In order to keep Ran-GTP in the nucleus and Ran-GDP in the cytoplasm, the RanGEF Chc1 (Rcc1) is found in the nucleus while RanGAP is found in the cytoplasm. Ranbp1, which binds to Ran and enhances the activity of RanGAP, is also found in the cytoplasm. The expression of Importin 4 (Ipo4; RanBP4) and Importin 7 (Ipo7/Imp7), Ran, Chc1, Ranbp1, and Nup62, a nucleoporin, was increased after γδ T cell activation.

γδ T cell Activation Leads to Changes in Cell Proliferation- and Apoptosis-Related Transcripts

The activation of γδ T cells led to the expression of both pro- and anti-apoptotic molecules (*Table 3.9*). Apoptotic cells can be stained using Annexin V because it binds to phosphatidylserine that appears on the cell surface during apoptosis. Transcripts for Phospholipid scramblase (Plscr1) were detected following activation. This enzyme is capable of moving phospholipids between lipid bilayers and may be responsible for the appearance of phosphatidylserine on the surface of apoptotic cells. However, it does not appear that all activated γδ T cells undergo apoptosis because some of these cells blast and divide and the expression of Myc was increased after activation. Myc is an important oncogene and it can regulate the expression of numerous growth-related genes.

When blasting and dividing, γδ T cells are expected to express cell cycle-associated proteins. In fact, transcripts for cell-cycle associated proteins, such as those for Chc1 (*Table 3.8*), Cyclin D2, Pcna, Cdkn1a (CIP1), and Cdc34, were all increased following activation. On the other hand, the expression of Cdc25b was lost after activation.

Increased expression of JunB was observed following activation and was accompanied by increased expression of the transcription factor Atf3. In the absence of c-Jun or JunB, Atf3 forms a homodimer that represses transcription (Chen, Liang et al. 1994). On the other hand, Atf3 can form a heterodimer with JunB that activates transcription (Hsu, Bravo et al. 1992). Thus, the expression of both JunB and Atf3 suggests that the resulting heterodimer should promote transcription.

Bcl-2 and Bcl2l1 (Bcl-XL) are anti-apoptotic molecules. After activation, the expression of Bcl2l1 was increased. Bcl2l1 prevents the activation of caspases by preventing the release of cytochrome c (Cycs), whose expression was increased after activation, from mitochondria.

Additionally, increases in expression following activation were observed with Apex1, Dusp2, Ier3, Mapk6 (Erk3), Pinx1, and Ssrp1, and transcripts of Nr4a1 (Nur77) and the related Nr4a2 (Nurr1) appeared following activation while those for Pdcd4 were reduced.

γδ T cell Activation Leads to Changes in the Wnt Signaling Pathway

The activation of γδ T cells led to a reduction in genes associated with Wnt signaling (*Table 3.10*). Wnt signaling revolves around the stabilization of β-catenin (Catnb) and is important in early T cell development. Normally, a complex of Glycogen synthase kinase-3 beta (GSK-3β; Gsk3b), Axin and Adenomatous polyposis coli (Apc) phosphorylates β-catenin, which leads to its degradation. In the absence of GSK-3β, β-catenin can accumulate and interact with transcription factors like LEF (Lef1) and TCF-1 (Tcf7), which leads to gene expression, including that of Cyclin D2. In addition to these proteins, numerous other proteins act to enhance or repress parts of this signaling pathway.

Ruvbl1 (Pontin52), binds to β-catenin and Lef1 and Tcf7 (Bauer, Huber et al. 1998) and integrin-linked kinase (Ilk) has been found to allow β-catenin to accumulate in the nucleus and interact with Lef1. Transcripts for Ruvbl1 were increased after activation suggesting that the ability of β-catenin to interact with Lef1 and Tcf7 was enhanced following γδ T cell activation. On the other hand, Ilk levels were found to decrease following activation, suggesting that the stabilization of β-catenin is reduced following γδ T cell activation.

Transcripts for Frat2 were reduced 12 hours after activation and transcripts for Frat1 were lost in one experiment and not detected in another. Frat2 is a homolog of Frat1 and both proteins are capable of binding to GSK-3β and Dishevelled. This leads to the stabilization of β-catenin, which can then associate with transcription factors like Lef1 and Tcf7. It has been found that a carcinoma cell line NT2/D1 that is induced to differentiate by adding retinoic acid also downregulates Frat2 (Freemantle, Portland et al. 2002). However, the upregulation of Frat1 and Frat2 is often observed in cancers where it promotes the accumulation of β-catenin. Given that Frat1, Frat2, and Ilk enhance the accumulation of β-catenin, reduced levels of these molecules may lead to a requirement for stronger Wnt signals following activation because there would be increased phosphorylation of β-catenin. However, transcripts for GSK-3β were also reduced after

activation, suggesting that γδ T cell activation may induce a reduction in the entire pathway.

In addition to the reduction in Frat2, Lef1 and Tcf7 levels were also greatly reduced following activation. Both of these proteins play an important role in T cell development (Staal and Clevers 2000). Similar to the loss of IL-7 receptor, the reduction in Frat2, Lef1, and Tcf7 indicates that the activation of G8 γδ T cells appears to change their requirements for survival.

Axin is often found downregulated in human hepatocellular carcinomas (HCCs), suggesting that these should exhibit increased signaling through the Wnt pathway due to a decreased phosphorylation and breakdown of β-catenin. It has been reported that the forced expression of Axin in the colon-cancer cell line LoVo leads to the expression of Axud1 (Axin1 up-regulated), suggesting that Axud1 expression is a sign of reduced signaling through the Wnt pathway (Ishiguro, Tsunoda et al. 2001). Axin appears to be only minimally downregulated following the activation of γδ T cells. However, Axud1 transcripts are increased after activation. Assuming that Axud1 is expressed in the absence of Wnt signaling, this suggests that Wnt signaling is reduced following the activation of γδ T cells. Along those lines, γδ IELs, which appear to be constitutively-activated γδ T cells, were previously found to express much lower levels of Lef1 and Tcf7 than mesenteric lymph node $CD8^+$ αβ T cells.

γδ T cell Activation Reduces the Expression of Krüppel-like Factors

Krüppel-like factors are related zinc-finger proteins. Constitutively-activated γδ IELs were found to express lower levels of some Krüppel-like factors than mesenteric lymph node $CD8^+$ αβ T cells. Similarly, γδ T cell activation led to the loss of expression of the Krüppel-like factors Klf3 and Klf7 and the expression of Klf13 was reduced (*Table 3.11*). Klf3 has been reported to be a strong transcriptional repressor in conjunction with CtBP2 (Turner and Crossley 1998). Klf7 has been shown to play a role in stopping cell-cycle progression by promoting G_1 arrest (Laub, Aldabe et al. 2001). Klf13, also known as RFLAT-1, is involved in the expression of RANTES and is translationally controlled.

γδ T cell Activation Induces the Expression of Some Cell-Surface Molecules

In order to identify activated γδ T cells that are participating in immune responses, it is helpful to know how these activated γδ T cells differ phenotypically from resting γδ T cells. The ability to detect activated γδ T cells could help in the identification of ligands that activate γδ T cells. The microarray data was thus analyzed for the expression of cell-surface markers following activation.

It addition to the expression of the very early maker of activation, CD69, γδ T cell activation led to the upregulation of BTLA, CD5 (Ly1), CD6, CD160, CTLA-4, Crtam, PD-1 (Pdcd1), Lag-3, and Sca-1/Ly6A (*Table 3.12*). All of these molecules, except for maybe CD160 and Crtam, appear to be involved in the attenuation of immune responses – mostly, through the recruitment of phosphatases that attenuate kinase cascades.

CD5 has been shown to lower T cell activation and the thymocytes of CD5-deficient mice exhibit more extreme levels of activation in response to CD3 stimulation (Tarakhovsky, Kanner et al. 1995). In addition, CD5-deficient peripheral T cells proliferate more than normal T cells following activation (Tarakhovsky, Kanner et al. 1995; Pena-Rossi, Zuckerman et al. 1999). It has also been found that T cells that are cultured in the absence of MHC show reduced levels of CD5 expression (Smith, Seddon et al. 2001). It has thus been postulated that CD5 helps tune TCR signaling in cases where the TCR can signal (Azzam, DeJarnette et al. 2001) and that it may play a similar role in some autoreactive B-1 B cells. It has been proposed that this is accomplished by recruiting the tyrosine phosphatase SHP-1.

CD6 and CD5 are closely related and map to nearly-adjacent loci. CD6 becomes phosphorylated after TCR ligation and may function as a co-stimulatory molecule but might also help prevent the apoptosis of cells following activating stimuli.

Stains for CD5 expression revealed that moderate levels are found on G8 γδ T cells and that their activation leads to higher levels of expression. While CD5 levels of naïve G8 γδ T cells were lower than those of αβ T cells, the fact that CD5 is expressed by naïve γδ T cells suggests that CD5 would not be exceptionally suitable for the identification of activated γδ T cells.

CTLA-4 is an important molecule involved in the attenuation of TCR signals. Mice deficient in CTLA-4 develop large numbers of autoreactive T cells, which suggests that CTLA-4 attenuates TCR signals (Waterhouse, Penninger et al. 1995). CTLA-4 binds B7-1 (Linsley, Brady et al. 1991) and B7-2 (Freeman, Gribben et al. 1993), which ensures that it can both associate with molecules on the antigen presenting cell side of the immunological synapse and compete with the costimulatory molecule CD28, thereby reducing the ability of CD28 to accumulate in the synapse. Similar to CD5, CTLA-4 can associate with SHP-1. In addition, it can associate with SHP-2 and PP2A. BTLA has also been reported to associate with SHP-1 and SHP-2 (Watanabe, Gavrieli et al. 2003).

PD-1 appears to have a similar function to CTLA-4 when it comes to preventing the appearance and proliferation of autoreactive T cells. It has been reported that C57Bl/6 mice that are deficient in PD-1 develop glomerulonephritis while similar mice on a BALB/c background develop dilated cardiomyopathy. These diseases are not as severe as those observed in CTLA-4 knockout mice, but nevertheless indicate the importance of this molecule in preventing autoimmune disease. PD-1 plays a role during thymocytes selection, where it may function similarly to CD5 by attenuating signals from the TCR. Thus, the absence of PD-1 may lead to increased negative selection since TCR signaling is stronger (Blank, Brown et al. 2003).

Stains for PD-1 expression revealed that naïve G8 γδ T cells expressed almost no PD-1 and that activated G8 γδ T cells expressed detectable levels thereof. In addition, PD-1 expression was found on some γδ T cells in normal mice and was usually accompanied by a lack of CD8α expression. Thus, PD-1 may be a suitable marker for the detection of activated γδ T cells. However, analyses of γδ T cells that bind T22 tetramers showed that their expression of PD-1 did not differ greatly from that of other γδ T cells, suggesting that PD-1 expression may not always be an indicator of γδ T cells that have recognized ligands through their γδ TCRs (*data not shown*).

Lag-3 (CD223) binds to MHC class II. It has been shown that this molecule can activate dendritic cells and that this molecule may, at the same time, play an inhibitory role in T cell activation. G8 γδ T cells do not recognize MHC class II through the γδ TCR. Thus, Lag-3 represents a molecule that is expressed and is not expected to interfere with the recognition of the actual ligand, T10/T22, suggesting that the activation of γδ T

cells results in the expression of large numbers of inhibitory molecules in the hope that some of these will downregulate their responses. This also suggests that G8 γδ T cells are desensitized and perhaps broadly tolerized following activation.

Stains for Lag-3 expression revealed that it, like PD-1, is not expressed on naïve G8 γδ T cells and is readily detectable on them after activation. Thus, Lag-3 may also be a suitable marker for the detection of activated γδ T cells. Interestingly, PD-1 appears to stain more γδ T cells in conventional mice than Lag-3. In addition, PD-1 and Lag-3 do not stain activated G8 γδ T cells on a narrow diagonal, suggesting that their levels may be independently regulated.

Somewhat in contrast to the expression of different inhibitory receptors, γδ T cell activation leads to the expression of CD160 (BY55), which binds MHC class I and MHC class I-like molecules. This molecule functions as an activating NK receptor (Barakonyi, Rabot et al. 2004) and is also found on activated cytotoxic T cells and all intraepithelial lymphocytes (Agrawal, Marquet et al. 1999). However, it does not signal on its own since it is attached to the surface of cells via a GPI anchor. It has been postulated that this molecule may be important in the generation of memory cells so that these cells continue to receive an activating signal from their environment even though their peptide/MHC ligands may no longer be present and their CD28 levels are reduced.

γδ T cell Activation Reduces the Levels of CD1d Transcripts

CD1d molecules are involved in the presentation of lipid antigens to T cells and are very important in the activation of NK T cells. Transcripts for CD1d1 and CD1d2 and transcripts for Prosaposin, which is involved in the loading and editing of lipids in CD1, were decreased following activation (*Table 3.13*). This suggests that activated γδ T cells are less likely to activate NK T cells. However, reduced surface levels of CD1d were not observed on G8 γδ T cells 24 hours after activation, suggesting that the effects of reduced levels of CD1d transcripts are not immediately observable due to existing CD1d or are counterbalanced by increased translation and/or increased total RNA levels.

γδ T cell Activation Leads to Changes in Metabolism-Associated Transcripts

Activation resulted in the upregulation of transcripts for Hexokinase 2 and Serine racemase (*Table 3.14*). The rest of the enzymes involved in glycolysis also tended to show increases following activation, but not as extreme. In addition, some of these enzymes may also be upregulated as a result of long-term culture.

Hexokinase 2 is responsible for the first committed step in the catabolism of glucose, which is present at a concentration of 2 grams per liter in RPMI 1640. This leads to the formation of glucose-6-phosphate at a cost of 1 ATP molecule. Unlike liver and muscle cells, lymphocytes are not known for having vast glycogen stores and there are only so many nucleotides that can be converted into triphosphates. Thus, transcript levels for this enzyme should be relatively low in resting cells and, at least at the 12 hour timepoint, were not upregulated solely in response to the presence of glucose in the media.

Serine racemase is normally seen as an enzyme that interconverts L-serine and D-serine. L-serine is an amino acid that is found in proteins. D-serine functions as a neurotransmitter by binding to the glycine site of N-methyl D-aspartate (NMDA) types of glutamate receptors (reviewed in (Schell 2004)). It is interesting that γδ T cell activation results in the upregulation of an enzyme that is capable of forming a neurotransmitter because this may allow the nervous system to detect the presence of an immune response. This enzyme has also recently been found to efficiently catalyze the elimination of serine to pyruvate (De Miranda, Panizzutti et al. 2002; Strisovsky, Jiraskova et al. 2003). Glycolysis also leads to the formation of pyruvate so the expression of this enzyme may have to do with the utilization of the 30 mg/l L-serine in the media in order to generate additional pyruvate.

Additional activation-induced changes were also observed in enzymes that are responsible for the synthesis of nucleotides. *De novo* nucleotide synthesis relies heavily on the folate cycle and an inhibitor thereof, Methotrexate, is used clinically to interfere with this process in order to prevent the DNA replication that must occur for proper cell division. Folate cannot be synthesized by mammalian cells and some of the transporters for folate, Rfc-1 and Folr4, are expressed following activation. The expression of receptors for folate has been observed in rapidly dividing cells during development

(Maddox, Manlapat et al. 2003). Serine and glycine allow for the initial conversion of tetrahydrofolate (THF) to N^5,N^{10}-methylene-THF. While the transcripts for the enzymes required for this step were not detected by microarray, this may have been due to issues with the detection of the transcripts. However, the enzymes that are capable of converting N^5,N^{10}-methylene-THF into N^5,N^{10}-methenyl-THF and then into N^{10}-formyl-THF, the NAD+ and NADP+ dependent methylene-THF dehydrogenases, were upregulated. In addition, transcripts for the enzyme Phosphoribosylglycinamide formyltransferase that converts N^{10}-formyl-THF back into THF were upregulated 12 hours after activation.

Many of the final enzymes required for the *de novo* synthesis and salvage of nucleotides were also upregulated following activation. These included CTP synthase, Adenylosuccinate lyase, Adenylosuccinate synthase, GMP synthase, IMP dehydrogenase 2, Dihydroorotate dehydrogenase, Uridine/Cytidine kinase, Adenylate kinase 2, and Thymidylate synthase. Given that activation leads to enhanced levels of RNA synthesis, DNA replication, and cell division, it makes sense that the expression of enzymes required for nucleotide synthesis and salvage need to be increased.

Activation Leads to the Activation of B Cells

During the activation of γδ T cells, it was observed that the γδ T cells were not the only cells that became $CD69^+$. A further analysis showed that a large percentage of B cells also became $CD69^+$, albeit at expression levels that were about 10-fold lower than those observed on γδ T cells.

It has been reported that the binding of MHC class II on immature dendritic cells by Lag-3 can induce the maturation of these cells (Andreae, Buisson et al. 2003; Buisson and Triebel 2003). In addition, it has recently been observed by members of Mark M. Davis' lab that T cell activation induces a brief calcium flux in B cells that serve as antigen presenting cells. Perhaps, the ligation of T10/T22 on B cells by G8 γδ T cells was directly inducing the expression of CD69 on both cells. Thus, experiments were designed to determine the source of CD69-expression by B cells and are discussed in Chapter 4.

Conclusions

Unlike the activation of G8 γδ IELs that was studied in Chapter 2, the activation of splenic G8 γδ T cells led to large changes in the transcripts they expressed. Among those changes, it appears that activated γδ T cells express genes associated with effector functions, such as Granzyme B and IFNγ, but also express genes that have been shown to diminish TCR signaling, such as BTLA, CD5, CD6, CTLA-4, Lag-3, and PD-1. Thus, activated γδ T cells may attain effector functions but may also shut down at the same time. It will be important to see if G8 γδ T cells can be activated in a way that does not result in their expression of inhibitory molecules. In addition, it will be important to determine whether the responses of *in vivo*-activated G8 γδ T cells differ from what has been observed *in vitro*.

Figure Legends

Figure 3.1: T10/T22 expression is strain dependent, inducible, and higher on B cells in the blood than in the spleen

(A) Splenocytes were isolated from BALB/c (blue), B10.BR (red), and C57Bl/6 mice (black) and stained using a biotin-conjugated anti-T10/T22 antibody (hamster; clone 7H9) and FITC- and PE-conjugated antibodies to identify NK cells (anti-CD49b; rat IgM; clone DX5), γδ T cells (anti-TCRδ; hamster; clone GL3), granulocytes (anti-Ly6G/Ly6C; rat IgG2b; clone RB6-8C5), αβ T cells (anti-TCRβ; hamster; clone H57-597), $CD19^+$ $B220^+$ and $B220^{low}$ B cells (anti-CD19; rat IgG2a; clone 6D5) (anti-B220; rat IgG2a; clone RA3-6B2), $CD11c^+$Mac-1^+ dendritic cells, and $CD11c^{neg}$Mac-1^+ monocytes/macrophages (anti-CD11c; hamster; clone HL3) (anti-Mac-1; rat IgG2b; clone M1/70.15). Macrophages/monocytes were further subdivided into granular (thin line) and non-granular (thick line) cells based on their side scatter profile. 7H9 was detected using allophycocyanin-conjugated streptavidin. Prior to the addition of any labeled antibodies, cells were blocked using 50 μl/well of 10 μg/ml of anti-CD16/CD32 in FACS wash (PBS with 5 mM EDTA, 0.1% sodium azide, and 5% FCS) for 20 minutes and then by adding 50 μl/well of 10 μg/ml anti-CD16/CD32, 10% hamster serum, 10% mouse serum, 300 μg/ml mouse IgG, and 300 μg/ml rat IgG in FACS wash for 20 minutes. Cells were then stained by adding 50 μl/well of labeled antibodies for an additional 30 minutes. (B) Splenocytes from a C57Bl/6 mouse were incubated with a mix of bacteria at 37°C for 2 hours and granulocytes were analyzed for T10/T22 expression. (C) Cells were isolated from the blood and spleen of a C57Bl/6 mouse and $CD19^+$ $B220^+$ and $B220^{low}$ B cells were analyzed for T10/T22 expression. (D) Splenic $CD19^+$ $B220^+$ and $B220^{low}$ B cells were further analyzed for CD5 and IgD expression.

Figure 3.2: γδ T cells and αβ T cells show a different distribution in the spleen, mesenteric lymph node, and thymus of a G8 BALB/c mouse

The spleen, mesenteric lymph node, and thymus of a G8 BALB/c mouse was frozen and cut into 10 μm sections. The sections were fixed using acetone and stained with FITC-conjugated anti-TCRβ antibodies (green) and PE-conjugated anti-TCRδ

antibodies (red) and nuclei were stained with DAPI (blue). The red, green, and blue channels of the inverted images are shown on the right.

Figure 3.3: Splenic G8 γδ T cells and αβ T cells express similar genes

Splenocytes of G8 BALB/c mice were stained with antibodies to the TCR β chain and the TCR δ chain and $2.0x10^6$ $\alpha\beta TCR^+\gamma\delta TCR^-$ and $1.6x10^6$ $\alpha\beta TCR^-\gamma\delta TCR^+$ cells were sorted on ice. Their RNA was isolated, amplified using two rounds of *in vitro* transcription, and analyzed using Affymetrix microarrays. Expression levels of transcripts that were not called absent in both samples are shown as plus signs where the *x* and *y* axis values represent their detected levels in αβ T cells and γδ T cells, respectively.

Figure 3.4: Lymphoid organs are different in G8 $RAG2^{KO}$ BALB/c mice

(A) The G8 $RAG2^{KO}$ BALB/c has a thymus that is small compared to what would be found in G8 BALB/c and BALB/c mice. (B) The G8 $RAG2^{KO}$ BALB/c mouse has small but detectable mesenteric lymph nodes. Sections from the (C) spleen and (D) small intestine were stained with antibodies to detect dendritic cells (CD11c; green) and γδ T cells (red) and nuclei were stained with DAPI (blue). The red, green, and blue channels of the inverted images are shown on the right.

Figure 3.5: G8 γδ T cell activation leads to TCR downregulation, the expression of CD69 and CD44, blasting, and cell division

G8 $RAG2^{KO}$ BALB/c splenocytes were cultured (A) alone or cocultured for either (B) 1 day or (C) 2 days in the presence of a five-fold excess of $H2^{b/d}$ BALB/c splenocytes and analyzed for CD69 expression (*x* axis) and γδ TCR levels (*y* axis). (D) The expression of the activation marker CD44 was assayed on G8 γδ T cells after 1 day of coculture with BALB/c (gray shaded area) or $H2^{b/d}$ BALB/c cells (black line). G8 γδ T cells were labeled with CFDASE and cocultured with either BALB/c splenocytes (shaded regions) or $H2^{b/d}$ BALB/c splenocytes (lines) for 14 (black/gray), 45 (blue), or 92 hours (red) and analyzed for (E) cell size based on forward scatter and (F) CFSE levels.

Figure 3.6: B10.BR and $H2^{k/d}$ BALB/c splenocytes do not activate G8 γδ T cells as well in cocultures as *b* haplotype-expressing splenocytes

G8 $RAG2^{KO}$ BALB/c splenocytes were incubated with a five-fold excess of (A) B10.BR or (B) $H2^{k/d}$ BALB/c splenocytes for 1 day and analyzed for γδ TCR levels and CD69 expression. $H2^{k/d}$ BALB/c splenocytes were obtained by crossing BALB/c mice with BALB.K mice.

Figure 3.7: G8 γδ T cell activation leads to large changes in gene expression

RNA was isolated from sorted splenic G8 $RAG2^{KO}$ BALB/c γδ T cells after coculture with a five-fold excess of either BALB/c or $H2^{b/d}$ BALB/c splenocytes and subjected to Affymetrix microarray analysis after PCR-based cDNA amplification. Gene expression levels were then compared between G8 $RAG2^{KO}$ BALB/c γδ T cells that had been cultured for 12 hours and those that had been cocultured for 4 days in the presence of a five-fold excess of either (A) BALB/c or (B) $H2^{b/d}$ BALB/c splenocytes. Gene expression levels were also compared after (C) 4 days or (D and E) 12 hours of coculture with BALB/c and $H2^{b/d}$ BALB/c stimulator cells. (A – D) Affymetrix U74 'A' arrays were analyzed for one experiment and (E) U74v2 'A,' 'B' and 'C' arrays were analyzed for another.

Table Legends

Tables 3.1 – 3.14: Microarray analysis of G8 γδ T cell activation

The first eight columns show the gene expression levels for genes in G8 γδ T cells after the indicated culture conditions. Numbers in gray indicate that the expression of a gene was called "absent" in that sample based on the probe set used for its detection. Some genes were detected by more than one probe set with differing efficiencies. "---" indicates that no value was available for a particular probe set (e.g., when the probe set was on a 'B' array and only an 'A' array was run).

The first four columns are for 12 hour and 4 day cocultures with BALB/c ($+H2^{d/d}$) and $H2^{b/d}$ BALB/c ($+H2^{b/d}$) splenocytes where PCR-based cDNA amplification was used prior to probe synthesis. Only the 'A' array of the U74 array set was used. The next three columns are for 12 hour cocultures with either BALB/c ($+H2^{d/d}$), $H2^{b/d}$ BALB/c, or a 50%/50% mix of the two (+Mix) where PCR-based cDNA amplification was also used prior to probe synthesis. All three arrays of the U74v2 array set were used. The next two columns are for sorted freshly-isolated γδ T cells and αβ T cells from a G8 BALB/c mouse where two rounds of *in vitro* transcription were used for probe synthesis. All three arrays of the U74 array set were used. The U74 and U74v2 array sets differ in that a large number of probe sets were erroneous in the U74 set. These erroneous probe sets are known and were omitted from the analysis.

The next two columns indicate the fold difference in expression between the genes in 12 hour samples that were incubated with either $H2^{b/d}$ BALB/c or BALB/c splenocytes. The first column is a comparison of columns 1 and 3. The second column is a comparison of columns 5 and 7. A positive number indicates that the expression of a gene was increased during G8 γδ T cell activation while a negative number indicates that the expression of a gene was decreased. A '1' or '-1' fold change indicates that the gene's expression did not change. A 2-fold change is indicative of a doubling in a gene's expression. The following Microsoft Excel formula was used for the fold change calculation, where *val_1* and *val_2* were the two expression values that were being compared:

=IF(ISNUMBER(*val_1*),EXP(ABS(LN(*val_2*/*val_1*)))*LN(*val_2*/*val_1*)/ABS(LN(*val_2*/*val_1*)),"---")

The next columns indicate the current gene's symbol in Entrez followed by the gene's name and probe set used for its detection in that row.

Figure 3.1: T10/T22 expression is strain dependent, inducible, and higher on B cells in the blood than in the spleen

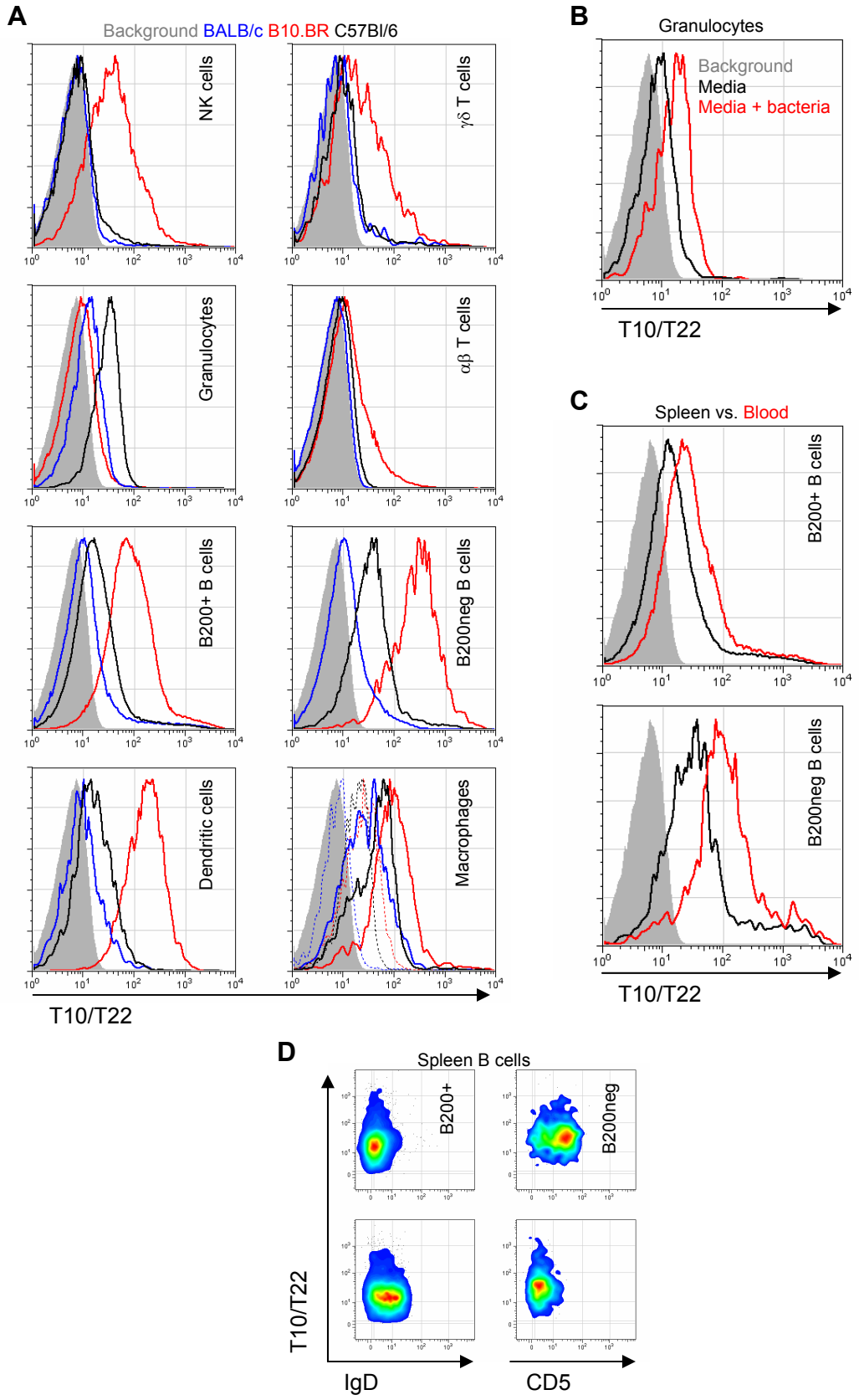

Figure 3.2: γδ T cells and αβ T cells show a different distribution in the spleen, mesenteric lymph node, and thymus of a G8 BALB/c mouse

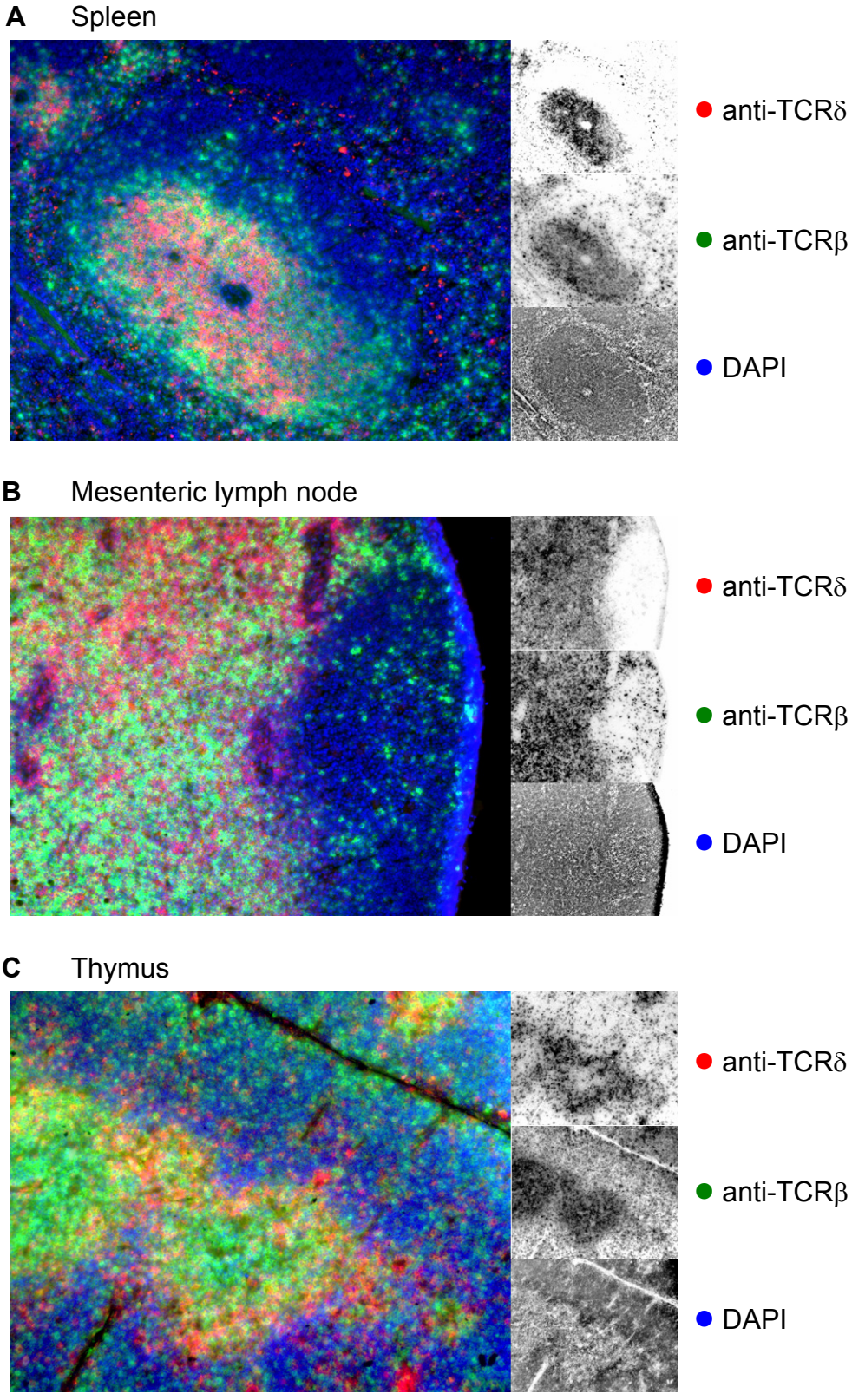

Figure 3.3: Splenic G8 γδ T cells and αβ T cells express similar genes

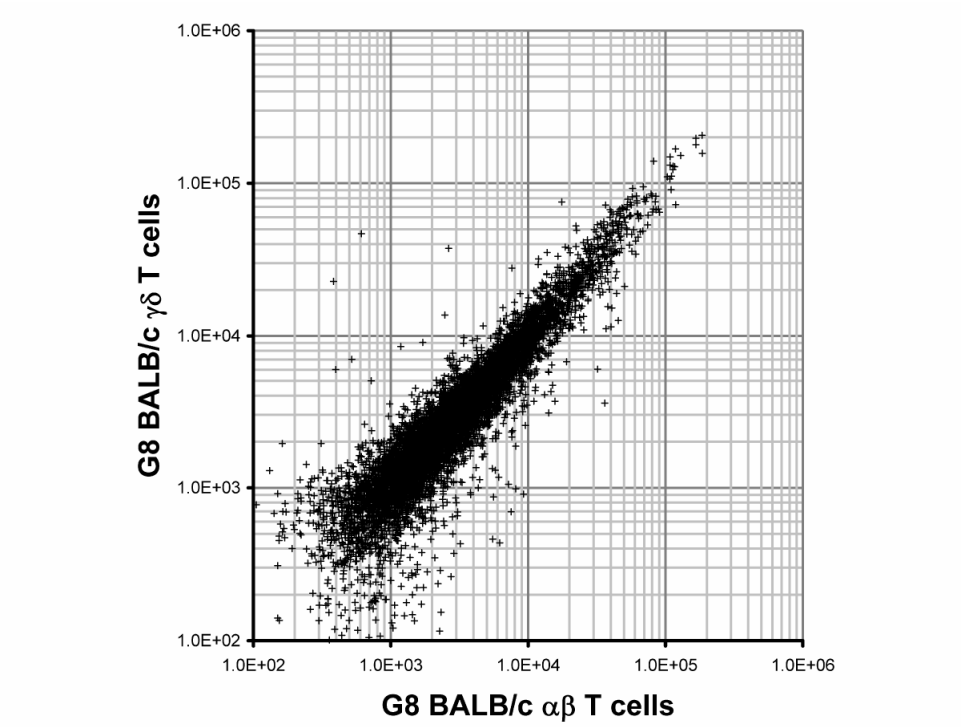

Figure 3.4: Lymphoid organs are different in G8 RAG2^{KO} BALB/c mice

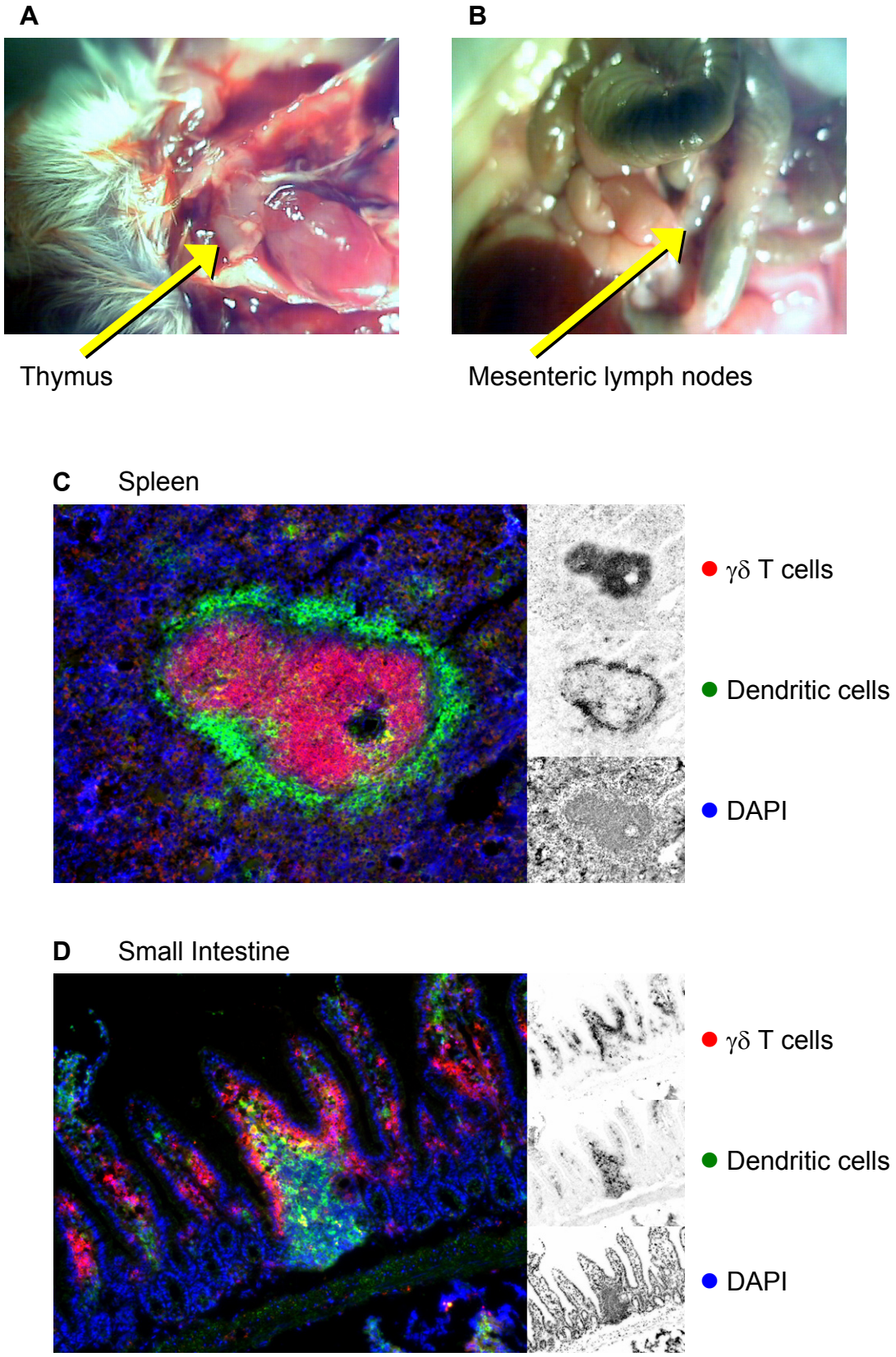

Figure 3.5: G8 γδ T cell activation leads to TCR downregulation, the expression of CD69 and CD44, blasting, and cell division

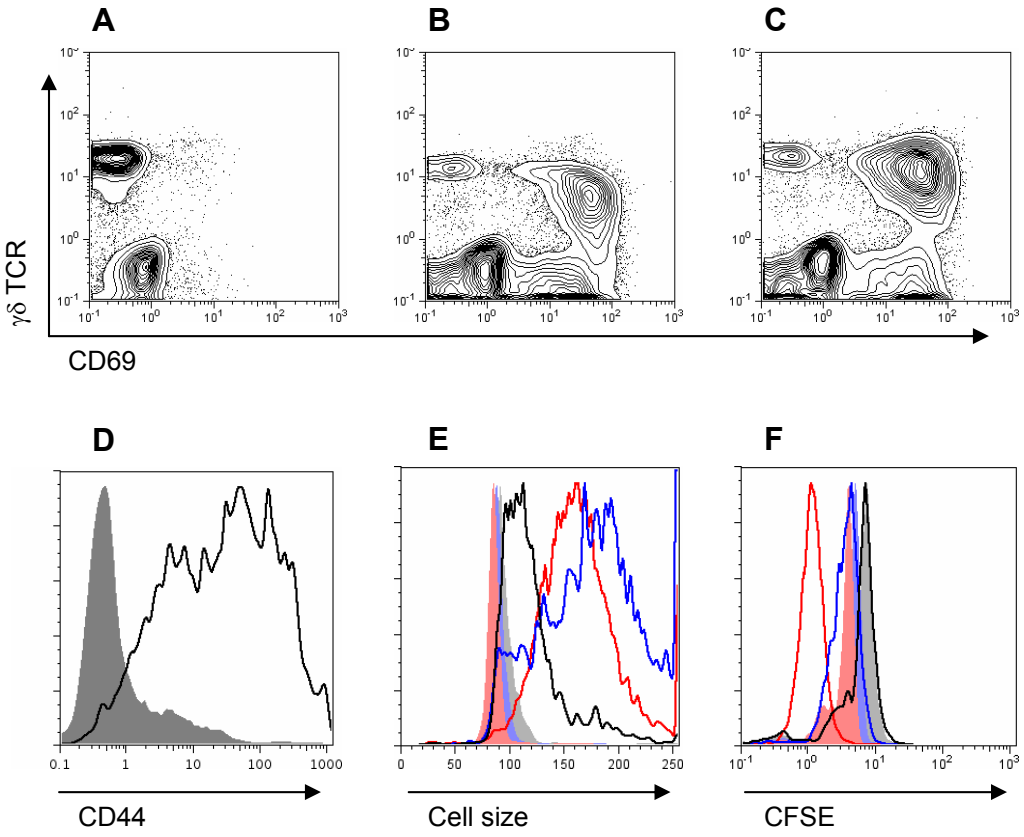

Figure 3.6: B10.BR and $H2^{k/d}$ BALB/c splenocytes do not activate G8 γδ T cells as well in cocultures as *b* haplotype-expressing splenocytes

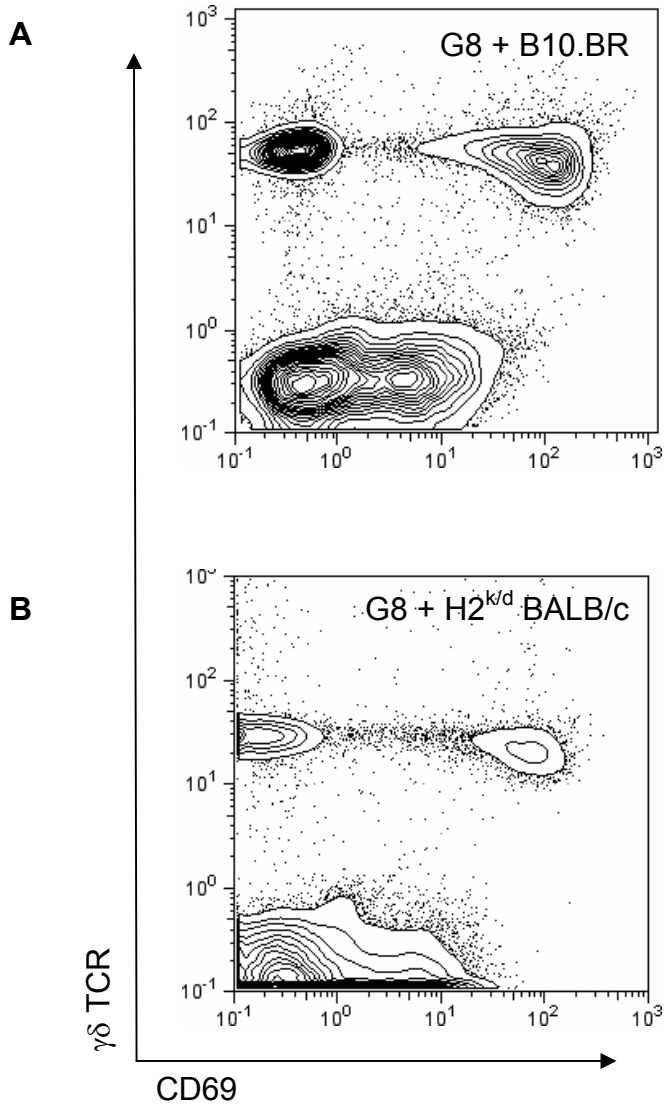

Figure 3.7: G8 γδ T cell activation leads to large changes in gene expression

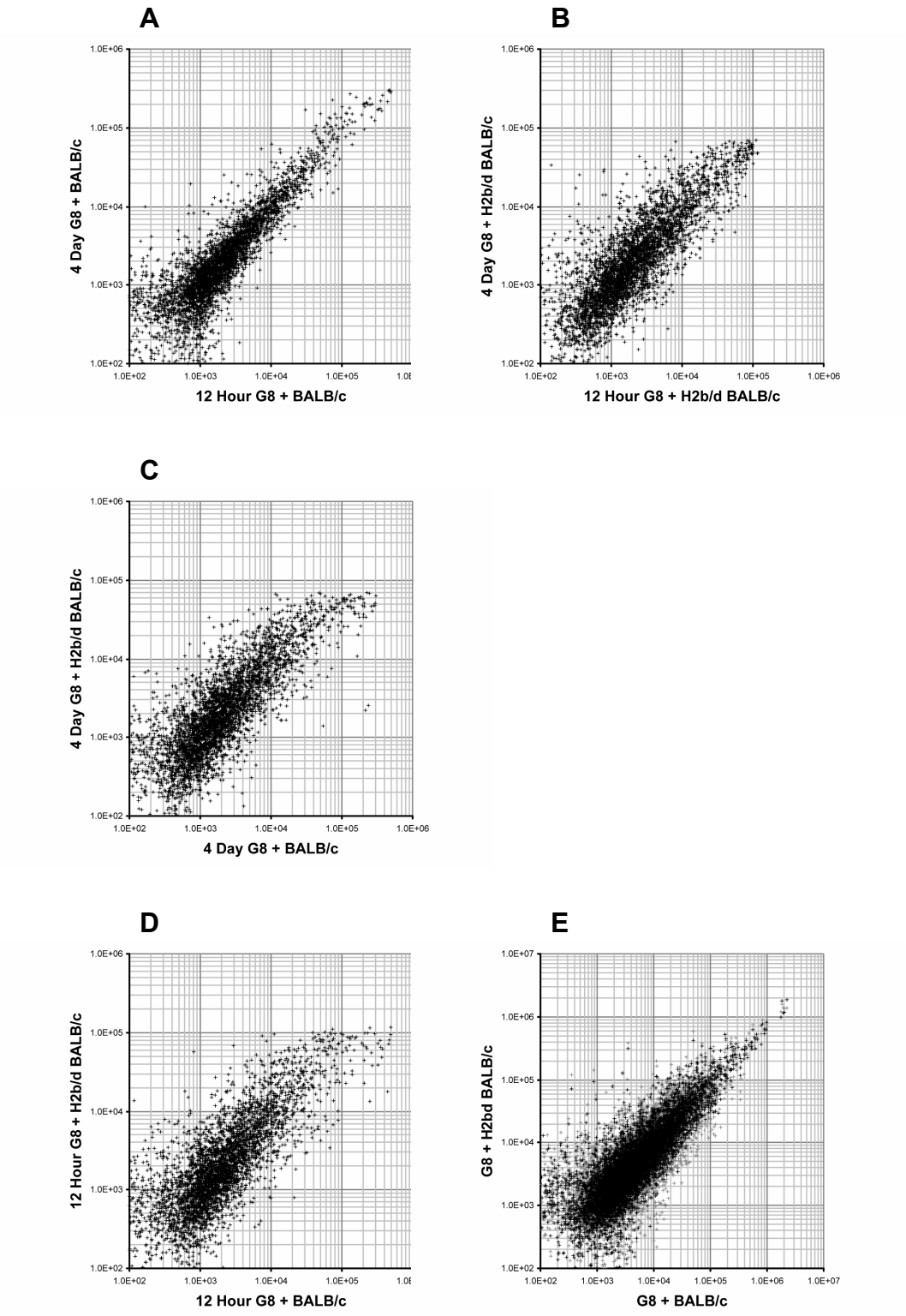

Table 3.1: Activation-induced changes

+H2$^{d/d}$ 12 hr	+H2$^{d/d}$ 4 day	+H2$^{b/d}$ 12 hr	+H2$^{b/d}$ 4 day	+H2$^{b/d}$ 12 hr	+Mix 12 hr	+H2$^{d/d}$ 12 hr	γδ T	αβ T	change		Gene	Name	Probe set
---	---	---	---	132896	127662	2815	---	---	---	47	Cd69	CD69 antigen	164220_at
1910	1666	13586	6410	7035	3853	1374	10443	14006	7	5	Itgav	integrin alpha V	104386_f_at
29211	36898	6962	52479	48807	118691	337806	21233	19656	-4	-7	Itgb7	integrin beta 7	100906_at
---	---	---	---	1166	1591	5141	---	---	---	-4	Itgb7	integrin beta 7	162193_f_at
3840	1734	1179	1607	2246	2597	6747	5155	4979	-3	-3	Sell	selectin, lymphocyte	102838_at

Table 3.2: TCR-associated transcripts

+H2$^{d/d}$ 12 hr	+H2$^{d/d}$ 4 day	+H2$^{b/d}$ 12 hr	+H2$^{b/d}$ 4 day	+H2$^{b/d}$ 12 hr	+Mix 12 hr	+H2$^{d/d}$ 12 hr	γδ T	αβ T	change		Gene	Name	Probe set
582	167	181	361	400	286	1506	682	598	-3	-4	Cd3d	CD3 antigen, delta polypeptide	92683_at
---	---	---	---	4571	7181	10215	22050	16928	---	-2	Cd3e	CD3 antigen, epsilon polypeptide	115906_at
12852	8547	4801	6176	7976	9735	15263	2724	5124	-3	-2	Cd3z	CD3 antigen, zeta polypeptide	102287_at
2784	3519	881	846	5543	7506	12954	6456	2801	-3	-2	Tec	cytoplasmic tyrosine kinase, Dscr28C related (Drosophila)	103539_at
2344	2122	682	2019	1593	4181	11520	2569	2560	-3	-7	Dock2	dedicator of cyto-kinesis 2	103462_at
24010	16952	4156	31136	11732	36725	93774	9668	12825	-6	-8	Dgka	diacylglycerol kinase, alpha	103596_at
---	---	---	---	1872	4034	5604	---	---	---	-3	Dgka	diacylglycerol kinase, alpha	165071_r_at
24010	16952	4156	31136	11732	36725	93774	9668	12825	-6	-8	Dgka	diacylglycerol kinase, alpha	103596_at
---	---	---	---	1872	4034	5604	---	---	---	-3	Dgka	diacylglycerol kinase, alpha	165071_r_at
---	---	---	---	2316	7730	16598	---	---	---	-7	Evl	Ena-vasodilator stimulated phosphoprotein	160667_at
---	---	---	---	17875	49534	152295	---	---	---	-9	Evl	Ena-vasodilator stimulated phosphoprotein	161808_f_at
---	---	---	---	1282	1468	2967	1849	3126	---	-2	Fyb	FYN binding protein	105541_at
---	---	---	---	2061	2703	4814	1218	586	---	-2	Fyb	FYN binding protein	110736_at
---	---	---	---	14040	31412	43509	49430	41791	---	-3	Fyb	FYN binding protein	110738_at
---	---	---	---	671	242	149	---	---	---	5	Fyb	FYN binding protein	166264_at
2677	1242	5551	1375	5122	5283	2121	5172	10411	2	2	Fyn	Fyn proto-oncogene	100133_at
---	---	---	---	3080	1850	439	---	---	---	7	Fyn	Fyn proto-oncogene	169541_i_at
11704	12225	13060	9386	10799	13642	15963	13327	12935	1	-1	Itk	IL2-inducible T-cell kinase	103028_at
45539	74597	14004	32394	8306	16489	35183	60680	54704	-3	-4	Itpr5	inositol 1,4,5-triphosphate receptor 5	101441_i_at
22179	32945	3485	13474	4995	8132	12455	17622	12194	-6	-2	Itpr5	inositol 1,4,5-triphosphate receptor 5	101442_f_at
---	---	---	---	1046	1281	1340	1893	2043	---	-1	Itpr5	inositol 1,4,5-triphosphate receptor 5	113336_at
2124	2286	2063	2441	4836	4261	5630	2418	1945	-1	-1	Lat	linker for activation of T cells	102228_at
4192	3075	5519	2632	12740	10812	4593	4852	4453	1	3	Lcp2	lymphocyte cytosolic protein 2	102957_at
8611	11818	10418	15997	57184	57958	72286	10277	13087	1	-1	Lck	lymphocyte protein tyrosine kinase	102809_s_at
---	---	---	---	9198	10973	16312	---	---	---	-2	Lck	lymphocyte protein tyrosine kinase	161265_f_at
---	---	---	---	13562	30800	114667	18959	8760	---	-8	Pitpnc1	phosphatidylinositol transfer protein, cytoplasmic 1	105610_at
2633	2685	475	1198	1107	1890	3485	7488	4278	-6	-3	Pitpnc1	phosphatidylinositol transfer protein, cytoplasmic 1	102922_at
---	---	---	---	3664	5433	14384	2947	3300	---	-4	Pitpnc1	phosphatidylinositol transfer protein, cytoplasmic 1	107400_at
---	---	---	---	6856	10358	18895	21383	15877	---	-3	Pitpnc1	phosphatidylinositol transfer protein, cytoplasmic 1	112381_at
---	---	---	---	1346	2196	2576	1552	2173	---	-2	Plcg1	phospholipase C, gamma 1	107396_at
---	---	---	---	2116	4302	15501	---	---	---	-7	Arhgap15	Rho GTPase activating protein 15	166860_at
7266	5005	1913	5243	3345	8261	20462	7450	5890	-4	-6	Arhgap9	Rho GTPase activating protein 9	103366_at
---	---	---	---	602	2579	15090	14421	15753	---	-25	Arhgef18	rho/rac guanine nucleotide exchange factor (GEF) 18	116815_at
2459	619	5740	5505	12050	5488	5031	2388	3887	2	2	Sh2d2a	SH2 domain protein 2A	100292_at
---	---	---	---	63832	18982	1444	655	3060	---	44	Stx11	syntaxin 11	134041_at
8650	9268	12162	4347	14162	17342	12280	20175	39102	1	1	Tcra	T-cell receptor alpha, constant	97944_f_at
8949	6285	4682	9338	14871	19068	32630	28045	19747	-2	-2	Tcrb	T-cell receptor beta, constant	93105_s_at
261992	136513	55665	44319	163914	220344	337448	33265	16472	-5	-2	A630038E17Rik	T-cell receptor delta, constant	92328_at
46287	46030	6512	28281	7757	24255	59967	46797	612	-7	-8	Tcrg	T-cell receptor gamma, constant	102744_at
26960	30104	6408	39141	18307	43293	116771	22766	383	-4	-6	Tcrg	T-cell receptor gamma, constant	102745_at
2101	2926	1335	969	2470	4360	7048	5004	721	-2	-3	Tcrg	T-cell receptor gamma, constant	102695_at
19090	12832	2689	1972	4345	15539	32205	7693	5530	-7	-7	Txk	TXK tyrosine kinase	104679_at
---	---	---	---	517	1668	2466	---	---	---	-5	Txk	TXK tyrosine kinase	162137_f_at
847	1403	2075	4742	10733	9982	8190	2890	2604	2	1	Vasp	vasodilator-stimulated phosphoprotein	101982_at
2333	1973	1612	3204	13196	11689	15259	2336	1386	-1	-1	Vav1	vav 1 oncogene	96511_s_at
2277	2161	2663	3233	11485	11228	10768	551	756	1	1	Vav1	vav 1 oncogene	99799_at
1058	1766	7364	3879	70374	47937	20084	1176	1664	7	4	Zap70	zeta-chain (TCR) associated protein kinase	93661_at
30521	29248	70828	23767	91417	79362	40408	16530	17174	2	2	Zap70	zeta-chain (TCR) associated protein kinase	93662_s_at

Table 3.3: NF-κB-associated transcripts

+H2$^{d/d}$		+H2$^{b/d}$		+H2$^{b/d}$	+Mix	+H2$^{d/d}$						
12 hr	4 day	12 hr	4 day	12 hr	12 hr	12 hr	γδ T	αβ T	change		Gene	Name	Probe set
---	---	---	---	14127	12221	708	2230	2031	---	20	AY078069	I kappa BNS	111316_at
1130	1771	885	1648	3186	3945	6316	440	508	-1	-2	Ikbkb	inhibitor of kappaB kinase beta	93706_at
---	---	---	---	26588	29152	28072	4833	4878	---	-1	Ikbkb	inhibitor of kappaB kinase beta	111615_at
---	---	---	---	6658	8225	11701	---	---	---	-2	Ikbkb	inhibitor of kappaB kinase beta	162716_at
1924	2306	1321	3590	1715	3799	7893	3138	3016	-1	-5	Ikbke	inhibitor of kappaB kinase epsilon	92301_at
2011	1229	847	848	1576	1120	628	904	1318	-2	3	Ikbkg	inhibitor of kappaB kinase gamma	103216_f_at
1032	1076	1223	1287	3388	3453	3724	1012	1157	1	-1	Ikbkg	inhibitor of kappaB kinase gamma	94196_at
---	---	---	---	1828	727	1095	1126	1250	---	2	Ikbkg	inhibitor of kappaB kinase gamma	106513_at
---	---	---	---	2350	573	472	1218	777	---	5	Ikbkg	inhibitor of kappaB kinase gamma	114642_at
---	---	---	---	17686	10363	3155	5724	10189	---	6	Malt1	mucosa associated lymphoid tissue lymphoma translocation gene 1	133562_at
11112	31800	95780	58024	96976	83856	23595	18091	18250	9	4	Nfkb1	nuclear factor of kappa light chain gene enhancer in B-cells 1, p105	98427_s_at
5631	8250	6758	3785	26548	33375	14638	4924	3595	1	2	Nfkbia	nuclear factor of kappa light chain gene enhancer in B-cells inhibitor, alpha	101554_at
2289	3683	2505	2315	3560	2338	1571	4466	5138	1	2	Nfkbia	nuclear factor of kappa light chain gene enhancer in B-cells inhibitor, alpha	104149_at
---	---	---	---	536194	529356	181027	---	---	---	3	Nfkbia	nuclear factor of kappa light chain gene enhancer in B-cells inhibitor, alpha	167965_f_at
2287	1469	3083	2828	10995	8186	6189	1632	2069	1	2	Nfkbib	nuclear factor of kappa light chain gene enhancer in B-cells inhibitor, beta	95715_at
1782	1946	4495	3454	33651	31501	9883	396	267	3	3	Nfkbib	nuclear factor of kappa light chain gene enhancer in B-cells inhibitor, beta	99982_at
732	1548	3323	1465	8293	6379	4320	211	244	5	2	Nfkb2	nuclear factor of kappa light polypeptide gene enhancer in B-cells 2, p49/p100	103614_at
348	807	442	688	1401	1756	1129	310	427	1	1	Nfkbie	nuclear factor of kappa light polypeptide gene enhancer in B-cells inhibitor, epsilon	101727_at
---	---	---	---	3500	3154	2816	1989	1524	---	1	Nfkbie	nuclear factor of kappa light polypeptide gene enhancer in B-cells inhibitor, epsilon	107985_at
---	---	---	---	40861	29736	10740	2161	3674	---	4	Tnip2	TNFAIP3 interacting protein 2	112472_at

Table 3.4: Effector function transcripts

+H2$^{d/d}$		+H2$^{b/d}$		+H2$^{b/d}$	+Mix	+H2$^{d/d}$						
12 hr	4 day	12 hr	4 day	12 hr	12 hr	12 hr	γδ T	αβ T	change		Gene	Name	Probe set
---	---	---	---	29227	21753	7424	---	---	---	4	Ecgf1	endothelial cell growth factor 1 (platelet-derived)	160292_at
2011	2634	3160	3880	3627	3010	3237	2479	3325	2	1	Ece1	endothelin converting enzyme 1	103456_at
---	---	---	---	11145	8684	2733	378	445	---	4	Ece1	endothelin converting enzyme 1	116065_at
2495	4572	29595	19534	197893	182734	45921	858	1512	12	4	Ephb4	Eph receptor B4	98446_s_at
206	934	233	1841	513	170	371	281	180	1	1	Gzma	granzyme A	102995_s_at
809	8344	57268	19122	143955	94952	871	135	1487	71	165	Gzmb	granzyme B	102877_at
62	113	1234	1127	2344	1622	94	336	165	20	25	Pla2g12a	phospholipase A2, group XIIA	104342_i_at
47043	74287	95097	60714	149593	122185	29620	29244	22941	2	5	Pla2g12a	phospholipase A2, group XIIA	104343_f_at
---	---	---	---	20262	16801	1334	26799	27296	---	15	Pdcd11	programmed cell death protein 11	112847_at
---	---	---	---	2373	1967	208	---	---	---	11	Pdcd11	programmed cell death protein 11	167856_s_at
608	4128	18120	12805	28132	21221	641	241	674	30	44	Serpinb9	serine (or cysteine) proteinase inhibitor, clade B, member 9	98405_at

Table 3.5: Cytokine-associated transcripts

+H2$^{d/d}$		+H2$^{b/d}$		+H2$^{b/d}$	+Mix	+H2$^{d/d}$							
12 hr	4 day	12 hr	4 day	12 hr	12 hr	12 hr	γδ T	αβ T	change		Gene	Name	Probe set
703	117	1522	297	1883	1871	937	646	314	2	2	Xcl1	chemokine (C motif) ligand 1	103199_at
1385	579	3150	89	5188	3132	1483	1090	835	2	3	Ccl3	chemokine (C-C motif) ligand 3	102424_at
231	206	2599	134	1985	1303	751	1388	1009	11	3	Ccl4	chemokine (C-C motif) ligand 4	94146_at
570	1833	3638	1868	10430	9580	1381	1166	2320	6	8	Cish	cytokine inducible SH2-containing protein	100022_at
1468	2583	4495	1754	5799	6204	1910	499	2831	3	3	Egr1	early growth response 1	98579_at
720	582	10331	1646	12981	11300	667	1246	2619	14	19	Egr2	early growth response 2	102661_at
---	---	---	---	2894	1660	80	126	64	---	36	Egr3	early growth response 3	132735_at
15490	17541	31738	11272	69783	61252	15502	6790	3913	2	5	Gpr65	G-protein coupled receptor 65	96553_at
1275	1154	1820	706	3161	4058	1092	441	698	1	3	Gadd45b	growth arrest and DNA-damage-inducible 45 beta	102779_at
---	---	---	---	25552	28216	2441	---	---	---	10	Gadd45b	growth arrest and DNA-damage-inducible 45 beta	161666_f_at
5919	2576	13214	14312	15118	14384	2742	3398	1239	2	6	Gfi1	growth factor independent 1	103259_at
679	2010	15181	10323	12032	13136	617	3042	2427	22	19	Icsbp1	interferon consensus sequence binding protein 1	98002_at
116	835	13776	28	13503	6887	27	72	429	119	498	Ifng	interferon gamma	99334_at
48	135	8430	1696	24477	20280	314	163	784	174	78	Irf4	interferon regulatory factor 4	92737_at
1498	3580	3875	905	5333	5505	1445	2635	2316	3	4	Isg20	interferon-stimulated protein	103432_at
4804	3161	1780	3478	1099	2482	4295	15024	17957	-3	-4	Il10rb	interleukin 10 receptor, beta	99491_at
2986	2035	910	1719	1723	4744	14662	17181	16020	-3	-9	Il16	interleukin 16	102029_at
1099	905	99	565	1867	4349	7584	837	517	-11	-4	Il17r	interleukin 17 receptor	99991_at
22862	17971	7660	5766	11672	16140	29528	19312	16758	-3	-3	Il17r	interleukin 17 receptor	99992_at
---	---	---	---	420	1202	3245	1509	1094	---	-8	Il17r	interleukin 17 receptor	114552_at
2825	3675	489	386	264	1043	2211	3234	3549	-6	-8	Il18r1	interleukin 18 receptor 1	101144_at
---	---	---	---	14461	10675	5040	7046	12180	---	3	Il2rb	interleukin 2 receptor, beta chain	112262_at
1548	2010	1156	115	1126	2899	7410	3576	6197	-1	-7	Il6ra	interleukin 6 receptor, alpha	104268_at
9592	3743	805	2269	970	3620	16045	20768	25871	-12	-17	Il7r	interleukin 7 receptor	99030_at
10890	6870	6758	9381	13590	20785	45726	13116	12621	-2	-3	Jak1	Janus kinase 1	98911_at
947	460	4061	650	5806	4609	321	424	939	4	18	Lta	lymphotoxin A	102630_s_at
27492	20434	10532	15774	19952	31809	123370	17922	22548	-3	-6	Rgs14	regulator of G-protein signaling 14	102711_at
1452	4849	16517	42324	387487	317515	3535	1895	3491	11	110	Rgs16	regulator of G-protein signaling 16	94378_at
---	---	---	---	58356	49562	958	---	---	---	61	Rgs16	regulator of G-protein signaling 16	161609_at
3363	4517	1022	594	3581	12892	17525	11634	4704	-3	-5	Socs3	suppressor of cytokine signaling 3	92232_at
---	---	---	---	1907	4798	6349	---	---	---	-3	Socs3	suppressor of cytokine signaling 3	162206_f_at
138	200	238	83	6491	7290	236	486	244	2	27	Tnf	tumor necrosis factor	102629_at

Table 3.6: Protein synthesis-associated transcripts

+H2$^{d/d}$ 12 hr	+H2$^{d/d}$ 4 day	+H2$^{b/d}$ 12 hr	+H2$^{b/d}$ 4 day	+H2$^{b/d}$ 12 hr	+Mix 12 hr	+H2$^{d/d}$ 12 hr	γδ T	αβ T	change		Gene	Name	Probe set
904	1550	1716	3536	6094	3739	1811	1169	427	2	3	Aars	alanyl-tRNA synthetase	94918_at
1999	2680	14309	3378	22227	25635	5458	2145	2925	7	4	Ddx21	DEAD (Asp-Glu-Ala-Asp) box polypeptide 21	94361_at
---	---	---	---	200165	114864	11169	1863	1854	---	18	Ddx21	DEAD (Asp-Glu-Ala-Asp) box polypeptide 21	106640_at
3450	2951	12331	4242	60828	47042	15234	1529	2659	4	4	D1Wsu40e	DNA segment, Chr 1, Wayne State University 40, expressed	95428_at
---	---	---	---	16290	14898	7258	1245	1490	---	2	D1Wsu40e	DNA segment, Chr 1, Wayne State University 40, expressed	116091_at
---	---	---	---	166189	112611	11323	9581	12978	---	15	Eef1e1	eukaryotic translation elongation factor 1 epsilon 1	111907_at
---	---	---	---	8724	6502	885	---	---	---	10	Eif1ay	eukaryotic translation initiation factor 1A, Y-linked	165199_f_at
---	---	---	---	3891	2465	742	---	---	---	5	Eif1ay	eukaryotic translation initiation factor 1A, Y-linked	168528_f_at
5420	4147	9968	4745	27051	21598	6447	1524	1534	2	4	Eif2s1	eukaryotic translation initiation factor 2, subunit 1 alpha	94253_at
---	---	---	---	11593	6752	2626	120	1026	---	4	Eif2b3	eukaryotic translation initiation factor 2B, subunit 3	115482_at
2502	1681	11148	2942	10928	8052	2208	2574	4674	4	5	Eif3s1	eukaryotic translation initiation factor 3, subunit 1 alpha	97205_at
2186	3811	10408	4389	51424	33266	16687	2856	4415	5	3	Eif3s9	eukaryotic translation initiation factor 3, subunit 9 (eta)	93973_at
2414	1613	18371	3859	9804	1644	2233	331	1163	8	4	Eif4g1	eukaryotic translation initiation factor 4, gamma 1	103926_at
1368	900	2159	1272	3639	2636	1630	3594	2336	2	2	Eif4a1	eukaryotic translation initiation factor 4A1	92816_r_at
---	---	---	---	6456	4015	1958	5234	4406	---	3	Eif4e	eukaryotic translation initiation factor 4E	137241_f_at
---	---	---	---	6072	4114	1335	---	---	---	5	Etf1	eukaryotic translation termination factor 1	160451_at
1315	1460	2794	1229	3567	3666	2351	2351	3356	2	2	Etf1	eukaryotic translation termination factor 1	98608_at
---	---	---	---	40218	16205	8192	---	---	---	5	Fbl	fibrillarin	160503_at
5969	6156	28647	4988	76736	58203	14577	2728	5231	5	5	Ftsj3	FtsJ homolog 3 (E. coli)	95756_at
---	---	---	---	21039	19997	6205	---	---	---	3	Gfm	G elongation factor	160226_at
---	---	---	---	6816	7120	4547	---	---	---	1	Gfm	G elongation factor	168366_at
1025	1169	2784	2777	18710	12599	1897	1248	1765	3	10	Gspt1	G1 to phase transition 1	93727_at
---	---	---	---	145986	111708	32984	8066	7910	---	4	Gemin6	gem (nuclear organelle) associated protein 6	108476_at
3105	4681	8770	7758	12520	13627	3828	1192	1420	3	3	Gtf2e2	general transcription factor II E, polypeptide 2 (beta subunit)	98515_at
4195	4618	17491	14220	60121	41830	17020	1844	1942	4	4	Gtf2f1	general transcription factor IIF, polypeptide 1	103762_at
---	---	---	---	72205	61315	24297	799	3000	---	3	Gtf2f1	general transcription factor IIF, polypeptide 1	108354_at
301	611	3114	640	34158	25440	3195	56	116	10	11	Grwd1	glutamate-rich WD repeat containing 1	103853_at
---	---	---	---	39308	37742	17806	---	---	---	2	Grwd1	glutamate-rich WD repeat containing 1	171003_r_at
1255	2514	8288	5500	6933	4752	1793	2225	3586	7	4	Eprs	glutamyl-prolyl-tRNA synthetase	96628_at
2882	2354	11123	1835	15286	7327	2733	5751	9092	4	6	Gtpbp4	GTP binding protein 4	99180_at
23065	22576	58275	22779	59828	44145	16617	5128	6166	3	4	Hars	histidyl-tRNA synthetase	92580_at
2963	2461	6197	1360	7551	6579	3178	1766	1832	2	2	Mki67ip	Mki67 (FHA domain) interacting nucleolar phosphoprotein	93342_at
---	---	---	---	27194	12993	5610	41	40	---	5	Mki67ip	Mki67 (FHA domain) interacting nucleolar phosphoprotein	108958_at
---	---	---	---	35087	18304	3196	238	504	---	11	Nolc1	nucleolar and coiled-body phosphoprotein 1	116139_at
---	---	---	---	13094	10039	4393	---	---	---	3	Nolc1	nucleolar and coiled-body phosphoprotein 1	163281_at
1462	345	3422	802	14042	11038	2937	2090	2288	2	5	Nol1	nucleolar protein 1	96804_at
1924	1272	10079	1344	6798	3193	334	999	2412	5	20	Nol5	nucleolar protein 5	92569_f_at
42093	93665	88043	39772	159667	148285	26690	13891	17795	2	6	Nol5a	nucleolar protein 5A	95109_at
13835	5074	55747	4655	116234	64181	25362	29795	22334	4	5	Nola1	nucleolar protein family A, member 1 (H/ACA small nucleolar RNPs)	104766_at
17846	32595	64865	52351	381557	345468	71097	13897	10293	4	5	Nola2	nucleolar protein family A, member 2	97824_at
5394	4599	30674	22678	94402	46925	16909	4992	8874	6	6	Ncl	nucleolin	100144_at
14821	20472	39396	25124	86076	65984	26585	6444	14851	3	3	Npm1	nucleophosmin 1	101634_at
1209	1110	6430	1541	6370	3931	1442	2537	4747	5	4	Pspc1	paraspeckle protein 1	103393_at
4301	5621	39129	21193	25912	19171	5151	3724	9327	9	5	Pabpc4	poly A binding protein, cytoplasmic 4	92775_at
---	---	---	---	12827	10684	3019	---	---	---	4	Prpf3	PRP3 pre-mRNA processing factor 3 homolog (yeast)	163951_at
---	---	---	---	83101	46734	23986	10518	9505	---	3	Prpf4	PRP4 pre-mRNA processing factor 4 homolog (yeast)	129169_at
15792	17842	44810	15479	83985	70108	25130	3571	5629	3	3	Rbm8	RNA binding motif protein 8	97254_at
5023	5791	27229	3779	31140	26192	6351	3953	5027	5	5	Rcl1	RNA terminal phosphate cyclase-like 1	98923_at
1483	1546	3937	1460	5933	4257	781	3825	4365	3	8	Rnu22	RNA, U22 small nucleolar	97838_at
18116	22452	58452	11831	103903	105430	17705	4875	6160	3	6	Rrs1	RRS1 ribosome biogenesis regulator homolog (S. cerevisiae)	96778_at
339	363	1228	642	1801	1168	357	427	488	4	5	Snrpd1	small nuclear ribonucleoprotein D1	100577_at
53898	65143	81951	39667	229615	194600	71630	22695	18084	2	3	Snrpd2	small nuclear ribonucleoprotein D2	95049_at
2154	3690	11019	11717	89530	73432	16770	1308	1380	5	5	Snrpa	small nuclear ribonucleoprotein polypeptide A	100101_at
1152	1586	3537	1004	6036	5375	2141	1169	1213	3	3	Snrpa1	small nuclear ribonucleoprotein polypeptide A'	101506_at
---	---	---	---	35548	30490	7469	7821	6745	---	5	Snrpf	small nuclear ribonucleoprotein polypeptide F	111352_at
1169	932	3374	653	7884	6371	2087	4526	4403	3	4	Sfrs9	splicing factor, arginine/serine rich 9	96834_at
9616	17135	26862	9703	39088	18345	7665	8643	7336	3	5	Sfrs3	splicing factor, arginine/serine-rich 3 (SRp20)	101004_f_at
---	---	---	---	7973	6022	2330	967	825	---	3	Taf3	TAF3 RNA polymerase II, TATA box binding protein (TBP)-associated factor	110578_at
430	494	1885	1039	6490	4031	704	1011	1122	4	9	Tars	threonyl-tRNA synthetase	95054_at
798	1173	2136	2576	5095	6096	3875	1614	1412	3	1	Wars	tryptophanyl-tRNA synthetase	98605_at
120	1445	2169	2422	7054	7831	929	327	128	18	8	Wars	tryptophanyl-tRNA synthetase	98606_s_at

Table 3.7: HSP and chaperone-associated transcripts

+H2$^{d/d}$		+H2$^{b/d}$		+H2$^{b/d}$	+Mix	+H2$^{d/d}$						
12 hr	4 day	12 hr	4 day	12 hr	12 hr	12 hr	γδ T	αβ T	change		Gene	Name	Probe set
---	---	---	---	6228	5767	1728	2333	2458	---	4	Cdc37l	cell division cycle 37 homolog (S. cerevisiae)-like	114373_at
---	---	---	---	8916	7684	6678	---	---	---	1	Cdc37l	cell division cycle 37 homolog (S. cerevisiae)-like	166321_at
---	---	---	---	8057	7919	5400	---	---	---	1	Cct2	chaperonin subunit 2 (beta)	160442_at
5323	9113	45071	24368	164427	165895	41825	4778	4222	8	4	Cct3	chaperonin subunit 3 (gamma)	98153_at
---	---	---	---	28083	27295	9074	---	---	---	3	Cct3	chaperonin subunit 3 (gamma)	161238_f_at
3358	3171	7442	5754	9033	6683	2460	7324	9569	2	4	Cct4	chaperonin subunit 4 (delta)	101011_at
1793	2059	7083	2937	15188	10522	6031	6461	8930	4	3	Cct5	chaperonin subunit 5 (epsilon)	93295_at
---	---	---	---	3628	2120	1195	---	---	---	3	Cct6a	chaperonin subunit 6a (zeta)	162279_f_at
---	---	---	---	40023	23107	10981	---	---	---	4	Cct7	chaperonin subunit 7 (eta)	160562_at
---	---	---	---	13443	8294	3704	---	---	---	4	Cct8	chaperonin subunit 8 (theta)	160102_at
6389	11139	12741	3558	17050	12374	5061	5734	7748	2	3	Dnajb11	DnaJ (Hsp40) homolog, subfamily B, member 11	98572_at
2296	5624	17940	2834	34567	30896	6519	1665	4820	8	5	Hspa5	heat shock 70kD protein 5 (glucose-regulated protein)	101955_at
11764	36157	56582	30280	74427	60059	8940	11828	9933	5	8	Hspe1	heat shock protein 1 (chaperonin 10)	92829_at
8641	10209	78525	13586	102172	81476	18366	15223	40749	9	6	Hspd1	heat shock protein 1 (chaperonin)	93277_at
1234	1522	5978	610	7336	2863	1435	2849	5003	5	5	Hspca	heat shock protein 1, alpha	95282_at
6198	18594	52479	33686	232032	168611	37352	9236	16381	8	6	Hspcb	heat shock protein 1, beta	95359_at
832	996	4412	766	16092	10593	2752	1816	2417	5	6	Hsp105	heat shock protein 105	98111_at
1488	1627	9099	6575	20818	12488	4616	2729	3169	6	5	Hspa4	heat shock protein 4	92571_at
---	---	---	---	8965	5025	3478	---	---	---	3	Hspa4	heat shock protein 4	161745_f_at
2655	2013	5815	5110	22226	16110	9440	373	633	2	2	Hspa4	heat shock protein 4	100353_g_at
4131	12157	18850	19295	36952	29855	10511	5936	9670	5	4	Hspa8	heat shock protein 8	96564_at
4604	7623	32170	14616	93272	74166	17368	16930	22207	7	5	Hspa9a	heat shock protein, A	97914_at
2469	5380	24484	18938	49714	34017	12238	2901	2379	10	4	St13	suppression of tumorigenicity 13	97309_at
1758	2566	6313	7492	23423	14088	8597	43	202	4	3	St13	suppression of tumorigenicity 13	97310_at
11948	15337	15564	5875	22693	16481	10802	3896	3387	1	2	Timm9	translocase of inner mitochondrial membrane 9 homolog (yeast)	94210_at
10669	12138	40600	10085	59054	49631	14107	3705	3420	4	4	Timm17a	translocator of inner mitochondrial membrane 17a	94860_at
4262	4480	3040	1746	9387	9137	11200	5347	3158	-1	-1	Timm17b	translocator of inner mitochondrial membrane 17b	96668_at
431	669	2053	1694	4749	1934	1124	530	856	5	4	Timm22	translocase of inner mitochondrial membrane 22 homolog (yeast)	93348_at
2212	2888	11775	14119	54242	52895	22898	968	1528	5	2	Timm44	translocator of inner mitochondrial membrane 44	98106_at
---	---	---	---	15855	8747	6187	805	814	---	3	Timm50	translocase of inner mitochondrial membrane 50 homolog (yeast)	108489_at

Table 3.8: Nuclear import-associated transcripts

+H2$^{d/d}$		+H2$^{b/d}$		+H2$^{b/d}$	+Mix	+H2$^{d/d}$						
12 hr	4 day	12 hr	4 day	12 hr	12 hr	12 hr	γδ T	αβ T	change		Gene	Name	Probe set
1528	1010	1882	1064	10366	7514	974	837	544	1	11	Chc1	chromosome condensation 1	99138_at
---	---	---	---	14339	9753	229	---	---	---	63	Chc1	chromosome condensation 1	162775_at
362	408	2850	204	2454	1198	381	2204	2632	8	6	Ipo4	importin 4	95034_f_at
112	181	1957	116	5646	4452	581	432	872	18	10	Ipo4	importin 4	95035_at
4089	7383	10178	5190	9131	6525	3007	1751	2104	2	3	Ipo7	importin 7	93970_at
---	---	---	---	5854	4086	1005	---	---	---	6	Ipo7	importin 7	164341_f_at
---	---	---	---	10729	10329	4318	---	---	---	2	Nup62	nucleoporin 62	160167_at
---	---	---	---	7342	5726	1605	---	---	---	5	Nup62	nucleoporin 62	166132_f_at
---	---	---	---	31795	23523	12744	---	---	---	2	Nup62	nucleoporin 62	166447_f_at
1318	1752	4152	994	8600	5590	1249	9052	7618	3	7	Ranbp1	RAN binding protein 1	98573_r_at
2887	3934	23698	6527	35103	18428	3465	12690	14088	8	10	Ran	RAN, member RAS oncogene family	102821_s_at
7124	11892	45005	8879	47660	29324	5758	35107	46240	6	8	Ran	RAN, member RAS oncogene family	101254_at

Table 3.9: Proliferation and apoptosis-associated transcripts

+H2$^{d/d}$		+H2$^{b/d}$		+H2$^{b/d}$	+Mix	+H2$^{d/d}$							
12 hr	4 day	12 hr	4 day	12 hr	12 hr	12 hr	γδ T	αβ T	change		Gene	Name	Probe set
1126	804	7307	3444	7660	5041	1189	769	494	6	6	Atf3	activating transcription factor 3	104155_f_at
185	83	1325	572	3004	2587	1108	71	149	7	3	Atf3	activating transcription factor 3	104156_r_at
1745	3140	18350	7363	105754	90426	12042	2297	2548	11	9	Apex1	apurinic/apyrimidinic endonuclease 1	93559_at
2150	1853	9190	5237	23546	13109	2692	1403	1804	4	9	Bcl2l1	Bcl2-like 1	99027_at
---	---	---	---	526	4496	11606	2123	2752	---	-22	Cdc25b	cell division cycle 25 homolog B (S. cerevisiae)	112364_at
1817	1931	3194	1955	11226	5906	3206	591	1329	2	4	Cdc34	cell division cycle 34 homolog (S. cerevisiae)	94048_at
78	170	1830	552	6643	3031	119	1097	2576	24	56	Ccnd2	cyclin D2	97504_at
202	2959	6439	30614	17137	11114	3847	2483	721	32	4	Cdkn1a	cyclin-dependent kinase inhibitor 1A (P21)	98067_at
11351	9579	27225	10483	60156	47163	37242	18060	14102	2	2	Cyc1	cytochrome c-1	95072_at
4926	10425	13243	8934	29726	27213	4286	1564	2066	3	7	Cycs	cytochrome c, somatic	98132_at
4461	2784	16348	4124	23915	25847	7320	7134	4267	4	3	Dusp2	dual specificity phosphatase 2	92758_at
106	1602	1731	1344	6667	6374	270	616	447	16	25	Ier3	immediate early response 3	94384_at
6878	13777	23388	17966	76208	107768	41868	328	459	3	2	Junb	Jun-B oncogene	102362_i_at
11205	17025	27584	18952	90391	119818	37248	1854	3013	2	2	Junb	Jun-B oncogene	102363_r_at
873	1274	3314	1851	11219	8086	2386	1713	1755	4	5	Mapk6	mitogen-activated protein kinase 6	103416_at
255	392	5853	789	8172	6689	819	715	1222	23	10	Myc	myelocytomatosis oncogene	104712_at
254	831	7056	989	9028	8071	139	335	2383	28	65	Nr4a1	nuclear receptor subfamily 4, group A, member 1	102371_at
295	86	2933	610	3831	1972	584	62	349	10	7	Nr4a2	nuclear receptor subfamily 4, group A, member 2	92248_at
589	192	5300	563	5820	3685	116	459	488	9	50	Nr4a2	nuclear receptor subfamily 4, group A, member 2	92249_g_at
435	808	6890	1821	16739	11922	966	460	910	16	17	Plscr1	phospholipid scramblase 1	102839_at
---	---	---	---	27823	20868	5842	827	770	---	5	Pinx1	PIN2/TRF1-interacting protein	109752_at
32152	22234	2952	9722	732	2225	11176	22628	38258	-11	-15	Pdcd4	programmed cell death 4	103029_at
2509	3221	5702	2740	6308	5370	1748	3353	4322	2	4	Pcna	proliferating cell nuclear antigen	101065_at
2969	5521	14911	21999	51526	31006	12265	6059	8037	5	4	Ssrp1	structure specific recognition protein 1	95069_at

Table 3.10: WNT-associated transcripts

+H2$^{d/d}$		+H2$^{b/d}$		+H2$^{b/d}$	+Mix	+H2$^{d/d}$							
12 hr	4 day	12 hr	4 day	12 hr	12 hr	12 hr	γδ T	αβ T	change		Gene	Name	Probe set
647	977	713	439	401	708	1194	443	586	1	-3	Apc	adenomatosis polyposis coli	101447_at
---	---	---	---	18849	20008	32102	---	---	---	-2	Axin	axin	160701_at
---	---	---	---	105829	108404	19493	15943	12786	---	5	Axud1	AXIN1 up-regulated 1	112908_at
---	---	---	---	3125	2715	4514	---	---	---	-1	Catnb	catenin beta	160430_at
78	170	1830	552	6643	3031	119	1097	2576	24	56	Ccnd2	cyclin D2	97504_at
76	915	337	278	576	591	2202	501	127	4	-4	Frat1	frequently rearranged in advanced T-cell lymphomas	92695_at
22417	14634	1814	3200	1189	3418	14666	2575	2525	-12	-12	Frat2	frequently rearranged in advanced T-cell lymphomas 2	103699_i_at
1954	770	882	641	571	889	1929	1017	1076	-2	-3	Frat2	frequently rearranged in advanced T-cell lymphomas 2	103700_r_at
---	---	---	---	196	286	1554	5525	6154	---	-8	Gsk3b	glycogen synthase kinase 3 beta	111399_at
---	---	---	---	10033	9920	20096	2996	2457	---	-2	Gsk3b	glycogen synthase kinase 3 beta	111732_at
---	---	---	---	2037	5990	6494	780	1065	---	-3	Gsk3b	glycogen synthase kinase 3 beta	140699_at
---	---	---	---	1340	1873	505	---	---	---	3	Gsk3b	glycogen synthase kinase 3 beta	162699_at
728	593	278	985	1863	1881	5070	1679	1051	-3	-3	Ilk	integrin linked kinase	101499_at
6451	6726	4064	4613	7594	15347	39521	7366	7848	-2	-5	Lef1	lymphoid enhancer binding factor 1	103628_at
62756	26486	5537	7026	15773	33446	78190	8937	11188	-11	-5	Lef1	lymphoid enhancer binding factor 1	103629_g_at
1313	1127	5502	1871	58549	37885	7726	1165	194	4	8	Ruvbl1	RuvB-like protein 1	99537_at
2175	2307	981	1302	3006	6533	22061	961	764	-2	-7	Tcf7	transcription factor 7, T-cell specific	97995_at

Table 3.11: Krüppel-like factor transcripts

+H2$^{d/d}$		+H2$^{b/d}$		+H2$^{b/d}$	+Mix	+H2$^{d/d}$						
12 hr	4 day	12 hr	4 day	12 hr	12 hr	12 hr	γδ T	αβ T	change		Gene	Name	Probe set
132	166	84	85	145	1271	2531	444	75	-2	-17	Klf3	Kruppel-like factor 3 (basic)	100010_at
1620	1320	465	191	1049	1298	2772	7514	7759	-3	-3	Klf3	Kruppel-like factor 3 (basic)	100011_at
---	---	---	---	5156	8425	24240	11387	12815	---	-5	Klf3	Kruppel-like factor 3 (basic)	113288_at
5447	2640	1051	1049	1858	2671	8352	2845	2508	-5	-4	Klf7	Kruppel-like factor 7 (ubiquitous)	104645_at
---	---	---	---	1142	1432	1836	976	780	---	-2	Klf7	Kruppel-like factor 7 (ubiquitous)	107020_at
---	---	---	---	524	2808	6148	15382	12120	---	-12	Klf7	Kruppel-like factor 7 (ubiquitous)	112898_at
---	---	---	---	15775	19415	44979	---	---	---	-3	Klf13	Kruppel-like factor 13	160617_at

Table 3.12: Activation-induced cell surface receptors

+H2$^{d/d}$		+H2$^{b/d}$		+H2$^{b/d}$	+Mix	+H2$^{d/d}$						
12 hr	4 day	12 hr	4 day	12 hr	12 hr	12 hr	γδ T	αβ T	change		Gene	Name	Probe set
---	---	---	---	49949	34136	11370	11150	36958	---	4	Btla	B and T lymphocyte associated	116608_at
363	257	7462	812	9649	7010	2417	4252	14673	21	4	Cd5	CD5 antigen	93637_at
1622	2003	16213	27619	42328	29349	5773	3681	15677	10	7	Cd6	CD6 antigen	92203_s_at
687	1405	8930	12405	21693	20346	5189	437	6221	13	4	Cd6	CD6 antigen	92204_at
2951	11184	68744	37007	75901	80469	1878	2579	1287	23	40	Cd160	CD160 antigen	102272_at
187	86	3318	1052	4003	3533	136	132	620	18	29	Crtam	cytotoxic and regulatory T cell molecule	98334_at
446	782	304	3748	676	746	1166	21	449	-1	-2	Ctla4	cytotoxic T-lymphocyte-associated protein 4	97718_at
1477	10721	6189	14002	7310	7346	1390	9724	3406	4	5	Ly6a	lymphocyte antigen 6 complex, locus A	93078_at
632	713	3908	15571	7062	6054	947	613	337	6	7	Lag3	lymphocyte-activation gene 3	98392_at
988	241	4920	6579	17095	11027	2055	156	215	5	8	Pdcd1	programmed cell death 1	98836_at

Table 3.13: CD1-associated transcripts

+H2$^{d/d}$		+H2$^{b/d}$		+H2$^{b/d}$	+Mix	+H2$^{d/d}$						
12 hr	4 day	12 hr	4 day	12 hr	12 hr	12 hr	γδ T	αβ T	change		Gene	Name	Probe set
10443	5068	2272	3058	4376	7417	26539	5876	2875	-5	-6	Cd1d1	CD1d1 antigen	101897_g_at
7178	3348	400	483	342	1518	6954	5661	4190	-18	-20	Cd1d1	CD1d1 antigen	103422_at
963	758	242	484	358	315	2710	943	593	-4	-8	Cd1d2	CD1d2 antigen	101896_at
6025	6221	2449	5265	6937	7501	19841	11622	12928	-2	-3	Psap	prosaposin	97114_at

Table 3.14: Metabolism-associated transcripts

+H2$^{d/d}$		+H2$^{b/d}$		+H2$^{b/d}$	+Mix	+H2$^{d/d}$								
12 hr	4 day	12 hr	4 day	12 hr	12 hr	12 hr	γδ T	αβ T	change		Gene	Name	Isoform	Enzyme #	Probe set
2564	2167	3120	2902	3268	3790	2091	2082	1000	1	2	Hk1	Hexokinase	1	2.7.1.1	99335_at
2313	9924	17864	15125	19313	17427	1591	114	167	8	12	Hk2		2		94375_at
---	---	---	---	5642	1835	10056	2478	2143	---	-2	Hk3		3		139274_at
43343	106861	33562	26002	20866	27020	29805	8243	10710	-1	-1	Gpi1	Glucose-6-phosphate isomerase		5.3.1.9	100573_f_at
347950	177164	79853	33970	109566	206927	228072	46370	56699	-4	-2					100574_f_at
3332	6442	5497	4892	29325	32153	27958	2735	1724	2	1	Pfkl	6-phosphofructokinase	liver	2.7.1.11	92637_at
359	1163	451	690	513	740	1489	274	163	1	-3	Pfkm		muscle		94438_at
2498	14529	6492	8546	10607	12306	11098	487	803	3	-1	Pfkp		platelet		97833_at
5307	25643	11687	20160	15566	15802	16519	1513	3452	2	-1					97834_g_at
---	---	---	---	5314	3073	1647	2391	1809	---	3					113570_at
---	---	---	---	4393	4222	2645	---	---	---	2					164250_at
---	---	---	---	9775	9311	7379	---	---	---	1	Aldo1	Fructose-bisphosphate aldolase	A	4.1.2.13	160090_f_at
98	91	59	264	206	424	509	37	63	-2	-2	Aldo2		B		101531_at
72	95	48	216	89	521	397	619	325	-1	-4					101532_g_at
7593	15986	10636	17140	60531	48722	36952	692	799	1	2	Tpi	Triosephosphate isomerase		5.3.1.1	99566_at
9747	21500	23549	24432	40321	34664	21547	7637	9936	2	2	Gapd	Glyceraldehyde 3-phosphate dehydrogenase		1.2.1.12	101214_f_at
7117	11447	11954	7607	18087	13572	8600	3273	4360	2	2	Pgk1	Phosphoglycerate kinase	1	2.7.2.3	93346_at
54	51	170	96	125	99	385	123	67	3	-3	Pgk2		2		101388_at
---	---	---	---	20951	15751	8213	---	---	---	3	Pgam1	Phosphoglycerate mutase	1	5.4.2.1	160091_at
82	54	58	44	45	46	51	50	50	-1	-1	Pgam2		2		92599_at
---	---	---	---	45541	42587	36143	9287	14328	---	1	Eno1	Phosphopyruvate hydratase	non-neuron	4.2.1.11	129223_at
---	---	---	---	3016	2298	3432	---	---	---	-1					169423_i_at
863	784	793	1445	2760	4366	3343	464	334	-1	-1	Eno2		neuronal		99045_at
1282	1376	897	2738	2025	2432	4988	968	1201	-1	-2	Eno3		muscle		96344_at
399	34	117	129	397	56	257	38	45	-3	2	Pklr	Pyruvate kinase	liver, RBC	2.7.1.40	101471_at
955	2942	2664	1005	8272	5572	3444	2858	4595	3	2	Pkm2		muscle		96066_s_at
1635	2944	27236	3555	42540	31909	5443	2992	3137	17	8	Srr	Serine racemase			93488_at
---	---	---	---	6122	3503	3520	1607	1819	---	2	Sds	L-serine ammonia-lyase		4.3.1.17	108574_at
38784	89712	100353	49909	339241	338405	250637	13934	18744	3	1	Ldh1	L-lactate dehydrogenase	A chain	1.1.1.27	96072_at
616	338	410	1043	576	373	761	772	657	-2	-1	Ldh2		B chain		101990_at
68	20	23	36	50	139	38	58	24	-3	1	Ldh3		C chain		93103_at
60	94	49	62	138	249	89	115	63	-1	2	Shmt1	Glycine hydroxymethyltransferase		2.1.2.1	104700_at
99	633	1014	632	1993	2241	522	556	210	10	4					98459_at
---	---	---	---	964	3428	2822	1392	1367	---	-3					113935_at
522	809	707	642	646	529	854	898	518	1	-1	Tyms	Thymidylate synthase		2.1.1.45	93236_s_at
1440	4454	1359	15630	2407	1687	947	799	1500	-1	3					93237_s_at
79	91	156	310	89	91	112	102	94	2	-1	Dhfr	Dihydrofolate reductase		1.5.1.3	104547_at
5556	6118	19678	4971	12634	10751	2888	6795	9035	4	4	Gart	Phosphoribosylglycinamide formyltransferase		2.1.2.2	100066_at
---	---	---	---	31087	21996	3378	991	1210	---	9	Mthfd1	Methylenetetrahydrofolate dehydrogenase (NADP+)		1.5.1.5	109735_at
---	---	---	---	1402	669	1568	404	426	---	-1					139125_at
---	---	---	---	1720	934	1532	---	---	---	1					167558_at
4588	26048	43875	37944	33735	49327	6734	21581	29763	10	5	Mthfd2	Methylenetetrahydrofolate dehydrogenase (NAD+)		1.5.1.15	100046_at
---	---	---	---	1289	1189	1390	---	---	---	-1	Prps1	Ribose-phosphate diphosphokinase	1	2.7.6.1	161897_f_at
895	1525	2947	1391	12632	10442	8519	1048	1255	3	1					95507_at
---	---	---	---	794	522	195	---	---	---	4	Prps2		2		161038_at
---	---	---	---	1763	2635	3766	---	---	---	-2					167174_at
304	957	496	365	240	659	563	66	137	2	-2	Ppat	Amidophosphoribosyltransferase		2.4.2.14	95553_at
81	154	97	59	583	83	116	51	82	1	5					95554_at
---	---	---	---	2533	395	1087	536	267	---	2	Paics	Phosphoribosylaminoimidazole carboxylase		4.1.1.21	140815_at
2786	2032	5111	1540	7070	7228	1694	3111	5174	2	4	Adsl	Adenylosuccinate lyase		4.3.2.2	98999_at
---	---	---	---	1381	1515	1244	1988	2951	---	1	Atic	Phosphoribosylaminoimidazolecarboxamide formyltransferase			112333_at
---	---	---	---	1563	251	283	---	---	---	6				2.1.2.3	163798_at
796	88	160	608	71	109	313	325	163	-5	-4	Adss	Adenylosuccinate synthase	muscle	6.3.4.4	98435_at
4910	4316	10946	10100	21452	17125	9190	2751	3626	2	2	Adss2		non-muscle		99038_at
1844	1590	5298	5151	16112	13434	8392	1398	1957	3	2					99039_g_at
---	---	---	---	6790	1985	1311	---	---	---	5					167296_r_at
798	1258	1310	599	3997	2148	1959	354	231	2	2	Impdh1	IMP dehydrogenase	1	1.1.1.205	98390_at
---	---	---	---	23184	17073	13708	7457	7349	---	2					105630_at
1101	1777	5128	8157	20193	13138	4123	1161	1898	5	5	Impdh2		2		100578_at
---	---	---	---	16099	9362	5631	---	---	---	3	Gmps	GMP synthase		6.3.4.1	162717_at

Chapter 4: Antigen-specific Activation of Splenic γδ T cells Leads to Broad Activation of B cells

Introduction

γδ T cells are one of the least understood components of the immune system. While they appear to contribute uniquely to host immune competence, it is not clear what mechanisms are associated with this. Some experiments suggest that γδ T cells contribute to a fast-acting early immune response (Boismenu and Havran 1997; Hayday and Tigelaar 2003). For instance, γδ T cell deficiency impairs the ability of mice to resist primary *Listeria monocytogenes* infections (Hiromatsu, Yoshikai et al. 1992; Skeen and Ziegler 1993). In addition, the presence of γδ T cells appears to be important in the control of virus levels during the first week of vaccinia virus infection (Selin, Santolucito et al. 2001). It has also been observed that γδ T cells act late in immune responses. In murine models of Influenza infection, γδ TCR mRNA-positive cells have been found to accumulate in the lung after an initial acute-phase αβ T cell response (Carding, Allan et al. 1990). The late appearance of γδ T cells has led to the suggestion that these cells contribute to the downregulation and resolution of the local immune responses (Carding and Egan 2000) as is evidenced during *Eimeria* infection of the small intestine where γδ T cell-deficient mice show a more severe pathology than RAG2-deficient mice (Roberts, Smith et al. 1996).

It has been proposed that late-acting γδ T cells recognize self antigens and there is no evidence that early-acting γδ T cells are pathogen specific. In addition, it has been observed that γδ T cells have the ability to recognize stress-induced self antigens, which has led to the idea that γδ T cells can act as sensors of physiological disturbance (Allison and Havran 1991). Further, it is recognized that the γδ TCR can recognize antigens directly without a requirement for antigen processing and presentation (Chien, Jores et al. 1996), which indicates that γδ T cells can respond to cells directly to initiate cellular immune responses without a requirement for prior antigen degradation or specialized antigen presenting cells.

Despite these advances, it has been difficult to define antigen-specific γδ T cell responses in either pathological or normal physiological processes. This is largely because it is unclear as to what most γδ T cells recognize. In terms of the possible

functions of γδ T cells during immune responses, early studies have shown that γδ T cells are cytolytic in redirected lysis assays (Borst, van de Griend et al. 1987; Brenner, McLean et al. 1987). Other studies have indicated that γδ T cell lines and clones are cytolytic and that they can secrete cytokines, chemokines, and growth factors after stimulation with antibodies to the γδ TCR complex or PMA (Cron, Gajewski et al. 1989). While these experiments have shown the functional potential of γδ T cells when triggered through their TCRs, it has been demonstrated that prolonged *in vitro* cultures (weeks to months) alter the nature of γδ T cell responses profoundly. Thus, it is unclear which of these responses are mounted when γδ T cells encounter cells bearing their cognate antigens *in vivo*. Further, while differential cytokine expression including that of IFNγ and IL-4 by γδ T cells has been observed in pathological situations including experimental asthma models (McMenamin, Pimm et al. 1994; Zuany-Amorim, Ruffie et al. 1998) and in coxsackievirus B3-induced myocarditis in BALB/c mice (Huber, Graveline et al. 2001), it has been shown that γδ T cells can also be activated by anti-Thy1 and anti-Ly6C antibodies (Cron, Gajewski et al. 1989). Thus, it is unclear what γδ T cell responses are antigen-specific.

In order to study γδ T cell activation through the γδ TCR, it is helpful to use an antigen that is a known ligand of γδ T cells. Even though the full scope of γδ T cell ligands has yet to be determined, it has been found that two independently-derived murine γδ T cell clones, G8 and KN6, recognize the MHC class Ib molecules T10 and T22 (Ito, Van Kaer et al. 1990; Schild, Mavaddat et al. 1994). The use of $T22^b$ tetramers has shown that as many as 0.2 – 2% of γδ T cells in normal mice appear to recognize these molecules and the direct binding of the Vγ2/Vα11 G8 γδ TCR to T10 and T22 has been demonstrated (Crowley, Fahrer et al. 2000). Although structurally similar to MHC class I molecules, neither T10 nor T22 appear to present peptides (Kaliyaperumal, Falchetto et al. 1995) or any other ligands.

Here, we utilize mice that are transgenic for the G8 γδ TCR (Dent, Matis et al. 1990) and are, thus, a source of primary γδ T cells with a known antigen specificity, as well as the 7H9 monoclonal antibody that identifies T10/T22-expressing cells, to analyze antigen-specific γδ T cell responses. We find that during a 24 hour coculture of G8 γδ

TCR-transgenic T cells and $H2^{b/d}$ BALB/c splenic cells, not only γδ T cells, but also B cells become activated as is evidenced by their expression of CD69, B7.2, and MHC class II. This is in large part due to the synergistic effects of IFNγ and IL-4 produced by the activated G8 γδ T cells. In addition, the expression of the G8 ligands, T10/T22, is upregulated on G8 γδ T cells, B cells, and other cells. Our results suggest ways through which γδ T cells sustain and amplify their responses in an antigen-specific manner as immune responses progress and provide mechanisms for enhancing local immune responses where γδ T cells may provide general non-cognate T cell help to B cells that may be of particular importance in B cell activation.

Materials and Methods

Mice

All experiments were conducted under protocols approved by the IACUC (A-PLAC) of Stanford University. G8 mice on a BALB/c background were crossed with $RAG2^{KO}$ mice on a BALB/c background (Taconic) to obtain G8 $RAG2^{KO}$ BALB/c mice. The presence of the transgene was identified by PCR using the following primers (5'->3'): *FWD-G8VD-71* TAC TTC TGT GCT GCT GAC ACG; *REV-G8J-71* CCA AAG ACG AGT TTG TCG GTA; *FWD-RAG2-307* CAT TCC ATT GAC GTG GTG TAT AGT; *REV-RAG2-307* GGG GAA GGT CCA CTC TTA TTC TAT. BALB/c mice were crossed with BALB.B mice (Harlan) to obtain $H2^{b/d}$ BALB/c mice that express both the *b* and *d* haplotypes on a BALB/c background.

G8 γδ T cell Activation

G8 $RAG2^{KO}$ BALB/c splenocytes were cultured with a five-fold excess of BALB/c or $H2^{b/d}$ BALB/c splenocytes in RPMI 1640 containing 10% FCS, non-essential amino acids, sodium pyruvate, β-mercaptoethanol, and glutamine/penicillin/streptomycin at 37°C. The final concentration was 10^7 cells/ml. Cells were cultured in 24-well flat-bottom plates containing 600 μl of cells per well or 96-well Vee-bottom plates containing 200 μl of cells per well. For Transwell studies, 6.5 mm Transwell inserts with 0.4 μm pore sizes (Corning) were added to the wells of the 24-well plates and 100 μl of BALB/c cells were added into the Transwells.

Cytokines and ELISA Analyses

Recombinant IFNγ and IL-4 (PeproTech, Inc.) were used at the indicated concentrations. Reagents for IFNγ, IL-2, and IL-4 ELISAs were obtained from eBioscience. Supernatants were tested at the original concentrations for the IL-4 ELISAs and were also diluted in assay diluent (eBioscience) for the IFNγ and IL-2 ELISAs, because the concentrations of these cytokines in the supernatants often exceeded the detectable range.

To deplete supernatants of cytokines, neutralizing sodium azide-free antibodies were added for at least 3 hours prior to their addition to cells. The neutralizing antibodies were anti-mouse IL-2 (clone S4B6, rat IgG_{2a}, BD Biosciences Pharmingen), anti-mouse IL-4 (clone 11B11, rat IgG_1, BD Biosciences Pharmingen), anti-mouse IFNγ (clone XMG1.2, rat IgG_1, BD Biosciences Pharmingen), anti-mouse MIP-1α (goat IgG, R&D Systems), anti-mouse MIP-1β (goat IgG, R&D Systems), and anti-mouse Lymphotactin (goat IgG, R&D Systems). The antibodies against IL-2, IL-4, and IFNγ were used at 5 μg/ml while the polyclonal antibodies against MIP-1α, MIP-1β, and Lymphotactin were used at 0.5 μg/ml.

To assay effects on only B cells, B cells were purified using anti-mouse CD19 MicroBeads, LS columns, and MidiMACS magnetic separators (Miltenyi Biotec) using the manufacturer's recommended protocol. Briefly, 100 μl of beads were mixed with 900 μl of culture media containing 10^8 splenocytes and incubated at 6°C for 15 minutes. Afterwards, the cells were washed once and resuspended in 500 μl of media. $CD19^+$ cells were then enriched by passing the cells through the columns and collecting the bound cells.

Flow Cytometry

HBSS (Ca^{2+} and Mg^{2+} free) containing 2% FCS, 5 mM EDTA, and 0.05% sodium azide was used to wash cells. Staining was performed by pre-incubating cells in this solution with 5% normal mouse serum, 5% normal hamster serum, and 0.5 μg/ml FcBlock (clone 2.4G2, BD Biosciences Pharmingen) and then adding the appropriate antibodies. Propidium iodide was included during the last wash to exclude dead cells. Biotin, FITC, PE, Allophycocyanin, and Cy7PE conjugates were used for staining. The Cytofix/Cytoperm Plus kit with GolgiStop (Monensin) (BD Biosciences Pharmingen) was used for intracellular cytokine staining according to the manufacturer's protocol. γδ T cells were stained using clone GL3 or the Vγ2-specific clone UC3-10A6 (BD Biosciences Pharmingen). B cells were stained with antibodies to either CD19 (clone 6D5) or B220 (clone RA3-6B2). Additional stains were for IFNγ (clone XMG1.2; BD Biosciences Pharmingen), B7.2 (clone GL1; BD Biosciences Pharmingen), CD44 (clone

IM7; BD Biosciences Pharmingen), CD69 (clone H1.2F3; BD Biosciences Pharmingen), PD-1 (clone J43; eBioscience), CD223/Lag-3 (clone C9B7W; BD Biosciences Pharmingen), and for T10/T22 (clone 7H9 (Crowley, Fahrer et al. 2000)). Flow cytometry was performed on either a BD LSR or a BD FACScan and data was analyzed using FlowJo software (Tree Star, Inc.). Cells were sorted on either a modified Cytomation MoFlo 11-color sorter or a BD Vantage SE/DiVa.

RT-PCR

Primers for CD45 (Virts, Barritt et al. 1998), IFNγ (Huang, McClellan et al. 2002) and IL-4 (Noma, Sideras et al. 1986) were based on published sequences. The sequences of the other primers were as follows (5'-3') and were designed to span at least one intron: *FWD-TCRβC* GTT TGA GCC ATC AAA AGC AGA; *REV-TCRβC* AGG ATC TCA TAG AGG ATG GT; *FWD-TCRδC* ACC AGA ACC TGA AAA TGA CAC A; *REV-TCRδC* CTG AAG CAC TGA GAA GTT GGA A; *FWD-GranzymeA* TGA CTG CTG CCC ACT GTA AC; *REV-GranzymeA* AAA TCT CCC CCA TCC TGC TGC TA.

RNA was isolated using Trizol (Invitrogen) and reverse transcribed using SuperScriptII (Invitrogen). SureStart Taq (Stratagene) was used for all PCR reactions. Reactions were initially denatured at 94°C for 10 minutes and then subjected to cycles of PCR using the following conditions: 1 minute denaturing at 94°C, 1 minute annealing at 55°C, and 2 minutes of extension at 72°C. The reactions were then incubated for an additional 10 minutes at 72°C.

Results

A T10/T22-Specific γδ T cell Activation System

Although T10 and T22 are less polymorphic than classical MHC class I molecules, there are differences between different alleles. The G8 γδ T cell clone, which was derived from BALB/c nude mice that had been immunized with B10.BR splenocytes, recognizes the T10 and/or T22 alleles present in C57Bl/10, B10.BR, and B10.S mice (Bluestone, Cron et al. 1988). G8 γδ TCR transgenic mice have been maintained on the BALB/c background because these mice do not have a functional gene encoding the constitutively-expressed T22 molecule (Ito, Van Kaer et al. 1990) and only express the activation-induced T10 molecule of the *d* haplotype, which is a non-stimulating allele of T10 for G8 γδ T cells. Thus, the transgenic γδ T cells appear to be naïve in BALB/c mice.

In order to study antigen-specific γδ T cell responses, we first crossed G8 BALB/c mice with $RAG2^{KO}$ BALB/c mice in order to generate G8 $RAG2^{KO}$ BALB/c mice that are deficient in B cells, αβ T cells, and γδ T cells of other specificities. We then cocultured splenocytes from G8 $RAG2^{KO}$ BALB/c mice with splenocytes from $H2^{b/d}$ BALB/c mice generated by crossing BALB/c mice with BALB.B mice. $H2^{b/d}$ BALB/c splenocytes were chosen to serve as stimulator cells for the G8 $RAG2^{KO}$ BALB/c splenocytes because they express the G8-stimulatory *b* alleles of T10 and T22 in addition to the non-stimulatory $T10^{d}$. In addition, $H2^{b/d}$ lymphocytes should not be alloreactive against $H2^{d}$-expressing cells in the G8 $RAG2^{KO}$ BALB/c spleen.

After 24 hours of coculture, activated G8 γδ T cells showed a 10 to 100-fold reduction in cell-surface γδ TCR levels (*Figure 4.1A*), a gradual increase in cell size (*Figure 4.1B*), and increased expression of the very early activation marker CD69 (*Figure 4.1A*) as well as of CD44, CD223/Lag-3, and PD-1 (*Figures 4.1C, D* and *E*). On the other hand, $T10^{d}$-expressing BALB/c stimulator cells did not lead to the activation of G8 γδ T cells.

γδ T cell Activation Leads to B cell Activation Through Soluble Factors

Unexpectedly, we found that, in addition to the G8 γδ T cells, B cells also became activated in this coculture system based, initially, on their expression of CD69. This was not observed when $H2^{b/d}$ BALB/c splenocytes were cultured alone or cocultured with $RAG2^{KO}$ BALB/c splenocytes (*Figure 4.2A*) and indicated that the activation of G8 γδ T cells was necessary for the observed B cell activation. In contrast, there was no observable increase of CD69 expression on αβ T cells.

To test if B cell activation requires cell-to-cell contact, transwell assays were performed. G8 $RAG2^{KO}$ BALB/c splenocytes were co-cultured with $H2^{b/d}$ BALB/c splenocytes in the lower chamber of the transwell and additional BALB/c splenocytes were added to the upper chamber. After 24 hours, we found that some of the B cells in the transwell that were not in direct contact with the activating G8 $RAG2^{KO}$ BALB/c γδ T cells also upregulated their expression of CD69, albeit to a lower level than the B cells in the lower chamber. This may have been due to the fact that diffusion was required for the soluble factor to move from the bottom of the well to the Transwell. There was a 1 mm separation between the cells in the well and the cells in the Transwell. The average squared distance for one-dimensional diffusion is given by 2*D*t. For a cytokine-sized molecule in water, the square root thereof leads to a value of 1 mm per hour and, thus, about a third of the cytokines released at any given time will appear in the Transwell after one hour (~32% of the area of a normal curve is beyond one standard deviation unit; one standard deviation unit is about equal to the root of the average squared distance; diffusion leads to a normal distribution). As expected, the expression of CD69 on B cells in the upper chamber was not induced when G8 $RAG2^{KO}$ BALB/c splenocytes were incubated with BALB/c splenocytes in the lower chamber.

Consistent with these results, B cells could be activated to express CD69 by culturing them in supernatants taken from cocultures containing G8 $RAG2^{KO}$ BALB/c and $H2^{b/d}$ BALB/c splenocytes (*Figure 4.2B*). On the other hand, B cells incubated in the combined supernatants from separate cultures of G8 $RAG2^{KO}$ BALB/c and $H2^{b/d}$ BALB/c splenocytes did not increase their levels of CD69 expression, indicating that

coculture was required. Thus, B cell activation occurred through the activation-induced production of one or more soluble factors.

Previously, we found that transcripts for IFNγ, IL-2, Lymphotactin, and MIP-1α were induced in activated G8 γδ T cells (*data not shown*). Therefore, to identify the soluble factors responsible for inducing B cell activation, we cultured splenocytes in the supernatants taken from cocultures of G8 RAG2^{KO} and H2$^{b/d}$ BALB/c splenocytes that had been depleted of IFNγ, IL-2, Lymphotactin, MIP-1α, MIP-1β, or combinations thereof using neutralizing antibodies. We found that only the inclusion of anti-IFNγ reduced the level of CD69 induction on B cells and the effect was only partial. This suggested that there were one or more factors produced in the stimulation assay that had not been identified. Since IL-4 production has been reported in systems where γδ T cells are found to be activated and IL-4 was first identified as a B cell stimulating cytokine (Noma, Sideras et al. 1986), we assayed whether IL-4 was made in our co-culture system.

ELISA analyses showed that between 14 and 68 (average 45) pg/ml of IL-4 was in the supernatants following one day of γδ T cell activation. In comparison, there was between 1 and 16 (average 3.5) ng/ml of IFNγ and between 2 and 4.5 ng/ml (average 3) of IL-2. Thus, a low amount of IL-4 was made in our system; albeit, at levels up to two orders of magnitude below those of IFNγ and IL-2.

As with IFNγ, the depletion of IL-4 from the coculture supernatants reduced their ability to induce CD69 expression on B cells (*Figure 4.2B)*. Significantly, when both IFNγ and IL-4 were depleted, the supernatant failed to induce CD69 expression on B cells. Both the anti-IFNγ and anti-IL-4 antibodies were of the same isotype and both were needed for the observed effect, which indicated that the effect was not due to the isotype of the antibody. Taken together, these results indicate that B cell activation was primarily induced by the combined effect of IFNγ and IL-4.

We then tested whether the production of IFNγ and IL-4 was also responsible for CD69 expression on B cells during the cocultures. Neutralizing antibodies against IFNγ and IL-4 were included in the coculture of G8 RAG2^{KO} BALB/c and H2$^{b/d}$ BALB/c splenocytes. We found that the inclusion of antibody to either of these two cytokines led to a reduction in the amount of CD69 expressed by B cells and the inclusion of both

antibodies led to an even greater reduction in CD69 staining (*Figure 4.2C*). However, a low level of CD69 induction on B cells remained that may have been due to directed cytokine secretion or other factors. Taken together, these experiments suggest that IFNγ and IL-4 induce CD69 expression by B cells but do not rule out the possibility that activation through other molecules such as T10 and T22 may also lead to increased CD69 expression by B cells.

Since the removal of IFNγ and IL-4 was found to abolish B cell activation in our system, we tested whether rIFNγ and rIL-4 could stimulate B cells. We found that using both of these cytokines together led to over 4-fold more $CD69^{+}$ B cells than when each of these cytokines was used alone – even at very high concentrations (*Figure 4.2D*). A titration of rIFNγ and rIL-4 (*Figure 4.2E*) indicated that these cytokines synergized to induce CD69 expression on around 80% of B cells compared to around 20% of B cells induced by either cytokine alone for both BALB/c and C57Bl/6 backgrounds.

The Expression of B7.2 is Upregulated on Splenic B cells in the Coculture

24 hour G8 $RAG2^{KO}$ BALB/c and $H2^{b/d}$ BALB/c cocultures and supernatants thereof also led to the upregulation of B7.2 on B cells (*Figure 4.3A*). rIFNγ and rIL-4 were thus tested for their ability to induce B7.2 expression on B cells (*Figure 4.3B*) . IL-4 appeared to be more effective than IFNγ. Additionally, a titration of these cytokines (*Figure 4.3C*) revealed that while IL-4 was more effective than IFNγ at upregulating B7.2, there was also a synergism between the two. In addition to B7.2, the supernatants were also observed to upregulate levels of MHC class II (*data not shown*).

The Expression of T10/T22 is Upregulated on Splenic Cells in the Coculture

While T22 is constitutively expressed, the expression of T10 is induced through the activation of cells (Crowley, Fahrer et al. 2000). In the coculture system using $T10/T22^{b}$-expressing stimulator cells, an upregulation of T10/T22 on G8 γδ T cells and B cells became apparent after 48 hours (*Figures 4.4A* and *B*). In contrast, the expression of CD69, CD223/Lag-3, and PD-1 on γδ T cells had already peaked after 24 hours (*Figure 4.1*). This is similar to what we reported previously for αβ T cells, where antigen

recognition-induced upregulation of T10/T22 was not observed until after 60 hours of incubation (Crowley, Fahrer et al. 2000). When rIFNγ and rIL-4 were tested for their ability to upregulate T10/T22 on B cells, only rIFNγ led to higher levels (*Figure 4.4C*). In addition, supernatants of activated γδ T cells were capable of inducing T10/T22 expression by B cells in an IFNγ-dependent manner (*data not shown*).

Activated γδ T cells Produce IFNγ and IL-4

To determine the kinetics of IFNγ, IL-2 and IL-4 production, we measured their transcripts by RT-PCR 0, 1, 2, 4, 6, 11, and 25 hours after initiating the cocultures (*Figure 4.5A*). The expression of CD45 was also analyzed because its levels were found to remain mostly unchanged following activation, although there were some changes in the isoforms thereof. IFNγ and IL-4 transcripts were found to increase over the course of 25 hours of activation. IL-2 transcripts were also found to increase but reached a peak level of production around 11 hours and then declined by 25 hours, which was in agreement with its detected levels in the supernatants (*data not shown*).

In order to determine whether IFNγ and IL-4 are made by G8 γδ T cells in this stimulation system, we cocultured G8 γδ T cells with T10/T22^{b}-expressing splenocytes for 12 hours instead of the previously-assayed 24 hours because, at this timepoint, the majority of G8 γδ T cells still had clearly-detectable levels of surface γδ TCRs that made it possible to purify G8 γδ T cells by FACS sorting. Allophycocyanin-labeled antibodies to the γδ TCR were then used to identify γδ T cells and FITC-labeled antibodies to 2B4, CD4, CD19, F4/80, Mac1, NK1.1, and to the αβ TCR were used to identify αβ T cells, B cells, NK cells, monocytes, and macrophages. FITC^{+} cells were removed using anti-FITC microbeads and the remaining cells were doubly sorted for live cells expressing the γδ TCR. After the first sort, a purity of 99.1% was obtained that was further increased to above 99.7% through the second sort. The sorted activated G8 γδ T cells were found to express transcripts for both IFNγ and IL-4 (*data not shown*).

We then determined if γδ T cells or cells other than γδ T cells were responsible for the majority of IFNγ and IL-4 transcripts in the coculture. After 24 hours of activation, cDNA was prepared from FACS-purified γδ T cells. cDNA was also prepared

from sorted B cells, αβ T cells, and *other* cells that stained for neither the γδ TCR, the αβ TCR, B220, nor high levels of CD69. These other cells included NK cells, macrophages, and dendritic cells.

RT-PCR was conducted on the sorted cell populations (*Figure 4.5B*). The majority of transcripts for IFNγ were detected in the sorted γδ T cells. The expression of IFNγ by activated γδ T cells was confirmed by intracellular cytokine staining (*Figure 4.5C*). IFNγ was also expressed to a lower extent by cells in the *other* population. It is possible that this population included γδ T cells that downregulated their γδ TCRs but did not express very high levels of CD69.

Transcripts for IL-4 were detected in the sorted γδ T cells. Similar to IFNγ, there was also a reduced level of IL-4 expressed in the *other* population. Again, this may have been due to contaminating γδ T cells that downregulated their surface γδ TCR levels. Approximately 10 times more cells were present in the γδ T cell population than in the *other* population during the sort so even identical amounts of transcripts in both populations would suggest that γδ T cells are responsible for 10 times more IL-4 production than the *other* population, assuming that the translation of IL-4 transcripts in both populations is equally efficient. It has been reported that activated splenic γδ T cells from KN6 BALB/c mice express IFNγ but do not express IL-4 (Kawaguchi-Miyashita, Shimada et al. 2000). This may have been due to their use of plate-bound anti-Vγ4 antibody as opposed to our use of ligand-expressing splenocytes.

Transcripts for Granzyme A, which appear to be constitutively expressed by γδ IELs (Fahrer, Konigshofer et al. 2001), were also detected in the activated G8 γδ T cells and were also detected in the *other* population. This indicated that this population likely contained NK cells, which are know to express cytotoxic molecules like Granzyme A.

The use of primers that amplify all isoforms of CD45 (Virts, Barritt et al. 1998) indicated that activated G8 γδ T cells expressed mostly the short RO isoform, which is characteristic of activated lymphocytes, while B cells, as expected, expressed mostly the large B220 isoform. αβ T cells expressed both the intermediate RB and short RO isoforms. Cells that were classified as *other* cells expressed both the RB and RO isoforms.

Discussion

Despite the observations that γδ T cells and αβ T cells are capable of similar effector functions, such as cytotoxicity and cytokine secretion, the contribution of γδ T cells to host immune competence is clearly distinct from that of αβ T cells. One major difference between αβ T cells and γδ T cells that may be responsible for this is their antigen recognition requirement (reviewed in (Chien, Jores et al. 1996)). Unlike αβ T cells, γδ T cells are not limited to recognizing antigens that are processed first and then presented by MHC molecules. Therefore, γδ T cells have the potential to be stimulated by many different types of cells.

Here, we analyzed the responses of G8 transgenic T cells to spleen cells that expressed the G8 γδ TCR ligands, $T10^b$ and $T22^b$. In the spleens of *b* haplotype mice, almost all cell populations express T10/T22 and some of the highest baseline levels are found on B cells (*data not shown*). We found that in our coculture system, T10/T22 levels are induced most prominently on B cells and G8 γδ T cells after activation. This suggests that during immune responses, the T10/T22-reactive γδ T cells can sustain, enhance and amplify as well as regulate their responses by increasing the expression of their ligands and recruiting and activating new cell types to serve as additional stimulator cells. Such a mechanism would be unique to γδ T cells because of their lack of a requirement for special antigen presenting cells and may compensate for the paucity of γδ T cells compared to αβ T cells.

Along this line, we have previously shown that T10/T22 can be induced on αβ T cells and B cells upon antigenic stimulation (Crowley, Fahrer et al. 2000). Our results here show that while T10/T22-induction on γδ T cells requires cell-to-cell contact, T10/T22-induction on B cells can also be obtained by IFNγ produced by activated γδ T cells.

One important observation is the early production of IL-4 by activated G8 γδ T cells. Although the Thy-1^{dull} subset of thymic γδ T cells has been found to produce IL-4 (Azuara, Grigoriadou et al. 2001), it has been reported that no IL-4 was detected when G8 clones (Cron, Gajewski et al. 1989) or KN6 BALB/c splenocytes (Kawaguchi-

Miyashita, Shimada et al. 2000) were stimulated using antibodies. This discrepancy could be due to differences between primary cells and clones and lines and the setup of the assays because we used non-irradiated splenocytes from $H2^{b/d}$ BALB/c mice as opposed to irradiated B10.BR splenocytes or plate-bound antibodies. Regardless, while substantially less IL-4 is produced than IFNγ in our system, IL-4 and IFNγ can synergize to lead to the expression of CD69 by over 80% of B cells and also lead them to upregulate B7.2 and MHC class II. These results suggest that through the activation of γδ T cells, B cells may become better antigen presenting cells. This aspect has not been anticipated before and provides a new way for γδ T cells to regulate αβ T cell responses. In addition, while Thy-1^{bright} γδ T cells have been reported to produce less IL-4 than Thy-1^{dull} γδ T cells, the reported amount produced by these cells (1 ng/ml after 3 days using $1.5x10^5$ activated cells) (Azuara, Grigoriadou et al. 2001) should be capable of mediating the same effects.

A synergism between IFNγ and IL-4 has been observed in other systems. For instance, these cytokines can increase the cyclic AMP-phosphodiesterase activity of monocytes and do so even at concentrations that are below detectable levels (Li, Chan et al. 1992). The combination of IFNγ and IL-4 has also been found to induce alveolar macrophages to produce superoxide anions (Bhaskaran, Nii et al. 1992) and to activate macrophages so that they produce TNFα and microbicidal nitrogen intermediates (Bogdan, Stenger et al. 1991; Stenger, Solbach et al. 1991). The combination also synergizes to lead to a reduction in the amount of soluble CD14 that is released by monocytes and macrophages (Landmann, Fisscher et al. 1992), perhaps making these cells more responsive to LPS.

Dendritic epidermal γδ T cells (DETCs) and splenic γδ T cells may be capable of similar responses because DETCs isolated from wound areas have been found to produce IFNγ (Jameson, Ugarte et al. 2002) and the production of IL-4 has been observed in cultured DETCs (Matsue, Cruz et al. 1993; Huber, Descossy et al. 1995). Thus, these cells may promote wound repair by producing keratinocyte growth factor and by enhancing local immune responses with IFNγ and IL-4 in order to minimize infections. Interestingly, NK T cells produce both IFNγ and IL-4 and do so in large amounts

following activation in response to α-galactosylceramide and this has also been found to induce the activation of B cells (Burdin, Brossay et al. 1999; Carnaud, Lee et al. 1999; Leite-De-Moraes, Hameg et al. 2001) suggesting that the function of cytotoxic cells also includes helping other cells, such as B cells, participate in immune responses.

Our results here also impart a possible mechanism for activated γδ T cells to provide help to B cells regardless of the specificity of the B cell receptor, but in an antigen-specific (for the γδ T cells) manner. In this context, clusters of γδ T cells have been found in B cell follicles within human secondary lymphoid tissues (Brandes, Willimann et al. 2003). Further, it has been observed that αβ T cell-deficient mice, where approximately 27% of γδ T cells show signs of activation, contain high levels of autoreactive antibodies of the T cell-dependent IgG and IgE isotypes that may be due to γδ T cell-produced IL-4 (Wen, Roberts et al. 1994). In addition, the migration and differentiation of self-reactive erythrocyte-specific B cells has also been reported in mice that are transgenic for both the 4C8 anti-erythrocyte antibody and the T10/T22-reactive KN6 γδ TCR (Watanabe, Ikuta et al. 2000). It is worth noting that human γδ T cell clones have also been reported to enhance immunoglobulin production by B cells but appear to do so in a contact-dependent manner (van Vlasselaer, Gascan et al. 1992) that is dependent on CD40/CD40L interactions (Horner, Jabara et al. 1995), and activated human γδ T cells have also been found to express OX40, ICOS and CD70 (Brandes, Willimann et al. 2003). This suggests that while activated murine γδ T cells do not appear to express CD40L ((Wen, Roberts et al. 1994) and data not shown) and influence B cell function using soluble factors like IFNγ and IL-4, human γδ T cells require cell-to-cell contact. Thus, by using a defined antigen-specific *in vitro* γδ T cell stimulation system, we have identified mechanisms and complexities that underlie the roles of γδ T cells during immune responses.

Figure Legends

Figure 4.1: γδ T cells activated by cells expressing T10/T22^{b} downregulate their cell-surface γδ TCR levels, blast, and express activation markers

(A, B, C) G8 RAG2^{KO} BALB/c splenocytes were incubated with either H2$^{b/d}$ BALB/c or H2$^{d/d}$ BALB/c splenocytes for 1 day. The cells were then stained with antibodies to CD69 (H1.2F3) and the γδ TCR (GL3) and analyzed by FACS. Propidium iodide and an antibody to B220 (RA3-6B2) were used to exclude dead cells and B cells, respectively. (A) The expression of CD69 and γδ TCR on the remaining cells is shown. (B) Combined γδ TCR^{+} and CD69^{hi} cells from (A) were then analyzed for cell size (forward scatter) and γδ TCR levels. In addition, G8 γδ T cells that were incubated in the presence (black line) or absence (shaded region) of H2$^{b/d}$ BALB/c splenocytes were analyzed for the expression of (C) CD44 (IM7), (D) CD223/Lag-3 (C9B7W) and (E) PD-1 (J43).

Figure 4.2: G8 γδ T cell activation induces CD69 expression on B cells in an IFNγ- and IL-4-dependent manner

The expression of CD69 was determined with either FITC or PE-labeled antibodies to CD69 (H1.2F3) and representative histograms of CD69 expression on B cells are shown in A – D. (A) H2$^{b/d}$ BALB/c spleen cells were cultured for 24 hours alone (gray shaded region) or cocultured with either RAG2^{KO} BALB/c (black shaded region) or G8 RAG2^{KO} BALB/c (black line) splenocytes. (B) BALB/c splenocytes were incubated for 24 hours with either culture media (gray shaded region), the supernatant of a 24 hour coculture of G8 RAG2^{KO} BALB/c and H2$^{b/d}$ BALB/c splenocytes (thick line) or this supernatant depleted of IFNγ (XMG1.2; Rat IgG1; dashed line), IL-4 (11B11; Rat IgG1; thin line), or both (black shaded region). (C) H2$^{b/d}$ BALB/c splenocytes (gray shaded region) or a mix of G8 RAG2^{KO} BALB/c and H2$^{b/d}$ BALB/c splenocytes was cultured for 24 hours in the absence (thick line) or in the presence of neutralizing antibodies to IFNγ (dashed line), IL-4 (thin line), or both (black shaded region). (D) BALB.B B cells were cultured for 24 hours in media (shaded region) or media containing either 1 μg/ml of rIFNγ (dashed line), 100 ng/ml of rIL-4 (thin line), or both (thick line).

(E) The percentage of B cells that are $CD69^+$ are shown after BALB.B B cells were cultured for 24 hours in the absence or presence of 10-fold dilutions of rIFNγ (between 1 pg/ml and 1 μg/ml) and rIL-4 (between 100 fg/ml and 100 ng/ml).

Figure 4.3: G8 γδ T cell activation induces B7.2 expression on B cells in an IFNγ- and IL-4-dependent manner

The expression of B7.2 was determined using clone GL1 and representative histograms of B7.2 expression on B cells are shown in (A) and (B). (A) BALB/c splenocytes were cultured for 24 hours in either culture media alone (shaded region) or supernatant of a 24 hour coculture of G8 $RAG2^{KO}$ BALB/c and $H2^{b/d}$ BALB/c splenocytes (thick line). (B) BALB.B B cells were cultured for 24 hours in media (shaded region) or media containing either 1 μg/ml of rIFNγ (dashed line), 100 ng/ml of rIL-4 (thin line) or both (thick line). (C) Mean levels (in fluorescence units) of B7.2 on B cells are shown after BALB.B B cells were cultured for 24 hours in the absence or presence of 10-fold dilutions of rIFNγ (between 1 pg/ml and 1 μg/ml) and rIL-4 (between 100 fg/ml and 100 ng/ml).

Figure 4.4: The activation of G8 γδ T cells induces T10/T22 expression on B cells and G8 γδ T cells during the coculture

(A, B) G8 γδ T cells were cultured in the presence of C57Bl/6 splenocytes and the expression of T10/T22 (7H9-biotin; streptavidin-allophycocyanin) was assayed after 48 hours on γδ T cells (GL3-PE) and B cells (RA3-6B2-PE). Representative histograms are shown of (A) T10 (7H9) levels on activated G8 γδ T cells (dark line) in comparison to those on G8 γδ T cells cultured in the absence of stimulator cells (shaded region) and of (B) T10/T22 levels on B cells cultured in the presence (dark line) or absence (shaded region) of G8 γδ T cells. (C) BALB.B B cells were cultured for 24 hours in media (shaded region) or media containing either 1 μg/ml of rIFNγ (dashed line), 100 ng/ml of rIL-4 (thin line), or both (thick line).

Figure 4.5: IFNγ and IL-4 are mostly produced by activated G8 γδ T cells in the cocultures of G8 RAG2^{KO} BALB/c and H2$^{b/d}$ BALB/c splenocytes

(A) RNA was isolated from approximately 2x10^6 cells after 0, 1, 2, 4, 6, 11, and 25 hours of coculture and analyzed for the expression of IFNγ, IL-2, IL-4, and the major isoforms of CD45 (B220, RBC, RB and RO) using 28 cycles of RT-PCR. (B) Cells that were cocultured for 24 hours were stained with antibodies to CD69 (H1.2F3-FITC), γδ TCR (GL3-PE), αβ TCR (H57-597-Allophycocyanin), and B220 (RA3-6B2-Cy7PE). Propidium iodide was used to exclude dead cells. γδ T cells, αβ T cells, B cells, as well as *other* cells that, based on their cell-surface phenotypes, were neither B cells nor T cells were sorted. cDNA was prepared from the sorted cells and approximately 100 cell-equivalents thereof per reaction were analyzed for the expression of CD45, Granzyme A, IFNγ, IL-4, and the constant regions of the TCR β and δ chains using 30 cycles of RT-PCR. αβ T cell, B cell, γδ T cell, and *other* samples are ordered left to right. (C) Monensin was added 11 hours after the start of cultures of G8 RAG2^{KO} BALB/c or H2$^{b/d}$ BALB/c splenocytes or cocultures thereof and cells were stained 4 hours afterwards with anti-Vγ2 (UC3-10A6) to detect the G8 γδ TCR and subsequently fixed, permeabilized, and stained with either anti-IFNγ (XMG1.2) or a rat IgG1 isotype control (R3-34).

Figure 4.1: γδ T cells activated by cells expressing T10/T22[b] downregulate their cell-surface γδ TCR levels, blast, and express activation markers

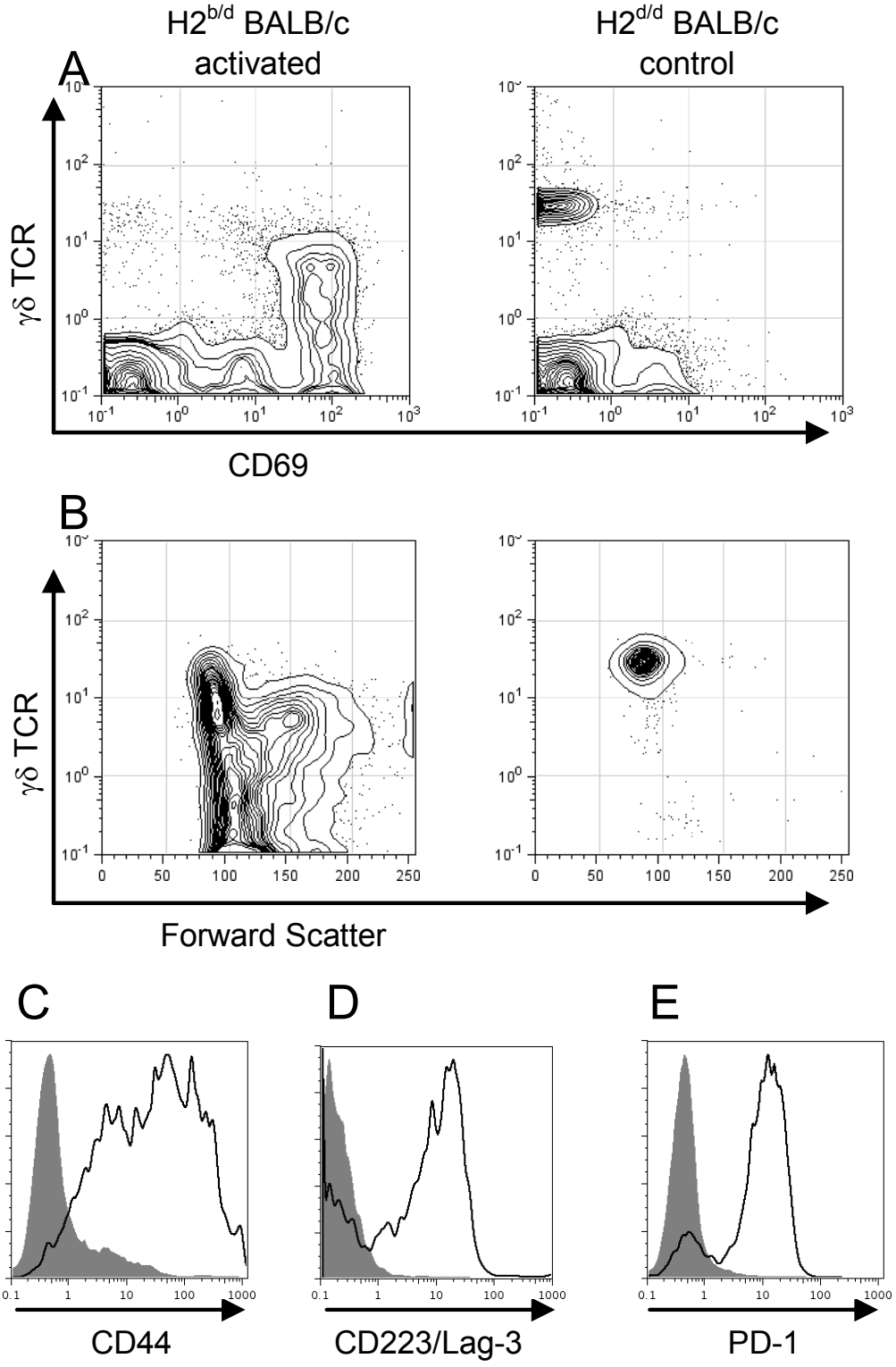

Figure 4.2: G8 γδ T cell activation induces CD69 expression on B cells in an IFNγ- and IL-4-dependent manner

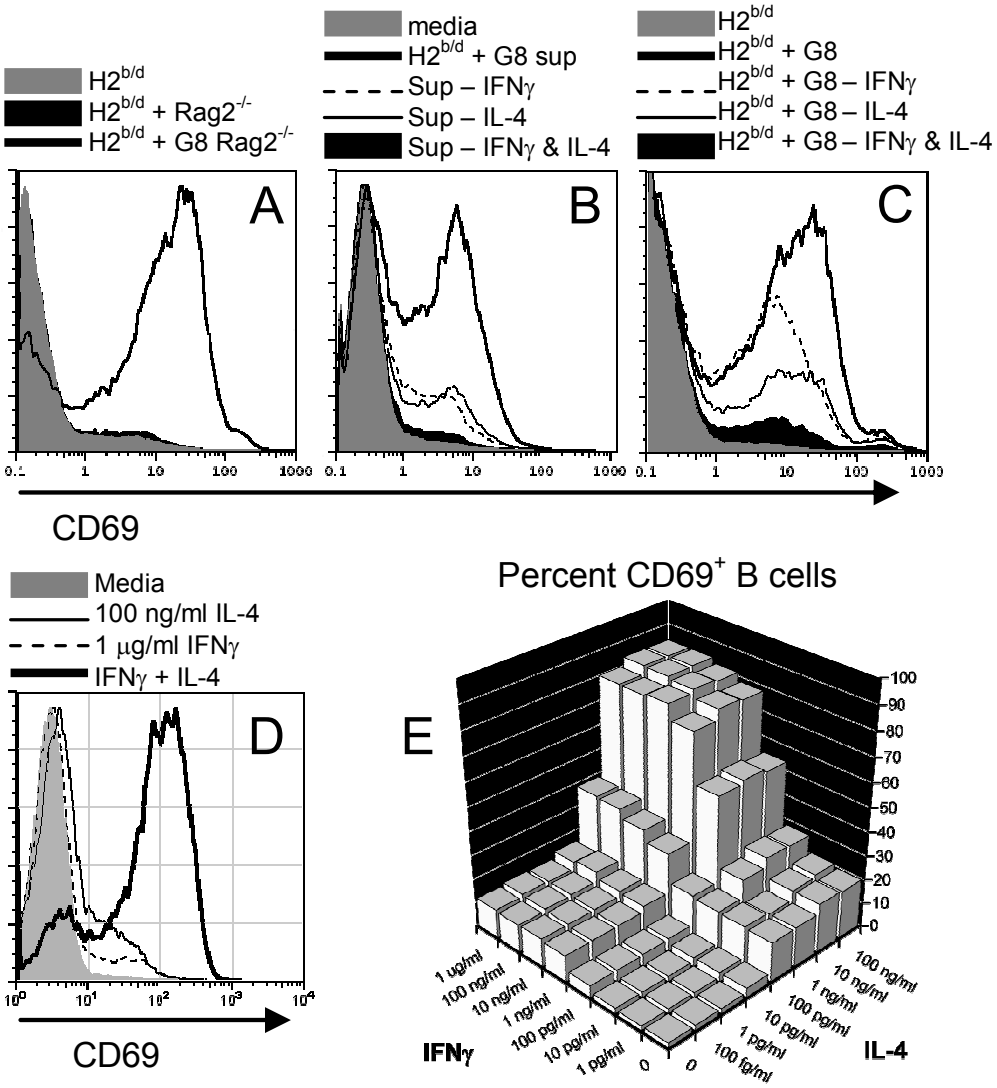

Figure 4.3: G8 γδ T cell activation induces B7.2 expression on B cells in an IFNγ- and IL-4-dependent manner

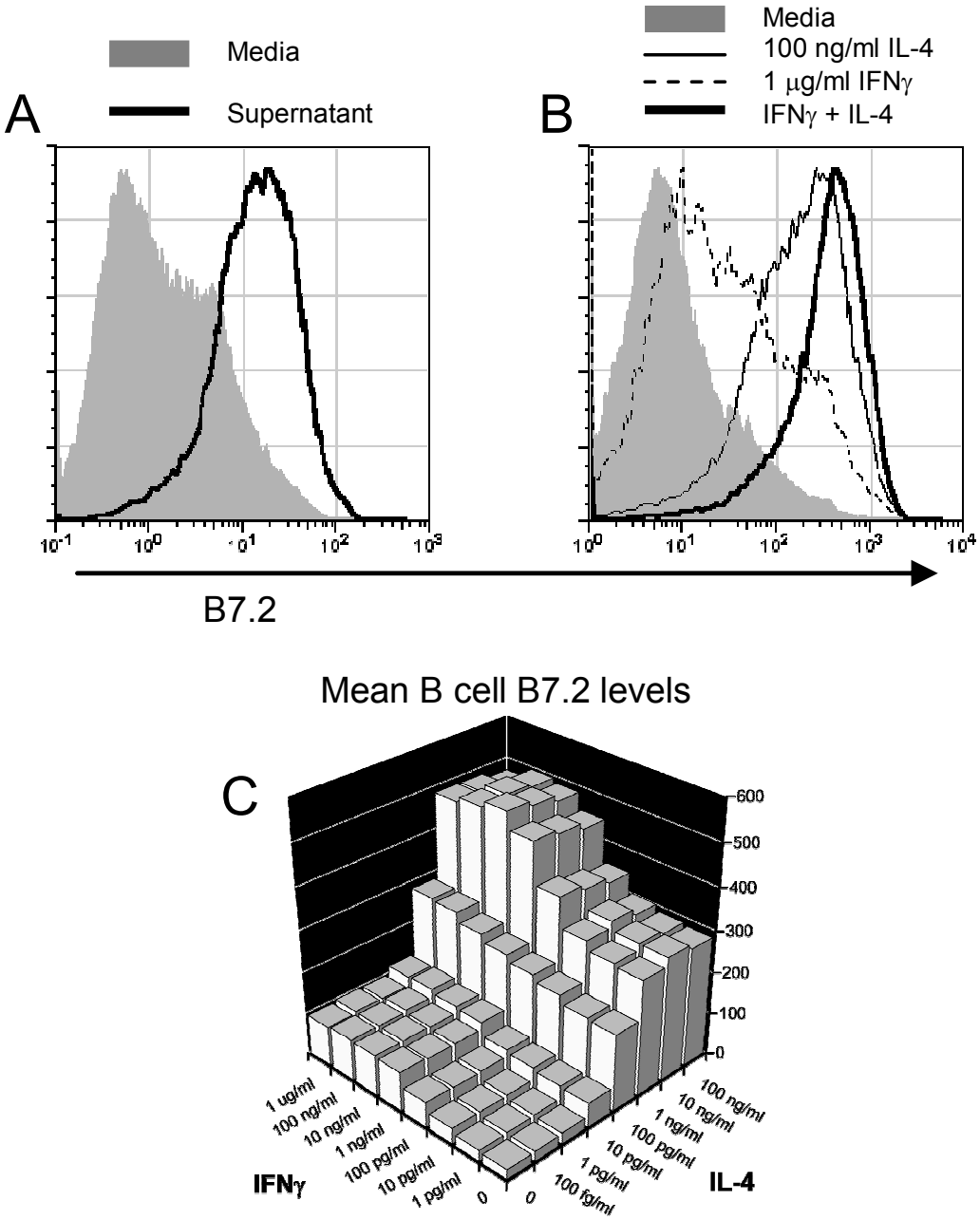

Figure 4.4: The activation of G8 γδ T cells induces T10/T22 expression on B cells and G8 γδ T cells during the coculture

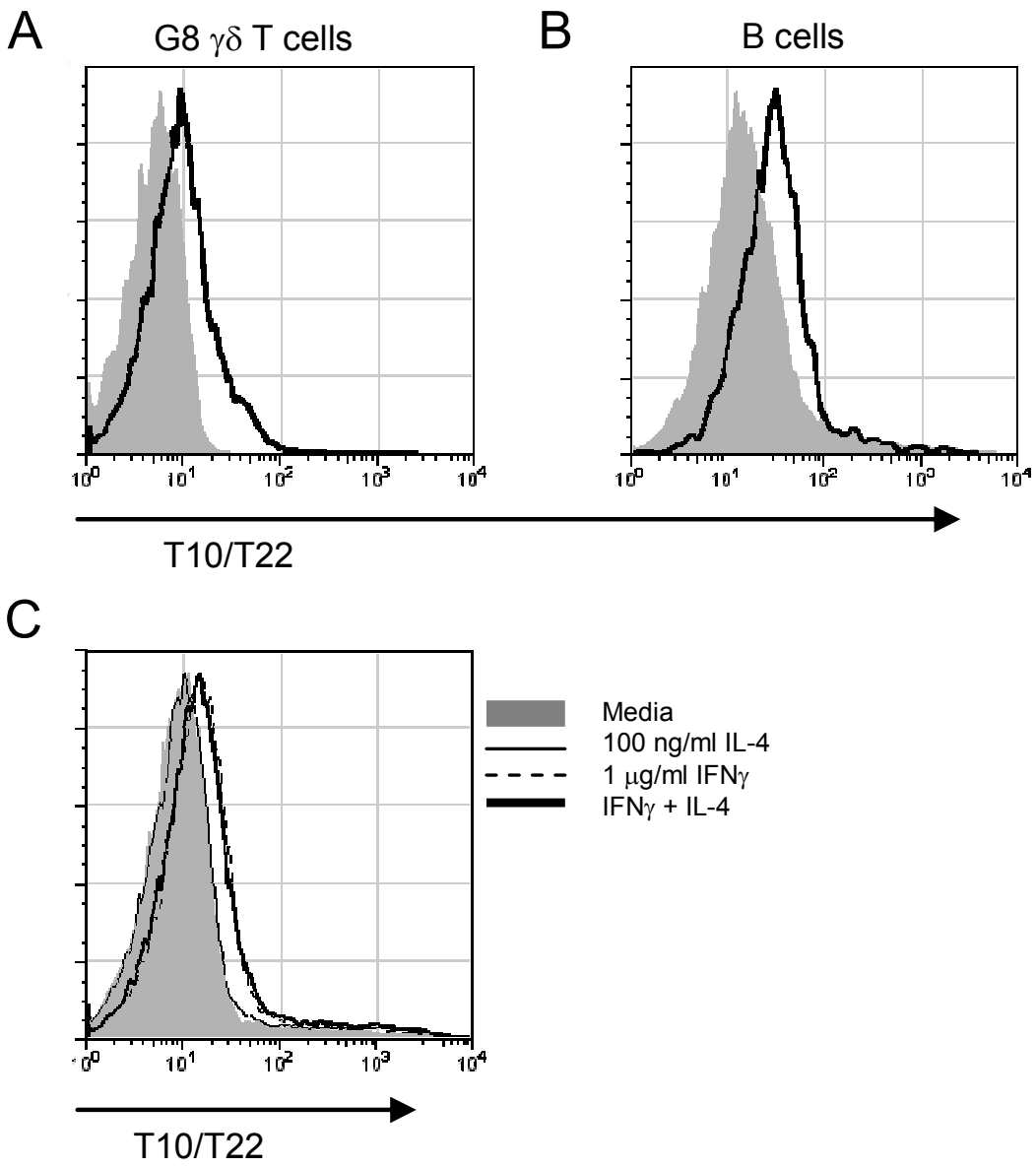

Figure 4.5: IFNγ and IL-4 are mostly produced by activated G8 γδ T cells in the cocultures of G8 RAG2^{KO} BALB/c and H2$^{b/d}$ BALB/c splenocytes

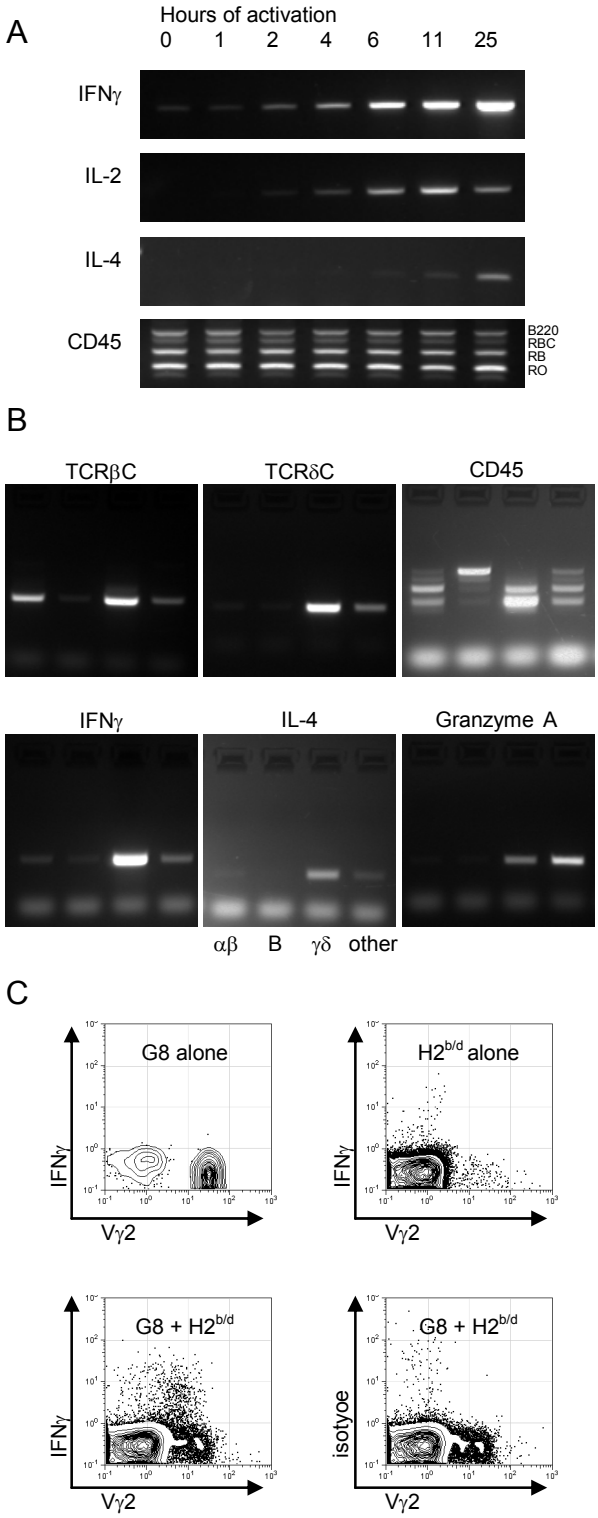

Chapter 5: A Simulation of Cell-to-Cell Contact in Order to Study Synapse Formation and T cell Activation

Foreword

"Physical Chemistry 5th Edition" by Gordon M. Barrow served as a general reference for this chapter.

Introduction

The interaction of a T cell with another cell can lead to the formation of a synapse if the T cell encounters agonist TCR ligands in the process. During synapse formation, the TCR actively moves towards the area where the T cell is in contact with the other cell (Wulfing and Davis 1998). In general, the TCR accumulates in the middle of the synapse and this is also accompanied by the accumulation of other molecules. For instance, MHC molecules bearing agonist peptides also accumulate in the middle of the synapse although, interestingly, MHC molecules bearing what would be thought of as irrelevant peptides do so as well. Unlike the TCR and MHC, ICAM-1 and LFA-1 accumulate in the area between the TCR and edge of the synapse. These central and peripheral distributions have been termed cSMACs and pSMACs by some (Monks, Freiberg et al. 1998) where c and p stand for central and peripheral, respectively, and SMACs stand for supramolecular activation clusters. As the term SMAC implies, many molecules accumulate and, over the last few years, ever-increasing numbers of different molecules have been found to accumulate.

In order to study the process of synapse formation further and its relevance to T cell activation, I designed a simulation of cell-to-cell contact. Simulations are very helpful in that, if properly designed, they allow one to design and obtain results from experiments that involve conditions that may be difficult to achieve in a laboratory setting. In addition, the design of simulations of biological processes exposes areas where additional research is needed in order to simulate these processes properly. An example of such a process is the general movement of the TCR to the synapse where it is unclear where each TCR is moving to and why it is moving there. Another example of such a process is the determination of whether or not a TCR is bound to an agonist peptide/MHC complex. It will be interesting and important to find answers to these questions. What follows are some of the results of the simulation that can only get more accurate as questions, like these, get answered.

Materials and Methods

On the use of JAVA

The simulation is written in the programming language JAVA. It currently contains a bit fewer than 10,000 lines of code. While JAVA programs rely on an interpreter and generally do not run as fast as compiled programs written in C++, they have the benefit of being easily portable to different computers and operating systems. The simulations shown in this chapter were either run on one of my computers, the lab's computers or, more likely, one of the many dual-processor UNIX-based computers that are part of Stanford's Leland computing cluster. Most simulations were completed in about a day.

The Simulation, In a Nutshell

The simulation is based on a model of two cells that touch each other at a contact area (*Figure 5.1A*). These two cells are represented by one or more spheres of which each contains a representation of the contact area. The contact area is divided into smaller regions. Molecules are found on the spheres and those inside the same region of the contact area can interact with each other. Molecules diffuse on the spheres and can also move towards a target. Concentrations of molecules are determined by using the area of each region and a confinement distance. On-rates for molecule binding are adjusted based on the membrane separations in the regions.

Cells

Cells are represented by one or more spheres. The reason for being able to represent two cells using more than two spheres is that this is a simulation of molecular interactions and images usually only have three color channels: red, green, and blue. This makes it difficult to tell more than three different types of molecules apart on the same sphere. Thus, in order to visualize the locations of a large number of different molecules and in order to be able to tell them apart, molecules can be assigned to different spheres. For each sphere, it is possible to specify the location of the sphere, the

radius of the sphere, the orientation of the contact area, the mean distance from the middle of the contact area for targets of directed molecule movement, the standard deviation of this distance, and whether or not the sphere is larger or smaller than a hemisphere.

Contact Area

It is possible to specify the radius of the contact area, which must be smaller or equal to the radii of all spheres. In order to use experimentally-determined on-rates, the contact area is divided into smaller regions (*Figure 5.1B*). It is possible to specify the maximum number of molecules that can be found inside each region on a cell and the number and height of virtual immobile bound molecules that contribute to the separation of membranes inside each region.

Molecules

For each type of molecule, it is possible to specify a large number of parameters. These include the name, the sphere it is located on, the color used to represent it, the height, the heights of all complexes formed with this type of molecule, the standard deviation for entering regions in an unbound state when the membranes are spaced closer together than the height of the molecule, the standard deviation for entering regions in a complexed state when the membranes are not separated by the height of the complex, the on-rates for forming potential complexes, the standard deviations of on-rate adjustments when the membranes are not separated by the heights of potential complexes, the confinement distance for adjusting on-rates, the off-rates for dissociating complexes, the velocity by which the unbound molecule moves towards a target, the velocities by which complexes move towards a target, the diffusion coefficient when unbound, the diffusion coefficients for complexes, the fraction that is initially intracellular, the fraction that is initially degraded, the rate of resynthesis, the target for exocytosis, the standard deviation of exocytosis, the rate of exocytosis, the rate of endocytosis when unbound and resting, the rate of endocytosis when unbound and activated, the rates of endocytosis when complexed and resting, the rates of endocytosis when complexed and activated, the rate

of degradation when resting and intracellular, the rate of degradation when activated and intracellular, the rate of deactivation when extracellular, the rate of deactivation when intracellular, and the duration of constant binding needed for activation.

Virtual Molecules

As will be discussed shortly, the separation of membranes inside the contact area is important. Virtual molecules act as immobile struts that reinforce a certain membrane separation inside the contact area. The larger the number of virtual molecules, the more likely it will be that the membrane separation inside a particular region of the contact area will be similar to the height of the virtual molecules. Virtual molecules are not used for any other computations.

Confinement Distance

On-rates are typically determined experimentally for volume and not area concentrations. In order to use on-rates determined for volume concentrations, the area concentrations are divided by so-called confinement distances (Bell, Dembo et al. 1984). While the separation of membranes in the contact area between two interacting cells typically ranges between 15 and 40 nm, the confinement distance has sometimes been reported to be as small as 2 nm (or orders of magnitude larger). This may be because, unlike in solution, molecules in membranes are oriented towards each other (or are separated such that they cannot bind). Then, once one receptor binds its ligand, the membrane close to that receptor is spaced optimally so that additional receptor/ligand complexes of the same type can form. This may then lead to larger areas where only certain receptors bind optimally to their ligands. A good general discussion of the confinement distance can be found in a review by M.L. Dustin (Dustin, Bromley et al. 2001).

Membrane Separation

When a molecule of type A on one cell binds to a molecule of type B on another cell, the membranes close to those molecules are spaced so that additional A to B binding

is favored. As more A to B binding takes place, this membrane spacing may be reinforced. On the other hand, other molecules whose complexes are taller or shorter than A/B complexes may not bind as readily because their interacting regions may not be optimally spaced (*Figure 5.1C*). In addition, the spacing of membranes affects whether molecules and complexes can enter regions (e.g., some may be too tall).

The separation of membranes in each region is calculated by taking a starting separation value for the region and multiplying it by the amount of virtual molecules that are causing that separation. The sum of all heights of complexes in that region is added to that value and the result is divided by the sum of virtual molecules and complexes in that region. The resulting separation is then used to modify the chance of a molecule binding to another molecule and the chance for a molecule or complex moving from one region to another.

Penalizing Sub-Optimal Distances

Some of the processes involved in molecule binding and region entry are modeled using normal distributions. While these processes may not necessarily behave according to normal distributions, they do have maximal values at their optima and lower values as the distance to the optima decreases or increases (*Figure 5.1D*). For these processes, it is possible to specify an optimal distance for membrane separation, which is the height of the dimer or monomer, as well as a standard deviation, σ, which is the distance from the optimum that corresponds to one standard deviation unit on the normal curve (1σ = 60.7% of the maximal value; 2σ = 13.5%; 3σ = 1.1%). The distance from the optimal distance, Δ, is then used in the following equation to obtain a ratio. This ratio, which lies between 0 and 1, is then used to adjust further calculations.

$$ratio = \frac{\frac{e^{-\frac{1}{2}\left(\frac{\Delta}{\sigma}\right)^2}}{\sigma\sqrt{2\pi}}}{\frac{1}{\sigma\sqrt{2\pi}}} = e^{-\frac{1}{2}\left(\frac{\Delta}{\sigma}\right)^2}$$

Adjusting the Rate of Association

When two molecules attempt to interact and the calculated distance between the membranes in the region containing the molecules is not the same as the length of the extracellular region of the potential complex, the k_{on} value is multiplied by the above ratio. Thus, at the optimal distance, the k_{on} value will be the specified k_{on} value, but at closer and further distances, the k_{on} value will be reduced.

Region Entry

The entry and exit of regions inside the contact area is regulated. For instance, complexes cannot leave the contact area because they are attached to both membranes. If complexes attempt to leave the contact area, they bounce off the edge. As molecules attempt to leave one region and enter another region, the likelihoods for these events are calculated and it is then determined if these events should take place. If a molecule is not allowed to enter a particular region, then it is moved back to its original location and it tries to move again.

When an unbound molecule attempts to enter a region where the membranes are spaced closer together than the height of the molecule, a random number between 0 and 1 is used to determine if this event can take place. The value of Δ is the absolute difference between the height of the molecule and the distance between the membranes in the region. The value of Δ is calculated for both the original and final region and *ratio* values are obtained for both regions. If the molecule is shorter than the distance between the membranes, a *ratio* value of 1 is used. The *ratio* value of the final region is divided by the *ratio* value of the original region to obtain the probability that the molecule can enter the final region. If the random number is smaller than that probability, then the event will take place. If not, then the program will attempt to move the molecule from the original location by a new distance in a new direction according to the same rules. Thus, the movement of tall molecules into narrowly-spaced regions can be prevented.

When a bound molecule attempts to enter a region where the membranes are spaced closer or further than the height of the complex, a random number between 0 and 1 is used to determine if this event can take place. The value of Δ is the difference

between the height of the complex and the distance between the membranes in the region. The value of Δ is calculated for both the original and final region and *ratio* values are obtained for both regions. If Δ does not differ in sign, then the *ratio* value of the final region is divided by the *ratio* value of the original region to obtain the probability that the complex can enter the final region. If Δ differs in sign, then the probability is the *ratio* value in the final region. If the random number is smaller than the probability, then the event will take place. Otherwise, the program will attempt to move the bound molecule from the original location by a new distance in a new direction until the event can take place. Thus, bound molecules tend to move into regions where the membrane separation is similar to the height of the complex and where they are also capable of rebinding with a more optimal k_{on} upon dissociation of the complex.

Simulating Receptor Dynamics

Initially, the simulation allocates space for all potential molecules. These molecules are then either randomly seeded onto the surfaces of spheres or treated as being internal or degraded. They are then put through iterations where a specified period of time is simulated. The shorter this period of time is, the more accurate the simulation becomes. Ideally, this time should be chosen such that molecules do not diffuse more than one region away in the contact area and do not all release and bind in each period of time. All rates use first-order rate constants except for k_{on}, which relies on second-order rate constants. In addition, receptor activation occurs after a fixed period of time and molecule synthesis does not rely on a random number to determine whether or not it should take place.

When using a first-order rate constant, *k*, the formula below is used to determine the probability, *p*, that an event will take place in a given amount of time, *t*. A random number between 0 and 1 is then generated and the event takes place if this number is lower than the calculated probability.

$$p = 1 - e^{-k \times t}$$

The simulation starts with the first molecule in a long list of molecules and puts it through the process illustrated in *Figure 5.2* and summarized below. If more than one thread is used (e.g., on multi-processor machines) then the list is divided evenly among threads and the starting molecules are chosen accordingly. Once the last molecule has been reached, a new round starts at the first molecule until a certain amount of total time has been simulated.

Molecules that are in a complex where they are the binding partner (i.e., the other molecule initiated the binding event) or that are currently internal or degraded are skipped.

Molecules that are part of a complex but are not the binding partner attempt to release from the binding partner using the specified k_{off}.

Molecules that are still part of a complex (i.e., they did not release) have their bound time increased. If this bound time or the bound time of their partners exceeds a specified amount, $t_{activate}$, they and/or their partners become activated.

Molecules attempt to internalize based on the applicable k_{endo} (active/inactive, bound/free). When bound molecules internalize, this dissociates the complex and the other molecule is freed.

External free molecules that are in an activated state attempt to deactivate based on the specified $k_{deactivate(ext)}$.

Molecules then move and/or diffuse and, if bound, their binding partner is moved to the same location in the contact area. If a molecule or complex is moved into a new region of the contact area, a test is performed to determine whether this move can take place. If not, another attempt is made to move and/or diffuse the molecule or complex. Complexes cannot leave the contact area and will bounce off the edge of the contact area.

Molecules that are not bound and are in the contact area then attempt to bind to other molecules inside the same region of the contact area based on the specified k_{on} values.

Internal molecules that are in an activated state attempt to deactivate based on the specified $k_{deactivate(int)}$.

Internal molecules that are in an inactive state attempt to externalize based on the specified $k_{exocytosis}$. During exocytosis, molecules can either randomly appear anywhere

on the surface of a sphere or can be biased to appear a certain distance from the middle of the contact area with a normal distribution.

Internal molecules that are in an inactive state and did not externalize may be degraded based of the specified $k_{degrade(inactive)}$.

Internal molecules that are in an activated state may be degraded based on the specified $k_{degrade(active)}$.

Degraded molecules are resynthesized if the current rate of synthesis (a fixed number per unit of time) dictates that additional molecules still need to be added. If a molecule is currently in a degraded state and molecules still need to be synthesized, then the molecule will be resynthesized.

Simulating Release

The probability, p_{rel}, that a complex will dissociate in a given amount of time is calculated using the standard formula for first-order reactions:

$$p_{rel} = 1 - e^{-k_{off} \times t}$$

A random number between 0 and 1 is generated and, if this random number is smaller than p_{rel}, the complex will dissociate.

Simulating Diffusion

In two-dimensional diffusion, the distance molecules diffuse in each dimension has a normal distribution. The average squared distance moved is the product of 4, the diffusion coefficient, and the time being simulated. Thus, in order to simulate diffusion, two random numbers, x_a and x_b, with Gaussian distributions, means of 0, and standard deviations of 1 are generated.

The distance moved, x, can be calculated from the values of x_a and x_b using the following equation:

$$x = \sqrt{x_a^{\,2} + x_b^{\,2}}$$

The average values of the squared values of x_a and x_b is 1 and thus the average value of the sum of the squared values is given by the following equation:

$$\overline{x^2} = 2$$

These numbers are then used with the following equation in order to obtain the distance, d_{diff}, that a given molecule or complex with a diffusion coefficient of D will diffuse in a random direction in a given amount of time.

$$d_{diff} = \sqrt{\frac{x_a^{\,2} + x_b^{\,2}}{2} \times 4 \times D \times t} = \sqrt{\left(x_a^{\,2} + x_b^{\,2}\right) \times 2 \times D \times t}$$

Simulating Directed Movement

In addition to diffusing, molecules can actively move towards targets. A new target is chosen each time a molecule is diffused and moved. These targets have specified average distances from the middle of the contact area and distribute normally over the surfaces of the spheres towards and away from the middle of the contact area with specified standard deviations. In order to move towards a target, a plane containing the molecule, the middle of the sphere and the target is intersected with a plane that is orthogonal to a vector from the molecule to the middle of the sphere. This yields a line and the molecule moves along the surface of the sphere in the direction of this line by a distance specified by its velocity and the amount of time being simulated. As the molecule could move either forwards or backwards in the direction of this line, its final location is the one where it ends up closer to the target.

This algorithm can yield an interesting result. If the sphere containing the molecule is smaller than a hemisphere, then, even if the targets are primarily inside the contact area, molecules outside the contact area tend to accumulate at the opposite end of the cell from the contact area. This is because, as a molecule moves either forwards or backwards along the line, the closer point to a target inside the contact area may not be

the closer point to the contact area. Antipodal accumulation has been reported in synapse formation (Costello, Gallagher et al. 2002).

Simulating Binding

Tracking the locations and interactions of individual molecules presents a computational challenge because each molecule could potentially interact with each other molecule. In order to get around this n-body problem at the expense of some precision, binding is calculated based on the concentrations of molecules in particular regions of the contact area.

When one deals with only two types of molecules, *A* and *B*, that bind each other, the following equation can be used to determine how many molecules, *x*, end up bound after a given amount of time.

$$\frac{(A-x)}{(B-x)} = \frac{A}{B} \times e^{k_{on} \times t \times (A-B)}$$

However, things are not as simple when one molecule, such as a TCR, can potentially bind to one of many different types of molecules, such as MHC molecules bearing different peptides, with different association rates. For this, a new equation is needed.

The rate of binding of a receptor to different types of ligands can be represented as follows where *A* is the concentration of the receptor, B_1, B_2, and B_n are the concentrations of the ligands, and k_1, k_2, and k_n are the rate constants for the binding of the receptor to particular ligands.

$$rate = Ak_1B_1 + Ak_2B_2 + \ldots + Ak_nB_n = A\left(k_1B_1 + k_2B_2 + \ldots + k_nB_n\right)$$

For a given final rate, the amount of receptor that binds to a particular ligand is proportional to the product of the rate constant for binding to that ligand and the concentration of that ligand divided by the sum of all products of rate constants and ligand concentrations.

$$rate(Ak_iB_i) = rate \times \frac{k_iB_i}{k_1B_1 + k_2B_2 + \ldots + k_nB_n}$$

This leads to the following equation for determining the total amount, x, of initially unbound receptor A that will be bound to a ligand after a given amount of time, t. At that time, the concentration of unbound A will be $A - x$.

$$\frac{dx}{dt} = k_1(A-x)\left(B_1 - \frac{k_1B_1}{k_1B_1+k_2B_2+\ldots+k_nB_n}x\right) + k_2(A-x)\left(B_2 - \frac{k_2B_2}{k_1B_1+k_2B_2+\ldots+k_nB_n}x\right) + \ldots + k_n(A-x)\left(B_n - \frac{k_nB_n}{k_1B_1+k_2B_2+\ldots+k_nB_n}x\right)$$

This can be integrated (with the help of Wolfram Research's Mathematica program) to obtain the probability, x/A, that any initially unbound receptor A will bind to a ligand during the time being simulated. The probability that receptor A will be bound to the particular ligand B_i is obtained by multiplying x/A by the rate of binding to B_i divided by the rate of binding to any ligand.

$$\frac{x}{A} = \frac{\left(\sum_{i=1}^{n} B_ik_i\right)^2 \times \left(1 - e^{\frac{t\times\left(A\times\sum_{i=1}^{n}B_ik_i^2 - \left(\sum_{i=1}^{n}B_ik_i\right)^2\right)}{\sum_{i=1}^{n}B_ik_i}}\right)}{\left(\sum_{i=1}^{n} B_ik_i\right)^2 - A\times\left(e^{\frac{t\times\left(A\times\sum_{i=1}^{n}B_ik_i^2 - \left(\sum_{i=1}^{n}B_ik_i\right)^2\right)}{\sum_{i=1}^{n}B_ik_i}}\right)\times\sum_{i=1}^{n}B_ik_i^2}$$

The simulation sequentially calculates release, diffusion and binding for each molecule and receptor/ligand complex. If a molecule ends up forming a receptor/ligand complex by binding to another molecule, then the other molecule is no longer treated separately and both molecules are treated as a complex for the duration of the interaction. Due to the sequential nature of the simulation, if a molecule does not end up binding

another molecule, this other molecule still has the chance to bind to the initial molecule once it is its turn to undergo diffusion and binding. Thus, the above probability, x/A, is too large when simulating binding sequentially for all molecules. The correct probability, p_{bind}, is obtained as follows:

$$p_{bind} = 1 - \sqrt{1 - \frac{x}{A}}$$

Results and Discussion

Testing the Binding and Release Algorithms

Each molecule is simulated sequentially. Thus, the first molecule is simulated under conditions where no molecules have yet bound or released from their ligands while the last molecule is simulated under conditions where this has taken place for all molecules. In addition, an algorithm was designed to calculate the likelihood that a molecule will bind to one of many potential ligands.

In order to validate this approach, the binding of immobile molecules on one cell to mobile molecules on another cell was simulated where, at equilibrium, 10, 50, or 90% of immobile molecules inside the contact area should have been bound. After 360 seconds the on-rates were set to zero so that the molecules could no longer associate with one another. The results are shown in *Figure 5.3* where the 10, 50, and 90% targets were obtained.

Binding Takes Place in Two Phases

Molecules diffuse over the surfaces of cells with different diffusion coefficients. These tend to reach maximal values around $1x10^{-13}$ m^2s^{-1} and are often quite smaller. Due to the viscosities of cell membranes that are about two orders of magnitude greater than that of water, the diffusion of cell-surface receptors is much slower than that of molecules in solution.

In order to study the equilibrium binding of two molecules, different numbers of immobile molecules were first seeded onto one cell. Appropriate numbers of mobile ligands were then seeded onto the other cell and confinement distances were chosen such that 90% of immobile molecules should have ended up being bound at equilibrium.

The results in *Figure 5.4* show that equilibrium levels of binding were more quickly approached when the amount of mobile molecules was in excess to the amount of immobile molecules. However, the actual time required to reach equilibrium should have been similar in all cases. In addition, binding occurred in two phases. First, the molecules inside the contact area had a chance to associate. This occurred in the first 10 seconds where there was an initial rapid phase of binding until 30% of immobile

molecules were bound. Additional molecules were then bound in the second phase as more mobile molecules diffused into the contact area.

The Diffusion Coefficient is Important in the Second Phase

In order to explore further the importance of diffusion in equilibrium binding, the mobility of molecules was reduced 10- and 100-fold. The results in *Figure 5.5* show that approximately 30% of immobile molecules were bound in the first phase due to the mobile molecules that were initially present in the contact area. Thereafter, additional immobile molecules were bound as equilibrium was slowly attained. The rate at which equilibrium was attained was dependent on the diffusion coefficients of the mobile molecules.

Accurate Diffusion Coefficients are Rare but Important

As was shown in *Figures 5.4* and *5.5*, there are two phases of binding. First, the molecules inside the contact area bind and then equilibrium is slowly reached as additional molecules diffuse, or are moved, into the contact area. Thus, the rate of diffusion likely affects synapse formation and, if relative numbers of molecules inside the synapse are important, then the rate of diffusion is very important. Unfortunately, very little experimental data exists on diffusion coefficients and, even when values are available, they may sometimes be of limited use.

First, the viscosities of cell membranes are cell type-dependent, may be dependant on the activation states of cells, and may be affected by some drugs. For instance, polymorphonuclear leukocytes have membrane viscosities that are about twice as great as those of red blood cells (Feinstein, Fernandez et al. 1975) and the drug cyclosporine has been found to increase the viscosity of lymphocyte membranes (Niebylski and Petty 1991). Thus, diffusion coefficients of cell-surface molecules need to be determined for the cells of interest.

Second, the viscosities of cell membranes are highly temperature-dependent and must be measured at 37°C, which may not be possible without the appropriate microscope add-ons. For instance, viscosities for erythrocyte membranes (of various

species) have been reported to be 76 cP at 37°C (Zachariasse, Vaz et al. 1982), 130 cP at 30°C (Koyama, Araiso et al. 1987), 180 cP at 25°C (Feinstein, Fernandez et al. 1975), 210 cP at 20°C (Koyama, Araiso et al. 1987), 330 cP at 10°C (Koyama, Araiso et al. 1987) and 570 cP at 5°C (Zachariasse, Vaz et al. 1982), suggesting that diffusion coefficients measured at 37°C could be 7.5-fold or greater than those measured at 5°C. Interestingly, physiological processes slow down about 2-fold for every 10°C reduction in temperature. A 32°C reduction in temperature from 37°C to 5°C would be expected to slow down reactions by 5-fold, which is close to the 7.5-fold increase in viscosity.

It should be kept in mind that the diffusion coefficient, D, is dependent on the temperature, T, and the viscosity, η, and can be calculated using the following formula:

$$D = \frac{RT}{6\pi r N \eta} = \frac{kT}{6\pi r \eta}$$

While the temperature-dependence of the diffusion coefficient is on a Kelvin scale and would not be expected to change much between 37°C and 5°C, this is not the case for viscosity on which the diffusion coefficient is also dependent. Thus, diffusion coefficients need to be measured at 37°C.

Third, the use of antibodies, gold beads, or anything that changes the size of the receptor being studied may lead to inaccurate diffusion coefficients. Membrane-bound proteins frequently have extracellular, transmembrane and intracellular domains. The diffusion coefficient of the whole molecule can be determined from the diffusion coefficients of the extracellular (D_E), transmembrane (D_T), and intracellular (D_I) domains (derived from the complexed receptor formula in (Coombs, Kalergis et al. 2002)).

$$D = \frac{D_E D_T D_I}{D_E D_T + D_E D_I + D_T D_I}$$

$$D = \left(\frac{kT}{6\pi}\right) \times \left(\frac{1}{r_E \eta_E + r_T \eta_T + r_I \eta_I}\right)$$

Because the membrane viscosity is ~100-fold greater than the viscosities of water (1 cP) and cytoplasm (2 cP) (Periasamy, Armijo et al. 1991) and because the transmembrane domain is not 100-fold smaller than the extracellular domain, *D* should be primarily dependent on the radius of the molecule's transmembrane domain, r_T, and the viscosity of the membrane, η_T.

However, it has been found that the diffusion coefficient of the GPI-anchored protein Thy-1 is highly dependent on its extracellular domain, which is only a single immunoglobulin V-type domain with a mass of about 18 kDa (Zhang, Schmidt et al. 1992). Assuming that immunoglobulin domains have radii of about 2 nm, this would suggest a diffusion coefficient of 1.14 x10^{-10} m^2s^{-1} in the absence of a transmembrane domain. The reported value is 3.2x10^{-13} m^2s^{-1}, which initially suggests that the GPI anchor inside a membrane could have a radius as large as 2 – 3 nm (although, due to the Stokes Paradox, it is not possible to rely on the initial formula for the diffusion coefficient to calculate the radius of the transmembrane domain). When, Thy-1 was detected using Fab, $F(ab)_2$, or whole IgG, its diffusion coefficient was reported to decrease to 2.0, 1.6, and 1.0x10^{-13} m^2s^{-1}, respectively. This suggests either that the antibody used to detect Thy-1 (MRC-OX7) was binding to Thy-1 such that it ended up inside the membrane or that there was a dense region just outside the cell membrane that had a similar viscosity to the cell membrane. Thus, antibodies and gold particles (and preferably not 100 nm gold beads, as were used to determine the diffusion coefficient for LFA-1 (Kucik, Dustin et al. 1996)), should not be used to determine diffusion coefficients because their size may affect the determined values.

Simulating the Benefits of LFA-1 Activation

Shortly after T cell activation, the affinity of LFA-1 for its ligand, ICAM-1, increases. This, in part, allows T cells to arrest on high endothelial venules (Bargatze,

Jutila et al. 1995) and leads to the formation of an LFA-1/ICAM-1 ring during synapse formation. The increase in affinity appears to be due to a conformational change in LFA-1 (Ma, Shimaoka et al. 2002) but it has also been reported that the diffusion coefficient of LFA-1 is increased after activation (Kucik, Dustin et al. 1996).

The simulation was thus used to determine the effects of increased affinity and increased mobility on the accumulation inside the synapse under optimal (2 nm confinement distance) and suboptimal (20 and 200 nm confinement distance) conditions. The interaction between resting LFA-1 and ICAM-1 has a reported k_{off} of 0.033 s^{-1} and k_{on} of 367 $M^{-1}s^{-1}$ where the association equilibrium constant increases from $1.1x10^4$ M^{-1} to $1.0x10^6$ M^{-1} following activation (Lollo, Chan et al. 1993). A similar association equilibrium constant, $2.0x10^6$ M^{-1}, for activated LFA-1 has been reported with k_{off} and k_{on} values of 0.1 s^{-1} and $2.0x10^5$ $M^{-1}s^{-1}$. Thus, activated LFA-1 appears to bind much faster than resting LFA-1 but also releases faster. As far as the mobility of LFA-1 is concerned, it has been reported to increase from a very slow $2.3x10^{-15}$ m^2s^{-1} to $2.9x10^{-14}$ m^2s^{-1} (Kucik, Dustin et al. 1996) that is similar to the mobility of other proteins with transmembrane domains. However, these values were determined using 100 nm gold particles, which could severely underestimate the mobility.

As shown in *Figure 5.6A – C*, activated fast-moving LFA-1 accumulated inside the synapse. In addition, resting fast-moving LFA-1 accumulated better than resting slow-moving LFA-1 but showed essentially no accumulation when a 200 nm confinement distance was used. Thus, in the absence of activation and properly-spaced membranes, there should not be appreciable LFA-1/ICAM-1 accumulation.

As shown in *Figure 5.6D – F*, activated fast-moving LFA-1 bound more ICAM-1 under optimal conditions than resting slow-moving LFA-1 whereas resting fast-moving LFA-1 only bound slightly more. When a 20 nm confinement distance was used, activated LFA-1 led to an order of magnitude more binding than resting LFA-1. When a 200 nm confinement distance was used, activated LFA-1 led to two orders of magnitude more binding than resting LFA-1.

Thus, the increase in affinity of LFA-1 for ICAM-1 after activation is primarily responsible for the accumulation of LFA-1 and ICAM-1 in the synapse. However, the increased mobility of LFA-1 after activation allows it to accumulate faster.

Everything that Binds and Diffuses Should Accumulate

An ever-increasing number of molecules are being found that accumulate inside the synapse. In fact, almost every molecule on one cell that has a ligand on the other cell seems to accumulate somewhere in the synapse. In some cases, such as with the TCR and CD2, this may be due to active movement towards the synapse. In other cases, this may be due to diffusion alone.

Figure 5.7 shows that any mobile molecule on one cell with a ligand on the other cell should be able to accumulate inside the synapse. Three different binding scenarios were analyzed.

In the first (*Figure 5.7A*), a molecule on one cell was immobile while the ligand on the other cell was mobile. This can be the case, for instance, when the immobile molecule is an adhesion molecule that is anchored to the cytoskeleton. In this case, there was initially a slight accumulation of the mobile ligand at the edge of the synapse that then spread more evenly over the entire synapse. Overall, accumulation of the ligand was limited by the fact that additional immobile molecules could not enter the synapse.

In the second (*Figure 5.7B*), both the molecule and its ligand were mobile and their complexes diffused with a 2-fold slower diffusion coefficient because these complexes were larger than the monomers and were bound in both membranes. This is the case for most complexes that are free to diffuse in both membranes and initially led to a preferential accumulation at the edge of the synapse that then evened out over the entire synapse. The overall accumulation was much greater than when one molecule was immobile (*Figure 5.7A*).

In the third (*Figure 5.7C*), both the molecule and its ligand were mobile and their complexes diffused with a 60-fold slower diffusion coefficient. This is the case for complexes that become anchored to the cytoskeleton after binding and led to a preferential and strong accumulation at the edge of the synapse.

Overall, both *Figures 5.7B* and *5.7C* could explain the LFA-1/ICAM-1 ring. As the TCR actively moves towards the middle of the synapse, its presence there may simply prevent the accumulation of LFA-1/ICAM-1 because TCR/MHC and LFA-1/ICAM-1 complexes lead to different membrane separations (15 nm in the case of TCR/MHC and

40 nm in the case of LFA-1/ICAM-1). LFA-1/ICAM-1 could also form a ring if their complexes become immobile after binding. Because LFA-1 is capable of signaling (Kim, Carman et al. 2003) this is possible but there does not appear to be any experimental data showing that bound LFA-1 becomes immobile.

Interestingly, *Figures 5.7B* and *5.7C* also show a slightly darker area around the synapse. In *Figure 5.7D*, all simulations were rerun with a curved, as opposed to flat, contact area. The amounts of molecules found at a given angle from the middle of the contact area were then analyzed and compared to the expected amounts. It became apparent that while diffusion-based synapse formation led to an accumulation of molecules inside the synapse, it also led to an area bordering the synapse where molecules were scarce. This border can be termed the event horizon of the synapse behind which interesting things happen.

A Study of Synapse Formation during T cell Activation

In order to study T cell synapse formation, simulations involving TCR, MHC, LFA-1, ICAM-1, CD2, and CD48 were set up. Different simulations involved differing amounts of agonist peptide/MHC complexes in the presence of irrelevant peptide/MHC complexes. In addition, some simulations were performed in the absence of CD2 or in the absence of active movement of the TCR and CD2 towards the synapse.

To simulate 24 hour T cell interactions with ligand-expressing cells, the radius of both cells was set to 5 μm because most lymphocytes have a diameter of about 10 μm. The radius of the contact area was set to 4 μm because the synapse is usually just smaller than the width of the cell. 50,000 TCRs and 50,000 MHC molecules were simulated where 50, 500, 5,000, or 25,000 of the MHC molecules were occupied by agonist peptides that were recognized according to reported data for 2B4 TCR interactions with MCC/IE^k (k_{off} = 0.063 s^{-1} and k_{on} = 1.57x10^3 $M^{-1}s^{-1}$). MHC molecules with irrelevant peptides were recognized with very fast dissociation rates (2.0 s^{-1}) and standard association rates (1.0x10^3 $M^{-1}s^{-1}$) (guesstimates from Lawren Wu in Mark M. Davis' lab) because TCR/MHC association is mostly peptide-independent (Wu, Tuot et al. 2002). It has been argued that TCR binding does not lead to enhanced TCR endocytosis (Liu, Rhodes et al. 2000) but increases in TCR endocytosis have been observed by others.

Based on reported data (Menne, Moller Sorensen et al. 2002), the simulation was configured so that 87% of the 50,000 TCRs were initially extracellular, intracellular TCRs exocytosed at a rate of 0.00167 s^{-1}, and resting TCR endocytosis rates of 0.00025 s^{-1} increased to 0.00197 s^{-1} after TCR ligation. T cell activation leads to the active movement of the TCR and CD2 towards the synapse and this velocity was set to a reported value of 0.05 $\mu m \cdot s^{-1}$ (Moss, Irvine et al. 2002).

Additional values used for the simulation could not be found in the literature and, thus, estimates were used. The confinement distances for all interactions were set to 2 nm and the standard deviation to penalize sub-optimal membrane separations was set to half the height of the complexes (e.g., 7.5 nm for the 15 nm TCR/MHC complex). The standard deviation to penalize sub-optimal membrane separations for complexes when entering new regions was set to one quarter the height of the complexes (e.g. 10 nm for 40 nm LFA-1/ICAM-1 complexes). The standard deviation to penalize unbound molecules entering regions where they are taller than the membrane separation was set to one quarter the height of the molecules (e.g., 1.75 nm for 7 nm CD2). The TCR is a large complex and, thus, would not be expected to diffuse quickly. Thus, the diffusion coefficient of unbound TCR was set to a very slow 5.0×10^{15} $m^2 s^{-1}$. Diffusion coefficients for ICAM-1, CD2, and CD48 were each set to 2.0×10^{14} $m^2 s^{-1}$, which is typical of most transmembrane receptors. Internal activated TCRs were degraded with rate constants of 0.1 s^{-1} while resting TCRs were not degraded. The dissociation rate of TCR/MHC complexes is known to be important in TCR activation (Matsui, Boniface et al. 1994) but TCR activation cannot be represented through a first-order reaction so TCRs were set to activate if bound continuously for 20 or more seconds. With a dissociation rate of 0.063 s^{-1}, the average bound time for 2B4/MCC/IE^k is about 16 seconds so a bit less than half of these interactions should lead to full TCR activation. Fully activated external and internal TCRs were set to deactivate with a rate constant of 0.01155 s^{-1}, which gives the activated receptor a half-life of one minute.

CD2 is an interesting molecule because CD2/CD48 complexes span a distance similar to that of TCR/MHC complexes. CD2 has a reasonably high affinity for CD48 where the k_{on} has been reported to be a fast 1.0×10^5 $M^{-1} s^{-1}$ but the k_{off} is also a very fast 6.0 s^{-1}, which is similar to what has been reported for TCR interactions with antagonist

peptide/MHC complexes. Because the confinement distance affects the formation of complexes, the role of CD2/CD48 complexes with their fast association rates may be to space the membranes in the middle of the synapse optimally so that TCR/MHC interactions with up to 100-fold slower association rates can then occur optimally. When CD2/CD48 interactions do not space the same distance as TCR/MHC, it has been found that T cell activation is severely compromised (Wild, Cambiaggi et al. 1999).

In order to simulate 24 hour interactions in simulations that each ran for about a day, the simulations were run using 10 second iterations, which had one caveat. The association and dissociation rates for CD2 were so fast that most CD2 molecules in the contact area released from and bound back to CD48 in each round. Thus, essentially all CD2 molecules in the contact area were bound to CD48 at any given time and enhanced the ability of TCRs to bind to peptide/MHC complexes.

As shown in *Figure 5.8A*, increased amounts of agonist peptide/MHC complexes led to increased amounts of internalization. The amount of extracellular signaling of fully-activated TCRs was also analyzed. When TCR/APC interactions lasted for 24 hours and 500 agonist peptide/MHC complexes were present, this led to constant signaling for the full 24 hours. On the other hand, 5,000 and 25,000 agonist peptide/MHC complexes led to stronger initial signals that then tapered off to the levels seen with 50 agonist peptide/MHC complexes. It has been proposed that continued signaling is important in determining the fate of T cells (Iezzi, Karjalainen et al. 1998) so these results show that agonist peptide levels may be important in determining the duration and strength of TCR signals.

It has been suggested that the synapse can form in the absence of directed movement towards the TCR where this was achieved, in part, by making the membrane separation in the synapse take on the shape of a parabola where separation in the middle of the parabola was favorable for TCR/MHC accumulation (Qi, Groves et al. 2001). However, active movement of the TCR and CD2 towards the synapse that is mediated, in part, by CD2-associated protein (CD2AP) (Dustin, Olszowy et al. 1998) may be important for synapse formation and activation because CD2AP-deficient mice cannot form organized synapses and show greatly reduced levels of TCR downregulation (Lee, Dinner et al. 2003).

In order to study the importance of TCR and CD2 clustering in synapse formation and T cell activation, the simulation was run is the absence of directed movement towards the synapse. As shown in *Figure 5.8B*, this led to greatly-reduced TCR internalization and about an order of magnitude less signaling TCRs than when active movement towards the synapse took place. A reason for this was that, in the simulation, LFA-1/ICAM-1 led to membrane separations of 40 nm that were not optimal for TCR/MHC interactions. Because the TCR is a large complex and likely diffuses slowly, LFA-1/ICAM-1 complexes could accumulate more rapidly and reinforce the 40 nm separation. On the other hand, when the TCR and CD2 actively moved into the synapse, their concentrations in the middle drove their association with MHC and CD48, respectively, and reinforced a 15 nm membrane separation that drove out LFA-1/ICAM-1 complexes to the periphery of the synapse.

To analyze the importance of CD2 in T cell activation, the simulation was run in the absence of CD2. As shown in *Figure 5.8C*, the absence of CD2 led to reduced levels of endocytosis and slightly reduced levels of TCR signaling. Most IELs do not express CD2 and this result is consistent with what was seen when the amount of TCR downregulation of IELs was compared to that of splenic T cells in cocultures with agonist ligand-expressing splenocytes; although, that difference may have also been due to differences in TCR signaling.

Simulating γδ T cell Activation

The comparison of splenic G8 γδ T cells to αβ T cells had suggested that there are very few major differences between these cells. Thus, signaling may also occur similarly.

To study γδ T cell activation, the same system was used except that the MHCs were replaced by 50, 100, 500, 1,000, 5,000, or 25,000 T10/T22 molecules and the G8 γδ TCR replaced the 2B4 αβ TCR. CD2 and CD48 were left out of the simulation.

As shown in *Figure 5.9*, the presence of both 5,000 and 25,000 T10/T22 molecules led to a profound downregulation of surface γδ TCR levels within 3 hours. In addition, the amount of signaling cell-surface γδ TCRs was greatly reduced after that

time. If prolonged TCR signaling is essential for some outcomes of T cell activation, then this may not be achievable if T10/T22 levels are high. In 12 hour cocultures between G8 RAG2^{KO} BALB/c γδ T cells and H2$^{b/d}$ BALB/c splenocytes (see Chapters 2, 3, and 4), γδ TCR transcripts were found in cells that did not express the γδ TCR. It is thus possible that these γδ TCR-negative γδ T cells encountered cells that expressed high levels of T10/T22.

When 500 T10/T22 molecules were present, the simulation predicted that cell-surface γδ TCR levels should become undetectable after 24 hours of activation. On the other hand, when twice or half as many T10/T22 molecules were present, γδ TCR levels could become undetectable in only 9 hours or did not decrease by much, respectively. This was similar to what was seen when G8 γδ T cells were cocultured with T10/T22^{b}-expressing splenocytes. As shown in Chapter 3, B cells are abundant T10/T22-expressing cells in the spleen and their T10/T22-levels have a normal distribution that spans about one order of magnitude. However, there are also outliers whose levels are an order of magnitude higher. Thus, the experimentally-observed amounts of G8 γδ TCR downregulation could be due to the distribution of T10/T22 on the B cells they are interacting with and, if the levels are really low as is the case with T10 in BALB.K, little to no downregulation may result.

Regardless of Peptide, the MHC Will Accumulate

It has been observed by Michelle Krogsgaard and others in Mark M. Davis' lab that synapse formation does not only lead to the accumulation of agonist peptide/MHC complexes in the synapse but also of MHCs presenting what may be irrelevant peptides. In order to analyze whether there is something special to the peptide accumulation, 10 minutes of synapse formation were simulated in 100 ms intervals using 50,000 TCRs, 5,000 MCC/IE^{k} complexes, and 50,000 irrelevant peptide/IE^{k} complexes.

As shown in *Figure 5.10A*, the synapse took shape over 10 minutes and required directed TCR movement. The red ICAM-1/LFA-1 ring was visible as was a central cluster of TCR, MHC, CD2, and CD48. In the absence of directed TCR movement, ICAM-1 and LFA-1 were spread out over the surface of the synapse.

The green and blue channels for the 10 minute timepoint were analyzed separately in *Figure 5.10B* in order to reveal the presence of the formerly blue 50,000 irrelevant peptide/IE^k complexes. These, along with CD48, were found to accumulate inside the central cluster as well.

Thus, MHC molecules bearing irrelevant peptides are expected to accumulate inside the synapse because the directed movement of TCRs towards the synapse leads to a high concentration of TCRs inside the synapse that drives their association with MHC molecules.

Future Directions

As was mentioned in the previous simulations, many important parameters still required estimations. For instance, many diffusion coefficients of important cell-surface molecules still need to be determined and these may end up being cell-type specific. In addition, in the previous simulations of T cell activation, a 20 second ligation time was used to initiate a signal from the TCR. As has been pointed out to me by the people in Mark M. Davis' lab who image T cell activation, T cell activation may occur much faster. However, the dissociation rate is clearly important in T cell activation and the T cell must be able to discriminate between many MHC complexes that bind for a fraction of a second and a few that bind for a few seconds. Thus, it will be important to uncover how TCRs determine that they are bound to agonist peptide/MHC complexes. This simulation currently penalizes the association of two complexes if the membranes are not spaced properly. It may be that the rate of dissociation needs to be increased if the membranes are spaced too far apart. In such a scenario, it would be possible to reduce the 20 second ligation time to something much shorter.

Figure Legends

Figure 5.1: An illustration of some concepts in the simulation

(A) The simulation is based around a model where two cells are in contact with each other at a contact area (*gray shaded*) where their molecules can interact with each other. (B) This contact area is subdivided into smaller regions (using various algorithms) that are shown as alternating black and white areas. Molecule concentrations are determined on a per-region basis and only molecules inside the same region can interact with each other. (C) Membrane separation inside of regions influences whether or not opposing molecules can bind to each other. If the membranes are properly spaced (*left*), the interacting areas (*circles*) of the opposing molecules (*stalks*) are all close together. If the membranes are too close to each other (*middle*), then the molecules can only bind if they are at an angle to each other. If the membranes are too far from each other (*right*), then the molecules can only bind if there are deformations in the membranes that bring some molecules closer together. (D) The association rate (k_{on}) is reduced if membranes are not properly spaced for binding (*left*). If the membranes are too close (*middle*) or too far apart (*right*), then the distance from the optimal separation, Δ, is calculated. The value of k_{on} is subsequently multiplied by a Δ-dependent factor that has a normal distribution.

Figure 5.2: Simulating receptor dynamics

During the simulation, molecules are synthesized and exported to the cell surface. There they diffuse and can interact with other molecules. After a certain amount of constant binding, molecules can activate and then also deactivate. Molecules can be endocytosed from the cell surface at rates that are dependent on whether they are bound and whether they are activated. Finally, intracellular molecules can be degraded.

Figure 5.3: The binding and release equations lead to proper equilibrium binding

The binding of two molecules was simulated using spheres where the contact area was $1/6^{th}$ of the surface area (cell radius = 5 μm; contact area radius = 4 μm; k_{on} = 1.57×10^{3} $M^{-1}s^{-1}$; k_{off} = 0.063 s^{-1}; D = 1×10^{-13} m^2s^{-1}). 10,000 immobile molecules were

seeded over the surface of one cell. 10,167, 10,833, or 11,500 mobile molecules were then seeded over the surface of the other cell and confinement distances of 12.3, 1.37, and 0.15 nm were used such that, at equilibrium, 10, 50, or 90% of immobile molecules inside the contact area should be bound, respectively. After 360 seconds the association rate constants were set to zero so that the molecules could no longer associate with one another. Each condition was simulated 5 times.

Figure 5.4: Receptor binding takes place in two phases

The binding of two molecules was simulated using spheres where the contact area was $1/6^{th}$ of the surface area (cell radius = 5 μm; contact area radius = 4 μm; k_{on} = $1.57x10^3$ $M^{-1}s^{-1}$; k_{off} = 0.063 s^{-1}; D = $1x10^{-13}$ m^2s^{-1}). Confinement distances were chosen such that 90% of immobile molecules should end up being bound at equilibrium. Binding was allowed for 360 seconds. 10,000 (*blue*), 30,000 (*green*), or 60,000 (*red*) immobile molecules served as the ligands for 11,500, 14,500, and 19,000 mobile molecules, respectively. Each condition was simulated five times.

Figure 5.5: Diffusion affects the second phase of binding

The binding of two molecules was simulated using spheres where the contact area was $1/6^{th}$ of the surface area (cell radius = 5 μm; contact area radius = 4 μm; k_{on} = $1.57x10^3$ $M^{-1}s^{-1}$; k_{off} = 0.063 s^{-1}). A confinement distance was chosen such that 90% of immobile molecules should end up being bound at equilibrium. Binding was allowed for 360 seconds. 60,000 immobile molecules served as the ligands for 19,000 mobile molecules that had diffusion coefficients of $1x10^{-13}$ (*red*), $1x10^{-14}$ (*green*), or $1x10^{-15}$ m^2s^{-1} (*blue*). Each condition was simulated five times.

Figure 5.6: The importance of affinity and mobility in LFA-1 activation

LFA-1 activation has been reported to lead to a higher affinity (k_{on} = $2.0x10^5$ $M^{-1}s^{-1}$ vs. 367 $M^{-1}s^{-1}$ and k_{off} = 0.1 s^{-1} vs. 0.033 s^{-1}) for ICAM-1 and increased mobility (D = $2.9x10^{-14}$ m^2s^{-1} vs. $2.3x10^{-15}$ m^2s^{-1}). To analyze the importance of changes in affinity and mobility under optimal and suboptimal binding conditions, the confinement distance was either set to (A, D) 2 nm (optimal), (B, E) 20 nm, or (C, F) 200 nm (suboptimal). (A, B,

C) 600 seconds of binding were simulated and LFA-1 accumulation inside the synapse was analyzed under conditions where LFA-1 bound and diffused as if it was activated (*solid lines*), bound and diffused as if it was resting (*short dashes*), or bound as if it was resting but diffused as if it was activated (*long dashes*). (D, E, F) In addition, the amount of bound fast-moving activated LFA-1 (*solid lines*) and bound fast-moving resting LFA-1 (*long dashes*) was compared to the amount of bound slow-moving resting LFA-1.

Figure 5.7. Whichever way mobile molecules bind, they always form a synapse

150,000 red molecules were randomly seeded onto one cell and 150,000 green molecules were seeded onto another cell. Both cells are represented using the same 5 μm radius sphere with a flat 4 μm radius contact area. Mobile free molecules had diffusion coefficients of 3.0×10^{-14} $m^2 s^{-1}$ while bound complexes were either (A) immobile or had diffusion coefficients of (B) 1.5×10^{-14} $m^2 s^{-1}$ or (C) 0.5×10^{-15} $m^2 s^{-1}$. At 0, 10, 60, 300, and 600 seconds, the amount of red molecules inside the contact area at a given distance from the middle of the contact area was analyzed (*right*). The affinities of the molecules for each other were based on the activated LFA-1 interaction with ICAM-1 ($k_{on} = 2.0 \times 10^5$ $M^{-1} s^{-1}$; $k_{off} = 0.1$ s^{-1}). The confinement distance inside the contact area was set to 2 nm. (D) The distribution of molecules from the middle of the contact area (0 degrees away) to the other end of the cell (180 degrees away) was analyzed after 600 seconds of binding using a model with a curved contact area.

Figure 5.8: Ligand numbers, directed movement, and CD2 are all important for T cell activation

(A) 24 hour interactions were simulated in 10 second intervals between 5 μm radius cells that used a 4 μm radius contact area. Initially, 50,000 evenly-distributed TCRs were simulated that bound to 50, 500, 5,000, or 25,000 peptide/MHC complexes with maximal on-rates of 1.57×10^3 $M^{-1} s^{-1}$ and off-rates of 0.063 s^{-1} and to additional (so that there are a total of 50,000 peptide/MHC complexes) irrelevant peptide/MHC complexes with maximal on-rates of 1.0×10^3 $M^{-1} s^{-1}$ and off-rates of 2.0 s^{-1}. TCRs moved to the contact area at 0.05 $\mu m \cdot s^{-1}$ and TCR/MHC complexes also actively moved at that rate. TCRs diffused with a very slow diffusion coefficient of 5.0×10^{-15} $m^2 s^{-1}$ and were set

to activate if bound continuously for 20 seconds. 0.0167 TCRs were synthesized per second. 13% of TCRs started out as being internal. The rate constant used for TCR externalization was 0.00167 s^{-1}. The rate constants used for resting and activated TCR internalization were 0.00025 and 0.00197 s^{-1}, respectively. The rate constant used for TCR deactivation was 0.01155 s^{-1}. In addition, there were 50,000 LFA-1, 50,000 ICAM-1, 14,000 CD2, and 50,000 CD48 molecules. CD2 and CD2/CD48 complexes moved to the synapse at a rate of 0.05 $\mu m \cdot s^{-1}$. Cell-surface TCR levels were analyzed (*left*) as well as levels of activated signaling TCRs (*right*). (B) The same 24 hour simulation as in (A) was run without active movement of the TCR and CD2 towards the contact area. (C) The same 24 hour simulation as in (A) was run in the absence of CD2.

Figure 5.9: The effects of T10/T22^b levels on G8 γδ T cell TCR levels and signaling

24 hour interactions were simulated in 10 second intervals between 5 μm radius cells that used a 4 μm radius contact area. Initially, 50,000 evenly-distributed G8 γδ TCRs were simulated that could bind to 50, 250, 500, 1,000, 5,000, or 25,000 T22^b MHC class 1b molecules with maximal on-rates of 6.53×10^4 $M^{-1}s^{-1}$ and off-rates of 8.1×10^{-3} s^{-1}. TCRs diffused with a very slow diffusion coefficient of 5.0×10^{-15} m^2s^{-1} and were set to activate if bound continuously for 20 seconds. In addition, TCRs moved to the contact area at 0.05 $\mu m \cdot s^{-1}$ and TCR/T22^b complexes also actively moved at that rate and diffused with a diffusion coefficient of 4.0×10^{-15} m^2s^{-1}. Unbound T22^b molecules diffused with a diffusion coefficient of 2.0×10^{-14} m^2s^{-1}. 0.0167 TCRs were synthesized per second. 13% of TCRs started out as being internal. The rate constant used for TCR externalization was 0.00167 s^{-1}. The rate constants used for resting and activated TCR internalization were 0.00025 and 0.00197 s^{-1}, respectively. The rate constant used for TCR deactivation was 0.01155 s^{-1}. In addition, there were 50,000 LFA-1 and 50,000 ICAM-1 molecules. Cell-surface levels of the G8 γδ TCR were analyzed (*top*) as well as activated signaling G8 γδ TCRs (*bottom*).

Figure 5.10: Peptide-independent MHC accumulation

(A) 10 minute interactions were simulated in 0.1 second intervals between 5 μm radius cells that used a 4 μm radius contact area. Initially, 50,000 evenly-distributed

TCRs were simulated that bound to 5,000 peptide/MHC complexes with maximal on-rates of $1.57x10^3$ $M^{-1}s^{-1}$ and off-rates of 0.063 s^{-1} and 50,000 additional irrelevant peptide/MHC complexes with maximal on-rates of $1.0x10^3$ $M^{-1}s^{-1}$ and off-rates of 2.0 s^{-1}. TCRs moved to the contact area at 0.15 $\mu m \cdot s^{-1}$ and TCR/MHC complexes also actively moved at that rate. TCRs were set to diffuse with a very slow diffusion coefficient of $5.0x10^{-15}$ m^2s^{-1} and were set to activate if bound continuously for 20 seconds. 0.0167 TCRs were synthesized per second. 13% of TCRs started out as being internal. The rate constant used for TCR externalization was 0.00167 s^{-1}. The rate constants used for resting and activated TCR internalization were 0.00025 and 0.00197 s^{-1}, respectively. The rate constant used for TCR deactivation was 0.01155 s^{-1}. In addition, there were 50,000 LFA-1, 50,000 ICAM-1, 14,000 CD2, and 50,000 CD48 molecules. CD2 and CD2/CD48 complexes moved to the synapse at a rate of 0.15 $\mu m \cdot s^{-1}$. The distribution of molecules was analyzed after 0 (*top left*), 3 (*top right*), and 10 (*bottom left*) minutes and also after 10 minutes in the absence of TCR and CD2 movement towards the contact area (*bottom right*). ICAM-1 (*red*), agonist peptide/MHC (*green*) and irrelevant peptide/MHC (*blue*) are shown on the lower left sphere. CD2 (*blue*) and CD48 (*green*) are shown on the upper middle sphere. LFA-1 (*red*) and TCR (*green*) are shown on the right lower sphere. (B) The green (*left*) and blue (*right*) channels of the 10 minute image were analyzed in order to locate the different MHC molecules and CD48 better.

Figure 5.1: An illustration of some concepts in the simulation

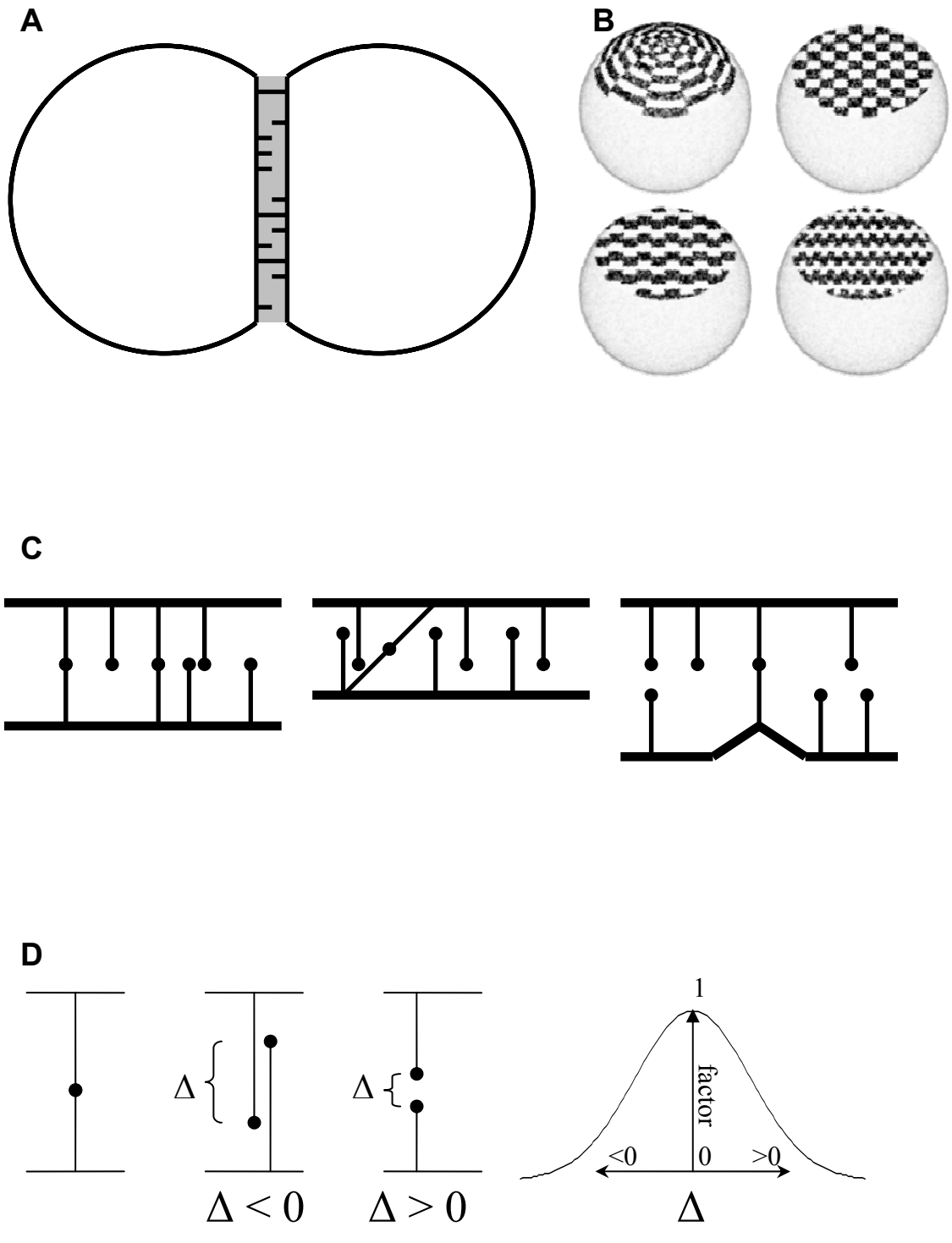

Figure 5.2: Simulating receptor dynamics

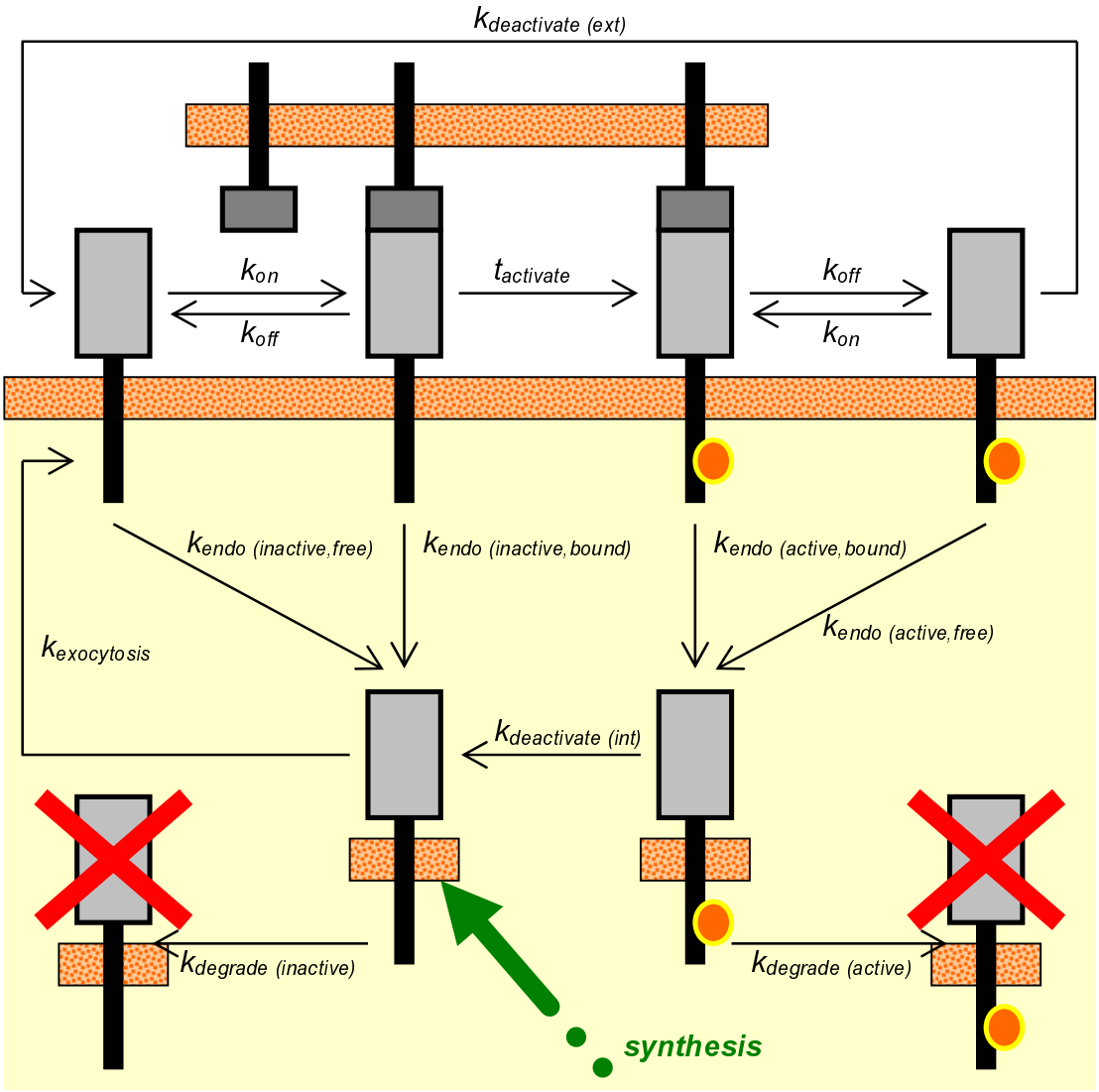

Figure 5.3: The binding and release equations lead to proper equilibrium binding

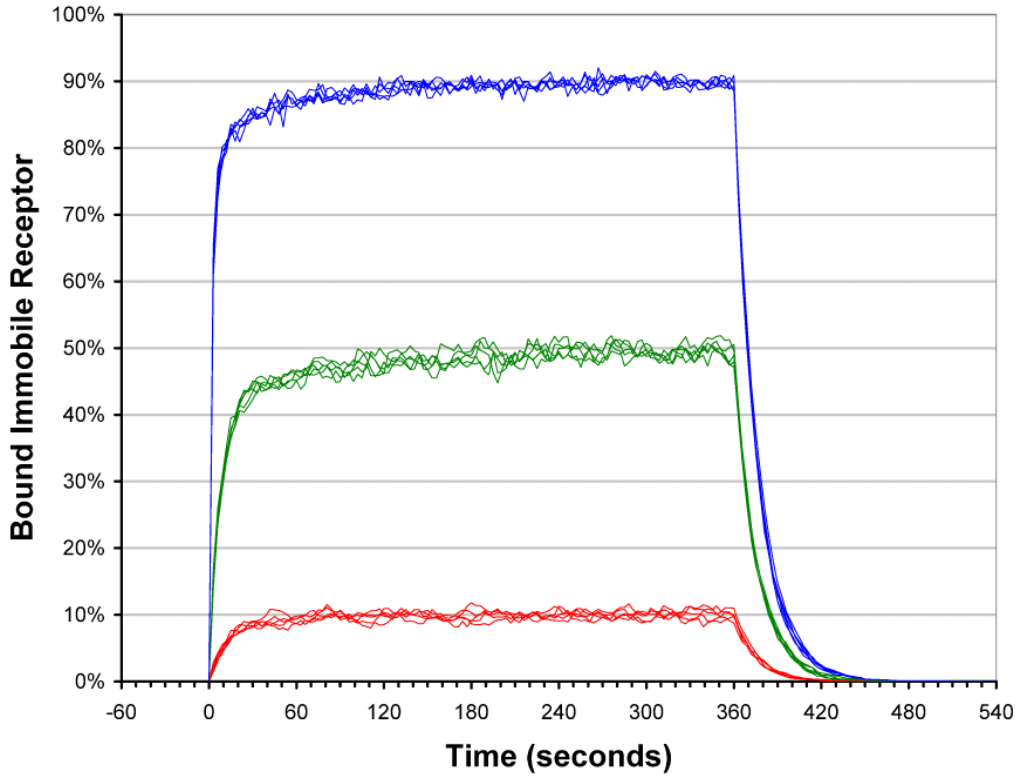

Figure 5.4: Receptor binding takes place in two phases

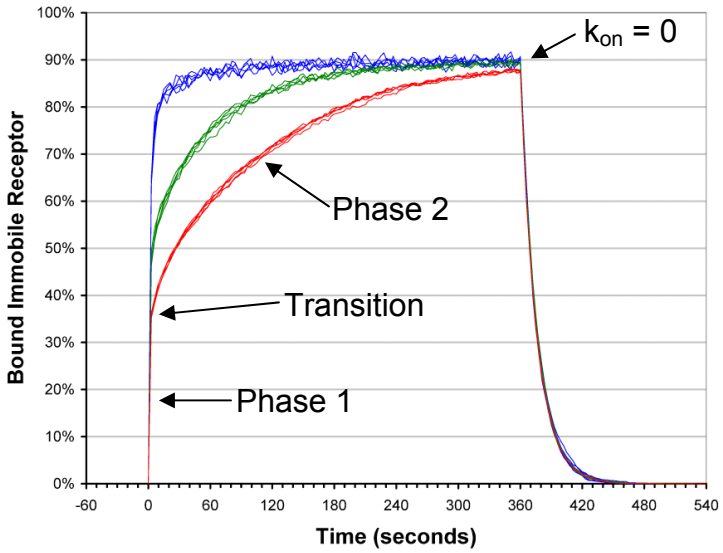

Figure 5.5: Diffusion affects the second phase of binding

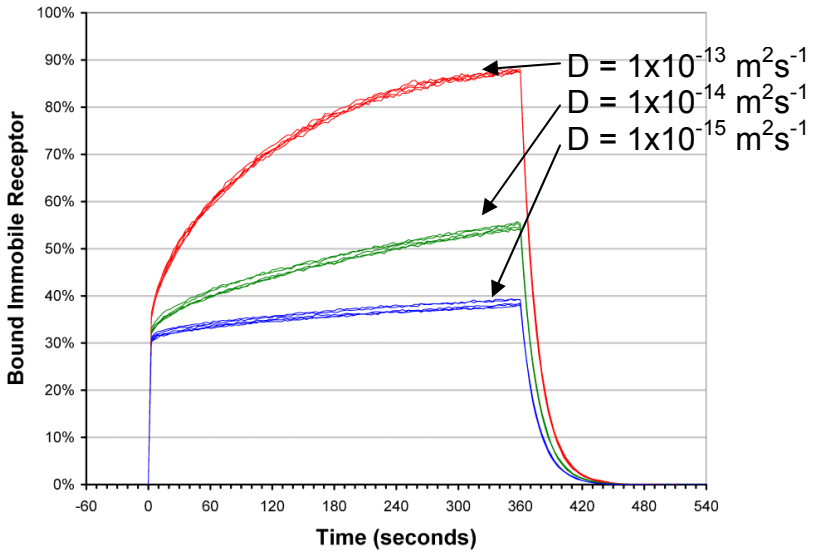

Figure 5.6: The importance of affinity and mobility in LFA-1 activation

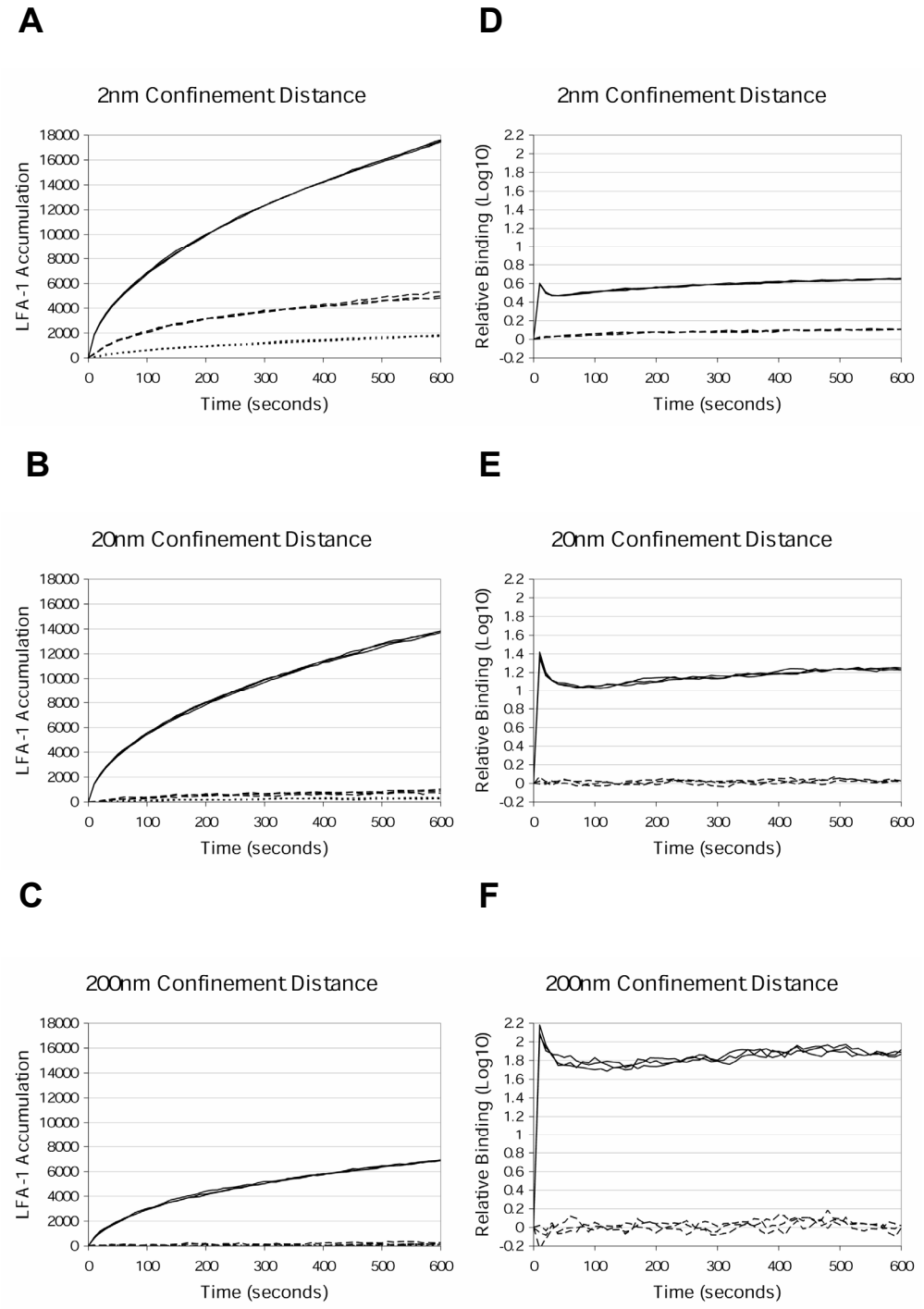

Figure 5.7: Whichever way mobile molecules bind, they always form a synapse

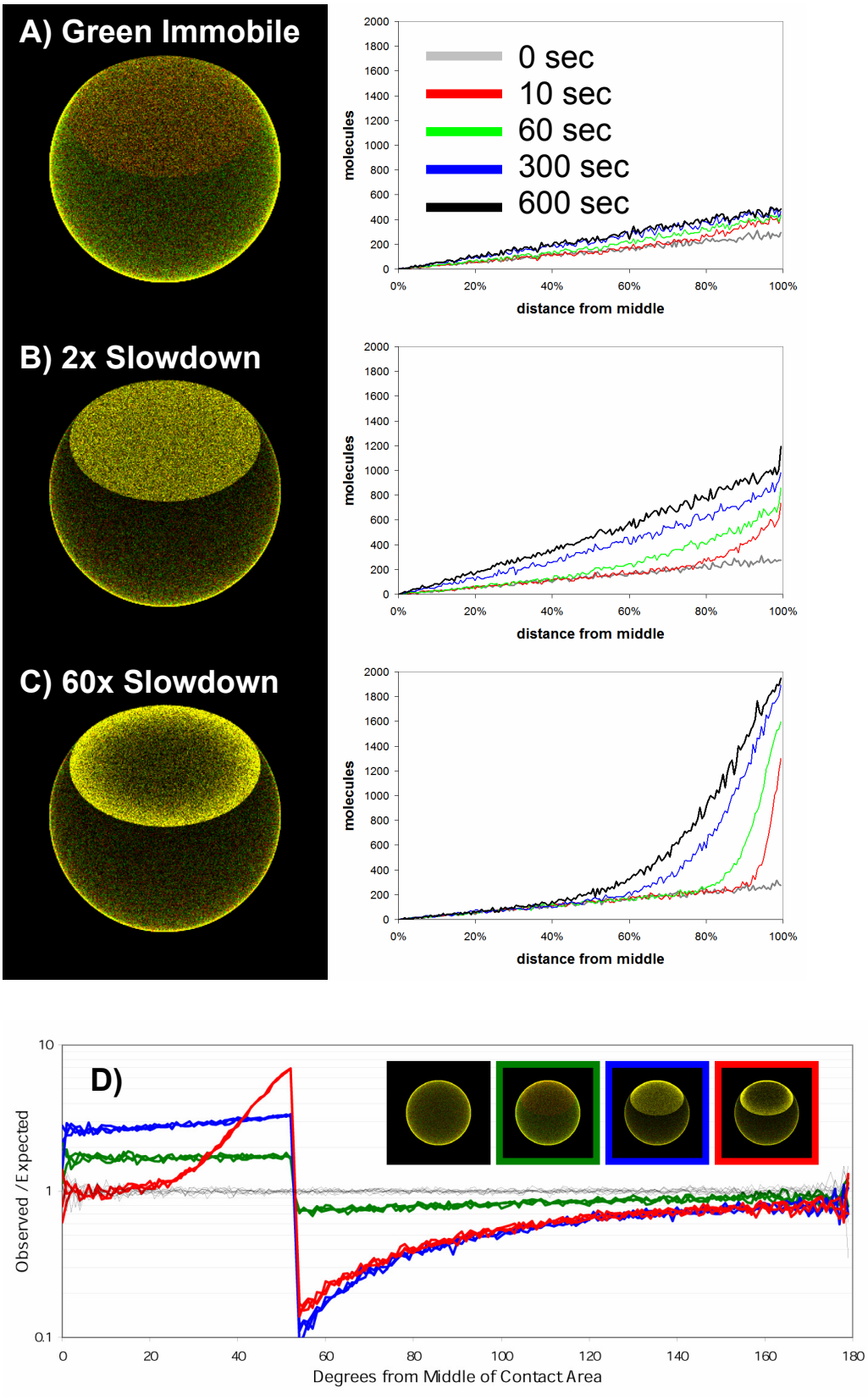

Figure 5.8: Ligand numbers, directed movement, and CD2 are all important for T cell activation

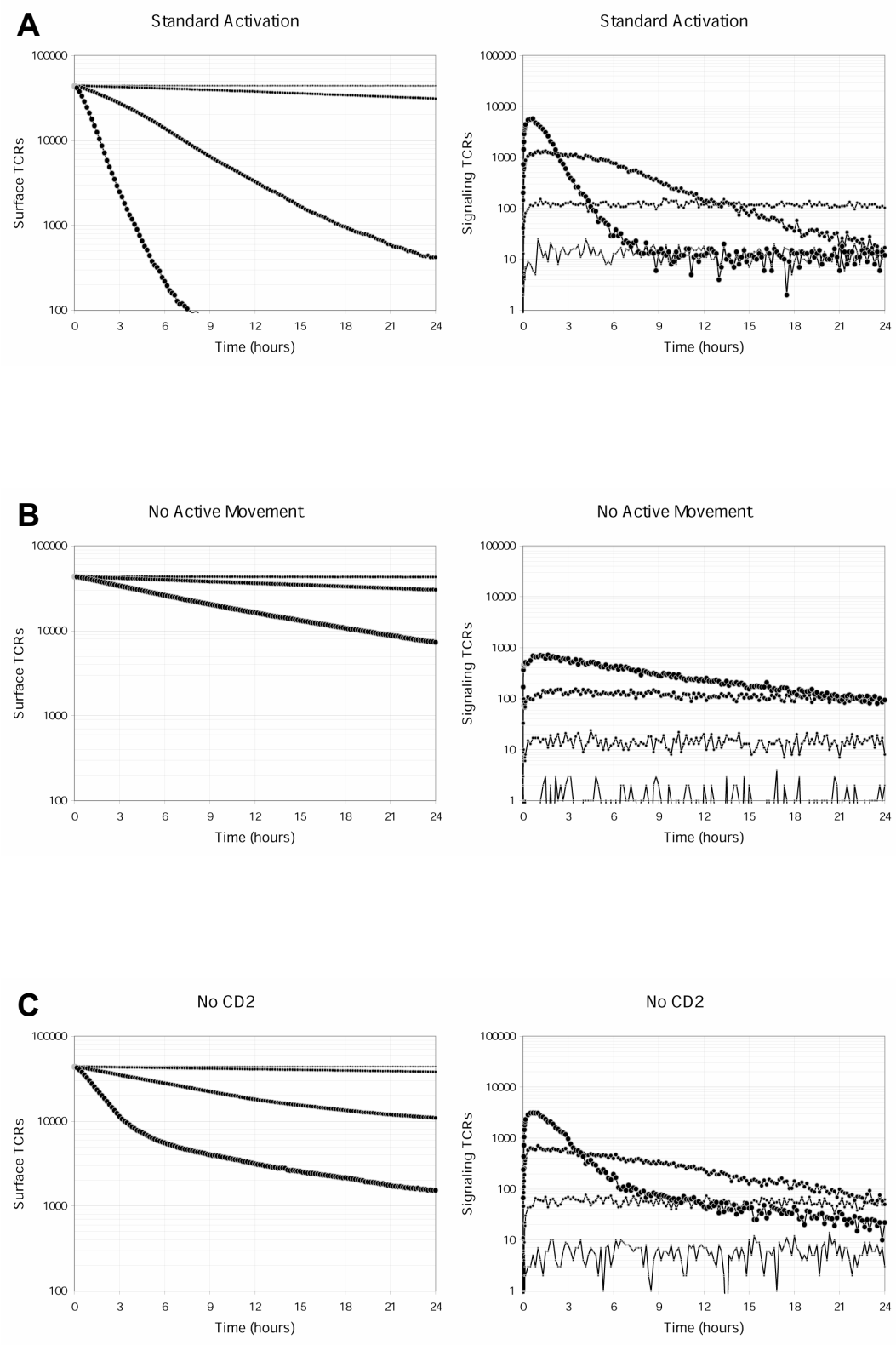

Figure 5.9: The effects of T10/T22^{b} levels on G8 γδ T cell TCR levels and signaling

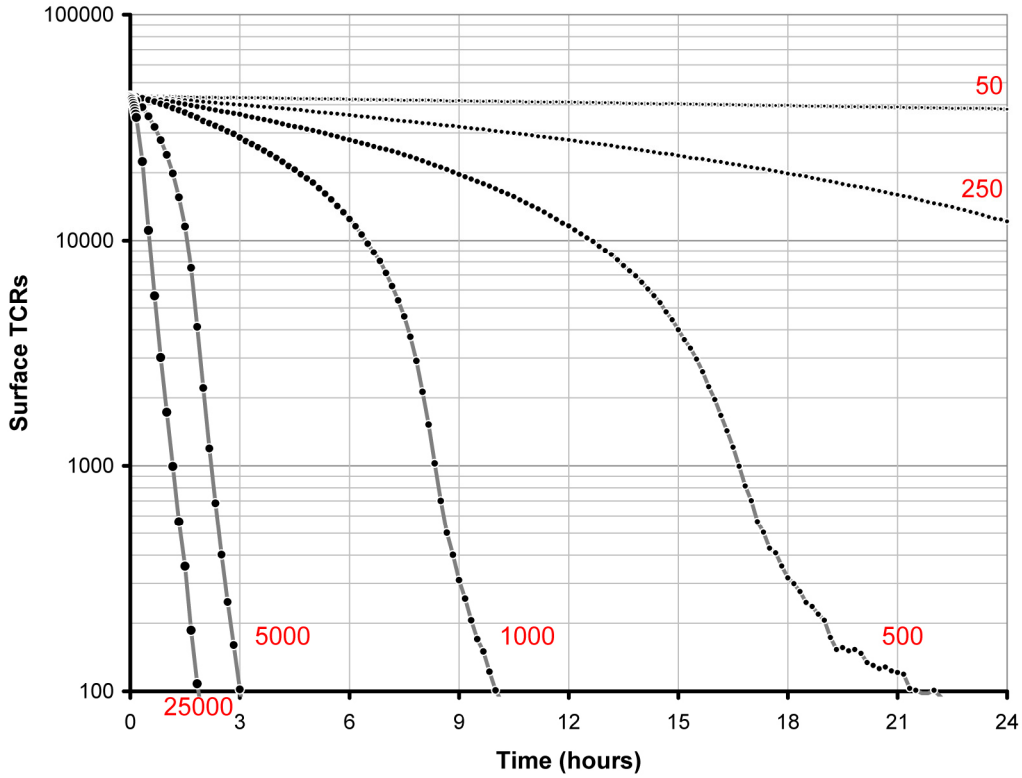

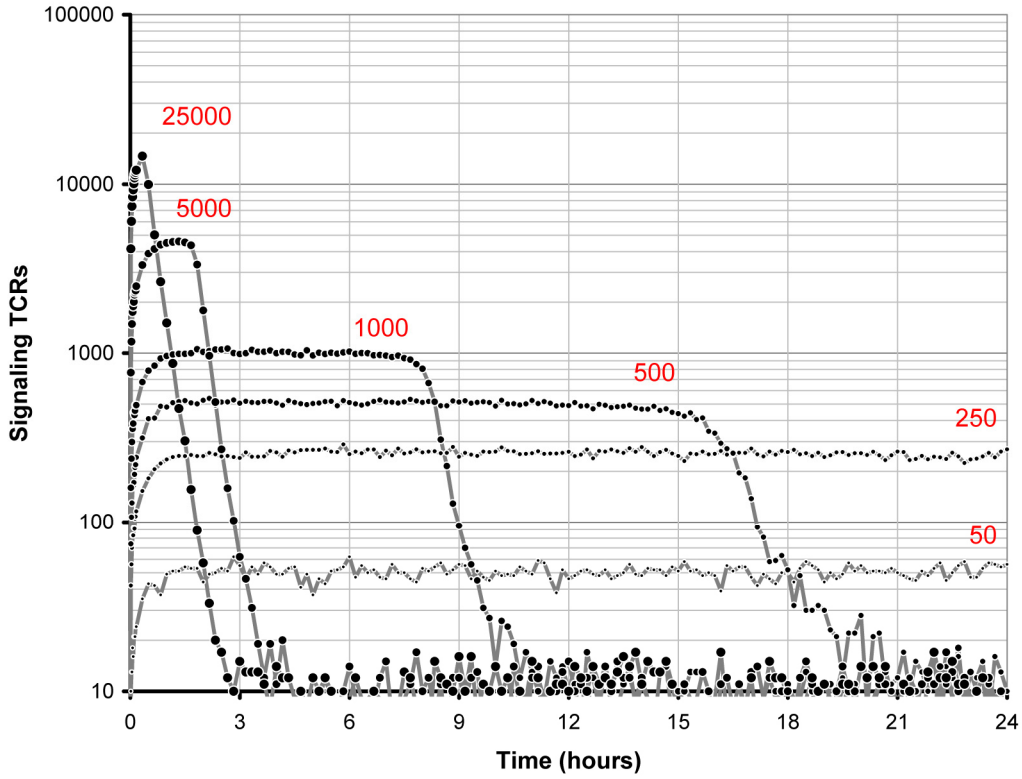

Figure 5.10: Peptide-independent MHC accumulation

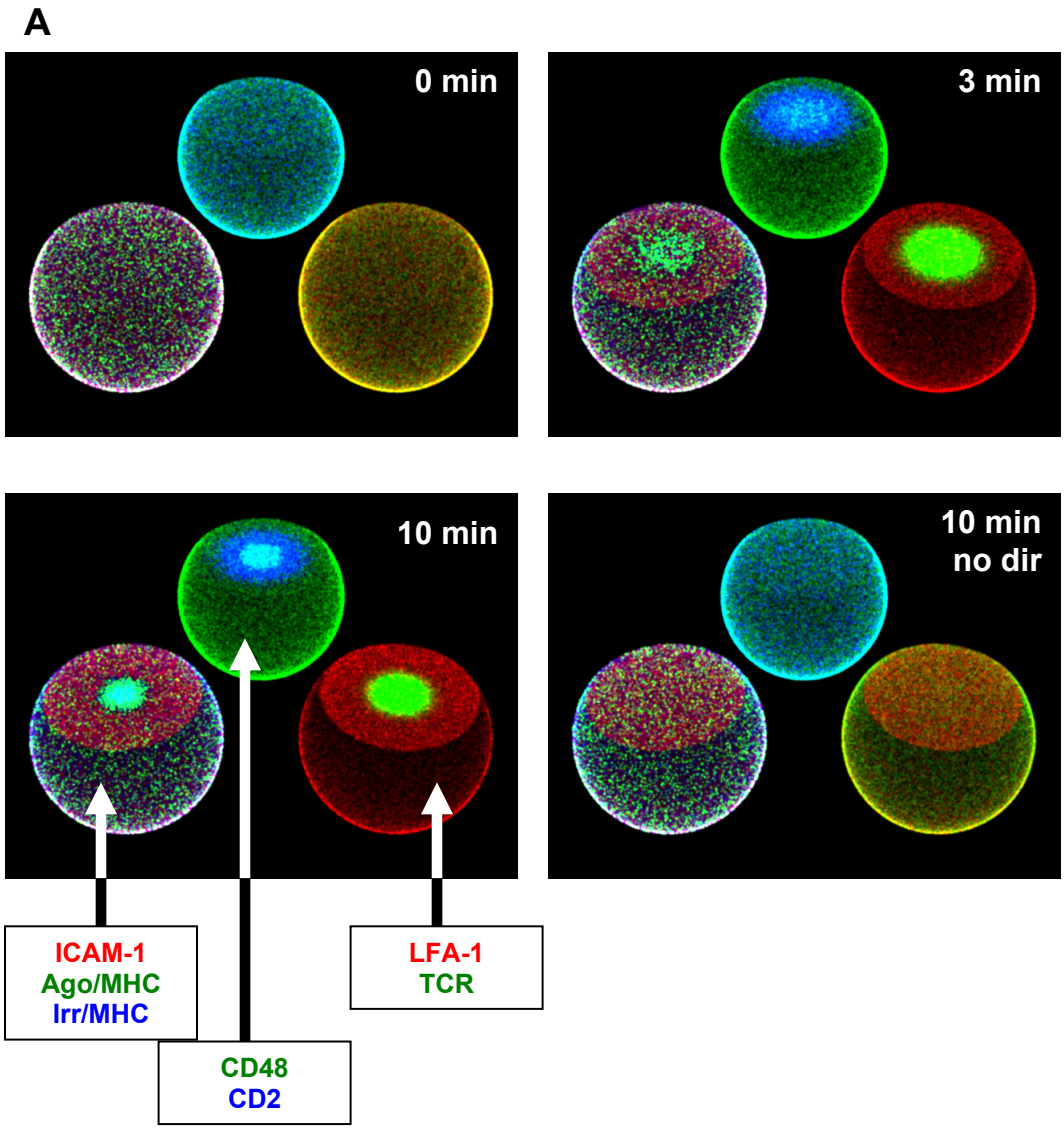

List of References

Agrawal, S., J. Marquet, G. J. Freeman, A. Tawab, P. L. Bouteiller, P. Roth, W. Bolton, G. Ogg, L. Boumsell and A. Bensussan (1999). "Cutting edge: MHC class I triggering by a novel cell surface ligand costimulates proliferation of activated human T cells." *J Immunol* **162**(3): 1223-6.

Allison, J. P. and W. L. Havran (1991). "The immunobiology of T cells with invariant gamma delta antigen receptors." *Annu Rev Immunol* **9**: 679-705.

Andreae, S., S. Buisson and F. Triebel (2003). "MHC class II signal transduction in human dendritic cells induced by a natural ligand, the LAG-3 protein (CD223)." *Blood* **102**(6): 2130-7.

Ariza, A., D. Lopez, E. M. Castella, C. Munoz, M. J. Zujar and J. L. Mate (1996). "Expression of CD15 in normal and metaplastic Paneth cells of the digestive tract." *J Clin Pathol* **49**(6): 474-7.

Asarnow, D. M., T. Goodman, L. LeFrancois and J. P. Allison (1989). "Distinct antigen receptor repertoires of two classes of murine epithelium-associated T cells." *Nature* **341**(6237): 60-2.

Ashkar, S., G. F. Weber, V. Panoutsakopoulou, M. E. Sanchirico, M. Jansson, S. Zawaideh, S. R. Rittling, D. T. Denhardt, M. J. Glimcher and H. Cantor (2000). "Eta-1 (osteopontin): an early component of type-1 (cell-mediated) immunity." *Science* **287**(5454): 860-4.

Azuara, V., K. Grigoriadou, M. P. Lembezat, C. Nagler-Anderson and P. Pereira (2001). "Strain-specific TCR repertoire selection of IL-4-producing Thy-1 dull gamma delta thymocytes." *Eur J Immunol* **31**(1): 205-14.

Azzam, H. S., J. B. DeJarnette, K. Huang, R. Emmons, C. S. Park, C. L. Sommers, D. El-Khoury, E. W. Shores and P. E. Love (2001). "Fine tuning of TCR signaling by CD5." *J Immunol* **166**(9): 5464-72.

Baixeras, E., B. Huard, C. Miossec, S. Jitsukawa, M. Martin, T. Hercend, C. Auffray, F. Triebel and D. Piatier-Tonneau (1992). "Characterization of the lymphocyte activation gene 3-encoded protein. A new ligand for human leukocyte antigen class II antigens." *J Exp Med* **176**(2): 327-37.

Barakonyi, A., M. Rabot, A. Marie-Cardine, M. Aguerre-Girr, B. Polgar, V. Schiavon, A. Bensussan and P. Le Bouteiller (2004). "Cutting edge: engagement of CD160 by its HLA-C physiological ligand triggers a unique cytokine profile secretion in the cytotoxic peripheral blood NK cell subset." *J Immunol* **173**(9): 5349-54.

Bargatze, R. F., M. A. Jutila and E. C. Butcher (1995). "Distinct roles of L-selectin and integrins alpha 4 beta 7 and LFA-1 in lymphocyte homing to Peyer's patch-HEV in situ: the multistep model confirmed and refined." *Immunity* **3**(1): 99-108.

Barrett, T. A., Y. Tatsumi and J. A. Bluestone (1993). "Tolerance of T cell receptor gamma/delta cells in the intestine." *J Exp Med* **177**(6): 1755-62.

Bauer, A., O. Huber and R. Kemler (1998). "Pontin52, an interaction partner of beta-catenin, binds to the TATA box binding protein." *Proc Natl Acad Sci U S A* **95**(25): 14787-92.

Beadling, C., K. M. Druey, G. Richter, J. H. Kehrl and K. A. Smith (1999). "Regulators of G protein signaling exhibit distinct patterns of gene expression and target G protein specificity in human lymphocytes." *J Immunol* **162**(5): 2677-82.

Bell, G. I., M. Dembo and P. Bongrand (1984). "Cell adhesion. Competition between nonspecific repulsion and specific bonding." *Biophys J* **45**(6): 1051-64.

Bhaskaran, G., A. Nii, S. Sone and T. Ogura (1992). "Differential effects of interleukin-4 on superoxide anion production by human alveolar macrophages stimulated with lipopolysaccharide and interferon-gamma." *J Leukoc Biol* **52**(2): 218-23.

Blank, C., I. Brown, R. Marks, H. Nishimura, T. Honjo and T. F. Gajewski (2003). "Absence of programmed death receptor 1 alters thymic development and enhances generation of CD4/CD8 double-negative TCR-transgenic T cells." *J Immunol* **171**(9): 4574-81.

Bluestone, J. A., R. Q. Cron, M. Cotterman, B. A. Houlden and L. A. Matis (1988). "Structure and specificity of T cell receptor gamma/delta on major histocompatibility complex antigen-specific CD3+, CD4-, CD8- T lymphocytes." *J Exp Med* **168**(5): 1899-916.

Bogdan, C., S. Stenger, M. Rollinghoff and W. Solbach (1991). "Cytokine interactions in experimental cutaneous leishmaniasis. Interleukin 4 synergizes with interferon-gamma to activate murine macrophages for killing of Leishmania major amastigotes." *Eur J Immunol* **21**(2): 327-33.

Boismenu, R., L. Feng, Y. Y. Xia, J. C. Chang and W. L. Havran (1996). "Chemokine expression by intraepithelial gamma delta T cells. Implications for the recruitment of inflammatory cells to damaged epithelia." *J Immunol* **157**(3): 985-92.

Boismenu, R. and W. L. Havran (1994). "Modulation of epithelial cell growth by intraepithelial gamma delta T cells." *Science* **266**(5188): 1253-5.

Boismenu, R. and W. L. Havran (1997). "An innate view of gamma delta T cells." *Curr Opin Immunol* **9**(1): 57-63.

Bonneville, M., K. Ito, E. G. Krecko, S. Itohara, D. Kappes, I. Ishida, O. Kanagawa, C. A. Janeway, D. B. Murphy and S. Tonegawa (1989). "Recognition of a self major histocompatibility complex TL region product by gamma delta T-cell receptors." *Proc Natl Acad Sci U S A* **86**(15): 5928-32.

Borst, J., R. J. van de Griend, J. W. van Oostveen, S. L. Ang, C. J. Melief, J. G. Seidman and R. L. Bolhuis (1987). "A T-cell receptor gamma/CD3 complex found on cloned functional lymphocytes." *Nature* **325**(6106): 683-8.

Brandes, M., K. Willimann, A. B. Lang, K. H. Nam, C. Jin, M. B. Brenner, C. T. Morita and B. Moser (2003). "Flexible migration program regulates gamma delta T-cell involvement in humoral immunity." *Blood* **102**(10): 3693-701.

Brenner, M. B., J. McLean, H. Scheft, J. Riberdy, S. L. Ang, J. G. Seidman, P. Devlin and M. S. Krangel (1987). "Two forms of the T-cell receptor gamma protein found on peripheral blood cytotoxic T lymphocytes." *Nature* **325**(6106): 689-94.

Brown, M. H., K. Boles, P. A. van der Merwe, V. Kumar, P. A. Mathew and A. N. Barclay (1998). "2B4, the natural killer and T cell immunoglobulin superfamily surface protein, is a ligand for CD48." *J Exp Med* **188**(11): 2083-90.

Buisson, S. and F. Triebel (2003). "MHC class II engagement by its ligand LAG-3 (CD223) leads to a distinct pattern of chemokine and chemokine receptor expression by human dendritic cells." *Vaccine* **21**(9-10): 862-8.

Burchert, A., D. Cai, L. Hofbauer, M. K. Samuelsson, E. P. Slater, J. Duyster, M. Ritter, A. Hochhaus, R. Mueller, M. Eilers, M. Schmidt and A. Neubauer (2003). "Interferon Consensus Sequence Binding Protein (ICSBP, IRF-8) antagonizes BCR/ABL and down-regulates bcl-2." *Blood*.

Burdin, N., L. Brossay and M. Kronenberg (1999). "Immunization with alpha-galactosylceramide polarizes CD1-reactive NK T cells towards Th2 cytokine synthesis." *Eur J Immunol* **29**(6): 2014-25.

Carding, S. R., W. Allan, S. Kyes, A. Hayday, K. Bottomly and P. C. Doherty (1990). "Late dominance of the inflammatory process in murine influenza by gamma/delta + T cells." *J Exp Med* **172**(4): 1225-31.

Carding, S. R. and P. J. Egan (2000). "The importance of gamma delta T cells in the resolution of pathogen-induced inflammatory immune responses." *Immunol Rev* **173**: 98-108.

Carnaud, C., D. Lee, O. Donnars, S. H. Park, A. Beavis, Y. Koezuka and A. Bendelac (1999). "Cutting edge: Cross-talk between cells of the innate immune system: NKT cells rapidly activate NK cells." *J Immunol* **163**(9): 4647-50.

Che, T., Y. You, D. Wang, M. J. Tanner, V. M. Dixit and X. Lin (2004). "MALT1/Paracaspase is a signaling component downstream of CARMA1 and mediates T cell receptor-induced NF-kappa B activation." *J Biol Chem*.

Chen, B. P., G. Liang, J. Whelan and T. Hai (1994). "ATF3 and ATF3 delta Zip. Transcriptional repression versus activation by alternatively spliced isoforms." *J Biol Chem* **269**(22): 15819-26.

Chen, C. Z., M. Li, D. de Graaf, S. Monti, B. Gottgens, M. J. Sanchez, E. S. Lander, T. R. Golub, A. R. Green and H. F. Lodish (2002). "Identification of endoglin as a functional marker that defines long-term repopulating hematopoietic stem cells." *Proc Natl Acad Sci U S A* **99**(24): 15468-73.

Chien, Y. H., R. Jores and M. P. Crowley (1996). "Recognition by gamma/delta T cells." *Annu Rev Immunol* **14**: 511-32.

Christmas, S. E. and A. Meager (1990). "Production of interferon-gamma and tumour necrosis factor-alpha by human T-cell clones expressing different forms of the gamma delta receptor." *Immunology* **71**(4): 486-92.

Coombs, D., A. M. Kalergis, S. G. Nathenson, C. Wofsy and B. Goldstein (2002). "Activated TCRs remain marked for internalization after dissociation from pMHC." *Nat Immunol* **3**(10): 926-31.

Costello, P. S., M. Gallagher and D. A. Cantrell (2002). "Sustained and dynamic inositol lipid metabolism inside and outside the immunological synapse." *Nat Immunol* **3**(11): 1082-9.

Cron, R. Q., T. F. Gajewski, S. O. Sharrow, F. W. Fitch, L. A. Matis and J. A. Bluestone (1989). "Phenotypic and functional analysis of murine CD3+,CD4-,CD8- TCR-gamma delta-expressing peripheral T cells." *J Immunol* **142**(11): 3754-62.

Crowley, M. P., A. M. Fahrer, N. Baumgarth, J. Hampl, I. Gutgemann, L. Teyton and Y. Chien (2000). "A population of murine gammadelta T cells that recognize an inducible MHC class Ib molecule." *Science* **287**(5451): 314-6.

Crowley, M. P., Z. Reich, N. Mavaddat, J. D. Altman and Y. Chien (1997). "The recognition of the nonclassical major histocompatibility complex (MHC) class I molecule, T10, by the gammadelta T cell, G8." *J Exp Med* **185**(7): 1223-30.

Crowley, M. T., C. R. Reilly and D. Lo (1999). "Influence of lymphocytes on the presence and organization of dendritic cell subsets in the spleen." *J Immunol* **163**(9): 4894-900.

De Miranda, J., R. Panizzutti, V. N. Foltyn and H. Wolosker (2002). "Cofactors of serine racemase that physiologically stimulate the synthesis of the N-methyl-D-aspartate (NMDA) receptor coagonist D-serine." *Proc Natl Acad Sci U S A* **99**(22): 14542-7.

De Vries, L., B. Zheng, T. Fischer, E. Elenko and M. G. Farquhar (2000). "The regulator of G protein signaling family." *Annu Rev Pharmacol Toxicol* **40**: 235-71.

Dent, A. L., L. A. Matis, F. Hooshmand, S. M. Widacki, J. A. Bluestone and S. M. Hedrick (1990). "Self-reactive gamma delta T cells are eliminated in the thymus." *Nature* **343**(6260): 714-9.

Droin, N. M., M. J. Pinkoski, E. Dejardin and D. R. Green (2003). "Egr family members regulate nonlymphoid expression of Fas ligand, TRAIL, and tumor necrosis factor during immune responses." *Mol Cell Biol* **23**(21): 7638-47.

Dustin, M. L., S. K. Bromley, M. M. Davis and C. Zhu (2001). "Identification of self through two-dimensional chemistry and synapses." *Annu Rev Cell Dev Biol* **17**: 133-57.

Dustin, M. L., M. W. Olszowy, A. D. Holdorf, J. Li, S. Bromley, N. Desai, P. Widder, F. Rosenberger, P. A. van der Merwe, P. M. Allen and A. S. Shaw (1998). "A novel adaptor protein orchestrates receptor patterning and cytoskeletal polarity in T-cell contacts." *Cell* **94**(5): 667-77.

Fahrer, A. M., Y. Konigshofer, E. M. Kerr, G. Ghandour, D. H. Mack, M. M. Davis and Y. H. Chien (2001). "Attributes of gammadelta intraepithelial lymphocytes as suggested by their transcriptional profile." *Proc Natl Acad Sci U S A* **98**(18): 10261-6.

Fanzo, J. C., C. M. Hu, S. Y. Jang and A. B. Pernis (2003). "Regulation of lymphocyte apoptosis by interferon regulatory factor 4 (IRF-4)." *J Exp Med* **197**(3): 303-14.

Feinstein, M. B., S. M. Fernandez and R. I. Sha'afi (1975). "Fluidity of natural membranes and phosphatidylserine and ganglioside dispersions. Effect of local anesthetics, cholesterol and protein." *Biochim Biophys Acta* **413**(3): 354-70.

Ferrick, D. A., M. D. Schrenzel, T. Mulvania, B. Hsieh, W. G. Ferlin and H. Lepper (1995). "Differential production of interferon-gamma and interleukin-4 in response to Th1- and Th2-stimulating pathogens by gamma delta T cells in vivo." *Nature* **373**(6511): 255-7.

Fiorini, E., I. Schmitz, W. E. Marissen, S. L. Osborn, M. Touma, T. Sasada, P. A. Reche, E. V. Tibaldi, R. E. Hussey, A. M. Kruisbeek, E. L. Reinherz and L. K. Clayton (2002). "Peptide-induced negative selection of thymocytes activates transcription of an NF-kappa B inhibitor." *Mol Cell* **9**(3): 637-48.

Freeman, G. J., J. G. Gribben, V. A. Boussiotis, J. W. Ng, V. A. Restivo, Jr., L. A. Lombard, G. S. Gray and L. M. Nadler (1993). "Cloning of B7-2: a CTLA-4 counter-receptor that costimulates human T cell proliferation." *Science* **262**(5135): 909-11.

Freemantle, S. J., H. B. Portland, K. Ewings, F. Dmitrovsky, K. DiPetrillo, M. J. Spinella and E. Dmitrovsky (2002). "Characterization and tissue-specific expression of human GSK-3-binding proteins FRAT1 and FRAT2." *Gene* **291**(1-2): 17-27.

Fu, Y. X., C. E. Roark, K. Kelly, D. Drevets, P. Campbell, R. O'Brien and W. Born (1994). "Immune protection and control of inflammatory tissue necrosis by gamma delta T cells." *J Immunol* **153**(7): 3101-15.

Furukawa, Y., T. Kawasoe, Y. Daigo, T. Nishiwaki, H. Ishiguro, M. Takahashi, J. Kitayama and Y. Nakamura (2001). "Isolation of a novel human gene, ARHGAP9,

encoding a rho-GTPase activating protein." *Biochem Biophys Res Commun* **284**(3): 643-9.

Glynne, R., S. Akkaraju, J. I. Healy, J. Rayner, C. C. Goodnow and D. H. Mack (2000). "How self-tolerance and the immunosuppressive drug FK506 prevent B-cell mitogenesis." *Nature* **403**(6770): 672-6.

Goodman, T. and L. Lefrancois (1988). "Expression of the gamma-delta T-cell receptor on intestinal CD8+ intraepithelial lymphocytes." *Nature* **333**(6176): 855-8.

Guehler, S. R., J. A. Bluestone and T. A. Barrett (1996). "Immune deviation of 2C transgenic intraepithelial lymphocytes in antigen-bearing hosts." *J Exp Med* **184**(2): 493-503.

Guehler, S. R., R. J. Finch, J. A. Bluestone and T. A. Barrett (1998). "Increased threshold for TCR-mediated signaling controls self reactivity of intraepithelial lymphocytes." *J Immunol* **160**(11): 5341-6.

Hayday, A. and R. Tigelaar (2003). "Immunoregulation in the tissues by gammadelta T cells." *Nat Rev Immunol* **3**(3): 233-42.

Hayday, A. C. (2000). "[gamma][delta] cells: a right time and a right place for a conserved third way of protection." *Annu Rev Immunol* **18**: 975-1026.

Hiromatsu, K., Y. Yoshikai, G. Matsuzaki, S. Ohga, K. Muramori, K. Matsumoto, J. A. Bluestone and K. Nomoto (1992). "A protective role of gamma/delta T cells in primary infection with Listeria monocytogenes in mice." *J Exp Med* **175**(1): 49-56.

Ho, I. C., J. P. Arm, C. O. Bingham, 3rd, A. Choi, K. F. Austen and L. H. Glimcher (2001). "A novel group of phospholipase A2s preferentially expressed in type 2 helper T cells." *J Biol Chem* **276**(21): 18321-6.

Hock, H., M. J. Hamblen, H. M. Rooke, J. W. Schindler, S. Saleque, Y. Fujiwara and S. H. Orkin (2004). "Gfi-1 restricts proliferation and preserves functional integrity of haematopoietic stem cells." *Nature* **431**(7011): 1002-7.

Hollinger, S. and J. R. Hepler (2002). "Cellular regulation of RGS proteins: modulators and integrators of G protein signaling." *Pharmacol Rev* **54**(3): 527-59.

Horner, A. A., H. Jabara, N. Ramesh and R. S. Geha (1995). "gamma/delta T lymphocytes express CD40 ligand and induce isotype switching in B lymphocytes." *J Exp Med* **181**(3): 1239-44.

Houlden, B. A., L. A. Matis, R. Q. Cron, S. M. Widacki, G. D. Brown, C. Pampeno, D. Meruelo and J. A. Bluestone (1989). "A TCR gamma delta cell recognizing a novel TL-encoded gene product." *Cold Spring Harb Symp Quant Biol* **54 Pt 1**: 45-55.

Hsu, J. C., R. Bravo and R. Taub (1992). "Interactions among LRF-1, JunB, c-Jun, and c-Fos define a regulatory program in the G1 phase of liver regeneration." *Mol Cell Biol* **12**(10): 4654-65.

Hu, C. M., S. Y. Jang, J. C. Fanzo and A. B. Pernis (2002). "Modulation of T cell cytokine production by interferon regulatory factor-4." *J Biol Chem* **277**(51): 49238-46.

Huang, X., S. A. McClellan, R. P. Barrett and L. D. Hazlett (2002). "IL-18 contributes to host resistance against infection with Pseudomonas aeruginosa through induction of IFN-gamma production." *J Immunol* **168**(11): 5756-63.

Huber, H., P. Descossy, E. Regier, R. van Brandwijk and J. Knop (1995). "Activation of phenotypically heterogeneous murine T cell receptor gamma delta + dendritic epidermal T cells by self-antigen(s)." *Int Arch Allergy Immunol* **107**(4): 498-507.

Huber, S. A., D. Graveline, W. K. Born and R. L. O'Brien (2001). "Cytokine production by Vgamma(+)-T-cell subsets is an important factor determining CD4(+)-Th-cell phenotype and susceptibility of BALB/c mice to coxsackievirus B3-induced myocarditis." *J Virol* **75**(13): 5860-9.

Huppa, J. B., M. Gleimer, C. Sumen and M. M. Davis (2003). "Continuous T cell receptor signaling required for synapse maintenance and full effector potential." *Nat Immunol* **4**(8): 749-55.

Iezzi, G., K. Karjalainen and A. Lanzavecchia (1998). "The duration of antigenic stimulation determines the fate of naive and effector T cells." *Immunity* **8**(1): 89-95.

Ishiguro, H., T. Tsunoda, T. Tanaka, Y. Fujii, Y. Nakamura and Y. Furukawa (2001). "Identification of AXUD1, a novel human gene induced by AXIN1 and its reduced expression in human carcinomas of the lung, liver, colon and kidney." *Oncogene* **20**(36): 5062-6.

Ito, K., L. Van Kaer, M. Bonneville, S. Hsu, D. B. Murphy and S. Tonegawa (1990). "Recognition of the product of a novel MHC TL region gene (27b) by a mouse gamma delta T cell receptor." *Cell* **62**(3): 549-61.

Iyer, V. R., M. B. Eisen, D. T. Ross, G. Schuler, T. Moore, J. C. Lee, J. M. Trent, L. M. Staudt, J. Hudson, Jr., M. S. Boguski, D. Lashkari, D. Shalon, D. Botstein and P. O. Brown (1999). "The transcriptional program in the response of human fibroblasts to serum." *Science* **283**(5398): 83-7.

Jacob, J. and D. Baltimore (1999). "Modelling T-cell memory by genetic marking of memory T cells in vivo." *Nature* **399**(6736): 593-7.

Jameson, J., K. Ugarte, N. Chen, P. Yachi, E. Fuchs, R. Boismenu and W. L. Havran (2002). "A role for skin gammadelta T cells in wound repair." *Science* **296**(5568): 747-9.

Janis, E. M., S. H. Kaufmann, R. H. Schwartz and D. M. Pardoll (1989). "Activation of gamma delta T cells in the primary immune response to Mycobacterium tuberculosis." *Science* **244**(4905): 713-6.

Kaliyaperumal, A., R. Falchetto, A. Cox, R. Dick, 2nd, J. Shabanowitz, Y. H. Chien, L. Matis, D. F. Hunt and J. A. Bluestone (1995). "Functional expression and recognition of nonclassical MHC class I T10b is not peptide-dependent." *J Immunol* **155**(5): 2379-86.

Kashiwakura, J., N. Suzuki, M. Takeno, S. Itoh, T. Oku, T. Sakane, S. Nakajin and S. Toyoshima (2002). "Evidence of autophosphorylation in Txk: Y91 is an autophosphorylation site." *Biol Pharm Bull* **25**(6): 718-21.

Kasper, L. H., T. Matsuura, S. Fonseka, J. Arruda, J. Y. Channon and I. A. Khan (1996). "Induction of gammadelta T cells during acute murine infection with Toxoplasma gondii." *J Immunol* **157**(12): 5521-7.

Kaufmann, S. H. (1996). "gamma/delta and other unconventional T lymphocytes: what do they see and what do they do?" *Proc Natl Acad Sci U S A* **93**(6): 2272-9.

Kawaguchi-Miyashita, M., S. Shimada, Y. Matsuoka, M. Ohwaki and M. Nanno (2000). "Activation of T-cell receptor-gammadelta+ cells in the intestinal epithelia of KN6 transgenic mice." *Immunology* **101**(1): 38-45.

Kerr, E. M. (1998). Yersinia pseudotuberculosis infection in C57BL/6 mice: Gene expression, kinetics, and essential cells in the immune response to a food-borne pathogen. Immunology program. Stanford, CA, Stanford University**:** 131.

Kim, M., C. V. Carman and T. A. Springer (2003). "Bidirectional transmembrane signaling by cytoplasmic domain separation in integrins." *Science* **301**(5640): 1720-5.

King, D. P., D. M. Hyde, K. A. Jackson, D. M. Novosad, T. N. Ellis, L. Putney, M. Y. Stovall, L. S. Van Winkle, B. L. Beaman and D. A. Ferrick (1999). "Cutting edge: protective response to pulmonary injury requires gamma delta T lymphocytes." *J Immunol* **162**(9): 5033-6.

Klein, J. R. (1986). "Ontogeny of the Thy-1-, Lyt-2+ murine intestinal intraepithelial lymphocyte. Characterization of a unique population of thymus-independent cytotoxic effector cells in the intestinal mucosa." *J Exp Med* **164**(1): 309-14.

Klein, J. R. and M. F. Kagnoff (1984). "Nonspecific recruitment of cytotoxic effector cells in the intestinal mucosa of antigen-primed mice." *J Exp Med* **160**(6): 1931-6.

Koduri, R. S., J. O. Gronroos, V. J. Laine, C. Le Calvez, G. Lambeau, T. J. Nevalainen and M. H. Gelb (2002). "Bactericidal properties of human and murine groups I, II, V, X, and XII secreted phospholipases A(2)." *J Biol Chem* **277**(8): 5849-57.

Komano, H., Y. Fujiura, M. Kawaguchi, S. Matsumoto, Y. Hashimoto, S. Obana, P. Mombaerts, S. Tonegawa, H. Yamamoto, S. Itohara and et al. (1995). "Homeostatic regulation of intestinal epithelia by intraepithelial gamma delta T cells." *Proc Natl Acad Sci U S A* **92**(13): 6147-51.

Koyama, T., T. Araiso and J. Nitta (1987). "Dynamics of membrane structure of frog erythrocyte ghosts measured with a nanosecond fluorometer." *Biorheology* **24**(3): 311-7.

Krause, M., A. S. Sechi, M. Konradt, D. Monner, F. B. Gertler and J. Wehland (2000). "Fyn-binding protein (Fyb)/SLP-76-associated protein (SLAP), Ena/vasodilator-stimulated phosphoprotein (VASP) proteins and the Arp2/3 complex link T cell receptor (TCR) signaling to the actin cytoskeleton." *J Cell Biol* **149**(1): 181-94.

Kucik, D. F., M. L. Dustin, J. M. Miller and E. J. Brown (1996). "Adhesion-activating phorbol ester increases the mobility of leukocyte integrin LFA-1 in cultured lymphocytes." *J Clin Invest* **97**(9): 2139-44.

Lacana, E. and L. D'Adamio (1999). "Regulation of Fas ligand expression and cell death by apoptosis-linked gene 4." *Nat Med* **5**(5): 542-7.

Landmann, R., A. E. Fisscher and J. P. Obrecht (1992). "Interferon-gamma and interleukin-4 down-regulate soluble CD14 release in human monocytes and macrophages." *J Leukoc Biol* **52**(3): 323-30.

Langlet, C., A. M. Bernard, P. Drevot and H. T. He (2000). "Membrane rafts and signaling by the multichain immune recognition receptors." *Curr Opin Immunol* **12**(3): 250-5.

Lanier, L. L., T. J. Kipps and J. H. Phillips (1985). "Functional properties of a unique subset of cytotoxic CD3+ T lymphocytes that express Fc receptors for IgG (CD16/Leu-11 antigen)." *J Exp Med* **162**(6): 2089-106.

Laub, F., R. Aldabe, V. Friedrich, Jr., S. Ohnishi, T. Yoshida and F. Ramirez (2001). "Developmental expression of mouse Kruppel-like transcription factor KLF7 suggests a potential role in neurogenesis." *Dev Biol* **233**(2): 305-18.

Lee, A. H., J. H. Hong and Y. S. Seo (2000). "Tumour necrosis factor-alpha and interferon-gamma synergistically activate the RANTES promoter through nuclear factor kappaB and interferon regulatory factor 1 (IRF-1) transcription factors." *Biochem J* **350 Pt 1**: 131-8.

Lee, K. H., A. R. Dinner, C. Tu, G. Campi, S. Raychaudhuri, R. Varma, T. N. Sims, W. R. Burack, H. Wu, J. Wang, O. Kanagawa, M. Markiewicz, P. M. Allen, M. L. Dustin, A. K. Chakraborty and A. S. Shaw (2003). "The immunological synapse balances T cell receptor signaling and degradation." *Science* **302**(5648): 1218-22.

Lefrancois, L. and T. Goodman (1989). "In vivo modulation of cytolytic activity and Thy-1 expression in TCR-gamma delta+ intraepithelial lymphocytes." *Science* **243**(4899): 1716-8.

Leite-De-Moraes, M. C., A. Hameg, M. Pacilio, Y. Koezuka, M. Taniguchi, L. Van Kaer, E. Schneider, M. Dy and A. Herbelin (2001). "IL-18 enhances IL-4 production by ligand-activated NKT lymphocytes: a pro-Th2 effect of IL-18 exerted through NKT cells." *J Immunol* **166**(2): 945-51.

Li, S. H., S. C. Chan, A. Toshitani, D. Y. Leung and J. M. Hanifin (1992). "Synergistic effects of interleukin 4 and interferon-gamma on monocyte phosphodiesterase activity." *J Invest Dermatol* **99**(1): 65-70.

Linsley, P. S., W. Brady, M. Urnes, L. S. Grosmaire, N. K. Damle and J. A. Ledbetter (1991). "CTLA-4 is a second receptor for the B cell activation antigen B7." *J Exp Med* **174**(3): 561-9.

Lippert, E., D. L. Yowe, J. A. Gonzalo, J. P. Justice, J. M. Webster, E. R. Fedyk, M. Hodge, C. Miller, J. C. Gutierrez-Ramos, F. Borrego, A. Keane-Myers and K. M. Druey (2003). "Role of regulator of G protein signaling 16 in inflammation-induced T lymphocyte migration and activation." *J Immunol* **171**(3): 1542-55.

Lipshutz, R. J., S. P. Fodor, T. R. Gingeras and D. J. Lockhart (1999). "High density synthetic oligonucleotide arrays." *Nat Genet* **21**(1 Suppl): 20-4.

Liu, H., M. Rhodes, D. L. Wiest and D. A. Vignali (2000). "On the dynamics of TCR:CD3 complex cell surface expression and downmodulation." *Immunity* **13**(5): 665-75.

Liu, W. K., P. F. Yen, C. Y. Chien, M. J. Fann, J. Y. Su and C. K. Chou (2004). "The inhibitor ABIN-2 disrupts the interaction of receptor-interacting protein with the kinase subunit IKKgamma to block activation of the transcription factor NF-kappaB and potentiate apoptosis." *Biochem J* **378**(Pt 3): 867-76.

Lohoff, M., H. W. Mittrucker, A. Brustle, F. Sommer, B. Casper, M. Huber, D. A. Ferrick, G. S. Duncan and T. W. Mak (2004). "Enhanced TCR-induced apoptosis in interferon regulatory factor 4-deficient CD4(+) Th cells." *J Exp Med* **200**(2): 247-53.

Lollo, B. A., K. W. Chan, E. M. Hanson, V. T. Moy and A. A. Brian (1993). "Direct evidence for two affinity states for lymphocyte function-associated antigen 1 on activated T cells." *J Biol Chem* **268**(29): 21693-700.

Lu, B., A. F. Ferrandino and R. A. Flavell (2004). "Gadd45beta is important for perpetuating cognate and inflammatory signals in T cells." *Nat Immunol* **5**(1): 38-44.

Lynch, E. A., C. A. Heijens, N. F. Horst, D. M. Center and W. W. Cruikshank (2003). "Cutting edge: IL-16/CD4 preferentially induces Th1 cell migration: requirement of CCR5." *J Immunol* **171**(10): 4965-8.

Ma, Q., M. Shimaoka, C. Lu, H. Jing, C. V. Carman and T. A. Springer (2002). "Activation-induced conformational changes in the I domain region of lymphocyte function-associated antigen 1." *J Biol Chem* **277**(12): 10638-41.

Maddox, D. M., A. Manlapat, P. Roon, P. Prasad, V. Ganapathy and S. B. Smith (2003). "Reduced-folate carrier (RFC) is expressed in placenta and yolk sac, as well as in cells of the developing forebrain, hindbrain, neural tube, craniofacial region, eye, limb buds and heart." *BMC Dev Biol* **3**(1): 6.

Matis, L. A., R. Cron and J. A. Bluestone (1987). "Major histocompatibility complex-linked specificity of gamma delta receptor-bearing T lymphocytes." *Nature* **330**(6145): 262-4.

Matsue, H., P. D. Cruz, Jr., P. R. Bergstresser and A. Takashima (1993). "Profiles of cytokine mRNA expressed by dendritic epidermal T cells in mice." *J Invest Dermatol* **101**(4): 537-42.

Matsui, K., J. J. Boniface, P. Steffner, P. A. Reay and M. M. Davis (1994). "Kinetics of T-cell receptor binding to peptide/I-Ek complexes: correlation of the dissociation rate with T-cell responsiveness." *Proc Natl Acad Sci U S A* **91**(26): 12862-6.

McMenamin, C., C. Pimm, M. McKersey and P. G. Holt (1994). "Regulation of IgE responses to inhaled antigen in mice by antigen-specific gamma delta T cells." *Science* **265**(5180): 1869-71.

Menne, C., T. Moller Sorensen, V. Siersma, M. von Essen, N. Odum and C. Geisler (2002). "Endo- and exocytic rate constants for spontaneous and protein kinase C-activated T cell receptor cycling." *Eur J Immunol* **32**(3): 616-26.

Mombaerts, P., J. Arnoldi, F. Russ, S. Tonegawa and S. H. Kaufmann (1993). "Different roles of alpha beta and gamma delta T cells in immunity against an intracellular bacterial pathogen." *Nature* **365**(6441): 53-6.

Monks, C. R., B. A. Freiberg, H. Kupfer, N. Sciaky and A. Kupfer (1998). "Three-dimensional segregation of supramolecular activation clusters in T cells." *Nature* **395**(6697): 82-6.

Mosley, R. L. and J. R. Klein (1992). "A rapid method for isolating murine intestine intraepithelial lymphocytes with high yield and purity." *J Immunol Methods* **156**(1): 19-26.

Moss, W. C., D. J. Irvine, M. M. Davis and M. F. Krummel (2002). "Quantifying signaling-induced reorientation of T cell receptors during immunological synapse formation." *Proc Natl Acad Sci U S A* **99**(23): 15024-9.

Nguyen, L. H., L. Espert, N. Mechti and D. M. Wilson, 3rd (2001). "The human interferon- and estrogen-regulated ISG20/HEM45 gene product degrades single-stranded RNA and DNA in vitro." *Biochemistry* **40**(24): 7174-9.

Niebylski, C. D. and H. R. Petty (1991). "Cyclosporine A induces an early and transient rigidification of lymphocyte membranes." *J Leukoc Biol* **49**(4): 407-15.

Niu, J., J. Profirovic, H. Pan, R. Vaiskunaite and T. Voyno-Yasenetskaya (2003). "G Protein betagamma subunits stimulate p114RhoGEF, a guanine nucleotide exchange factor for RhoA and Rac1: regulation of cell shape and reactive oxygen species production." *Circ Res* **93**(9): 848-56.

Noma, Y., P. Sideras, T. Naito, S. Bergstedt-Lindquist, C. Azuma, E. Severinson, T. Tanabe, T. Kinashi, F. Matsuda, Y. Yaoita and et al. (1986). "Cloning of cDNA encoding the murine IgG1 induction factor by a novel strategy using SP6 promoter." *Nature* **319**(6055): 640-6.

Ogasawara, T., M. Emoto, K. Kiyotani, K. Shimokata, T. Yoshida, Y. Nagai and Y. Yoshikai (1994). "Sendai virus pneumonia: evidence for the early recruitment of gamma delta T cells during the disease course." *J Virol* **68**(6): 4022-7.

Ouellette, A. J., R. M. Greco, M. James, D. Frederick, J. Naftilan and J. T. Fallon (1989). "Developmental regulation of cryptdin, a corticostatin/defensin precursor mRNA in mouse small intestinal crypt epithelium." *J Cell Biol* **108**(5): 1687-95.

Paterson, H. F., J. W. Savopoulos, O. Perisic, R. Cheung, M. V. Ellis, R. L. Williams and M. Katan (1995). "Phospholipase C delta 1 requires a pleckstrin homology domain for interaction with the plasma membrane." *Biochem J* **312 (Pt 3)**: 661-6.

Pena-Rossi, C., L. A. Zuckerman, J. Strong, J. Kwan, W. Ferris, S. Chan, A. Tarakhovsky, A. D. Beyers and N. Killeen (1999). "Negative regulation of CD4 lineage development and responses by CD5." *J Immunol* **163**(12): 6494-501.

Pennington, D. J., B. Silva-Santos, J. Shires, E. Theodoridis, C. Pollitt, E. L. Wise, R. E. Tigelaar, M. J. Owen and A. C. Hayday (2003). "The inter-relatedness and

interdependence of mouse T cell receptor gammadelta+ and alphabeta+ cells." *Nat Immunol* **4**(10): 991-8.

Periasamy, N., M. Armijo and A. S. Verkman (1991). "Picosecond rotation of small polar fluorophores in the cytosol of sea urchin eggs." *Biochemistry* **30**(51): 11836-41.

Qi, S. Y., J. T. Groves and A. K. Chakraborty (2001). "Synaptic pattern formation during cellular recognition." *Proc Natl Acad Sci U S A* **98**(12): 6548-53.

Rameh, L. E. and L. C. Cantley (1999). "The role of phosphoinositide 3-kinase lipid products in cell function." *J Biol Chem* **274**(13): 8347-50.

Robbins, S. H., S. C. Terrizzi, B. C. Sydora, T. Mikayama and L. Brossay (2003). "Differential regulation of killer cell lectin-like receptor G1 expression on T cells." *J Immunol* **170**(12): 5876-85.

Roberts, K., W. M. Yokoyama, P. J. Kehn and E. M. Shevach (1991). "The vitronectin receptor serves as an accessory molecule for the activation of a subset of gamma/delta T cells." *J Exp Med* **173**(1): 231-40.

Roberts, S. J., A. L. Smith, A. B. West, L. Wen, R. C. Findly, M. J. Owen and A. C. Hayday (1996). "T-cell alpha beta + and gamma delta + deficient mice display abnormal but distinct phenotypes toward a natural, widespread infection of the intestinal epithelium." *Proc Natl Acad Sci U S A* **93**(21): 11774-9.

Rock, E. P., P. R. Sibbald, M. M. Davis and Y. H. Chien (1994). "CDR3 length in antigen-specific immune receptors." *J Exp Med* **179**(1): 323-8.

Sakane, F. and H. Kanoh (1997). "Molecules in focus: diacylglycerol kinase." *Int J Biochem Cell Biol* **29**(10): 1139-43.

Sanui, T., A. Inayoshi, M. Noda, E. Iwata, M. Oike, T. Sasazuki and Y. Fukui (2003). "DOCK2 is essential for antigen-induced translocation of TCR and lipid rafts, but not PKC-theta and LFA-1, in T cells." *Immunity* **19**(1): 119-29.

Schell, M. J. (2004). "The N-methyl D-aspartate receptor glycine site and D-serine metabolism: an evolutionary perspective." *Philos Trans R Soc Lond B Biol Sci* **359**(1446): 943-64.

Schild, H., N. Mavaddat, C. Litzenberger, E. W. Ehrich, M. M. Davis, J. A. Bluestone, L. Matis, R. K. Draper and Y. H. Chien (1994). "The nature of major histocompatibility complex recognition by gamma delta T cells." *Cell* **76**(1): 29-37.

Sciammas, R., P. Kodukula, Q. Tang, R. L. Hendricks and J. A. Bluestone (1997). "T cell receptor-gamma/delta cells protect mice from herpes simplex virus type 1-induced lethal encephalitis." *J Exp Med* **185**(11): 1969-75.

Selin, L. K., P. A. Santolucito, A. K. Pinto, E. Szomolanyi-Tsuda and R. M. Welsh (2001). "Innate immunity to viruses: control of vaccinia virus infection by gamma delta T cells." *J Immunol* **166**(11): 6784-94.

Seoh, M. L., C. H. Ng, J. Yong, L. Lim and T. Leung (2003). "ArhGAP15, a novel human RacGAP protein with GTPase binding property." *FEBS Lett* **539**(1-3): 131-7.

Shires, J., E. Theodoridis and A. C. Hayday (2001). "Biological insights into TCRgammadelta+ and TCRalphabeta+ intraepithelial lymphocytes provided by serial analysis of gene expression (SAGE)." *Immunity* **15**(3): 419-34.

Siebrecht, M. S., E. Hsia, C. Spychalski and C. Nagler-Anderson (1993). "Stimulation of murine intestinal intraepithelial lymphocytes by the bacterial superantigen staphylococcal enterotoxin B." *Int Immunol* **5**(7): 717-24.

Silva-Santos, B., D. J. Pennington and A. C. Hayday (2005). "Lymphotoxin-mediated regulation of gammadelta cell differentiation by alphabeta T cell progenitors." *Science* **307**(5711): 925-8.

Sim, G. K. (1995). "Intraepithelial lymphocytes and the immune system." *Adv Immunol* **58**: 297-343.

Skeen, M. J. and H. K. Ziegler (1993). "Induction of murine peritoneal gamma/delta T cells and their role in resistance to bacterial infection." *J Exp Med* **178**(3): 971-84.

Smith, K., B. Seddon, M. A. Purbhoo, R. Zamoyska, A. G. Fisher and M. Merkenschlager (2001). "Sensory adaptation in naive peripheral CD4 T cells." *J Exp Med* **194**(9): 1253-61.

Song, A., Y. F. Chen, K. Thamatrakoln, T. A. Storm and A. M. Krensky (1999). "RFLAT-1: a new zinc finger transcription factor that activates RANTES gene expression in T lymphocytes." *Immunity* **10**(1): 93-103.

Staal, F. J. and H. Clevers (2000). "Tcf/Lef transcription factors during T-cell development: unique and overlapping functions." *Hematol J* **1**(1): 3-6.

Stenger, S., W. Solbach, M. Rollinghoff and C. Bogdan (1991). "Cytokine interactions in experimental cutaneous leishmaniasis. II. Endogenous tumor necrosis factor-alpha production by macrophages is induced by the synergistic action of interferon (IFN)-gamma and interleukin (IL) 4 and accounts for the antiparasitic effect mediated by IFN-gamma and IL 4." *Eur J Immunol* **21**(7): 1669-75.

Strisovsky, K., J. Jiraskova, C. Barinka, P. Majer, C. Rojas, B. S. Slusher and J. Konvalinka (2003). "Mouse brain serine racemase catalyzes specific elimination of L-serine to pyruvate." *FEBS Lett* **535**(1-3): 44-8.

Sun, J., C. H. Bird, V. Sutton, L. McDonald, P. B. Coughlin, T. A. De Jong, J. A. Trapani and P. I. Bird (1996). "A cytosolic granzyme B inhibitor related to the viral apoptotic regulator cytokine response modifier A is present in cytotoxic lymphocytes." *J Biol Chem* **271**(44): 27802-9.

Sun, Z., C. W. Arendt, W. Ellmeier, E. M. Schaeffer, M. J. Sunshine, L. Gandhi, J. Annes, D. Petrzilka, A. Kupfer, P. L. Schwartzberg and D. R. Littman (2000). "PKC-theta is required for TCR-induced NF-kappaB activation in mature but not immature T lymphocytes." *Nature* **404**(6776): 402-7.

Takagaki, Y., A. DeCloux, M. Bonneville and S. Tonegawa (1989). "Diversity of gamma delta T-cell receptors on murine intestinal intra-epithelial lymphocytes." *Nature* **339**(6227): 712-4.

Takeba, Y., H. Nagafuchi, M. Takeno, J. Kashiwakura and N. Suzuki (2002). "Txk, a member of nonreceptor tyrosine kinase of Tec family, acts as a Th1 cell-specific transcription factor and regulates IFN-gamma gene transcription." *J Immunol* **168**(5): 2365-70.

Tarakhovsky, A., S. B. Kanner, J. Hombach, J. A. Ledbetter, W. Muller, N. Killeen and K. Rajewsky (1995). "A role for CD5 in TCR-mediated signal transduction and thymocyte selection." *Science* **269**(5223): 535-7.

Tsujimura, H., T. Nagamura-Inoue, T. Tamura and K. Ozato (2002). "IFN consensus sequence binding protein/IFN regulatory factor-8 guides bone marrow progenitor cells toward the macrophage lineage." *J Immunol* **169**(3): 1261-9.

Turner, J. and M. Crossley (1998). "Cloning and characterization of mCtBP2, a co-repressor that associates with basic Kruppel-like factor and other mammalian transcriptional regulators." *Embo J* **17**(17): 5129-40.

Valdez, A. C., J. P. Cabaniols, M. J. Brown and P. A. Roche (1999). "Syntaxin 11 is associated with SNAP-23 on late endosomes and the trans-Golgi network." *J Cell Sci* **112 (Pt 6)**: 845-54.

Van Huffel, S., F. Delaei, K. Heyninck, D. De Valck and R. Beyaert (2001). "Identification of a novel A20-binding inhibitor of nuclear factor-kappa B activation termed ABIN-2." *J Biol Chem* **276**(32): 30216-23.

van Vlasselaer, P., H. Gascan, R. de Waal Malefyt and J. E. de Vries (1992). "IL-2 and a contact-mediated signal provided by TCR alpha beta + or TCR gamma delta + CD4+ T cells induce polyclonal Ig production by committed human B cells. Enhancement by IL-5, specific inhibition of IgA synthesis by IL-4." *J Immunol* **148**(6): 1674-84.

Verburg, M., I. B. Renes, D. J. Van Nispen, S. Ferdinandusse, M. Jorritsma, H. A. Buller, A. W. Einerhand and J. Dekker (2002). "Specific responses in rat small intestinal epithelial mRNA expression and protein levels during chemotherapeutic damage and regeneration." *J Histochem Cytochem* **50**(11): 1525-36.

Viney, J. L. and T. T. MacDonald (1992). "Lymphokine secretion and proliferation of intraepithelial lymphocytes from murine small intestine." *Immunology* **77**(1): 19-24.

Virts, E., D. Barritt and W. C. Raschke (1998). "Expression of CD45 isoforms lacking exons 7, 8 and 10." *Mol Immunol* **35**(3): 167-76.

Wang, E., L. D. Miller, G. A. Ohnmacht, E. T. Liu and F. M. Marincola (2000). "High-fidelity mRNA amplification for gene profiling." *Nat Biotechnol* **18**(4): 457-9.

Wang, J., M. Whetsell and J. R. Klein (1997). "Local hormone networks and intestinal T cell homeostasis." *Science* **275**(5308): 1937-9.

Watanabe, N., M. Gavrieli, J. R. Sedy, J. Yang, F. Fallarino, S. K. Loftin, M. A. Hurchla, N. Zimmerman, J. Sim, X. Zang, T. L. Murphy, J. H. Russell, J. P. Allison and K. M. Murphy (2003). "BTLA is a lymphocyte inhibitory receptor with similarities to CTLA-4 and PD-1." *Nat Immunol* **4**(7): 670-9.

Watanabe, N., K. Ikuta, S. Fagarasan, S. Yazumi, T. Chiba and T. Honjo (2000). "Migration and differentiation of autoreactive B-1 cells induced by activated gamma/delta T cells in antierythrocyte immunoglobulin transgenic mice." *J Exp Med* **192**(11): 1577-86.

Waterhouse, P., J. M. Penninger, E. Timms, A. Wakeham, A. Shahinian, K. P. Lee, C. B. Thompson, H. Griesser and T. W. Mak (1995). "Lymphoproliferative disorders with early lethality in mice deficient in Ctla-4." *Science* **270**(5238): 985-8.

Wen, L., S. J. Roberts, J. L. Viney, F. S. Wong, C. Mallick, R. C. Findly, Q. Peng, J. E. Craft, M. J. Owen and A. C. Hayday (1994). "Immunoglobulin synthesis and generalized autoimmunity in mice congenitally deficient in alpha beta(+) T cells." *Nature* **369**(6482): 654-8.

Wild, M. K., A. Cambiaggi, M. H. Brown, E. A. Davies, H. Ohno, T. Saito and P. A. van der Merwe (1999). "Dependence of T cell antigen recognition on the dimensions of an accessory receptor-ligand complex." *J Exp Med* **190**(1): 31-41.

Wu, L. C., D. S. Tuot, D. S. Lyons, K. C. Garcia and M. M. Davis (2002). "Two-step binding mechanism for T-cell receptor recognition of peptide MHC." *Nature* **418**(6897): 552-6.

Wulfing, C. and M. M. Davis (1998). "A receptor/cytoskeletal movement triggered by costimulation during T cell activation." *Science* **282**(5397): 2266-9.

Yokoyama, W. M., F. Koning, G. Stingl, J. A. Bluestone, J. E. Coligan and E. M. Shevach (1987). "Production of a T cell hybridoma that expresses the T cell receptor gamma/delta heterodimer." *J Exp Med* **165**(6): 1725-30.

Zachariasse, K. A., W. L. Vaz, C. Sotomayor and W. Kuhnle (1982). "Investigation of human erythrocyte ghost membranes with intramolecular excimer probes." *Biochim Biophys Acta* **688**(2): 323-32.

Zhang, F., W. G. Schmidt, Y. Hou, A. F. Williams and K. Jacobson (1992). "Spontaneous incorporation of the glycosyl-phosphatidylinositol-linked protein Thy-1 into cell membranes." *Proc Natl Acad Sci U S A* **89**(12): 5231-5.

Zhu, J., L. Guo, B. Min, C. J. Watson, J. Hu-Li, H. A. Young, P. N. Tsichlis and W. E. Paul (2002). "Growth factor independent-1 induced by IL-4 regulates Th2 cell proliferation." *Immunity* **16**(5): 733-44.

Zuany-Amorim, C., C. Ruffie, S. Haile, B. B. Vargaftig, P. Pereira and M. Pretolani (1998). "Requirement for gammadelta T cells in allergic airway inflammation." *Science* **280**(5367): 1265-7.